

See discussions, stats, and author profiles for this publication at: <https://www.researchgate.net/publication/338655242>

Heat Transfer Enhancement of a Counter Flow Shell and Tube Heat Exchanger

Thesis · October 2016

CITATIONS

0

READS

632

3 authors, including:



Zena K. Kadhim

Wasit University

51 PUBLICATIONS 100 CITATIONS

[SEE PROFILE](#)

Some of the authors of this publication are also working on these related projects:



CFD Study to Enhance the Heat Transfer in Heat Exchanger by Change the Outer Surface of the Inner Tube and Use Nano Fluid [View project](#)



Experimental study o Free Convection Inside Curvy Surfaces Porous Cavity [View project](#)

Republic of Iraq
Ministry of Higher Education
and Scientific Research
Wasit University
College of Engineering
Mechanical Engineering Department



Heat Transfer Enhancement of a Counter Flow Shell and Tube Heat Exchanger

A Thesis

Submitted to the Council of the College of Engineering/
Wasit University in Partial Fulfillment of the Requirements
for the Degree of Master of Science in Power
Generation/ Mechanical Engineering

By

Safaa Abd Mohammad
(B.Sc.1998)

Supervised By
Prof. Dr. Zena K. Kadhim

بِسْمِ اللَّهِ الرَّحْمَنِ الرَّحِيمِ

اللَّهُ أَكْبَرُ)
اللَّهُ الَّذِي خَلَقَ سَبَعَ سَمَاوَاتٍ وَمِنَ الْأَرْضِ مِثْلَهُنَّ
يَنْزَلُ الْأَمْرَ بَيْنَهُنَّ لِتَعْلَمُوا أَنَّ اللَّهَ عَلَى كُلِّ شَيْءٍ قَدِيرٌ
وَأَنَّ اللَّهَ قَدْ أَحَاطَ بِكُلِّ شَيْءٍ عِلْمًا

١٢

صدق الله العلي العظيم

سورة الطلاق: الآية ١٢

DEDICATION

To my father ... best man in my life

To the soul of my mother

To my wife ... Patience and support within my crucial time.

To my children ... Who fill my life with joy and pleasure.

To my brothers ... Pure brotherhood.

To my friends ... Who supported me in my studies.

To my teachers at all educational stages.

I dedicate this modest endeavor.

Safaa Abd Mohammed

2016

Acknowledgements

Maximal appreciation is to the Almighty Allah for the celestial intervention in this modest effort.

Candid gratitude is hereby extended to the following who never desisted in helping to achieve this thesis:

Prof. Dr. Zena K. Kadhim, my supervisor, for her guidance, support and unlimited help during the period of research.

Mech. Eng. Dept. Staff and Lecturers.

My family and friends, for the moral support.

My friend, Firas Abd, for his support throughout the ANSYS learns.

Safaa Abd Mohammed

2016

Supervisors' Certification

I certify that the thesis entitled "**Heat Transfer Enhancement of a Counter Flow Shell and Tube Heat Exchanger**" was prepared by (Safaa Abd Mohammed) under my supervision at Wasit University / Engineering College/ the Mechanical Engineering Department in a partial fulfillment of the requirements for the degree of Master of Science in Mechanical Engineering.

*ic/IC. Al-shamari
Zener*

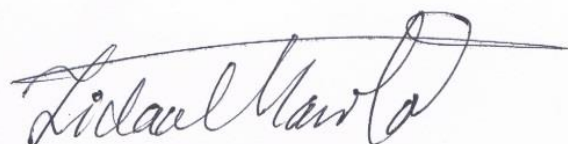
Professor Dr. Zena K. Kadhim

10 / 10 / 2016

Supervisor

Linguistic Certification

I certify that this thesis entitled “ Heat Transfer Enhancement of a Counter Flow Shell and Tube Heat Exchanger ”, prepared by (Safaa Abd Mohammed) was linguistic supervision. It was amended to meet the style of English language.



Asst. Prof. Dr. Fida al-Mawla

Language Expert

٢٩ / ١ / 2017

Examination Committee Certification

We the members of examining committee certify that after reading the thesis entitled "**Heat Transfer Enhancement of a Counter Flow Shell and Tube Heat Exchanger**" and examining the student (Safaa Abd Mohammed) in its contents. We think it meets the standards and it is adequate for the award of the Degree of Master of Science in Mechanical Engineering.



Prof. Dr.

Arkan KH. Husain AL-Taie

21 / 5 / 2017

(Chairman)



Ass. Prof. Dr.

Ahmed Waheed Mustafa

21 / 5 / 2017

(Member)



Ass. Prof. Dr.

Abbas Jassem Jubear

16 / 5 / 2017

(Member)



Prof. Dr.

Zena Khalefa Kadhim

16 / 5 / 2017

(Supervisor)

Approved for the University of Wasit

Ass. Prof. Dr.

Ali Nasser Hello

/ / 2017

Dean of the College of Engineering

ABSTRACT

This work is deals with experimental and numerical implementing to recover the benefit by changing the shape of the tube in heat exchanger and improving the heat transfer using water as the working fluid for heat transfer in the first case, then was using Nano fluids as a heat transfer working fluid.

The experimental tests were carried out in a manufactured and design a complete test system for counter flow heat exchanger. The test on a system consisting of a copper tube with 1m length 17.05 mm inner diameter 19.05 mm outer diameter, fixed concentric within the outer tube was made of a Polyvinyl Chloride (P.V.C) with an inner diameter 43 mm and outer diameter 50 mm isolated from the outside by using white foam to reduce heat loss. The modified tube was manufactured containing transverse grooves with 0.5 mm depth this is equal to the half thickness of the copper tube with the ratio $z/d = 1, 0.5$ (z : distance from center to center of groove, d : outer pipe diameter)

The laboratory experiment used the hot water volumetric flow rate ranging between 1to5 LPM and Re from 3000 to 25000, passing within the inner copper tube. The cooling water was used in the first experiment with the volumetric flow rate ranging between 3to7 LPM and Re from 500 to 2200. But in the second experiment, then additives to the working fluid the nanomaterial's of alumina AL_2O_3 in concentration 0.8%.Three temperatures were the hot fluid is the adoption of 40, 50 and 60 °C and cold water temperature is 25 °C.

The experimental result showed on improvement in overall heat transfer coefficient are ranging from 54.54% to 55.72% at a temperature of 40 °C, 52.93% to 56.24% at a temperature of 50 °C and 51.21% to 57.27% at a temperature of 60 °C, for both corrugated tubes with respect to smooth tube without using nanoparticles.

When adding the nanoparticles of alumina AL_2O_3 with diameter 20nm diffused in the working fluid (water as basic fluid) with concentration of 0.8% practically increase in heat transfer by 11.70%.

Numerical simulation of heat exchanger analysis Nano fluid and heat transfer are carried out using ANSYS-FLUINT 14.0 software. The software has been used to solve energy, momentum and continuity equations to analyze fluid flow through the heat exchanger. Analysis was performed for each pipe using cold fluid without and with nanoparticles imposing a state of preprocessing, Newtonian behavior and three dimensions of flow. The numerical simulation done at hot water volumetric flow rate 1to5 LPM and Re from 3000 to 25000, the cold water volumetric flow 3to7 LPM and Re 500 to 2200. Nano fluid AL_2O_3 used with volume fraction 0.8%.

The results showed the slight divergence among experimental and the numerical results by percentage 8.97% to 11.35% for corrugated tubes $z/d=1$, 0.5 respectively, but it clearly shows that they have the same behavior and phenomenon.

The experiential equations were achieved for the value of Reynolds and Nusselt number as shown in chapter 5, for all variables and tube geometry with and without Nano fluid by using LAB FIT program, designed by Universidad Federal de Campina Grande, Brazil. Equations are show

$$\text{Nu}_c = 449.8 + 1443R_e^{0.1749} \quad (1)$$

$$\text{Nu}_{cn} = 621.3 + 1157R_{en}^{0.1096} \quad (2)$$

Table of Contents

Abstract	I
List of Contents	III
Nomenclature	VII
Chapter 1 Introduction	1
1.1 Introduction	1
1.2 Heat Exchanger Application	2
1.3 Objective of Present Study	4
1.4 Structure of The Thesis	5
Chapter 2 Literature Review	6
2.1 The Experimental Study	6
2.2 The Numerical Study	10
Chapter 3 Theories and Numerical Solution	16
3.1 Introduction	16
3.2 Numerical Models	16
3.2.1 Design of Geometry	16
3.3 Numerical Simulation	17
3.3.1 Computational Domain	17
3.3.2 Assumption	17
3.3.3 Governing Equation for Laminar and Turbulent Flow	18
3.4 Mesh Generation	20
3.5 Mesh Topology	20
3.6 Computing Time and total Cell Number	21
3.7 Boundary condition	21
3.8 Control Parameters	22
3.8.1 Convergence	22
3.8.2 Relaxation Factor	22
3.9 Number of Iteration	23
3.10 Solution Procedure	23

3.11 Model Characterization	24
Chapter 4 Experimental Work	30
4.1 Introduction	30
4.2 Enhancing Tube Surface	32
4.3 Experimental System	32
4.3.1 Test Section	32
4.3.2 Electrical Control Unit	33
4.3.3 Hot Water Vessel	33
4.3.4 Cold Water Vessel	33
4.3.5 Water Pump	33
4.3.6 Water Valves	33
4.3.7 Flow Meter	33
4.3.8 Cooling Unit	34
4.3.9 Thermocouples	34
4.3.9.1 Thermocouples Calibrations	34
4.3.10 Data Logger Thermometer	35
4.4 Manometer	35
4.5 Fundamental of Nano Fluids	35
4.6 Thermal Conductivity of Nano Fluids	36
4.6.1 Volume Fraction	36
4.6.2 Thermal Conductivity of Nano Fluid	37
4.7 Theories and Equation	39
4.7.1 Assumption of Energy Balance Equation	39
4.8 Preparation of Nano Fluid	39
4.9 Base Fluid and Nanoparticles	39
4.10 Use Ultrasonic Vibration Device	40
4.11 Experiment Set Up and Operation Procedure	40
Chapter 5 Results and Discussion	42
5.1 Introduction	42
5.2 Effect of Hot Water Flow Rate on Temperature Difference in	43

Tube-side	
5.3 Effect of Hot Water Flow Rate on Temperature Difference for shell-side	43
5.4 Effect of Cold Water Mass Flow Rate on Temperature Difference	43
5.5 Effect of Hot Water Mass Flow Rate on Heat Dissipation for Tube and Shell- sides	44
5.6 Effect of Cold Water Mass Flow Rate on Heat Dissipation for Tube and Shell-sides	44
5.7 Effect of Hot Water Mass Flow Rate on Overall Heat Transfer Coefficient for Tube and Shell-sides	45
5.8 Effect of Cold Water Mass Flow Rate on Overall Heat Transfer Coefficient for Tube and Shell-sides	45
5.9 Effect of Hot Water Mass Flow Rate on Nusselt Number for Tube-side	46
5.10 Effect of Hot Water Mass Flow Rate on Nusselt Number for Shell-side	47
5.11 Effect of Cold Water Mass Flow Rate on Nusselt Number	47
5.12 Effect of Hot Water Mass Flow Rate on Friction Factors	47
5.13 Effect of Cold Water Mass Flow Rate on Friction Factors	48
5.14 Effect of Water Mass Flow Rate and Tube Geometry on Pressure Drop in Tube-side	48
5.15 Effect of Water Mass Flow Rate and Tube Geometry on Pressure Drop in Shell-side	49
5.16 Effect of Water Mass Flow Rate and Tube Geometry on Number of Transfer Unit and Effectiveness (NTU)	49
5.17 Performance of Heat Exchanger with Nano fluid	50
5.18 Effect of Nano Fluid on Temperature Difference	50
5.19 Effect of Nano Fluid on Heat Dissipation	50
5.20 Effect of Nano Fluid on Overall Heat Transfer Coefficient	51
5.21 Effect of Nano Fluid on Nusselt Number	51
5.22 Effect of Nano Fluid on Effectiveness of Heat Exchanger	51
5.23 Numerical Results Analysis	51
5.24 Comparison between Experimental and Numerical Results	53
5.25 Experiential Equations	53

Chapter 6 Conclusions and Recommendations	80
6.1 Conclusions	80
6.2 Recommendations	81
References	82
Appendixes	

Nomenclature		
Symbol	Description	Units
A	Area	m^2
A_s	Surface area	m^2
A_c	Cross section area	m^2
C_p	Specific Heat	$\text{J/kg. } ^\circ\text{C}$
D, D_s	Diameter of outer tube (shell)	m
D_e	Equivalent diameter	m
D_h	Hydraulic diameter	m
d	Diameter of inner tube (tube)	m
F	Correction factor	...
f	Friction factor	...
h	Heat transfer coefficient	$\text{W/m}^2.^\circ\text{C}$
k	Thermal conductivity	$\text{W/m. } ^\circ\text{C}$
L	Length	m
m	Mass	kg
\dot{m}	Mass flow rate	kg/sec
N	Number of grove	...
Nu	Nusselt number	...
P	Perimeter	m
P_e	Equivalent perimeter	m
Pr	Prandtl number	...
P	Pressure	Pa
ΔP	Pressure drop	Pa
Q	Heat dissipation	W
Re	Reynold number	...
S	Width of corrugated	...
T	Temperature	$^\circ\text{C}$
T_{hi}	Inlet temperature of hot water	$^\circ\text{C}$
T_{ci}	Inlet temperature of cold water	$^\circ\text{C}$
T_{ho}	Outlet temperature of hot water	$^\circ\text{C}$
T_{co}	Outlet temperature of cold water	$^\circ\text{C}$
T_m	Mean temperature	$^\circ\text{C}$
u	Velocity	m/sec
U	Overall heat transfer coefficient	$\text{W/m}^2.^\circ\text{C}$
\dot{v}	Volumetric flow rate	$1/\text{m}$
(u, v, w)	Velocity component	m/sec
(u', v', w')	Fluctuating velocity component	m/sec
(\bar{u} , \bar{v} , \bar{w})	Mean velocity component	m/sec
z/d	Corrugated ratio	...

Greek symbols

Symbol	Description	Units
μ	Dynamic viscosity	kg/m. sec
ρ	Density	kg/m ³
φ	Volume concentration	...
Δ	Difference between values	...
ε	Heat exchanger effectiveness	...
α	Under relaxation factor	...
π	PI equal to 3.145926	...

Subscripts

Symbol	Description
bf	Base fluid
nf	Nano fluid
c	Cold
h	Hot
i	Inner
min.	Minimum
max.	Maximum
o	Outer
p	Particle
s	Surface

Abbreviations

Symbol	Description
CFD	Computational fluid dynamic
LMTD	Log mean temperature difference
NTU	Number of transfer unit
RNG	Renormalization group
SIMPLE	Semi implicit method for pressure-linked equation

CHAPTER ONE

INTRODUCTION

1.1 Introduction

“A heat exchanger is a device that is used to transfer heat between two or more fluids that are at different temperatures. Heat exchangers are essential elements in a wide range of systems, including the automobiles, computers, power plants, and comfort heating/cooling equipment”[1].

A generally utilized type of heat exchangers is the shell-and-tube heat exchanger (STHE), the enhancement of heat transfer rate which is the principle target of this work. Specialists are consistently being requested to enhance procedures and increment effectiveness. These solicitations may emerge as a consequence of the need to expand prepare throughput, increment productivity, or suit capital confinements. Forms which utilize warm exchange hardware should much of the time be enhanced hence. Once in a while expanding heat exchanger execution may not come about because of increments in throughput or higher obligations [2].

Heat exchanger is a vital unit operation that adds to effectiveness numerous procedures May be the most well-known sort of heat exchanger in modern enforcement STHE, as appeared in figure (1-1). Shell and tube heat exchanger have countless (infrequently a few hundred) stuffed in a shell with their parallel to that of the shell. Warm exchange happens as one liquid streams inside tubes and other liquid streams outside through the shell. Baffles are ordinarily put in shell to drive shell-side liquid to stream over a shell to upgrade warm exchange and to keep up uniform dispersing between tubes. In spite of their across the

board utilize, shell and tube warm exchangers are not appropriate for use in car and air ship applications in view of their generally extensive size and weight [3].

The major reason for this measurement is that shell and tube innovation is a financially savvy, demonstrated answer for a wide assortment of heat exchange prerequisites. There are impediments connected with the innovation which incorporate wasteful use of shell side weight drop, low or dead stream zones around the baffles where fouling and erosion can happen, and stream initiated tube vibration, which can eventually bring about hardware disappointment. A heat exchanger is a segment that permits the exchange of heat starting with one liquid (fluid or gas) to another fluid[4]. Increasing heat exchanger execution for the most part means exchanging more obligation or working the exchanger at a nearer temperature approach. This can be proficient without an emotional increment in surface area [2].

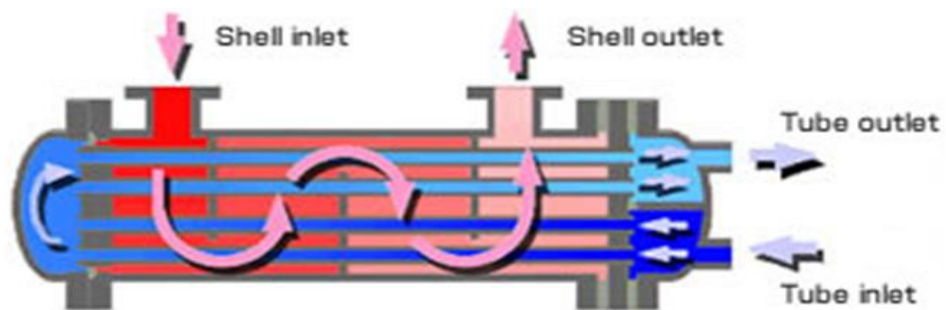


Figure (1-1) Structure of shell and tube type heat exchanger [2]

1.2 Heat Exchanger Application

Today's heat exchangers must meet an assortment of exceptionally requesting prerequisites. As far as execution, they need to guarantee most extreme heat exchange while keeping size to a base. Moreover, the solidness of heat exchangers must be to a great degree high, giving inconvenience free execution

all through its administration life at low assembling cost [5]. Heat exchanger are designed for heat transfer and mostly applied in the processes:

1. Heating, cooling , ventilation, condensation and evaporation.
2. Power generation (including nuclear).
3. Heat exchanger for automotive applications[6], marine application[14], and aircraft [16].
4. Refineries/Petrochemical, Bio-gas [7].
5. Personal computer cooling, to keep components within permissible operating temperature limits. Components that are susceptible to temporary malfunction or permanent failure if overheated include integrated circuits such as CPUs, chipset, graphics cards, and hard disk drives [8].
6. Manufacturing process like food, steel casting and automotive parts[9].
7. Air cooled exchangers [10].
8. Heat exchangers for hygienic use [11].
9. Aerospace applications [12].
10. Energy saver heat exchangers use for sun oriented water warming frameworks [13].
11. Steam condensation in numerous synthetic procedures, steam is required, or comes about from production [15].
12. In the petrochemical businesses [17].
13. Nano fluid applications in
 - a. Electronic applications.
 - b. Transportation.
 - c. Industrial cooling application.
 - d. Nuclear systems cooling.
 - e. Space applications.
 - f. Medical application.
 - g. Cooling of microchips.

1.3 Objective of Present Study

The main objectives of this study are:

1. To enhance heat transfer coefficient for shell and tube heat exchanger.
2. Perform shell and tube heat exchanger.
3. To study the effect of Nano fluid stream parameter on heat transfer coefficients.
4. Design and implement a test section to get heat transfer coefficient for modified tube.
5. Manufacture the heat exchanger from P.V.C. with modified copper tubes.
6. The experimental measurements effect for different water volumetric flow rate for hot and cold water". Water temperature and stream rate on heat transfer coefficient for modified tubes.
7. Study the effect of Nano fluid stream parameter on heat transfer coefficients
8. Analyses data, quantification of full measuring process.
9. Obtain experimental equations for Reynolds Number, Nusselt Number of using hot and cold water and a Nano fluid.
10. Simulation the 3D geometry for modified exchanger by ANSYS-FLUENT 14.0 software.
11. Compare the experimental results with numerical results from ANSYS-FLUENT and show the percentage of error and it's causes.
12. Put forward method to reduce these cases.

1.4 Structure of The Thesis

This work is divided into six chapters as portrayed beneath and some other applicable data are given in the appendix:

Chapter 1: Presents an introduction to the thesis, defining the problems, aims of the study and structure of the thesis.

Chapter 2: Reviews the published literature of theoretical and experimental study, as well as experimental and numerical study, the use of Nano fluid in heat transfer enhancement.

Chapter 3: Describes of mathematical formulation including the assumption and setup of the ANSYS-FLUENT 14.0 software.

Chapter 4: Present the experimental apparatus; design and manufacturing of the test sample, description of the devices and instruments and the uncertainty analysis of the experimental work.

Chapter 5: Illustrates the results and discussions of the experimental work and comparing the results with the theoretical results and other research.

Chapter 6: Bring together all the conclusions from this work recommendation for further works are also provided.

CHAPTER TWO

Literature Review

2.1 The Experimental Study

K. Boomsma et al., 2003, [20] performed experiments with water that were scaled to estimate the heat exchangers' performance, when used with a 50% water-ethylene glycol solution. Open-cell metal foams with an average cell diameter of 2.3 mm were manufactured from [6101-T6] aluminum alloy and were compressed and fashioned into compact heat exchangers measuring [40 mm × 40 mm × 2 mm high], possessing a surface area to volume ratio on the order of [10,000 m²/m³]. They were placed into a forced convection arrangement using water as the coolant. Heat fluxes measured from the heater-foam interface ranged up to [688 kW m⁻²], which corresponded to Nusselt number up to 134 when calculated based on the heater-foam interface area of [1600 mm²] and a Darcian coolant flow velocity of approximately 1.4 m/s. The compressed open-cell aluminum foam heat exchangers generated thermal resistances that were 2-3 times lower than the best.

N. Sahiti et al., 2005, [21] demonstrated that the proposed technique for exchange upgrades is a great deal more powerful than present strategies, since it brings about an expansion in exchange region pin fins furthermore an increment in the heat exchange coefficient. Significant upgrades were exhibited in that work by utilizing little round and hollow sticks on surfaces of heat exchangers.

Wang et al., 2009, [22] presented experimental work done on shell and tube heat exchanger by blocking the gaps between the baffle and the shell by using the sealers. Results of closing the small gaps in the shell side increase the heat transfer coefficient by [18.2-25.5%], the overall heat transfer coefficient

increase by [15.6-19.7%] and the exergy efficiency increased by [12.9-14.1%]. Increase losses in pressure [44.6-48.8%], but rise in pump power wanted can be neglected compared with the rise of heat flux.

Chinaruk et al., 2009, [23] investigated the impacts of the pitch and contort proportion on normal heat exchange coefficient and the weight misfortune when they are resolved in a round tube with the completely created stream for the Reynolds number in the range of 12,000 to 44,000, two dimpled tubes with various space proportions of dimpled surfaces ($PR = 0.7$ and 1.0). Three curved tapes with diverse bend proportions ($y/w = 3, 5$, and 7) are utilized, tentatively utilizing air as working liquid. The exploratory results uncover that both heat exchange coefficient and grating component in the dimpled tube fitted with the contorted tape, are higher than those in the dimple tube acting alone and plain tube. It is additionally found that the exchange coefficient and contact calculate joined gadgets increment as the space proportion and contort proportion (y/w) diminish.

Qasim et al., 2013, [24] investigated experimentally the heat exchanger with different wire coils insert in the tube with different pitches for Reynolds number ranging between [5000 to 40000] inside the tube and counter flow arrangement to the working fluid (water in two side). The results show that the heat transfers as well as friction factor increase with increasing the intensity of coils or decreasing the coiling pitches and enhancement by wire coils is more effective at low values of Reynolds number than high values. For Reynolds number range, a maximum increase in Nusselt number of 2.43 is obtained, corresponding to an increase in friction factor of 4.75.

Eiyad Abu-Nada, 2009, [30] studied the experimental data for viscosity which take into account the dependence of these properties on temperature and nanoparticle volume fraction. Different viscosity and thermal conductivity models are used to evaluate heat transfer enhancement in the annulus. It was observed that for $Re \geq 10^4$, the average Nu was reduced by increasing the

volume fraction of nanoparticles. However, for $Re = 10^3$, the average Nu increased by increasing the volume fraction of nanoparticles. For ($Re \geq 10^4$) Nu was deteriorated everywhere around the cylinder surface especially at high expansion ratio. Completely different predictions for ($Re \geq 10^4$) where the difference in prediction of Nusselt number reached 30%. However, this difference was less than 10% at $Re = 10^3$.

Anoop et al., 2009, [31] investigated effect of Nano-particles size in heat transfer coefficient experimentally, two molecule sizes were utilized, one with normal molecule of 45 nm and other with 150 nm in laminar district. It was watched that both Nano liquids indicated higher exchange qualities than the base liquid and the Nano liquid (45 nm) particles demonstrated higher heat exchange coefficient than that (150 nm). It was additionally watched that in the creating locale, the heat exchange coefficients indicate higher improvement than in the created area.

In **Leonga et al.**, 2012, [32] the recovery shell and tube heat exchanger in biomass heating plant was studied. The results after use the application of Nano fluid in enhancement of heat transfer. It was shown that the convective and overall heat transfer coefficient increased with the application of Nano fluid compared to base fluids. Heat transfer enhancement is about 7.8%. It is found with addition of (1%) copper Nano-particles in ethylene glycol with mass flow rate of the flue gas (26.3 kg/s) and (116.0 Kg/s) for coolant.

Reza Aghayari et al., 2014 [33] performed experiments on double tube heat exchanger. The tube was made of a soft steel (ID=6mm) and (OD=8mm). Nano fluid used the containing nanoparticles ($\gamma\text{-AL}_2\text{O}_3$) with particle size 20 nm and volume fraction (0.1- 0.3%). The effects of temperature and concentration of Nano-particles on Nusselt number and heat transfer coefficient are examining. The experimental results show a considerable increase in heat transfer coefficient and Nusselt number up to (19% - 24%), respectively.

V. Santhosh Cibi et al., 2014, [34] studied experimentally the using system contains shell and tube heat exchanger. The graphite powder mixed with the water to prepare the aqueous solution of graphite. The mixture makes with different concentration (0.025, 0.05, and 0.075) wt% of graphite in water. The m of hotter fluid is constant at (1 LPM) and m cold water is varied from (1 to 5 LPM). From the results, it was observed that the thermal conductivity increases with increase in the concentration. With the addition of (0.025, 0.05, 0.075) wt%, the thermal conductivity will be in rang (1.8, 3.2, 4.3), whereas water has only (0.618W/m. k).

Aphichat Danwittayakul et al., 2015, [35] presented experimental study to find the heat transfer efficiency by using several percentage weight of alumina Nano-particles. Alumina Nano-particles (less than<50 nm) in size was used. Used five concentrations of Nano fluid were applied in the hot line. Flow rate of Nano fluid was set as $30 \text{ cm}^3/\text{s}$ and m cold were change from (10 to 50) cm^3/s . The result is show that the highest heat transfer coefficient was at concentration of (0.25%) with enhancement about 10%.

Arun Kumar Tiwari, 2015, [36] studied experimentally, analysis of shell and tube heat exchanger with Al_2O_3 /water Nano fluid and the effect of using it with different particle volume concentrations (0.5 to 3%). It was found that the effectiveness of shell and tube heat exchanger increments by 6.2% because of increment in volume focus from (0.5% to 3%). Less coolant pumping force is required for exchanger worked with Al_2O_3 Nano liquid contrasted with base liquid. Subsequently, there is change in execution of shell and tube heat exchanger because of the utilization Nano fluid.

Somchandra Patel et al., 2015, [37] conducted an experimental work on a system containing a shell and tube heat exchanger. Nano fluid was heated and it flows inside tubes. The Nano fluid with average particle size (20, 40, 60, 80 nm) with concentration of (0.012 % Vol.) was used. From experimental work find

that the (20 nm) particle give better heat transfer and also higher friction facture among the entire particle being used. If the diameter of nanoparticles is decrease the thermal conductivity of fluid is increased and due to higher thermal conductivity the heat transfer coefficient is also increase.

Asmaa H.Dhiaa et al., 2015 [38] conducted an experimental study by using Nano fluid $\text{TiO}_2/\text{water}$. The average diameter of the nanoparticles is (10 nm) and with (0.1%) Vol. concentrations and the temperature work range of (20-60 °C) and the velocity has been changed from 0.032 to 0.192 m/s. The experimentations explain that the suspended Nano-particles extraordinarily enhance performance of the base fluid transfer of heat, and the Nano fluid of $\text{TiO}_2/\text{water}$ has a better heat transfer coefficient compared with pure water in the similar Reynolds number. As contrasted with water, the convective heat transfer coefficient of Nano fluid has improved to 37% for the Nano fluid at 0.192 m/s under 60°C. The Nano fluid $\text{TiO}_2/\text{water}$ changes the structure of the besides fluid and the thermal conductivity increase. These changes near the wall lead to increase the energy exchange rates and increase heat transfer between the fluid and the wall.

2.2 The Numerical Study

K. Vijay et al., 2014, [25] designed the heat exchanger and tested experimentally the inner tube was corrugated twisted and the outer tube was normal tube. Numerical work made by use ANSYS FLUENT 14.0 software the result was showed that the heat transfer rate and temperature distribution were greater in corrugated twisted tube than that of normal tube in heat exchangers.

Shweta et al., 2014, [26] presented a comparative analysis of a water/water shell and tube heat exchanger, to analyze the heat transfer coefficient and pressure drop for range of mass flow rates and temperature outlets, by using Kern, Bell and Bell Delaware methods. The results showed that the shell side heat transfer coefficient rises with increasing mass flow in all three methods, but

the heat transfer given by Bell Delaware method is more than the other two methods. Also the shell side pressure increased rapidly with increased flow rate and this increase was again more in Bell Delaware method as compared to others.

- **Kern method**
$$h = 0.36 * (k/D_e) * (R_e^{0.55}) * (P_r^{0.33}) * \left[\left(\frac{\mu_s}{\mu_w} \right)^{0.14} \right]$$
- **Bell method**
$$h_{shell} = h_{co} * F_n * F_w * F_b * F_L$$
- **Bell Delaware method**
$$h = j_i * C_{ps} * \left(\frac{m_s}{S_m} \right) * \left[\left(\frac{1}{P_{rs}} \right) - \left(\frac{2}{3} \right) \right] * \left[\left(\frac{\mu_s}{\mu_w} \right)^{0.14} \right]$$

Sidi et al., 2006, [27] investigated a numerical technique in view of the "control-volume" approach that was utilized to illuminate the arrangement of non-linear and coupled representing conditions. Established κ - ϵ model was utilized so as to model the turbulence, together with stunned non-uniform network framework. Numerical outcome demonstrates that consideration of Nano-particles into base liquid has created a growth of the heat exchange coefficient, which has been found to increment obviously with an expansion of particles volume fixation. Such helpful impact has all the earmarks of being more claimed for streams with direct to high Re. In turn around, the nearness of Nano-particles has actuated a fairly intense impact on the divider shear push that has likewise been found to increment with molecule stacking. Another relationship is proposed to ascertain the fully-developed heat transfer coefficient for the Nano fluid considered.

$$Nu_{fd} = 0.085 Re^{0.71} Pr^{0.35}$$

2.1

Resat et al., 2006, [1] dealt with the optimal design of heat exchanger, by utilizing the LMTD method to decide exchange zone for offered design setup (the exchanger outline is the assessment of the base exchange zone required for a given heat obligation). Genetic algorithms (GA) have been effectively connected for the ideal plan of the heat exchanger. External tube width, tube design, number of tube passes, external shell distance across, confound separating and cut, it is changed to made the best design of heat exchanger.

Paisarn et al., 2008, [28] investigated the enhancement heat transfer rate by changing properties of transport fluid and flow. Heat tube with de-ionic water, alcohol and Nano fluid were tested. Titanium nanoparticles with ($D=21\text{ nm}$) are used where blends of liquor and Nano-particles are readied utilizing an ultrasonic homogenizer. Impacts of charge measure of working liquid, heat tube tilt edge and Nano-particles focuses on heat effectiveness of heat tube are considered. Nano-particles significantly affect the improvement of heat productivity of heath tube. The heat productivity is 10.60% for the tube with 0.10% nanoparticles volume fixation higher respect to based fluid.

Saqheeb Ali et al., 2015, [29] studied the effect of thickness of fin tube in temperature and the mass flow rat theoretically. The CFD examination is finished by utilizing the ANSYS. The outcomes acquired with three diverse sorts of material's steel, aluminum and copper, finding to exceptionally minor changes happen in the weight and speed with increment of blade thickness and get high temperature at outlet in the event of Aluminum and copper contrasted with steel material. At the point when increment the balance thickness the temperature of the chilly liquid at the outlet of the heat exchanger increments. By diminishing the mass stream rate for there is expanding the estimation of temperature.

B. Chandra sekhar et al., 2014, [4] presented numerical investigation for Pressure drop variations in multi tube pass shell and tube heat exchanger as well as the heat transfer coefficient was obtained. Pressure drop for 1,2,4,6 tube pass shell and tube heat exchanger were found by using “C PROGRAMING” and compared with “Bell Manual Method” values. It was concluded that 4 tube pass is to be better than 6 tubes pass since 4 tubes pass and Pressure drop is less than its allowable.

A review in the literature as seen in table (2.1), reveals the using of different effective techniques to enhance heat transfer from heat exchanger tube outer surface. Also, some investigations have studied the different parameters like

fins, blocked gaps, used dimpled tube, used insert in tube, used corrugated inner surface tube and used different types of Nano fluid.

However, very little research has been done with combined of these techniques. The Numerical and Experimental Investigation to enhance the heat transfer in heat exchanger by changing the outer surface of the inner tube and use Nano fluid, the objective of the present work is to study the effect of change the outer surface of the inner tube from normal to corrugated and used Nano to enhance heat transfer. The heat transfer by using the transverse groove on the outer surface of the inner tube with the temperature 40, 50 and 60 °C and volumetric flow rate for cold water 3, 4, 5, 6 and 7 LPM and volumetric flow rate for hot water 1, 2, 3, 4 and 5 LPM and Nano fluid with concentration of 0.8%.

Table (2.1) Summary of the literature

No	Author	Type of investigation	Finding
1	Boomsma et al., 2003 (20)	Experimentally	At coolant velocity= 1.4 m/s, The compressed open-cell aluminum foam heat exchangers generated thermal resistances that were 2-3 times lower than the best.
2	Sahiti et al, 2005, (21)	Experimentally	Considerable enhancements were demonstrated in the work by using small cylindrical pins on surfaces of heat exchangers.
3	Wang et al., 2009, (22)	Experimentally	Increase the heat transfer coefficient and the overall heat transfer coefficient.
4	Chinaruk et al., 2009, (23)	Experimentally	At $Re = 12000 - 24000$, found that the heat transfer coefficient and friction factor in the combined devices increase as the pitch ratio (PR) and twist ratio (y/w) decrease.
5	Qasim et al., 2013, (24)	Experimentally	At the condition [$Re=5000-40000$, $m=0.1-0.15 \text{ kg/s}$, $Thi=60-70^\circ\text{C}$, $Tci= 20^\circ\text{C}$]. Enhancement by wire coils is more effective at low values of Reynolds number than high values, $Re = 5000 - 40000$.

6	Eiyad Abu-Nada 2009, (30)	Experimentally	At the condition [Re \geq 10000]. The average Nu increased by increasing the volume fraction of nanoparticles.
7	Anoop et al., 2009, (31)	Experimentally	At the condition [average particle size= 45nm] by use Nano fluid 45 nm particles the heat transfer coefficients show higher enhancement than in the developed region.
8	Leonga et al., 2012, (32)	Experimentally	At the condition [\dot{m} =26.3 kg/s flow gas, \dot{m} =116 kg/s coolant]The addition of 1% copper nanoparticles in ethylene glycol based fluid, lead to enhancement in heat transfer about 7.8%.
9	Reza Aghayari et al., 2014, (33)	Experimentally	At the condition [average particle Size=20nm, Re=8000-32000].The experimental results show a considerable increase in heat transfer coefficient up to19%.
10	V. Santhosh et al., 2014, (34)	Experimentally	At the condition [Nano fluid 6 vol. %, Re= 800, flow rate=1-5 LPM] The thermal conductivity increase with increase in the concentration.
11	Aphichat et al., 2015, (35)	Experimentally	[\dot{m} =10-50 cm ³ /s, average particle size <50nm].The highest heat transfer coefficient was achieved at the concentration of 0.25% alumina with about 10% enhancement.
12	Arun Kumar 2015, (36)	Experimentally	At the condition [\dot{m} =0.1-0.35 kg/s, average particle size= 0.005-0.03 nm, Re=10200-11000]. There is an overall improvement in the performance of the shell and tube heat exchanger due to the use of Al ₂ O ₃ /water Nano fluid.
13	Somchandra et al., 2015, (37)	Experimentally	At the condition [\dot{m} =0.05-0.12kg/s, average particle size= 20-80 nm]. The diameter of nanoparticles is decrease the thermal conductivity of fluid is increased and the heat transfer coefficient is also increase.
14	Asmaa H. et al., 2015, (38)	Experimentally	At the condition [T= 20-60 °C, Re=4000-10000, average particle size= 10 nm]. The Nano fluid TiO ₂ /water changes the structure of the besides fluid and the thermal conductivity increase.

15	K. Vijay et al., 2014, (25)	Numerically	At [Thi=100°C, Tci=30°C]. The heat transfer rate and the temperature distribution were better in corrugated twisted tube than that of normal tube in heat exchangers.
16	Shweta et al., 2014, (26)	Numerically	At [Re = 200-400, \dot{m} =0.01-0.04 kg/s]. The heat transfer given by Bell Delaware method is more than Kern and Bell methods
17	Sidi et al., 2006, (27)	Numerically	The inclusion of nanoparticles into the base fluid has produced an augmentation of the heat transfer coefficient.
18	Resat et al., 2006, (1)	Numerically	Genetic algorithms (GA) have been successfully applied for the optimal design of the heat exchanger.
19	Paisarn et al., 2008, (28)	Numerically	At the condition [average particle size= 21 nm]. The thermal efficiency is 10.60% for the heat tube with 0.10% nanoparticles volume concentration higher than that with the based working fluid.
20	Saqheeb et al., 2015, (29)	Numerically	At the condition [Re = 1000-1500, Tin = 313 k, \dot{m} =0.320 kg/s]. When increase the fin thickness the temperature of the cold fluid at the outlet of the heat exchanger increases.
21	B. Chandra et al., 2014, (4)	Numerically	At the condition [Q_{oil} = 43.33 m ³ /hr, Q_{water} = 200 m ³ /hr. Tiw= 32°C]. It is concluded that 4 tube pass is to be preferred than 6 tubes pass since 4 tubes pass calculated pressure drop is less than its allowable pressure drop.

CHPTER THREE

NUMERICAL MODELLIES

3.1 Introduction

In this chapter the numerical analysis of enhancement heat exchanger by using the effect of the different tube shape and Nano fluid on the performance of the system are represented. The main purpose of this part is to determine the validity of the results which are got from the experimental work, as well as to simulate the experiments and apply them in order to minimize cost and time.

The numerical study in this chapter includes:

- Study the effect of changing the surface geometry of the copper tube, use Nano fluid (Al_2O_3), and study the effect of volumetric flow rate and temperature by simulating the experimental work by using ANSYS FLUENT 14.0 software.
- This chapter involves also a series of equations and the theories which are adopted in this work to finalize the solution.

3.2 Numerical Models

Numerical analysis is used to simulate the heat exchange in a countercurrent flow heat exchanger between water/water and water/Nano fluid [hot water flow in tubes and cold water or Nano fluid flow in shell] through the tubes wall. The simulation is done by ANSYS FLUINT 14.0 software with the same conditions of the experimental work.

3.2.1 Design of Geometry

The test sections for smooth copper tube has the dimensions (17.05 and 19.05 mm) as inner and outer diameter and (42.6 and 50 mm) inner and outer

diameter for P.V.C outer tube respectively, With a length of 1m. The Sketch by using a SOLID WORK PREMIUM 2015 program, as shown in figure (3-1). After the geometry was drawn and saved, it was exported to GAMBIT 2.3.6 to make meshing and other activities for all volumes and then saved. Then it exported to ANSYS 14.0 to be read and be ready for model boundary conditions and start simulation in ANSYS FLUENT 14.0 software.

3.3 Numerical Simulation

Numerical simulation was done to analyze advanced phenomena in engineering implementation without including a costly prototype for experimental study. It is the analysis of a system including fluid flow, heat transfer and other parameters on various departments of science. The numerical simulation across three-dimensional model for the heat exchanger adopting by using ANSYS FLUENT 14.0 software, in order to analyze the flow field in the heat exchanger using the solution of energy equation, momentum equation and conservation continuity. Comparison of results for smooth and corrugated tubes was carried out. Numerical method will be expressed in the following part.

3.3.1 Computational Domain

Computational fields in sitting project are shown as in and out of both cold and hot water in the shell and tube. Flow is counter flow on both sides. Corrugated are made on the outer surface of the inner copper pipe.

3.3.2 Assumptions

The following assumptions were made during the present study for hot and cold water:

1. Steady state.
2. Newtonian fluid.
3. Incompressible.

4. Three dimensional.
5. Turbulent flow in inner side hot water ($3000 < \text{Re} < 25000$).
6. Laminar flow in outer side cold water ($500 < \text{Re} < 2200$).
7. Negligible buoyancy.
8. Radiation heat transfer is not considered.

3.3.3 Governing Equations for Laminar and Turbulent Flow

1. Laminar Flow

The governing equations for energy, momentum and continuity are described in the following sections [39]:

- a) Continuity Equation

$$\frac{\partial u}{\partial x} + \frac{\partial v}{\partial y} + \frac{\partial w}{\partial z} = 0 \quad (3.1)$$

- b) Momentum Equation

$$\rho_n \left(u \frac{\partial u}{\partial x} + v \frac{\partial v}{\partial y} + z \frac{\partial w}{\partial z} \right) = - \frac{dp}{dx} + \mu_n \left(\frac{\partial^2 u}{\partial x^2} + \frac{\partial^2 u}{\partial y^2} + \frac{\partial^2 u}{\partial z^2} \right) \quad (3.2)$$

$$\rho_n \left(u \frac{\partial u}{\partial x} + v \frac{\partial v}{\partial y} + z \frac{\partial v}{\partial z} \right) = - \frac{dp}{dy} + \mu_n \left(\frac{\partial^2 v}{\partial x^2} + \frac{\partial^2 v}{\partial y^2} + \frac{\partial^2 v}{\partial z^2} \right) \quad (3.3)$$

$$\rho_n \left(u \frac{\partial w}{\partial x} + v \frac{\partial w}{\partial y} + z \frac{\partial w}{\partial z} \right) = - \frac{dp}{dz} + \mu_n \left(\frac{\partial^2 w}{\partial x^2} + \frac{\partial^2 w}{\partial y^2} + \frac{\partial^2 w}{\partial z^2} \right) \quad (3.4)$$

- c) Energy Equation

$$\rho_n C_p n \left(u \frac{\partial T}{\partial x} + v \frac{\partial T}{\partial y} + w \frac{\partial T}{\partial z} \right) = k_n \left(\frac{\partial^2 T}{\partial x^2} + \frac{\partial^2 T}{\partial y^2} + \frac{\partial^2 T}{\partial z^2} \right) \quad (3.5)$$

2 .Turbulent Flow

The governing equations for energy, momentum and continuity are described in the following sections [40]:

- a) Continuity Equation

$$\frac{\partial \bar{u}}{\partial x} + \frac{\partial \bar{v}}{\partial y} + \frac{\partial \bar{w}}{\partial z} = 0 \quad (3.6)$$

b) Momentum Equation

$$\left(\bar{u} \frac{\partial \bar{u}}{\partial x} + \bar{v} \frac{\partial \bar{u}}{\partial y} + \bar{w} \frac{\partial \bar{u}}{\partial z} \right) + \left(\frac{\partial}{\partial x} \overline{(u'^2)} + \frac{\partial}{\partial y} \overline{(u'v')} + \frac{\partial}{\partial z} \overline{(u'w')} \right) = - \frac{1}{\rho} \frac{\partial P}{\partial x} + \gamma \nabla^2 \bar{u} \quad (3.7)$$

$$\left(\bar{u} \frac{\partial \bar{u}}{\partial x} + \bar{v} \frac{\partial \bar{u}}{\partial y} + \bar{w} \frac{\partial \bar{u}}{\partial z} \right) + \left(\frac{\partial}{\partial x} \overline{(u'^2)} + \frac{\partial}{\partial y} \overline{(u'v')} + \frac{\partial}{\partial z} \overline{(u'w')} \right) = - \frac{1}{\rho} \frac{\partial P}{\partial x} + \gamma \nabla^2 \bar{u} \quad (3.8)$$

$$\left(\bar{u} \frac{\partial \bar{u}}{\partial x} + \bar{v} \frac{\partial \bar{u}}{\partial y} + \bar{w} \frac{\partial \bar{u}}{\partial z} \right) + \left(\frac{\partial}{\partial x} \overline{(u'^2)} + \frac{\partial}{\partial y} \overline{(u'v')} + \frac{\partial}{\partial z} \overline{(u'w')} \right) = - \frac{1}{\rho} \frac{\partial P}{\partial x} + \gamma \nabla^2 \bar{u} \quad (3.9)$$

c) Energy Equation

$$\bar{u} \frac{\partial \bar{T}}{\partial x} + \bar{v} \frac{\partial \bar{T}}{\partial y} + \bar{w} \frac{\partial \bar{T}}{\partial z} = \alpha \nabla^2 \bar{T} + \left(- \frac{\partial}{\partial x} \overline{(u'T')} - \frac{\partial}{\partial y} \overline{(v'T')} - \frac{\partial}{\partial z} \overline{(w'T')} \right) \quad (3.10)$$

d) Transport Equations

- K Equation

$$\rho_n \left(\bar{u} \frac{\partial K}{\partial x} + \bar{v} \frac{\partial K}{\partial y} + \bar{w} \frac{\partial K}{\partial z} \right) = \left[\left(\mu_n + \frac{\mu_t}{\sigma_K} \right) \left(\frac{\partial^2 K}{\partial x^2} + \frac{\partial^2 K}{\partial y^2} + \frac{\partial^2 K}{\partial z^2} \right) \right] + G_K - \rho_n \in \quad (3.11)$$

- ϵ Equation

$$\rho_n \left(\bar{u} \frac{\partial \epsilon}{\partial x} + \bar{v} \frac{\partial \epsilon}{\partial y} + \bar{w} \frac{\partial \epsilon}{\partial z} \right) = \left[\left(\mu_n + \frac{\mu_t}{\sigma_\epsilon} \right) \left(\frac{\partial^2 \epsilon}{\partial x^2} + \frac{\partial^2 \epsilon}{\partial y^2} + \frac{\partial^2 \epsilon}{\partial z^2} \right) \right] + C_{1\epsilon} \frac{\epsilon}{K} G_K - C_{2\epsilon} \rho_n \frac{\epsilon^2}{K_n} \quad (3.12)$$

Where:

$$G_K = \mu_t S^2 \quad (3.13)$$

S = the modulus of the main rate-of-strain tensor.

G_K = generation of turbulent kinetic energy due to mean velocity gradients.

3.4 Mesh Generation

Unstructured mesh is applied in the present study to discretize the computational field into a finite number of control volumes by using the finite-volume scheme. Structured mesh is ruled out because it is favorable for easy cases and it becomes insufficient and time consumed for complicated geometries. By using GAMBIT software, the model was meshed. It is worth mentioning that convenient numerical control and modeling techniques are very important to step up convergence and stability during the calculation. By adopting control-volume technique, FLUENT shifts the governing equations to algebraic equations that can be solved numerically. The control volume is technique involves of integrating the governing equations inside each control volume, yielding discrete equations [21].

3.5 Mesh Topology

Unstructured solver was used in FLUENT software for unstructured mesh which was mentioned in section (3.4). In unstructured mesh, the example of associations differs from indicate point. Additionally, the network of the work must be unequivocally depicted by a fitting information structure. These making arrangement calculations are more costly than those of organized lattices. In any case, the more prominent geometrical adaptability offered by unstructured work can be pivotal when managing spaces of complex geometries or when the work must be an embraced to entangled components of the stream field. In this way, it offers pliability to utilize the better work topology for modern geometries. Familiar programming can utilize different component sorts for work topology. The quantity of work hubs and the hub mode in regards to with component shapes is limited by the kind of component [41].Triangular element type is used in meshing of the surface. Tetrahedron element is employed for 3D geometry; because it has favor in advanced geometries. Mesh of present model is shown in figure (3-2) and mesh topology is shown in figure (3-3).

3.6 Computing Time and Total Cell Number

In this study, it is known that the complication of geometry makes the simulation take a long time for suitable solutions. When dealing with complex flows, the complicated geometry of the model and its mesh resolutions may impose limitations on the computational time step. Basically, the intense mesh resolution would restrict the time step. The number of cells used in this study is as shown in the table (3.1). The simulation took (21hour) as maximum time to be convert.

Table (3.1) number of cells

No.	Case	No. of cells
1	Smooth inner tube	3,741,120
2	Corrugated inner tube ($y/d=1$)	3,680,203
3	Corrugated inner tube ($y/d=0.5$)	3,742,822

3.7 Boundary Conditions

The performance rating of the heat exchanger in this work, some requirements of the physical sample are defined adequately as follows:

- **Inlet Boundary Conditions:**

Inlet velocity was fixed for inner (hot section) and outer (cold section) sides during this study. The temperature inlet of the hot section are (40, 50, 60°C) and in the cold section is (25°C).

- **Pressure Outlet Boundary Conditions :**

Outlet field was set as pressure outlet for the hot and cold section.

- **Wall B.C.:**

No slip was set in wall of the copper pipe. This condition for both fluid and solid region is used.

3.8 Control Parameters

The modeling techniques and convenient numerical is significant to step up convergence and stable the calculation. By choose control–volume technique, FLUENT shifts the governing equations to algebraic equations that can be solved numerically. The control volume technique was involves of integrating the governing equations inside each control volume, yielding discrete equations[42].

3.8.1 Convergence

In this study, the scaled residual for continuity, energy and velocities equations monitored during the solutions. The values are taken into consideration for the convergences are shown in table (3.2).

Table (3.2) residual values for different parameters

Continuity	Velocities	Energy	κ	ϵ
10^{-4}	10^{-4}	10^{-6}	10^{-3}	10^{-3}

3.8.2 Relaxation Factor

The default setting of under relaxation factor is used because the convergence is achieved without any change. The default setting is shown in table (3.3).

Table (3.3) the under relaxation factor

Pressure	Momentum	Energy	TKE	TDR
0.3	0.7	1	0.8	0.8

3.9 Number of Iterations

The number of iterations needed in this work was (4200) as shown in figure (3-4). It is the most extreme number of emphases expected to get the convert.

3.10 Solution Procedure

The following steps were performed in the numerical simulation as follows:

1. Read the mesh.
2. Check the mesh and convert the drawing scale.
3. Select the appropriate solver in FLUENT 14.0 software, there are three solvers provided:
 - The first is used for incompressible flow called the separated solver. This will solve the governing equation in a sequential method.
 - The other solvers solve the governing equation in synchronous method and used for compressible flow.

In this project a first type of solver has been used.

4. Select the model, active energy equation, $k-\epsilon$ (RNG) model and standard wall functions are used.
5. Insert the properties of the materials:
 - Hot water in inner pipe.
 - Cold water or Nano fluid in the shell.
 - Copper tube.
6. Insert the boundary conditions, section (3.7).
7. Set the control parameter:
 - The under-relaxation factor as default setting, section (3.8.2).
 - For the series of differential equations select:
 - i. Pressure = standard
 - ii. Momentum = second order upwind

- iii. Pressure–velocity coupling = SIMPLE
 - iv. Turbulent kinetic energy = second order upwind
 - v. Turbulent dissipation rate = second order upwind
8. Set current flow.
 9. Run the calculation with notice the scaled residual operation.
 10. Save the result.

Figure (3-5) shows SIMPLE algorithms [43].

3.11 Model Characterization.

Heat exchanger shell and tube type will be used. The shell was made from P.V.C. and smooth and two corrugated tubes were made from copper. Figures (3- 6) show all dimensions. Table (3.4) shows the dimension.

Table (3.4) dimension of the shell and tube

Shell	Outer diameter	50 mm
	Inner diameter	42.6 mm
	Thickness	3.7 mm
	Length	1000 mm
Smooth tube	Length	1000 mm
	Inner diameter	17.05 mm
	Outer diameter	19.05 mm
	Thickness	1 mm
Corrugated tube	Corrugation ratio	$z/d=1$
		$z/d=0.5$
	No. of corrugation in outer surface	$z/d=1 , N=49$
		$z/d=0.5 , N=99$

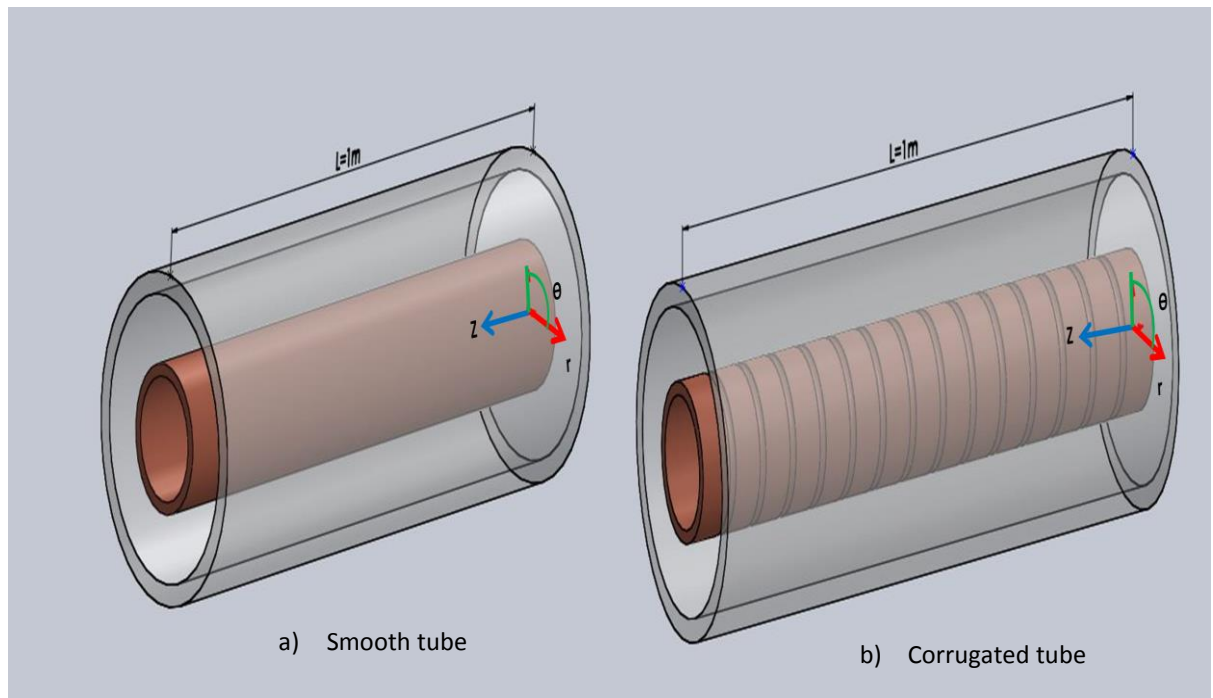


Figure (3-1a, b) Test section geometry

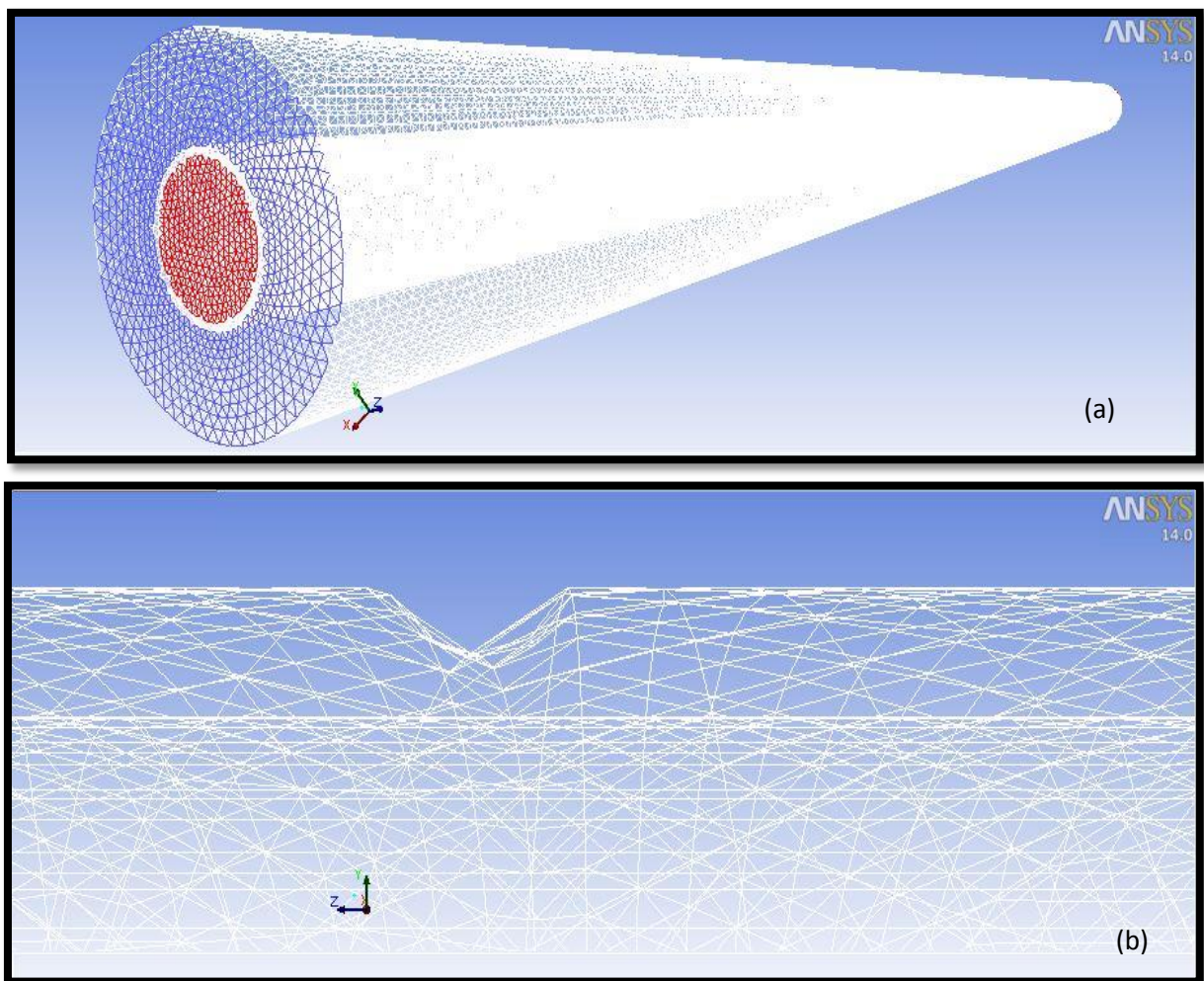


Figure (3-2a, b) Mesh of present model

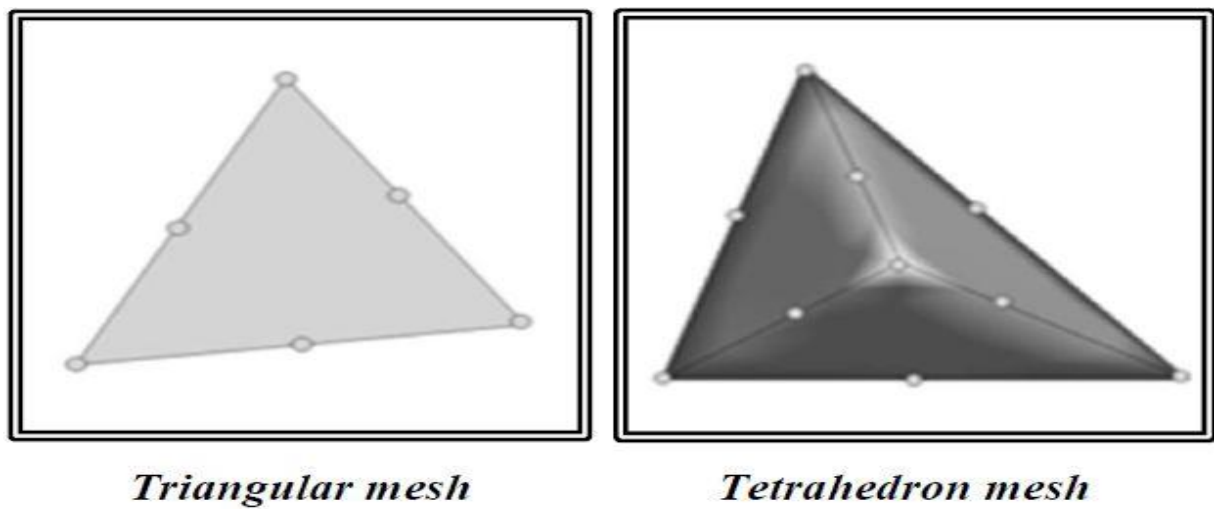


Figure (3-3) Mesh topology [43]

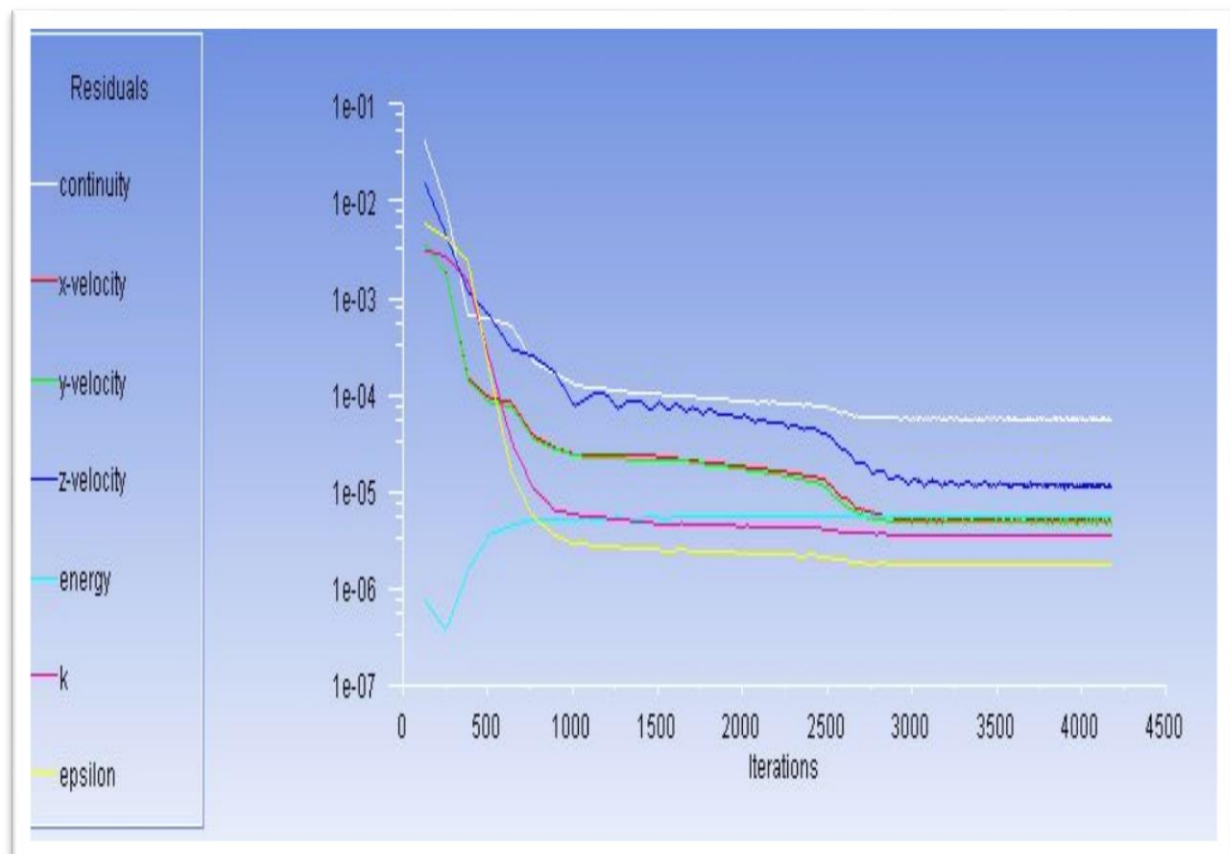


Figure (3-4) Residual for numerical simulation of present study

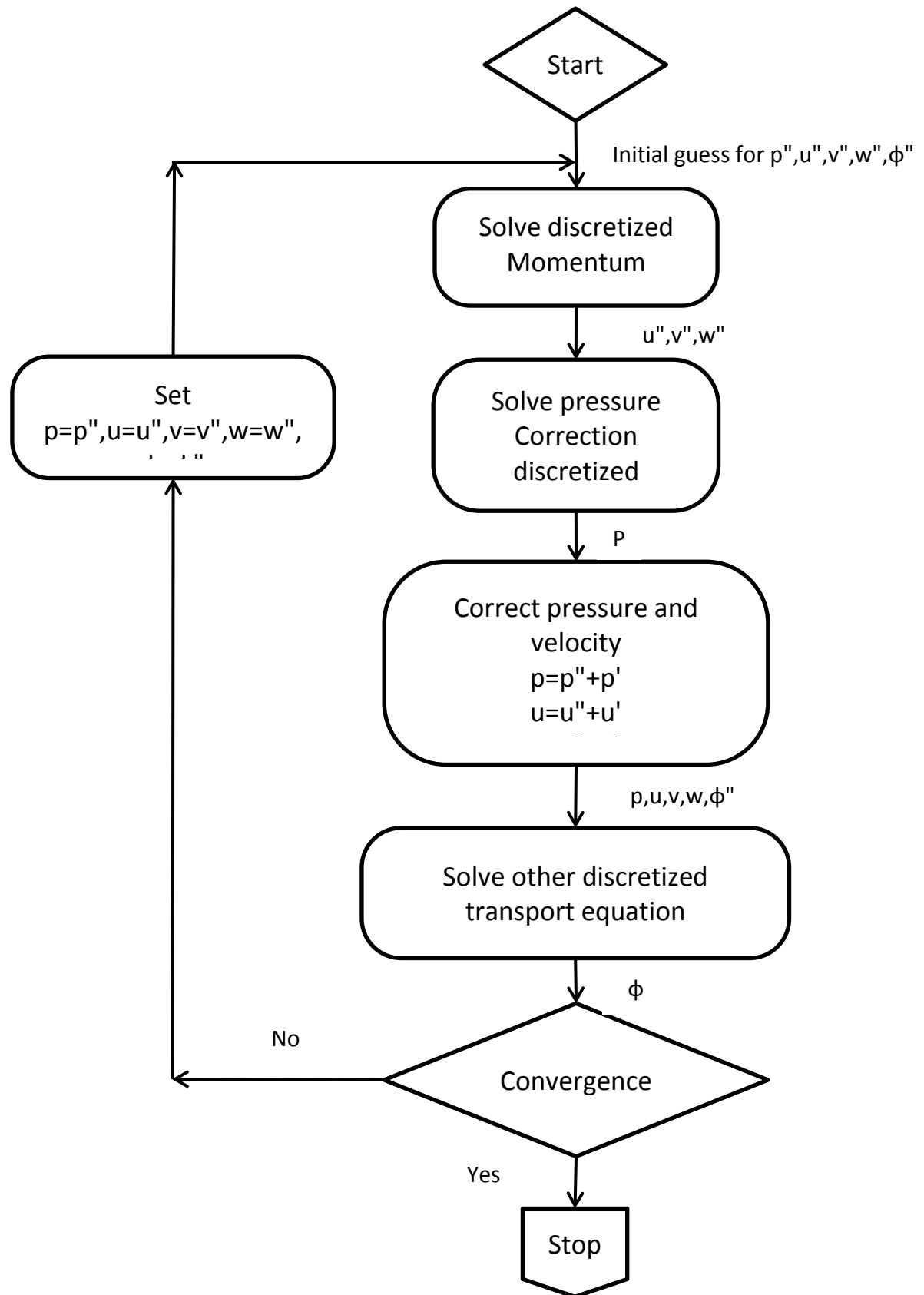
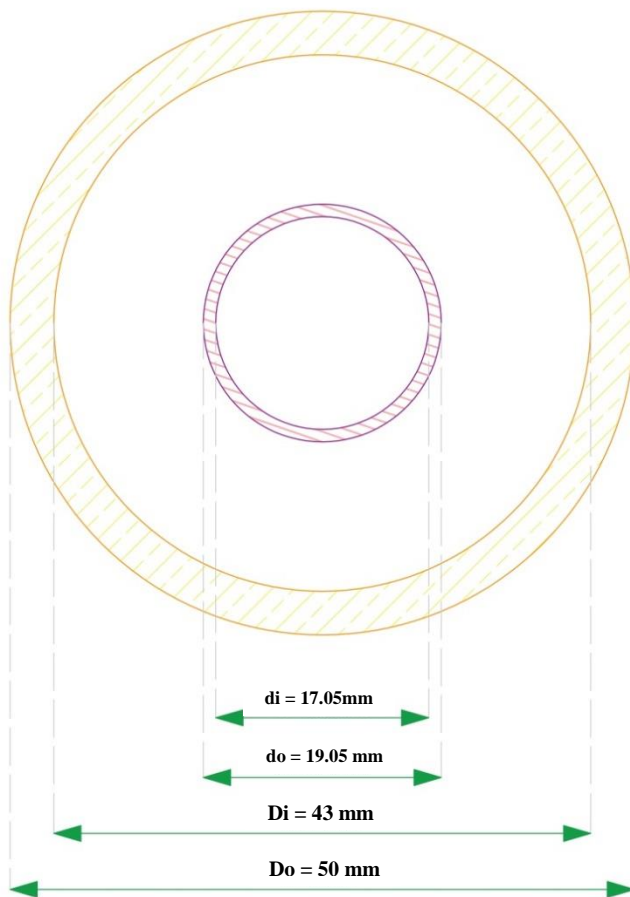
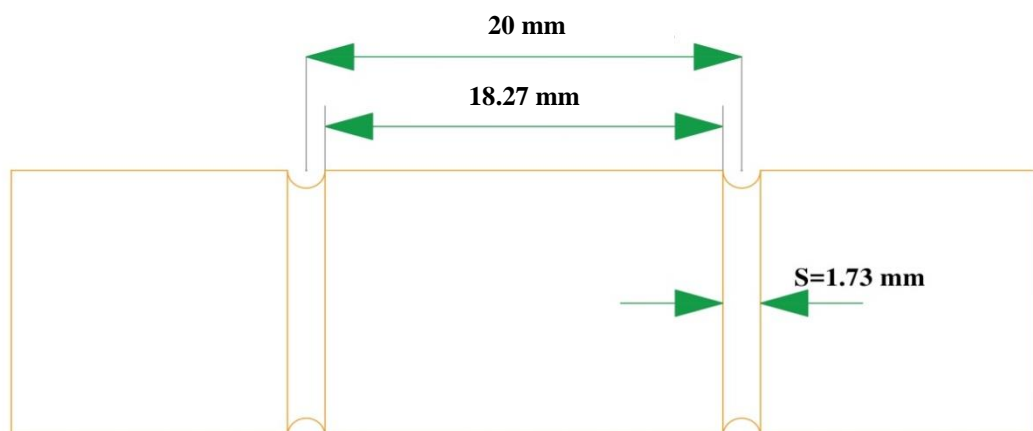


Figure (3-5) SIMPLE algorithms [43]



(a) shell and tube dimensions

(b) corrugated ($z/d=1$) dimensions

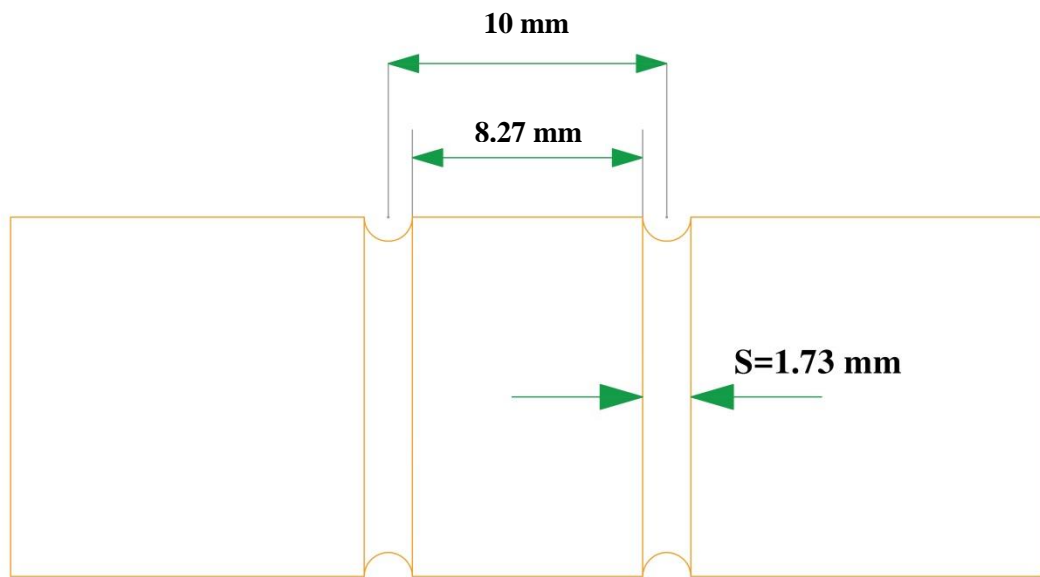
(c) corrugated ($z/d=0.5$) dimensions

Figure (3-6a, b and c) dimension of the test section

CHAPTER FOUR

EXPERIMENTAL WORK

4.1 Introduction

The experimental work in this study is implemented in the postgraduate laboratories of the Engineering College of Wasit University and it has operated at the ambient laboratory conditions.

These investigations dealt with the change of the pipe shape from smooth pipe to corrugate pipe with different values of corrugation ($z/d = 0, 1$ and 0.5), under different temperature $40, 50$ and 60°C . The volumetric water flow rates were $1, 2, 3, 4$ and 5 LPM for hot fluid. At a temperature of 25°C volumetric cold water flow rate at $3, 4, 5, 6$ and 7 LPM , was used. This study discusses the impact of these parameters on enhancing heat transfer coefficient in the exchanger. In comparison to the actual results and numerical results from the ANSYS FLUENT 14.0, it also included the devices and equipment which are needed to succeed this experimentally project in this chapter. Figure (4-1) show test section, figures (4-2) and (4-3) show schematic illustrations of the total system and installation of all devices. All equations used in the study for hot and cold sides and Nano fluid are shown in the appendix [A] with a sample of calculations in appendix [B].

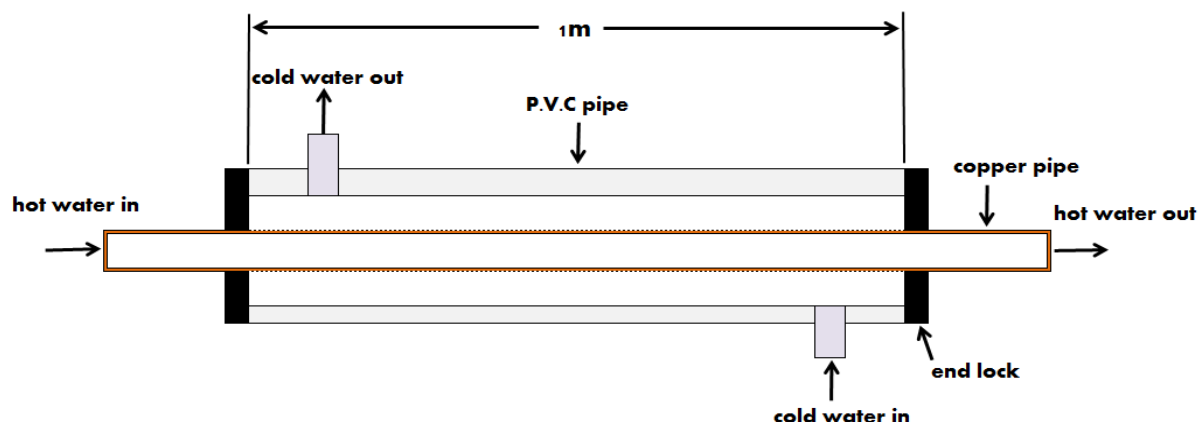


Figure (4-1) schematic test section

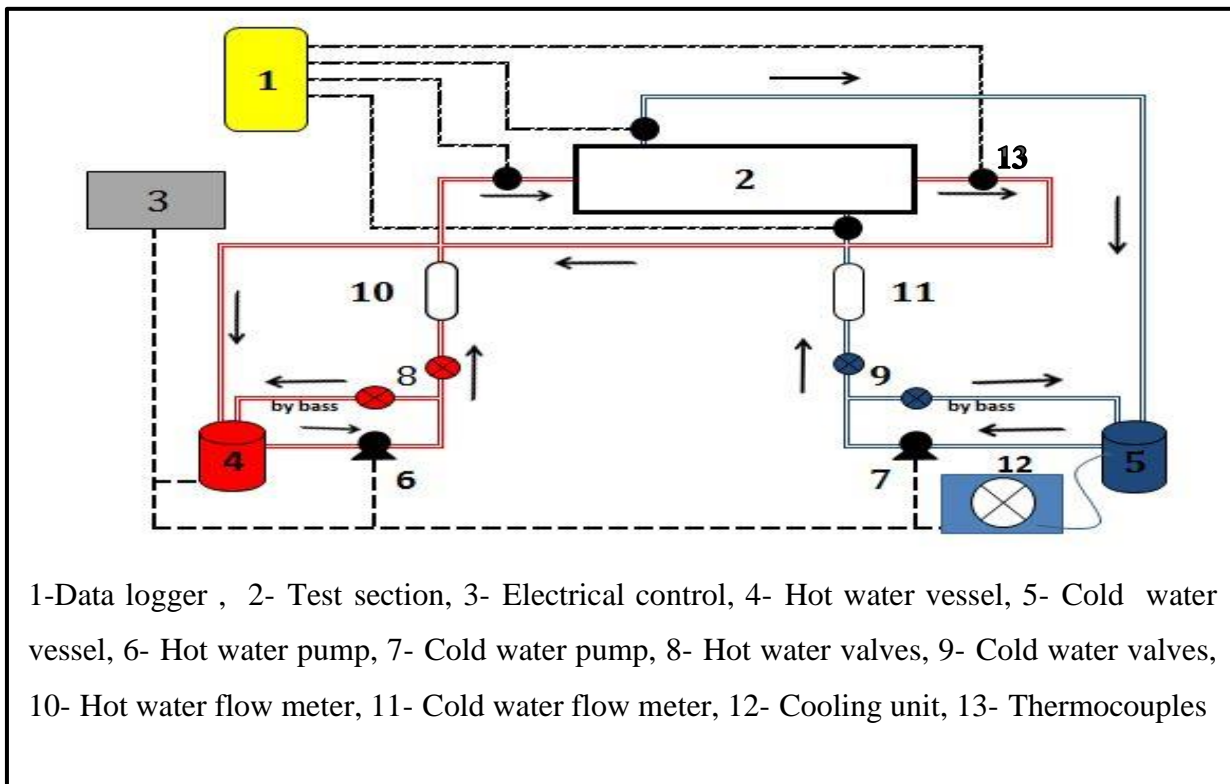


Figure (4-2) schematic layout of experimental rig



Figure (4-3) photography of total equipment of the system

4.2 Enhancing Pipe Surface

There are a lot of experimental works to enhance heat transfer coefficient by changing geometric of pipe surface, by added fins or pin to increase the surface area larges then the heat transfer by better increase. The corrugated pipe leads to increase heat transfer coefficient because the swirl flow creates turbulence resulting in higher heat transfer coefficient in tube side [44].

4.3 Experimental System

In order to obtain the goal of the project required design and fabricate heat exchanger with different type of pipes.

4.3.1 Test Section

The test section is an important part of a heat exchanger, which contains the inner pipe made of copper material and outer pipe made of Polyvinyl Chloride (P.V.C), choose respect to the standard pitch between the pipes in the heat exchanger [45]. It includes two parts, the first part is an internal copper pipe, smooth and two corrugated pipes with ratio ($z/d=1, 0.5$). The smooth pipe has (1m) long and (17.05mm, 19.05mm) inner and outer diameter respectively. The corrugated pipes with the ratio ($z/d = 1, 0.5$), pipe length is (1m), (17.05mm) inner diameter, (19.05mm) outer diameter. In the first ratio have ($N=49$) and in the second ratio ($N=99$) where (N) is number of corrugated in the outer surface of copper pipe. Thickness of the used copper pipe is (1mm) and the corrugated value is half pipe thickness shown in figure (C-1a, b, c, and d), it is made by using pipe cutter. The second part is P.V.C. of (50mm) outer diameter, (42.6mm) inner diameter, (1m) length and (3.7mm) thickness. It is insulated by white foam and roll insulation which has (20mm) thickness. Insulation is used to minimize losses to surrounding in minimum value. The test is made by fixing three Thermocouples one on the outer surface of the shell, one on the outer surface of the white foam

and the last in the surrounding temperature. The three temperatures are found (25, 33.7, 36 °C) respectively, as shown in figure (C-2).

4.3.2 Electrical Control Unit.

It hosts the main supply of electrical power for: heater, cooling system and water motors.

4.3.3 Hot Water Vessel.

It is made from iron with volume 0.2m^3 and contains electrical heater with capacity 6000 watt to heat the water as wanted in the work, shown in figure (C-3).

4.3.4 Cold water vessel

It is made from plastic with volume (0.1) m^3 to contain cold water, as shown in figure (C- 4).

4.3.5 Water Pump

Two water pumps are used in this work. They are electrical motors, and they are used to circulate the hot and cold water from vessel to the exchanger and back to vessel in any water flow rate. Specifications of water pump are volumetric flow 10-30LPM, maximum head 30m and horsepower 0.5 kW, shown in figure (C-5).

4.3.6 Water Valves

Four valves were used two for cold side and two for hot side, one connected with flow meter and the other work as by pass to control the amount of water flow needed in the work, as shown in figure (C-6).

4.3.7 Flow Meter

Two flow meters were used to measure the cold and hot water flow rates interring the heat exchanger, as shown in figure (C-7). The flow meter working range is from (2-18) LPM. The flow meter were calibrated, shown in figure (C-12).

4.3.8 Cooling Unit

This unit contains a compressor and a radiator with fan working with R134a gas with capacity 1ton of refrigeration (outdoor split unit). It is used to cool water in the vessel using radiator in the water to make cool (indoor radiator split unit), as shown in figure (C-8).

4.3.9 Thermocouples

To gauge temperature of inlet and outlet fluid (cold and hot) four thermocouples types (k) were used. Thermocouples were distributed in inlet and outlet water of exchanger, it's fixed in plastic pipe by making holes until (1mm) and material was put to prevent leakage (Epo putty two part type adhesive), as shown in figure (C-9).

4.3.9.1 Thermocouples calibrations

Thermocouples have been calibrated by the Central Organization for Standard and Quality Control according to COSQC working instruction (W1-06-01-03). The calibration results are listed in photograph (C-13). Table (4.1) and figure (4-3) show the result of the calibration.

Table (4.1) Calibration Results of thermocouples

Set	Actual value °C	Indicate value °C	Correlation value °C
25	25.1408	25	0.1408
40	40.47	39.9	0.57
50	50.59	49.9	0.697
60	60.75	59.3	1.453

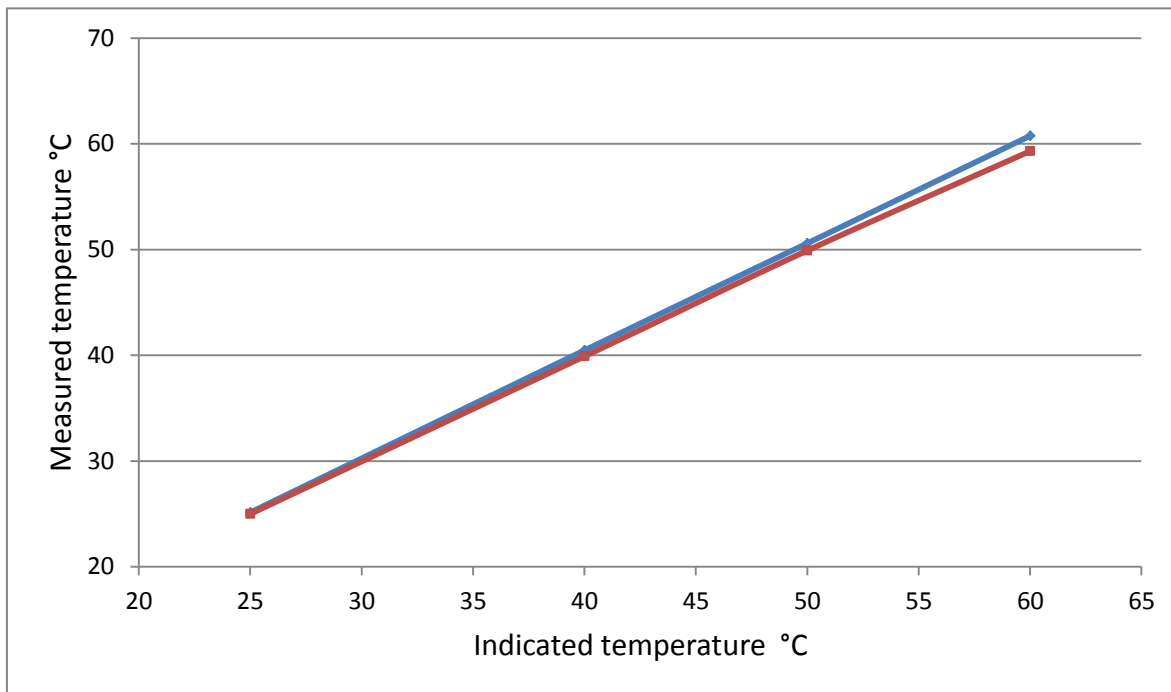


Figure (4-3) The relationship between the measured and indicated values

4.3.10 Data Logger Thermometer

Data logger thermometer type “CENTER 309” four channel’s thermocouples type (k) used to temperature read out. Data logger made by Shenzhen Laesent Technology CO., LTD in Taiwan.

4.4 Manometer

The experimental system contains several parts to enable the work, one of these “Manometer PM-9107” used to measure pressure drop between inlet and outlet points of water along the test section. The manometer working range is (1-7000) mbar made by Lutron Electronic Features, as shown in figure (C-10).

4.5 Fundamentals of Nano Fluids

Heat transfer is the most remarkable process in many manufacturing and consumer output. The originally poor thermal conductivity of the traditional fluids

set a major limit on heat transfer. Scientists and engineers have made great efforts to break this fundamental limit by dispersing millimeter or micrometer sized particles in liquid. However, the major problem with the use of such large particles is the rapid settling of these particles in fluids. Because extended surface technology has already been adapted to its limits in the design of thermal management systems, technologies with the potential to improve a fluid's thermal properties are of great interest once again[3].

The idea and emersion of Nano fluids is related immediately to miniaturization and nanotechnology. The connotation of Nano fluids is the idea that particle volume of main importance in developing stable and strongly conductive Nano fluids.

Milestones in thermal conductivity measurement:

1. Nano fluids have high temperature conductivity with respect to the base fluid. Water-based Nano fluids containing AL_2O_3 nanoparticles show a (2to4) fold rise in (k) enhancement during a small temperature zone.
2. The size of hanging Nano-particles is important to thermal properties of Nano fluids.

In the present work (AL_2O_3) was used with Nanoparticle diameter of 20nm as shown in figure (C-11)

4.6 Thermal Conductivity of Nano Fluids

4.6.1 Volume Fraction

Thermal conductivity is one of the important properties and assistance to the process of heat transfer. Thermal conductivity at temperature range from (30-80) °C for different concentrations of AL_2O_3 -water Nano fluid vary in the range from 0.2% to 1.0%. The thermal conductivity of Nano fluids is enhanced with increased nanoparticle volume fraction with rise in fluid temperature. In

volume fraction of 0.8% and 1.0%, thermal conductivity gets enhanced by 44% to 55% when temperature is increased to (80°C) as shown in photograph (4-4)[34].

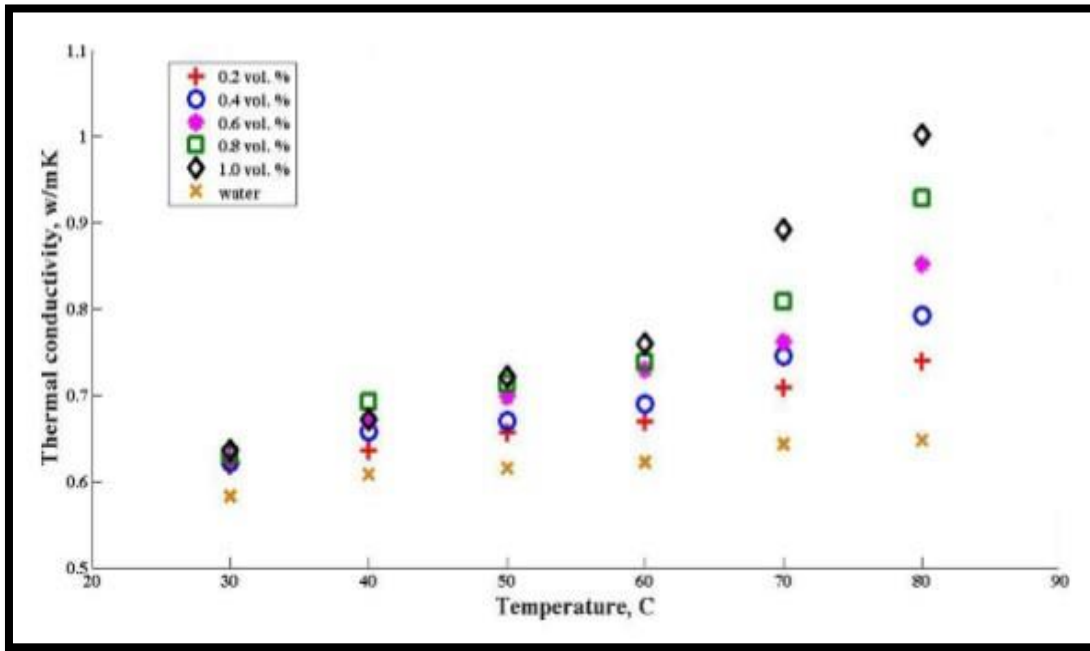


Figure (4-4) enhanced in thermal conductivity by Nano fluid [34]

4.6.2 Thermal Conductivity of Nano Fluid

To find the best value of thermal conductivity different equations were used:

Maxwell and **Garnett** equation is [46]:

$$\frac{k_{nf}}{k_{bf}} = \frac{(1-\varphi)(k_p + 2k_{bf}) + 3\varphi k_p}{(1-\varphi)(k_p + 2k_{bf}) + 3\varphi k_{bf}} \quad (4.1)$$

Yi and **Choi** formed a correction for Maxwell equation and called this new finding as modified Maxwell equation [47]:

$$\frac{k_{nf}}{k_{bf}} = \frac{k_p + 2k_{bf} + 2.662(k_p - k_{bf})\varphi}{k_p + 2k_{bf} - 1.331(k_p - k_{bf})\varphi} \quad (4.2)$$

Buongiorno equation [48]:

$$k_{nf} = k_{bf}(1 + 7.47\varphi) \quad (4.3)$$

When: *nf* : Nano-fluid

pf : base fluid

φ : volume fraction

In the present work equation (4.3) was used to calculate the thermal conductivity because it gives highest value as shown in the table (4.2) and figure (4-5).

Table (4.2) value of thermal conductivity of Nano fluid for different equation

φ	k particle W/m. $^{\circ}$ C	T $^{\circ}$ C	Base fluid W/m. $^{\circ}$ C	Equ.(4.1) W/m. $^{\circ}$ C	Equ.(4.2) W/m. $^{\circ}$ C	Equ.(4.3) W/m. $^{\circ}$ C
0.8	40	20	0.60220	0.61612	0.62078	0.63818
		21	0.60380	0.61776	0.62243	0.63988
		22	0.60560	0.61960	0.62428	0.64179
		23	0.60739	0.62143	0.62613	0.64369
		24	0.60919	0.62327	0.62798	0.64560
		25	0.61099	0.62511	0.62983	0.64750
		26	0.61279	0.62695	0.63168	0.64941
		27	0.61453	0.62873	0.63348	0.65125
		28	0.61615	0.63039	0.63515	0.65297
		29	0.61777	0.63204	0.63681	0.65469
		30	0.61940	0.63370	0.63848	0.65641

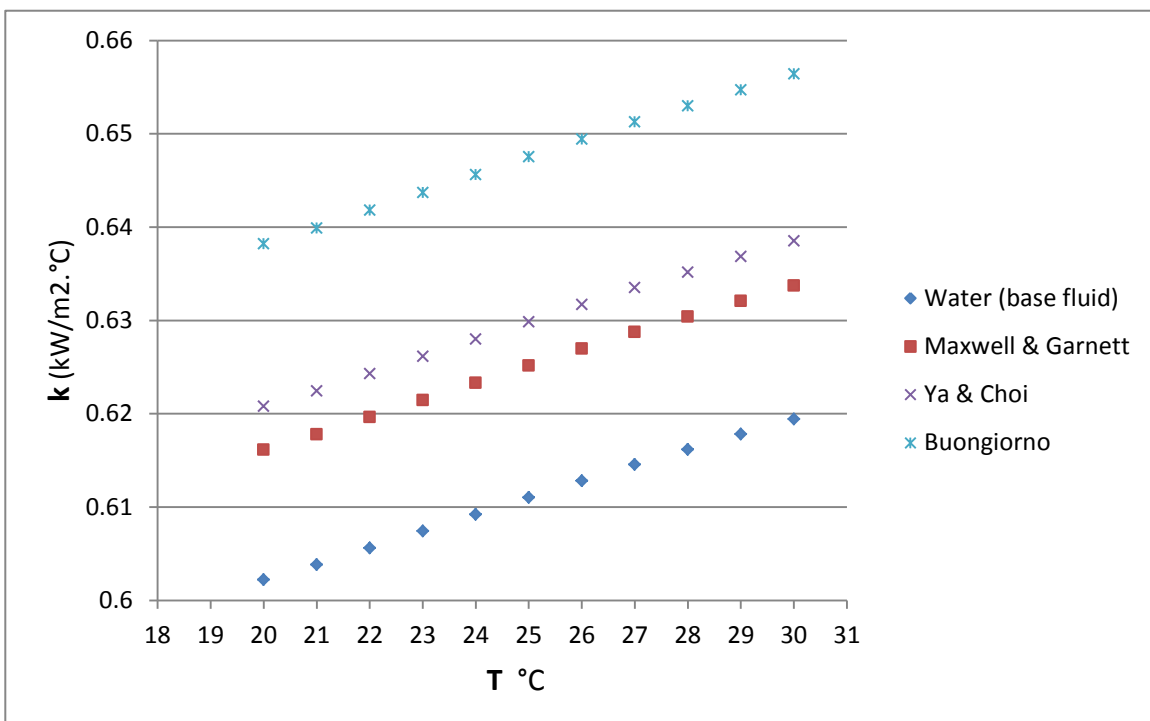


Figure (4-5) value of thermal conductivity of Nano fluid for different equation

4.7 Theories and Equations

This part involves all the equations and mathematic relations which are employed in this study to reach the required solution.

4.7.1 Assumptions of Energy Balance Equation

Energy balance is to calculate the rate of heat transfer rate by following assumptions [3]:

1. No heat exchange between the fluid and the surroundings (adiabatic flow).
2. Neglect the axial conduction in the tubes.
3. At the average temperature value of inlet and outlet temperature the fluid specific heats of fluid are constant.
4. Neglect the change in potential and kinetic energy.
5. The overall heat transfer coefficient is constant.
6. Flow is steady.

4.8 Preparation of Nano Fluids

“Nano fluid can be defined as a fluid in which solid particles with the sizes under 100 nm are suspended and dispersed uniformly in a fluid. The base fluid used is the same as traditional heat transfer fluids in this work used water [49].

4.9 Base fluid and Nanoparticles

During the present work, (Al_2O_3) nanoparticles have been used and base fluid used is water. The specifications of (Al_2O_3) nanoparticles are shown in table (4.3) [50].

Table (4.3) specification of Nano particles

Type	D (nm)	ρ (kg/m ³)	K (W/m.°C)	C_p (kJ/kg.°C)
Al_2O_3	20	3970	40	765

4.10 Using Ultrasonic Vibration Device

The ultrasonic device is used show in (C-14) to mix the nanoparticle of Al_2O_3 with the base fluid (water); in this work water is used as base fluid. The mixing work is done according to the following relation [51]:

$$\varphi\% = \frac{\left(\frac{m_p}{\rho_p}\right)}{\left(\frac{m_p}{\rho_p}\right) + \left(\frac{m_{bf}}{\rho_{bf}}\right)} \quad (4.4)$$

From the above equation, by fixing the water value at (5litter) in all the tests the value of nanoparticle needed to be mixed is calculated. The volume concentration used was (0.8%) [34], of concentration is (160.6 gram). The ultrasonic vibration device was switched for 14hours. To get the best Nano fluid mixture with no sedimentation or agglomeration, many tests were made during the work [52].

4.11 Experiment Set up and Operation Procedure

This work is completed according to the following procedure:

1. Water level was checked first to be in the required level.
2. All connecting wires (thermocouples, and AC power cable) and other necessary electrical parts were checked.
3. Check all connecting pipeline in the system to avoid any leakage.
4. Check connecting pipeline of the manometer to read the pressure drop.
5. Start the data logger thermometer and select time of reading temperature (time select is 30 sec.)
6. Start the pressure manometer.
7. Supply AC power to cooling system unit to (1-2) hour to get water at temperature (25°C).
8. Supply AC power to electrical heater to (1-6) hour to get water at temperature (40, 50 and 60°C).

9. Supply AC power to the electrical pumps (hot and cold) then change the valve to gate the value of water flow rate in cold and hot line by change and check the flow meters.
10. Start to record temperature and pressure drop after (45min.) when the system is steady state. And the experimental works in each case continue to 30min.

Repeat all steps for experimental work for all test sections. The above procedure was repeated for all cases (smooth pipe, two corrugated pipes) with and without Nano fluid. All test repeat three time to make sure the results.

CHAPTER FIVE

RESULTS AND DISCUSSION

5.1 Introduction

This chapter includes the results obtained experimentally and numerically. The experimental and numerical data more obtained for smooth pipe, two types of corrugated pipes with and without Nano fluids

The experimental work includes the investigation of effectiveness of the corrugated tubes with $z/d=1, 0.5$ as well as with and without Nano fluid in heat exchanger.

Heat transfer rate is calculated for the inner copper tube has been with and without corrugated pipe and the result of adding nanoparticles AL_2O_3 in the cold side and change volumetric flow rate of the hot side, then comparison between them. Then derive empirical equations to describe the results of this study.

The numerical works was a 3D simulation of a heat exchanger. The simulation was carried out in smooth tube, corrugated tubes with and without Nano fluid in the cold side. Turbulent and laminar flow have been provided for inner and outer sides of pipe respectively. The simulation was done by $k-\varepsilon$ (RNG) model.

Different parameters were studied numerically to check the enhancement in heat exchanger like Nano fluid, hot volumetric flow rate =1, 2, 3, 4 and 5 LPM, cold volumetric flow rate =3, 4, 5, 6 and 7 LPM, hot water temperature and corrugated ratio. For the review and discussion of some diagrammatic figures and all other results see in appendix [D] and the other percentage for all work see in appendix [E]. The calculation of the uncertainty of experimental results show in appendix [F].

5.2 Effect of the Hot Water Volumetric Flow Rate on Temperature Difference in Tube-side

Figures (5-1a) to (5-3a) clarify the relation between change of hot water volumetric flow rate for smooth and two type of corrugated tubes $z/d=1, 0.5$ for different hot temperature, When you install the value of cold volumetric flow rate water. It was found that increase in temperature difference by change the tube geometry and decrease in temperature difference by increase the hot volumetric flow rate water. This change attributed to the hot water that still has heat when leave the tube because the time to exchange the heat is less. The enhancement range of temperature difference for corrugated tube are (14.94%, 43.2%) for corrugated tube $z/d=1, 0.5$ respectively in respect to smooth tube at temperature 60°C and cold volumetric flow rate 7LPM.

5.3 Effect of Hot Water Volumetric Flow Rate on Temperature Difference for Shell-side

Figures (5-1b) to (5-3b) clarify the relation between change hot volumetric flow rate and cold temperature difference cold pressure drop for smooth and two corrugated tubes $z/d=1$ and 0.5 for different hot water temperatures. When you install the value of cold volumetric flow rate at 3LPM, it shows a decrease in the temperature difference due to the change of tube geometry. This temperature is difference increases the hot volumetric flow rate. This change due to the cold water stick on for long time to leave the shell-tube respect to hot water and the new hot water inter the tube have high temperature. The enhancement of temperature difference for corrugated tube are (52.14%, 29.34%) for corrugated tube $z/d=1, 0.5$ respectively respect to smooth tube at temperature 40°C and cold volumetric flow rate 7LPM.

5.4 Effect of Cold Volumetric Flow Rate on Temperature Difference

Figures (5-4a) to (5-6a) show the increase in hot temperature difference with increase cold volumetric flow rate, because water in the shell inter with low

temperature and the large different in temperature lead to exchange more heat from hot water. Figures (5-4b) to (5-6b) show in used corrugated tube $z/d=1$ increase in cold temperature difference in volumetric flow rate 3LPM and don't see large different at volumetric flow rate 7LPM, but in use corrugated tube $z/d=0.5$ show the cold temperature different increase in volumetric flow rate 7LPM and don't see large change in volumetric flow rate 3LPM.

5.5 Effect of Hot Water Volumetric Flow Rate on Heat Dissipation for Tube and Shell- sides

Figures (5-7) to (5-9) illustrate the relation between change hot volumetric flow rate and heat dissipation in hot and cold side for smooth and two corrugated tubes $z/d=1,0.5$, for different hot temperature 40°C , 50°C and 60°C . It can be appears from this figures the heat dissipation of two corrugated tubes is higher than of smooth tube. The enhancement happened due to increase in outer surface area that happened by made grooves. Then can see the enhancement in heat dissipation reach to max value for corrugated $z/d=1$ and be more in corrugated $z/d=0.5$. The enhancement percentage are (15.29%, 45.65%) for corrugated $z/d=1, 0.5$ respectively with respect to smooth tube for tube side, the percentage are (52.14%, 10.34%) for shell side at temperature 40°C and cold volumetric flow rate 7LPM.

5.6 Effect of Cold Water Volumetric Flow Rate on Heat Dissipation for Tube and Shell-sides

The relation between change of cold volumetric flow rate water and heat dissipation in hot and cold side for smooth and two corrugated tubes $z/d=1,0.5$, show in figures (5-10) to (5-12). The heat dissipation in hot side increase by increase cold water volumetric flow rate and change tube from smooth to corrugated, figures (5-10a) to (5-12a)show use corrugated tube $z/d=0.5$ give large heat dissipation in volumetric flow rate 7LPM. Figures (5-10b) to (5-12b) show increase in heat dissipation in volumetric flow rate 7LPM more than flow

rate 3LPM when use corrugated $z/d=1$ and 0.5. The heat dissipation have large change at use high volumetric flow rate and don't have large change in use low volumetric flow rate.

5.7 Effect of Hot Water Volumetric Flow Rate on Overall Heat Transfer Coefficient for Tube and Shell-side

Overall heat transfer coefficient is the capacity of the conductive and the convective resistance to the heat transfer. It is usually used to observe the heat transfer in the exchange. Figures (5-13a) to (5-15a) explain the relation between overall heat transfer coefficient in tube side and hot volumetric flow rate. The overall heat transfer coefficient increase when install the value of cold volumetric flow rate at 3LPM. The overall heat transfer coefficient increasing by change the tube geometry and be higher in the corrugated tube $z/d=1$. The overall heat transfer coefficient for tube side increase by (22.36%, 47.89%) by change the tube geometry from smooth to corrugated $z/d=1$ and $z/d=0.5$ respectively at temperature 40°C and cold volumetric flow rate 7LPM.

Figures (5-13b) to (5-15b) show the increase in overall heat transfer coefficient in the shell side in percentage (23.46%, 49.36%). The enhancement of overall heat transfer coefficient in tube and shell sides increase by increase the heat dissipation at temperature 40°C and cold volumetric flow rate 7LPM.

5.8 Effect of Cold Water Volumetric Flow Rate on Overall Heat Transfer Coefficient for Tube and Shell-Sides

The change of cold water volumetric flow rate show in figure (5-16) to (5-18). The overall heat transfer coefficient in tube side, from figures (5-16a) to (5-18a) increase by use corrugated tube $z/d=1$ and 0.5 respect to smooth tube and the increase at (54.54%, 55.72%) at temperature 40°C and cold volumetric flow rate 7LPM.

From figure (5-16b) and (5-18b) the overall heat transfer coefficient for shell side increase at cold flow rate 7LPM, the enhancement percentage are (55.66%, 58.91%) in shell side by using two corrugated tubes at temperature 40°C and cold volumetric flow rate 7LPM.

5.9 Effect of Hot Water Volumetric Flow Rate on Nusselt Number for Tube-Side

The variation of hot volumetric flow rate in tube side with Nusselt number for different hot temperature depicts in table (5.1). The Nusselt number increases by increasing the hot volumetric flow rate and change the hot temperature. This is due to the actuality that Nusselt number is a function of heat transfer coefficient. The hot side doesn't have noticeable change because the properties of water don't have large change and the inner tube shape still smooth.

Table (5.1) Nusselt Number in Tube-side

\dot{V}_c	\dot{V}_h	Nu _h at 40°C			Nu _h at 50°C			Nu _h at 60°C				
		L/M	L/M	smooth	z/d=1	z/d=0.5	smooth	z/d=1	z/d=0.5	smooth	z/d=1	z/d=0.5
3	1	14.73	14.75	14.8	15.75	15.81	15.86	16.76	16.86	16.98		
3	2	25.67	25.75	25.78	27.49	27.54	27.67	29.31	29.33	29.65		
3	3	35.54	35.62	35.69	38.09	38.17	38.37	40.63	40.69	41.07		
3	4	44.79	44.88	44.97	48.07	48.12	48.38	51.25	51.33	51.82		
3	5	53.65	53.76	53.78	57.63	57.63	57.9	61.46	61.38	62.03		
4	1	14.68	14.8	14.74	15.69	15.8	15.85	16.74	16.83	16.99		
4	2	25.63	25.73	25.73	27.41	27.63	27.67	29.17	29.4	29.6		
4	3	35.5	35.65	35.68	38.01	38.27	38.4	40.52	40.8	41.09		
4	4	44.74	44.92	44.95	48	48.25	49.42	51.22	51.49	51.83		
4	5	53.63	53.74	53.87	57.55	57.77	57.94	61.44	61.66	61.97		
5	1	14.64	14.72	14.75	15.66	15.75	15.85	16.71	16.78	16.94		
5	2	25.58	25.64	25.74	27.35	27.44	27.67	29.16	29.23	29.54		
5	3	35.45	35.52	35.67	37.96	38.01	39.14	40.51	40.51	40.96		
5	4	44.7	44.75	44.937	47.92	47.91	49.36	51.15	51.08	51.69		
5	5	53.52	53.57	53.76	57.4	57.31	59.08	61.29	61.08	61.88		
6	1	14.63	14.73	14.75	15.63	15.77	15.81	16.64	16.81	16.9		
6	2	25.56	25.69	25.75	27.33	27.54	27.65	29.06	29.33	29.49		
6	3	35.44	35.59	35.67	37.96	38.17	38.34	40.31	40.72	40.9		
6	4	44.68	44.84	44.937	47.89	48.14	48.33	50.9	51.36	51.58		
6	5	53.5	53.67	53.78	57.36	57.64	57.83	61.06	61.46	61.72		
7	1	14.68	14.71	14.74	15.64	15.76	15.81	16.65	16.82	16.89		
7	2	25.59	25.76	25.72	27.31	27.5	27.621	29.1	29.36	29.46		

7	3	35.47	35.55	35.65	37.87	38.14	39.05	40.37	40.69	40.87
7	4	44.7	44.79	44.91	47.8	48.09	49.23	50.95	51.31	51.54
7	5	53.52	53.63	53.65	57.21	57.53	57.66	61.04	61.42	61.7

5.10 Effect of Hot Water Volumetric Flow Rate on Nusselt Number for Shell-Side

Figures (5-19a) to (5-21a) depict the variation of hot volumetric flow rate in shell side with Nusselt number for different hot temperature and at cold volumetric flow rate 3LPM. The Nusselt number increases by change the tube geometry from smooth to corrugated $z/d=1$ and more than for $z/d=0.5$. The increase percentages are (37.81%, 39.9%) for corrugated $z/d=1, 0.5$ respectively. It could be concluded that the increasing in Nusselt numbers due to increasing in the surface area which due to increases the heat transfer.

5.11 Effect of Cold Water Volumetric Flow Rate on Nusselt Number for Shell Side

The effect of cold volumetric flow rate on the Nu is shown in figures (5-19b) to (5-21b). The large effect can be seen in the shell side, due to change in all water properties for instance velocity and Reynold's number. The enhancement in Nu ranging between (66.1%, 68.32%) for corrugated tubes $z/d=1, 0.5$ respectively at temperature 40°C.

5.12 Effect of Hot Water Volumetric Flow Rate on Friction Factors

The relation between hot volumetric flow rate and friction factors in inner side of the tube is shown in figures (5-22a) to (5-24a). The increase of friction factor value is reaches to max and decrease by increase the water volumetric flow rate due to the change from laminar in the inlet to turbulent. The value of friction factors nearly constant and not affected by change the tube geometry because the inner tube still smooth and the Reynolds number doesn't have large change. From figure (5-22b) to (5-24b). It is noted that the friction factor decrease by increase the flow rate and change tube geometry because the

boundary layer doesn't remain for long distance and effect by corrugated pitch, because grooves in the outer tube surface lead to make suction in the boundary layer then reduced momentum and therefore less thickness.

5.13 Effect of Cold Water Volumetric Flow Rate on the Friction Factors

The friction factor in tube side does not show any change but in the cold side occurs decrease with increases the cold volumetric flow rate as shown in figure (5-22) to (5-27). The percentage fraction factor in cold side is (70.34%, 64.65%) for corrugated tube $z/d=1, 0.5$ respectively at temperature 40°C and cold water volumetric flow rate 7LPM.

5.14 Effect of Water Volumetric Flow Rate and Tube Geometry on Pressure Drop in Tube-side

Table (5.2) shows the pressure drop behavior in coupling with friction factor because the drop in pressure decreases and increase in directly proportional with friction factor. The pressure drop indicates change inversely with increase in cold volumetric flow rate and change the tube geometry from smooth to two corrugated tubes.

Table (5.2) pressure drop in tube-side

\dot{V}_c	\dot{V}_h	Nu _h at 40°C			Nu _h at 50°C			Nu _h at 60°C			
		L/M	smooth	$z/d=1$	$z/d=0.5$	smooth	$z/d=1$	$z/d=0.5$	smooth	$z/d=1$	$z/d=0.5$
			Pa	Pa	Pa	Pa	Pa	Pa	Pa	Pa	Pa
3	1	5.91	2.69	2.18	5.73	2.05	1.55	5.55	2.01	1.08	
3	2	9.53	8.34	7.46	12.81	8.03	5.58	12.15	7.9	3.7	
3	3	20.82	18.69	15.4	20.9	17.99	9.76	19.55	17.64	5.55	
3	4	42.79	33.1	24.88	39.99	31.49	14.88	37.33	30.86	7.41	
3	5	55.18	51.32	34.99	50.21	48.82	15.5	50.67	48.01	7.71	
4	1	6.22	1.96	1.56	5.42	1.94	1.16	4.63	1.88	0.85	
4	2	9.26	7.82	5.6	11.7	7.72	4.53	10.27	7.41	3.21	
4	3	19.16	17.57	11.9	22.41	17.29	9.76	17.47	16.59	7.08	
4	4	35.78	31.22	18.41	33.43	30.65	15.87	31.67	29.23	11.6	
4	5	58.87	48.58	26.43	50.19	47.66	23.24	48.66	45.55	16.97	
5	1	6.22	1.86	1.43	5.42	1.78	1.39	4.63	1.73	1.29	
5	2	9.26	7.42	5.6	10.08	7.04	5.39	17.28	6.79	5.12	

5	3	18.78	16.69	12.46	17.79	15.81	11.86	26.09	14.86	11.25
5	4	33.08	29.66	21.65	31.33	28	20.83	33.75	26.17	19.75
5	5	50.17	46.32	33.44	47.36	43.71	32.16	47.1	40.11	30.09
6	1	6.07	1.78	1.37	4.96	1.72	1.35	3.86	1.65	1.31
6	2	23.02	6.85	5.48	18.6	6.64	5.33	14.19	6.49	5.22
6	3	15.38	14.98	12.28	15.05	14.51	11.93	17.76	14.03	11.68
6	4	27.59	26.5	21.8	26.46	25.55	21.1	26.89	24.79	20.59
6	5	43.28	41.25	33.95	42.96	39.52	32.74	41.69	38.62	31.82
7	1	6.22	1.68	1.33	4.96	1.65	1.09	3.85	1.61	0.93
7	2	8.64	6.66	5.29	9.22	6.59	4.25	14.19	6.39	3.61
7	3	18.99	14.88	11.88	18.91	14.76	9.4	21.77	14.35	7.97
7	4	29.62	26.38	21.11	27.68	26.14	16.61	36.89	25.44	14.07
7	5	48.86	40.98	32.88	42.98	40.77	24.79	41.54	39.51	20.83

5.15 Effect of Water Volumetric Flow Rate and Tube Geometry on Pressure Drop in Shell-side

Figure (5-28) to (5-30) shows the effect of hot volumetric flow rate on the pressure drop for different temperature and different geometry. The pressure drop change inversely with increase in hot volumetric flow rate and change tube geometry. The maximum value for pressure drop at smooth tube for cold volumetric flow rate =3 and 7 LPM, but the corrugated tube reduce this value in general for cold volumetric flow rate 3 LPM but in 7 LPM the corrugated tube $z/d=1$ best than $z/d=0.5$, this due to the turbulent flow bring forth eddy connected with other generated the large swirl working to increase energy losses and reduce the amount of heat transfer as a result of increasing the number of grooves on the surface of the outer tube. The percentage enhancement for corrugated tubes respect to smooth tube is (88.34%, 83.44%) at temperature 40°C.

5.16 Effect of Water Volumetric Flow Rate and Tube Geometry on Number of Transfer Unit and Effectiveness (NTU)

Heat transfer effectiveness is the ratio of the actual heat transfer to the maximum possible heat that can be transferred. The relations between the effectiveness and NTU with the different volumetric flow rate are shown in

figure (5-31) to (5-36). These figures show that the effectiveness increases with increasing NTU, as well as they show for the volumetric flow rate 7LPM and corrugated tube $z/d=0.5$ give the higher effectiveness than for 3LPM and smooth tube. This behavior attributed to the effectiveness increasingly being adopted on increasing heat transfer coefficient which increases directly proportional with volumetric flow rate and different tube geometry. The percentage enhancement for corrugated tubes respect to smooth tube is (50.68%, 55.18%) at temperature 40°C.

5.17 The Performance of Heat Exchanger with Nano fluid

Performance of heat exchanger with different tubes geometry and Nano fluid has been researched to find the effect of both Nano fluid and geometry on heat transfer enhancement. The thermal performance of heat exchanger with Nano fluid for hot volumetric flow rate 3LPM and temperature 40°C is shown in the following paragraphs and the flow rate 4, 5, 6 and 7 LPM can be seen in appendix [D].

5.18 Effect of Nano Fluid on Temperature Difference

A comparison of figures (5-37) to (5-39) illustrates the Nano fluid effect on hot temperature difference. These figures clarify the double effect for used corrugated tubes and Nano fluid. The enhancement percentage where used Nano fluid compared with base fluid is 11.70 %. And from figures (5-40) to (5-42) appears the enhancement in cold temperature different by used Nano fluid and tube geometry.

5.19 Effect Nano Fluid on Heat Dissipation

The variation of heat dissipation with different hot volumetric flow rate for Nano fluid is clear in figures (5-43) to (5-45). It is obvious that heat dissipation increases by increasing hot volumetric flow rate and used Nano fluid. Enhancement percentage in heat dissipation by using Nano fluid is (45.17%,

53.41%). Besides, the effect of Nano fluid on cold heat dissipation is shown in figures (5-46) to (5-48).

5.20 Effect of Nano Fluid on Overall Heat Transfer Coefficient

The variation of overall heat transfer coefficient for different hot volumetric flow rate and temperature for water and Nano fluids in hot and cold sides are shown in figures (5-49) to (5-54).The value of this parameter for Nano fluids is higher than that for base fluid. This value increases with rise in the volumetric flow rate and the thermal conductivity rise by Nano particle in base fluid. This study is take attention a lot of designer of the heat exchangers for economic and compactness requests.

5.21 Effect Nano Fluid on Nusselt Number

The value of the Nusselt number in tube side is illustrated in figures (5-55) to (5-57). This form does not show a distinct change in behavior because all the inner boundary condition still constant. Figures (5-58) to (5-60) show the enhancement in Nusselt number in cold side. The major cause of this enhancement is due to the rise in both h and k of Nano fluid.

5.22 Effect Nano Fluid on Effectiveness of Heat Exchanger

The relation between the NTU and effectiveness of base fluid and Nano fluid is clarified in figures (5-61) to (5-63). The effect of adding Nano fluid on performance of corrugated tubes heat exchanger can be seen. It is increase in heat dissipation by adding nanoparticles because the particles which added to the base fluid that leads to increase its thermal conductivity. The enhancement in effectiveness is (21.1%), (33.18%) and (34.99%) for smooth, corrugated $z/d=1$ and corrugated $z/d=0.5$ respectively.

5.23 Numerical Results Analysis

In order to validate numerical simulation, a comparison has done with prior numerical results completed by **Özden Ağra et.al [58]** which presented the

numerical studies for different tubes and covering a vast range of Reynolds from 12000 to 57000, and study the effect of the form geometry and change its parameter as helix angle and effect of corrugated in inner and outer tube surface.

They have performed a numerical study for predicting temperature different, heat dissipation and fraction factor. In general, the good convention of behavior between these results has been found which denote the accepted validation of present simulation.

The goal of numerical studies is to explore the effect of corrugated tube and Nano fluid in the heat transfer rate and temperature different as well as velocity by using ANSYS FLUENT 14.0 software, to solve the continuity and momentum and energy equations as described in chapter 3. The present study included different parameters such as different hot volumetric flow rate change from 1 to 5LPM, its temperature ranging from 40 to 60°C and cold volumetric flow rate are change for change the cold volumetric flow rate from 3 to 7 LPM at inlet cold temperature 25°C. This is done for all tube with and without Nano particles.

The longitudinal section in tubes shown in figure (5-64) illustrated the turbulence flow that occurs in the boundary layer which create from corrugated in outer surface, as well as from figure (5-65) can indicate the change in velocity flow behavior due to the change in the (z/d) and the surface area due to corrugated surface tube. The turbulence in this case assists to increase the heat transfer at volumetric flow rate 3 LPM.

Figures (5-66) to (5-68) cross section at 50cm for test section can indicate the conduct of fluid in tube and shell side and the change that occurs by change the cold water flow rate and tube geometry.

Figures (5-69) to (5-71) cross section at 50cm for test section, show the dual effect of used Nano fluid instead of water in shell side and use of different ratio

of corrugated tube, as well as the potential advantages due to include higher thermal conductivity than the pure fluid .

5.24 Comparison between Experimental and Numerical Results

Experimental results of the test section are validated by numerical 3D simulation created by ANSYS FLUENT 14.0 software as shown in figure (5-72). Good matching observed with difference between results in experimental and numerical works. The difference in the numerical results more than the experimental work results in percentage from (8.97% to 10.05%) for smooth tube, (9.52% to 10.96 %) and (10.68% to 11.35%) for corrugated tubes z/d=1, 0.5 respectively. This difference is the result of the numerical work done in ideal conditions like ambient temperature, mixing in water tank, the speed sense of thermocouples and the human error.

5.25 Experiential Equations

Experiential equation have been derived to control the experimental results of Nusselt number for two corrugated tubes with different ratio z/d=1, 0.5 by using the LAB FIT program. The empirical equations in this study are divided into two groups, the first indicates to Nu without Nano.

Equation (5.1) represents an empirical equation to calculate the Nusselt number for cold side without Nano for all temperature range, all the hot and the cold volumetric flow rates and for all tube geometries.

$$\text{Nu}_c = 449.8 + 1443R_e^{0.1749} \quad (5.1)$$

The second group of empirical equation calculated the Nusselt number for the hot and the cold side with use Nano fluid in the cold side. Equation (5.2) represents an empirical equation to calculate the Nusselt number for cold side with used Nano fluid for all temperature range, all hot and cold flow rates and for all tube geometries.

$$\text{Nu}_{cn} = 621.3 + 1157R_{en}^{0.1096} \quad (5.2)$$

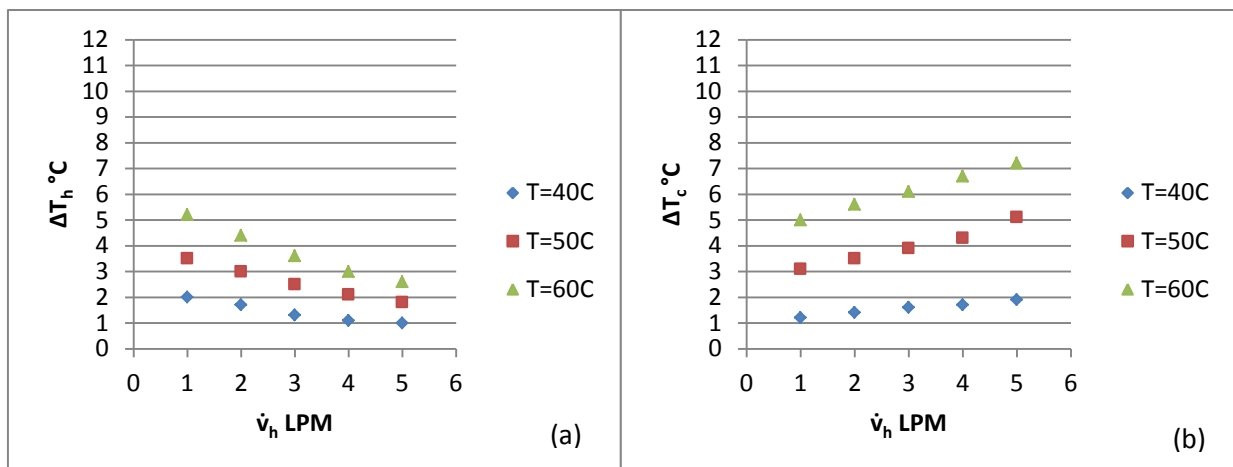


Figure (5-1) Effect of hot volumetric flow rate on temperature difference in smooth tube at $\dot{v}_c = 3$ LPM in different temperatures

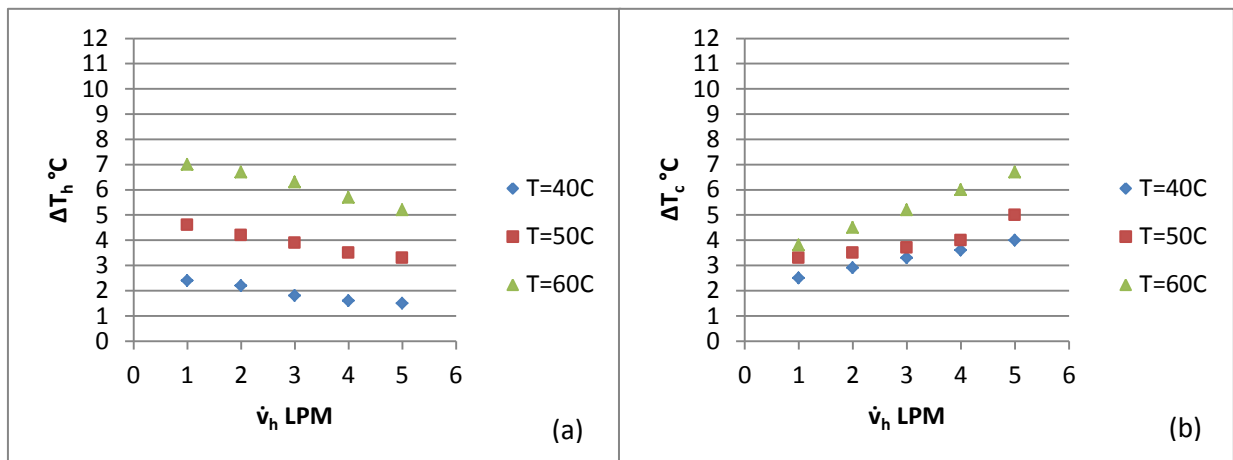


Figure (5-2) Effect of hot mass flow rate on temperature difference in corrugated tube ($z/d = 1$) at $\dot{v}_c = 3$ LPM in different temperatures

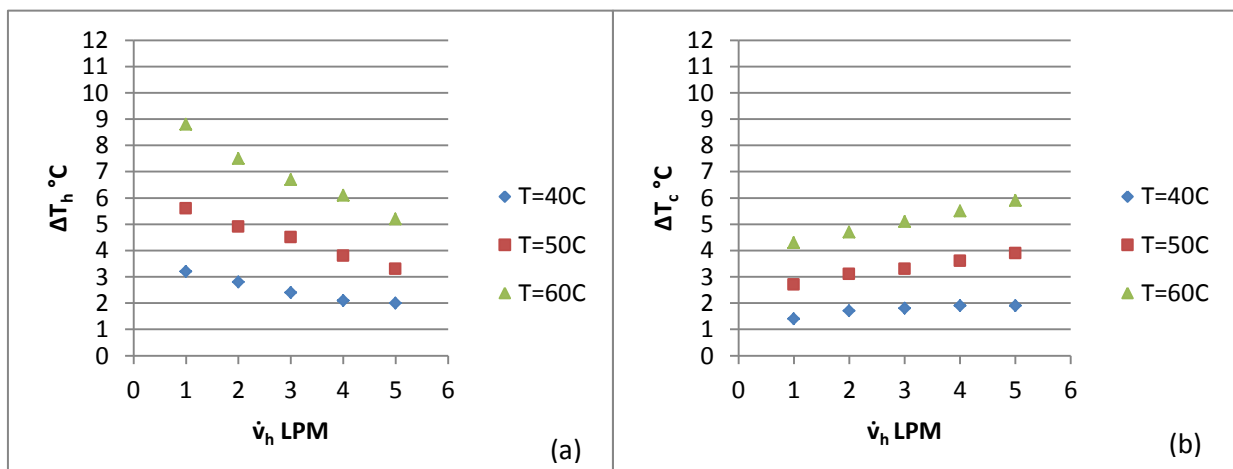


Figure (5-3) Effect of hot mass flow rate on temperature difference in corrugated tube ($z/d = 0.5$) at $\dot{v}_c = 3$ LPM in different temperatures

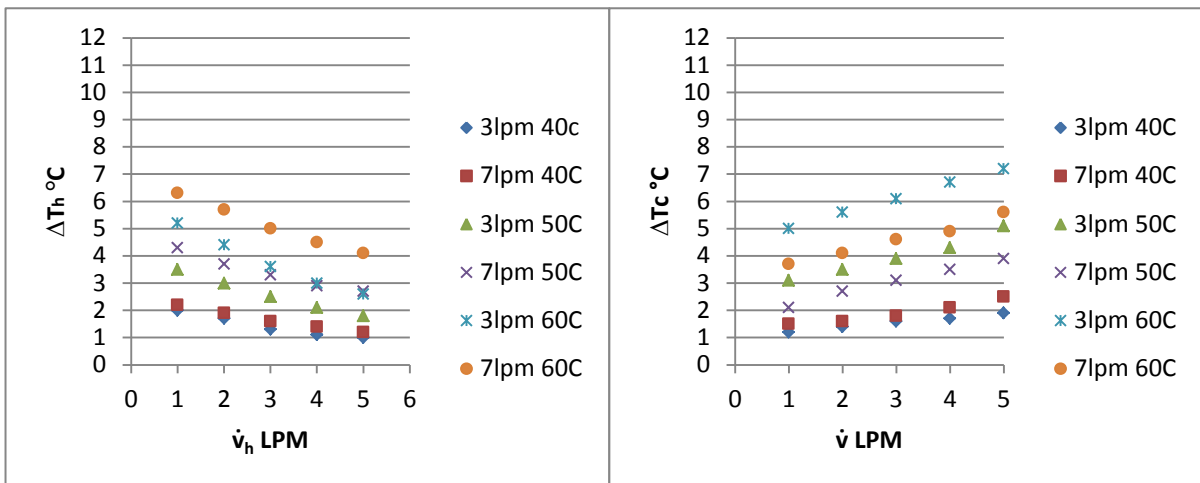
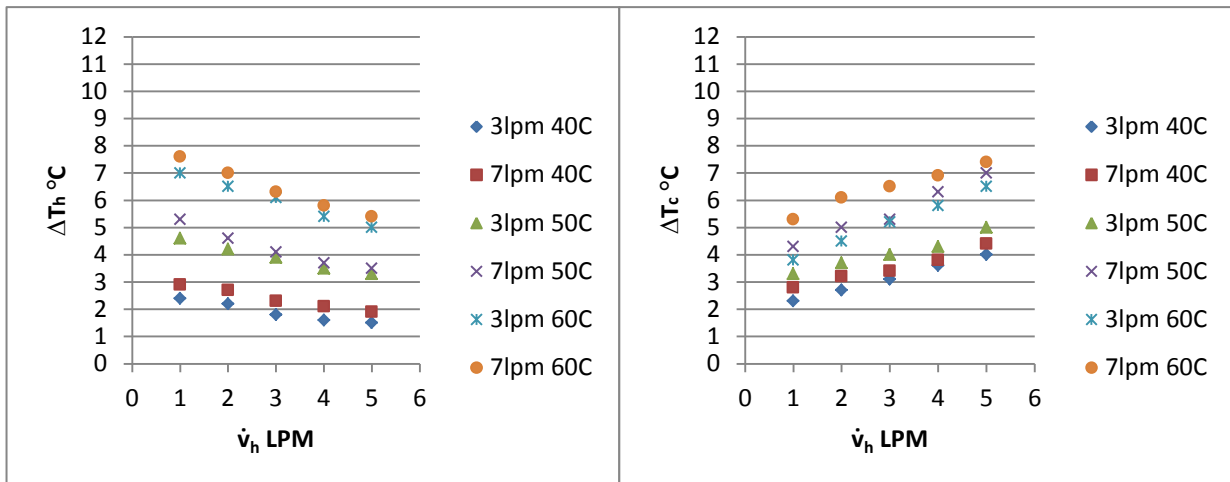
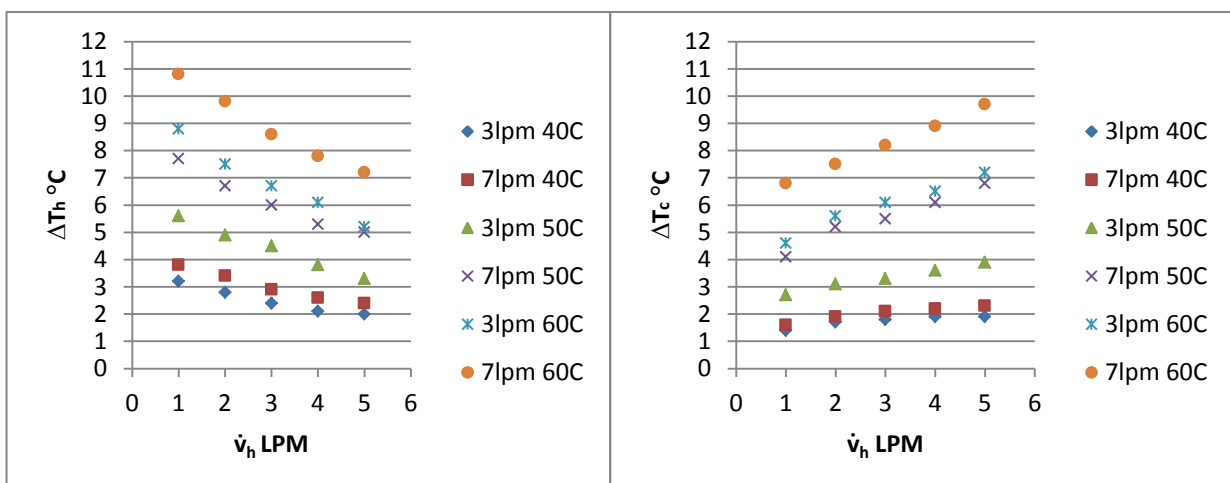


Figure (5-4) Effect of cold volumetric flow rate on temperature difference in smooth tube

Figure (5-5) Effect of cold volumetric flow rate on temperature difference in corrugated tube ($z/d=1$)Figure (5-6) Effect of cold volumetric flow rate on temperature difference in corrugated tube ($z/d=0.5$)

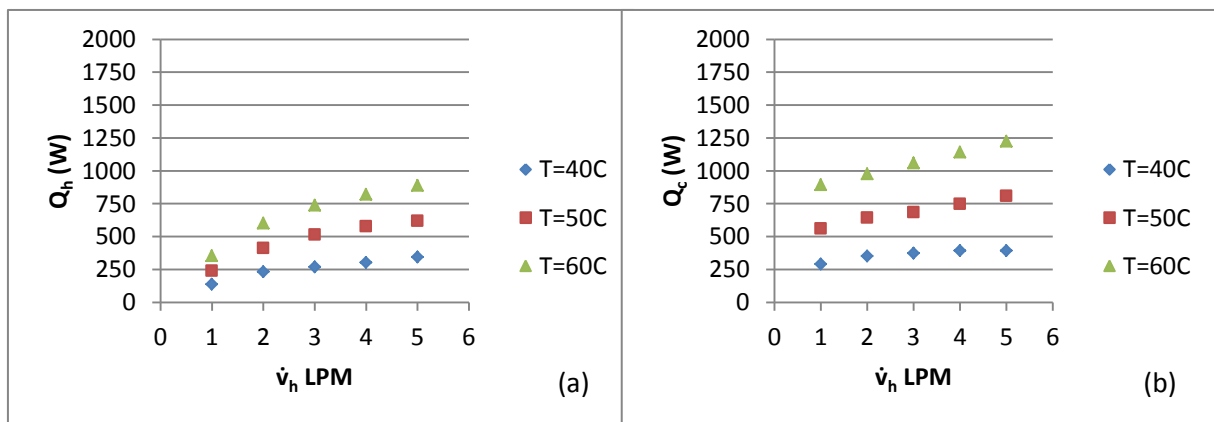


Figure (5-7) Effect of hot mass flow rate on heat dissipation in smooth tube at $\dot{v}_c=3$ LPM in different temperatures

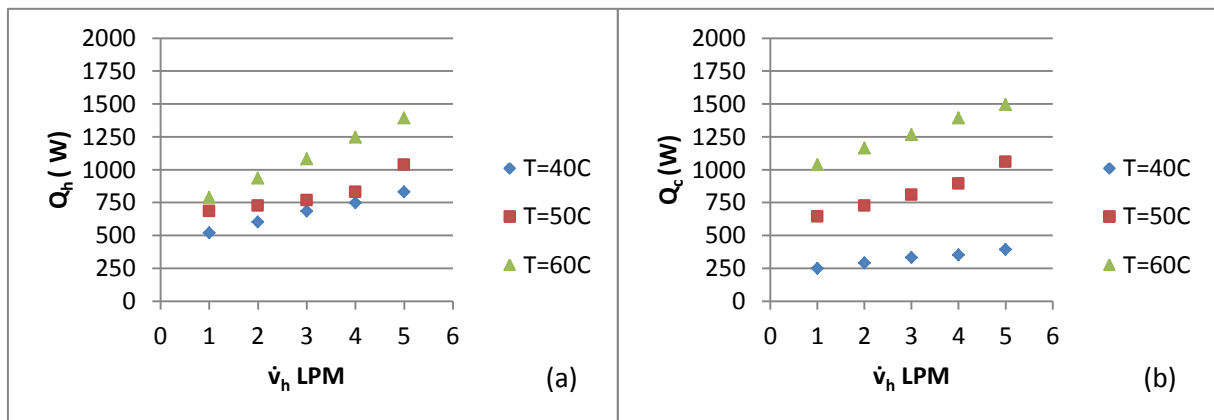


Figure (5-8) Effect of hot mass flow rate on heat dissipation in corrugated tube ($z/d=1$) at $\dot{v}_c=3$ LPM in different temperatures

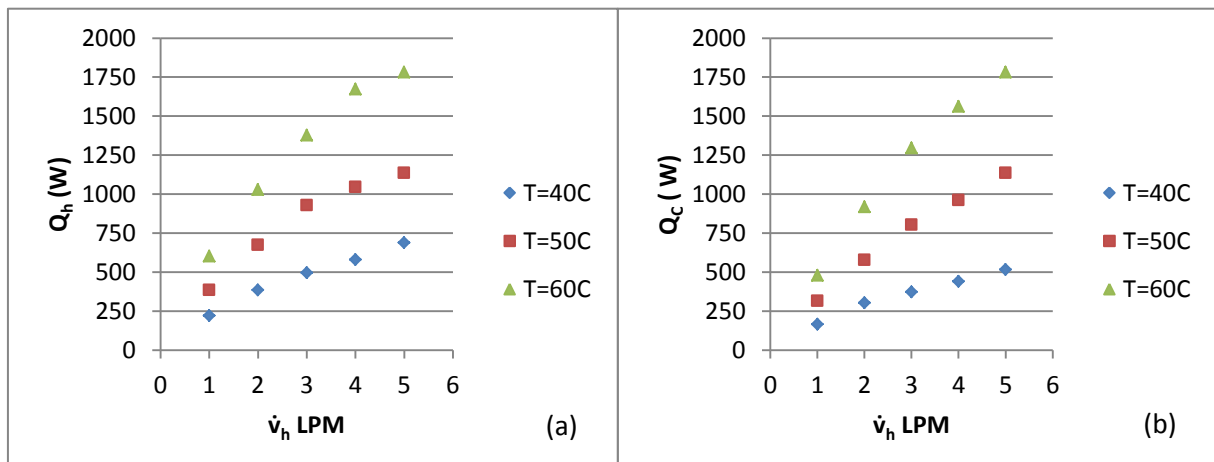


Figure (5-9) Effect of hot mass flow rate on heat dissipation in corrugated tube ($z/d=0.5$) at $\dot{v}_c=3$ LPM in different temperatures

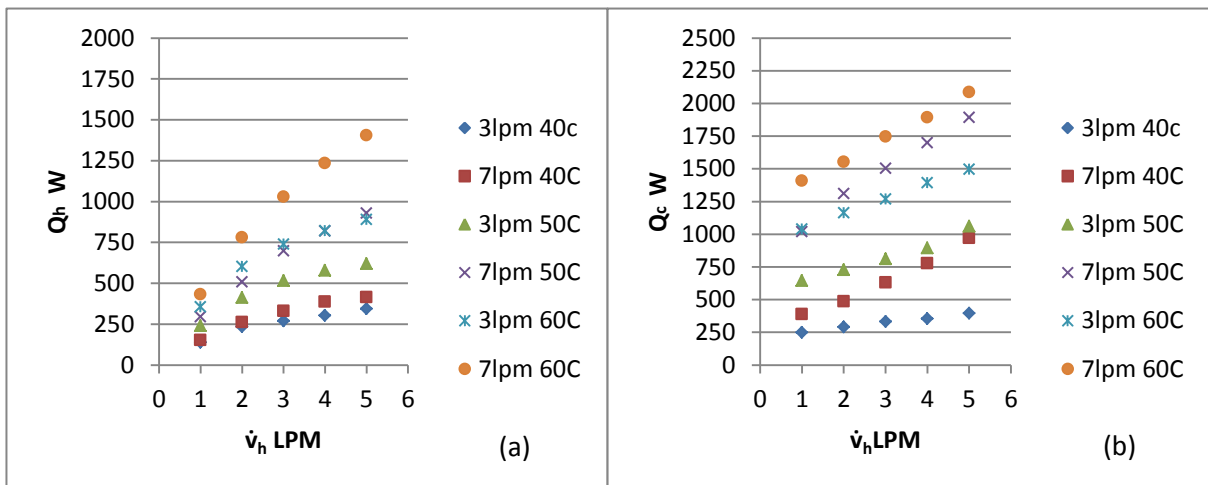
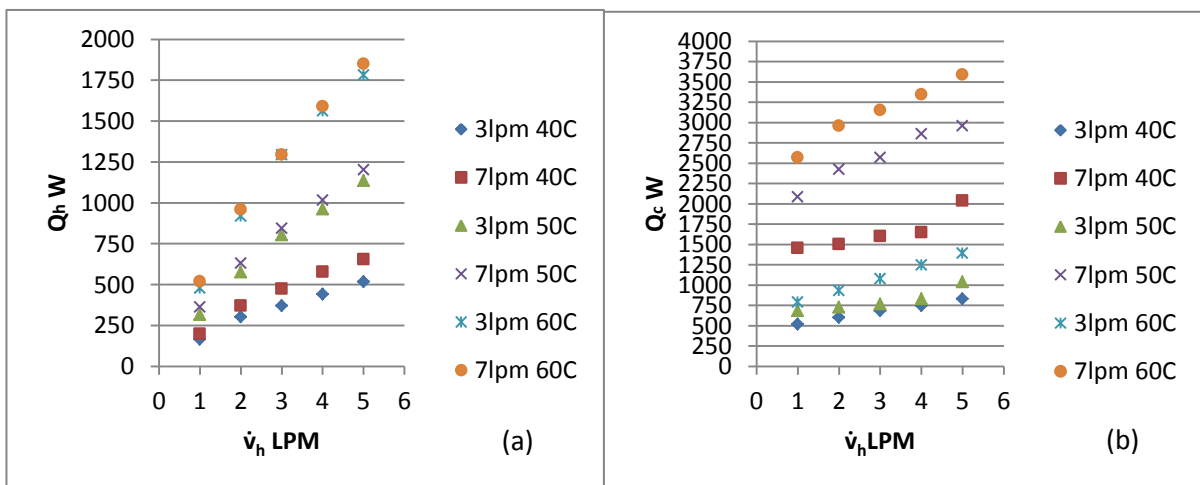
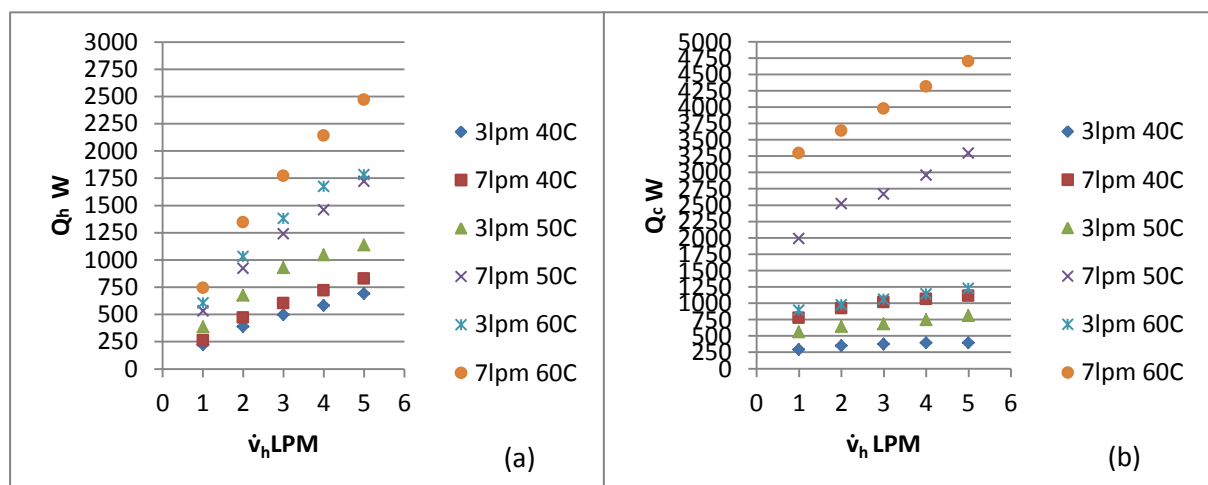


Figure (5-10) Effect of cold volumetric flow rate on heat dissipation in smooth tube

Figure (5-11) Effect of cold volumetric flow rate on heat dissipation in corrugated tube ($z/d=1$)Figure (5-12) Effect of cold volumetric flow rate on heat dissipation in corrugated tube ($z/d=0.5$)

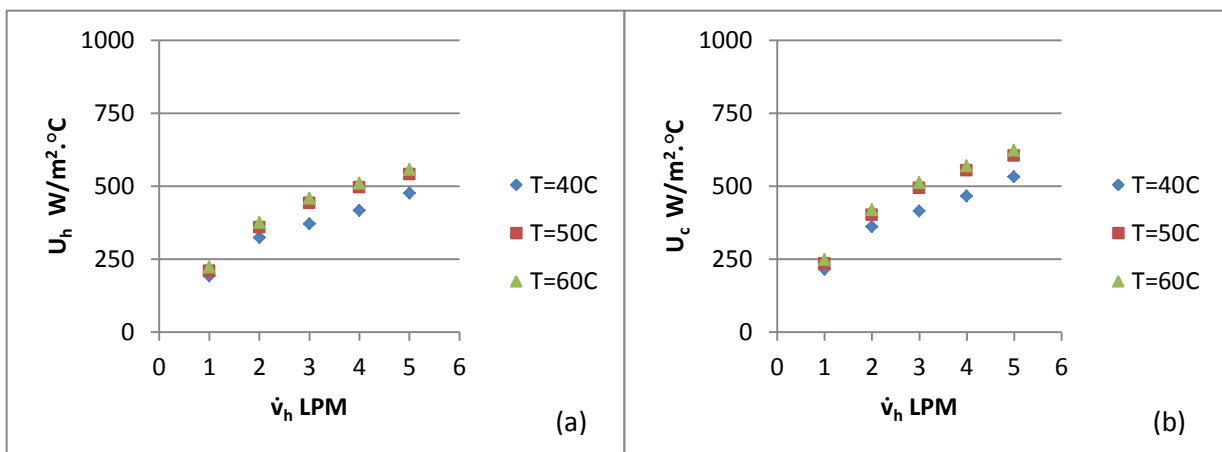


Figure (5-13) Effect of hot mass flow rate on overall heat transfer coefficient in smooth tube at $\dot{v}_c=3$ LPM in different temperatures

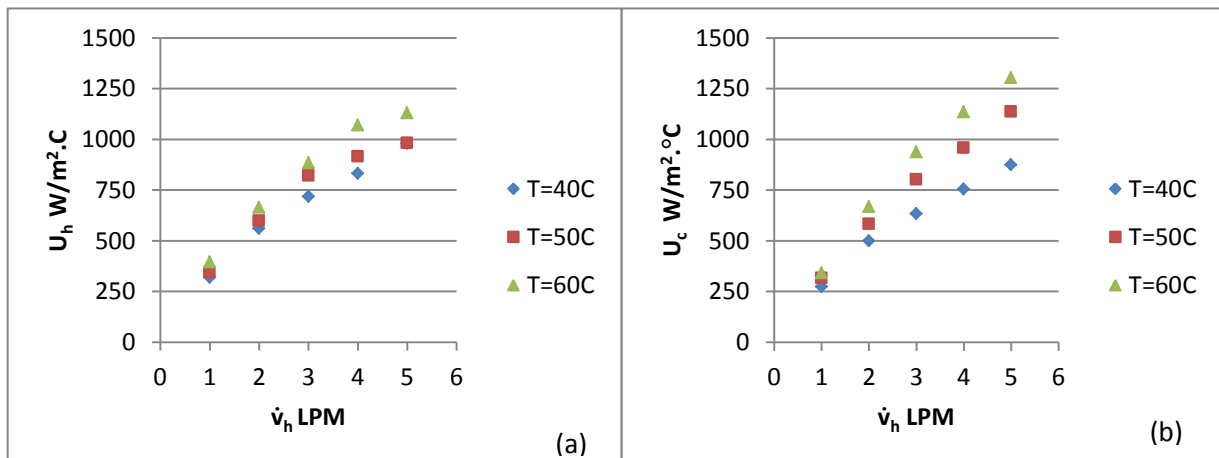


Figure (5-14) Effect of hot mass flow rate on overall heat transfer coefficient in corrugated tube ($z/d=1$) at $\dot{v}_c=3$ LPM in different temperatures

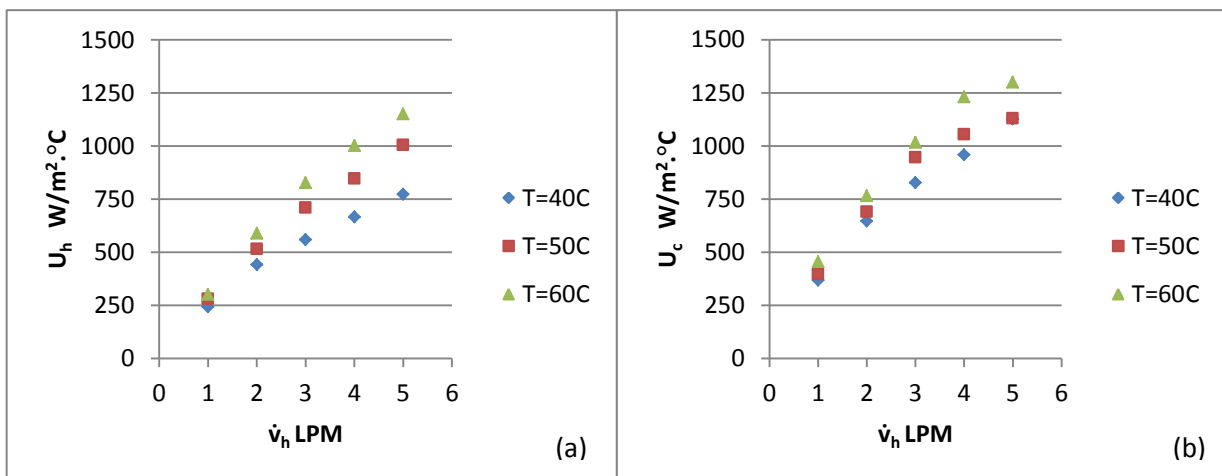


Figure (5-15) Effect of hot mass flow rate on overall heat transfer coefficient in corrugated tube ($z/d=0.5$) at $\dot{v}_c=3$ LPM in different temperatures

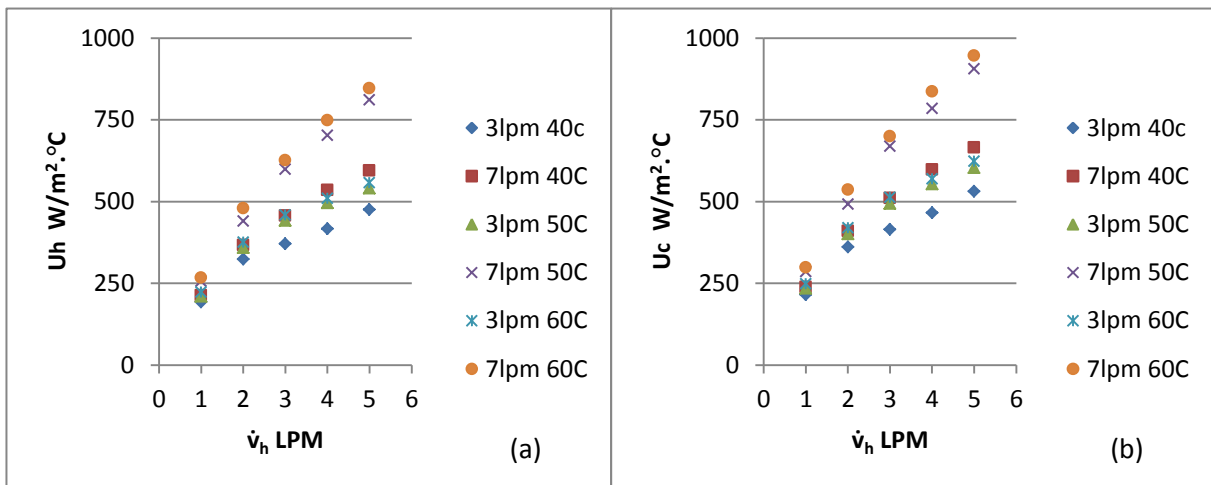


Figure (5-16) Effect of cold volumetric flow rate on overall heat transfer coefficient in smooth tube

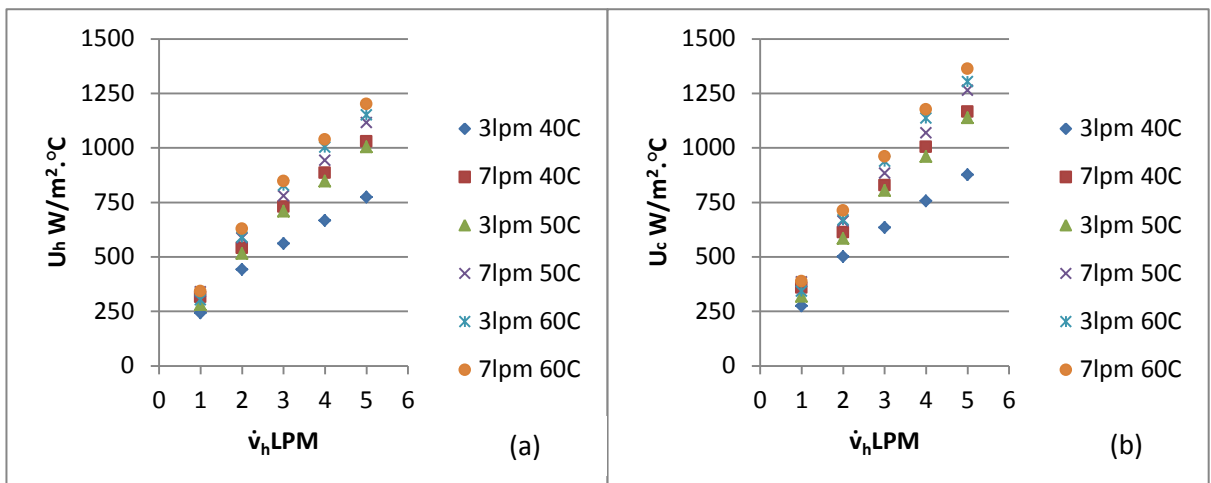


Figure (5-17) Effect of cold volumetric flow rate on overall heat transfer coefficient in corrugated tube ($z/d=1$)

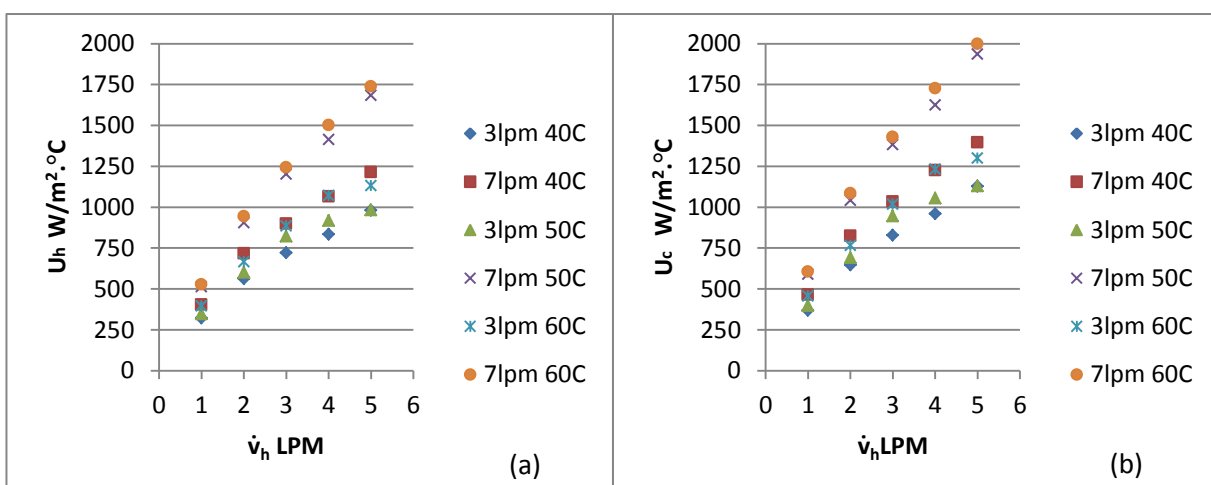


Figure (5-18) Effect of cold volumetric flow rate on overall heat transfer coefficient in corrugated tube ($z/d=0.5$)

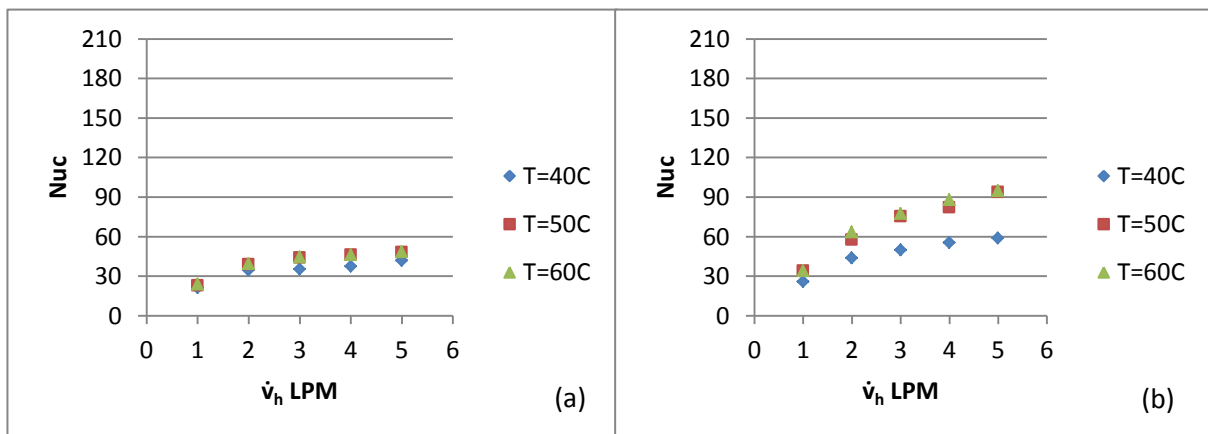


Figure (5-19) Effect of hot mass flow rate on Nusselt Number in smooth tube
at (a) $\dot{v}_c=3\text{LPM}$ (b) $\dot{v}_c=7\text{LPM}$

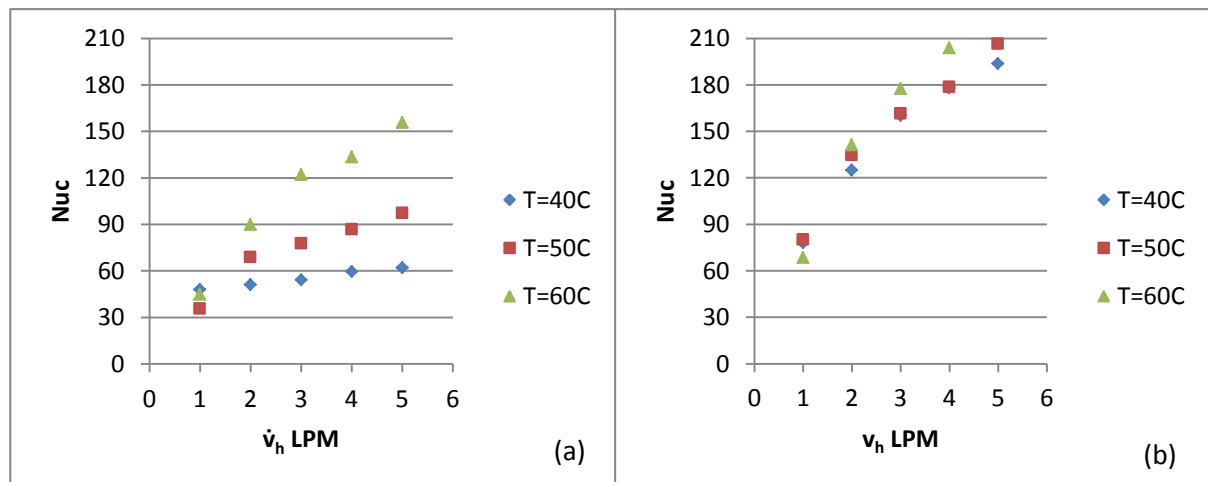


Figure (5-20) Effect of hot mass flow rate on Nusselt Number in corrugated tube ($z/d=1$)
at (a) $\dot{v}_c=3\text{LPM}$ (b) $\dot{v}_c=7\text{LPM}$

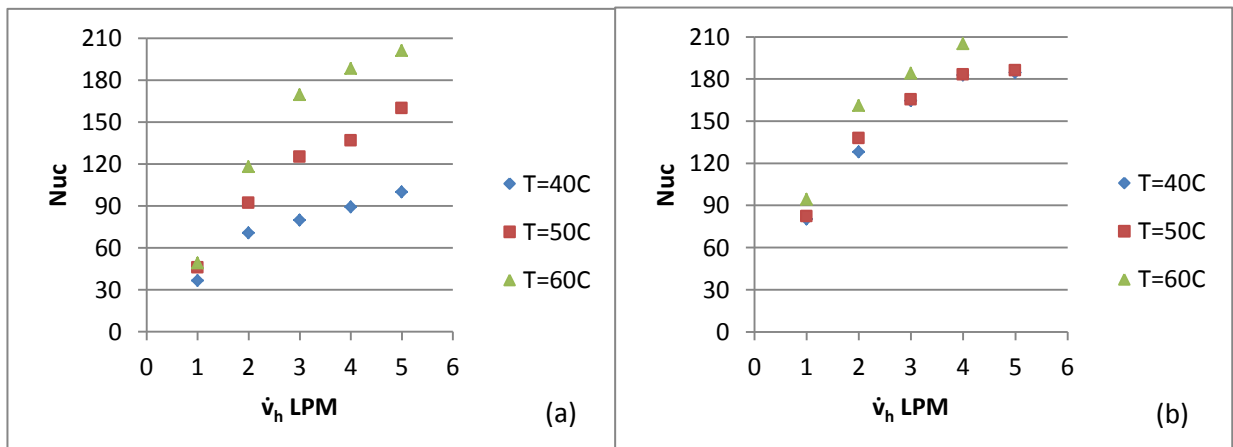


Figure (5-21) Effect of hot mass flow rate on Nusselt Number in corrugated tube ($z/d=0.5$)
at (a) $\dot{v}_c=3\text{LPM}$ (b) $\dot{v}_c=7\text{LPM}$

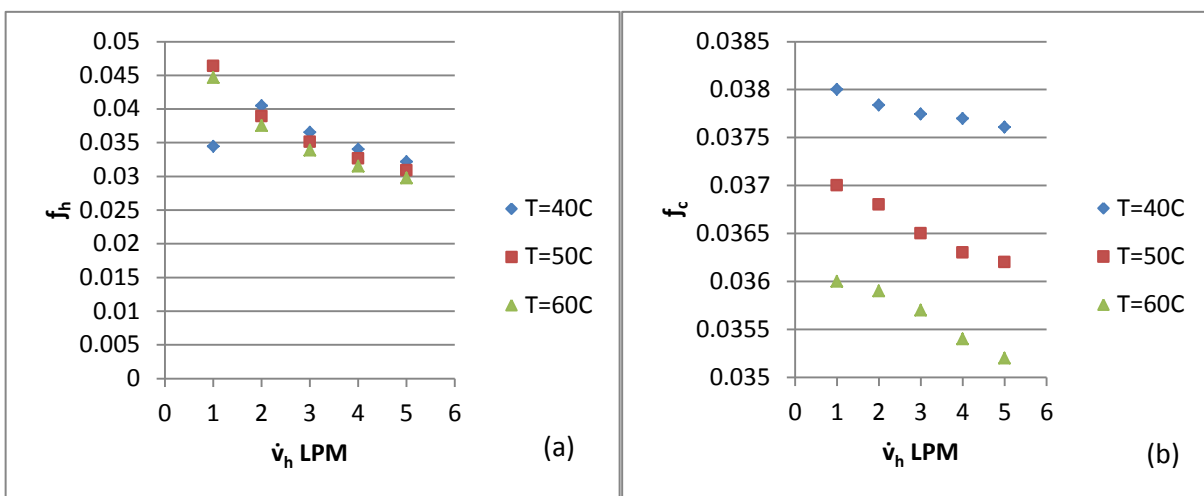


Figure (5-22) Effect of hot mass flow rate on fraction factor in smooth tube at $\dot{v}_c = 3$ LPM in different temperatures

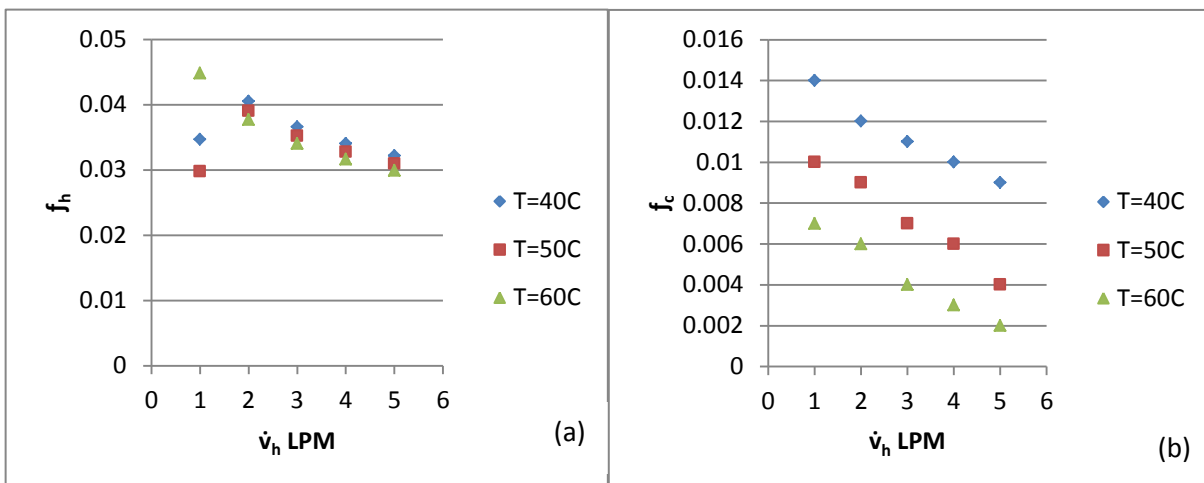


Figure (5-23) Effect of hot mass flow rate on fraction factor in corrugated tube ($z/d = 1$) at $\dot{v}_c = 3$ LPM in different temperatures

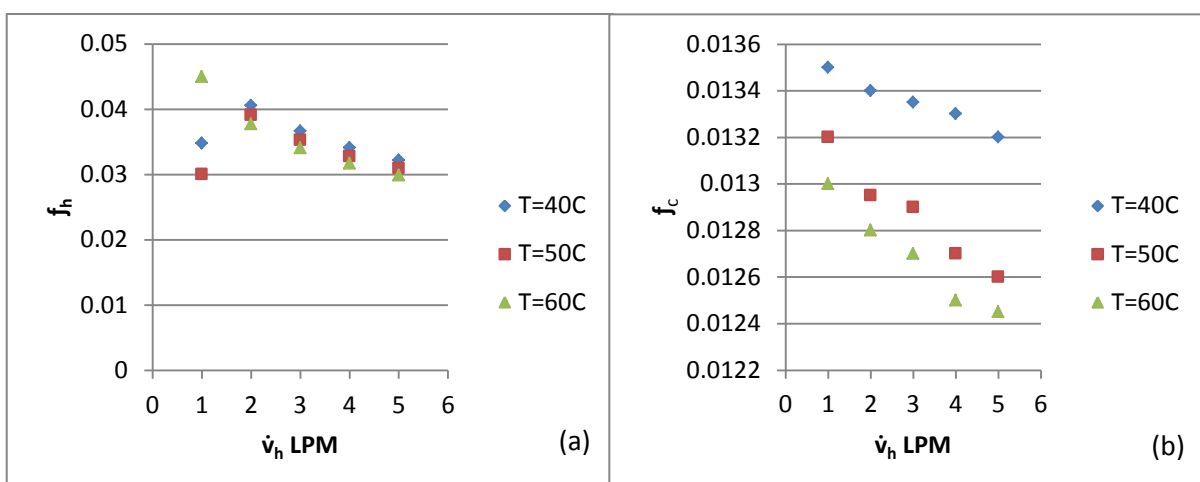


Figure (5-24) Effect of hot mass flow rate on fraction factor in corrugated tube ($z/d = 0.5$) at $\dot{v}_c = 3$ LPM in different temperatures

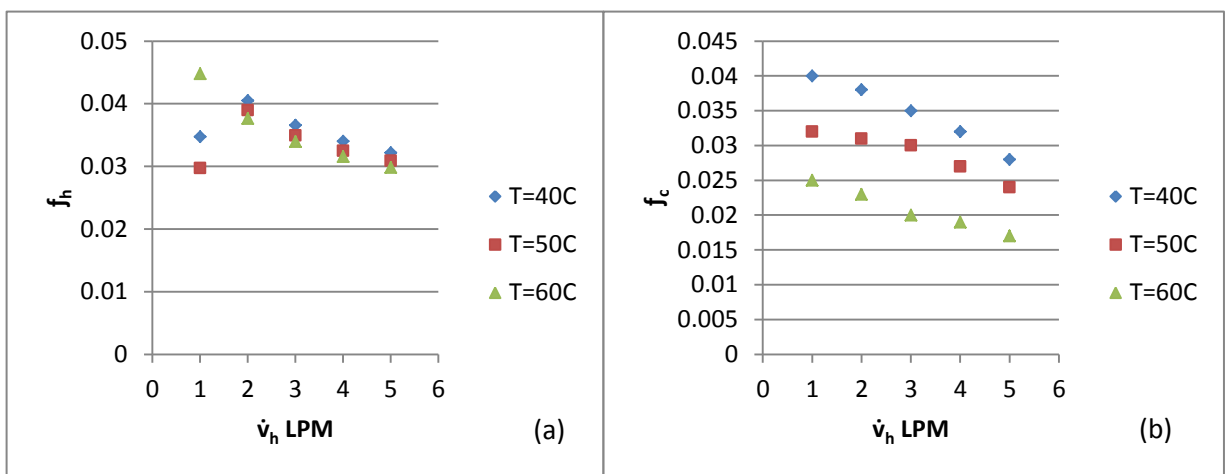


Figure (5-25) Effect of hot mass flow rate on fraction factor in smooth tube at $\dot{v}_c = 7$ LPM in different temperatures

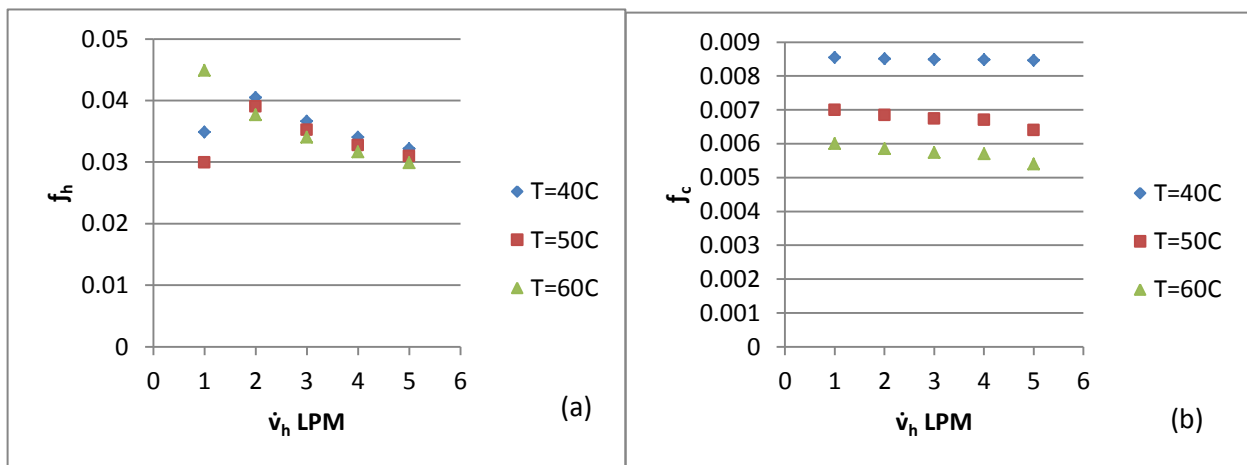


Figure (5-26) Effect of hot mass flow rate on fraction factor in corrugated tube ($z/d = 1$) at $\dot{v}_c = 7$ LPM in different temperatures

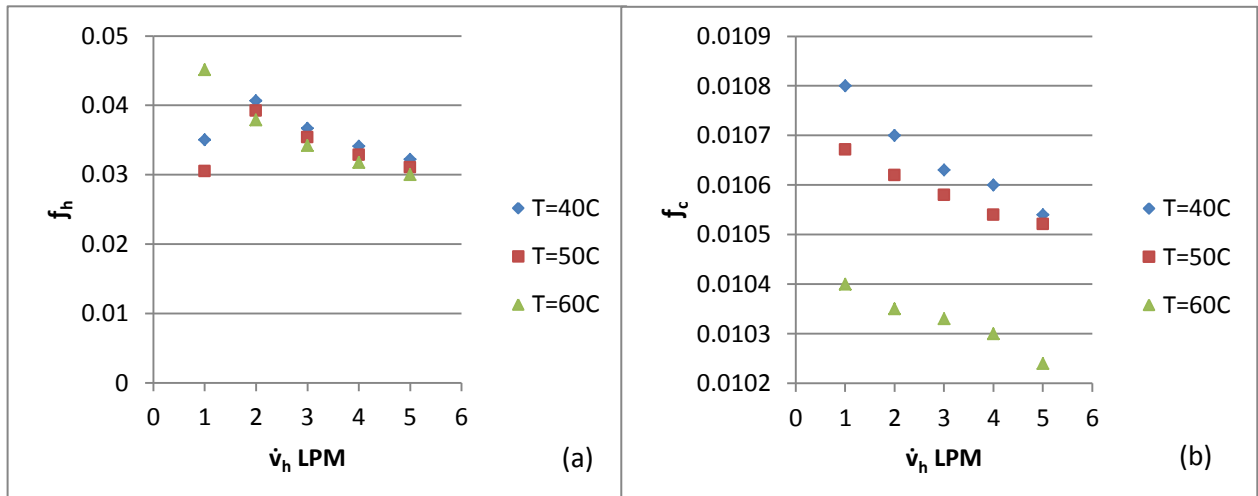


Figure (5-27) Effect of hot mass flow rate on fraction factor in corrugated tube ($z/d = 0.5$) at $\dot{v}_c = 7$ LPM in different temperatures

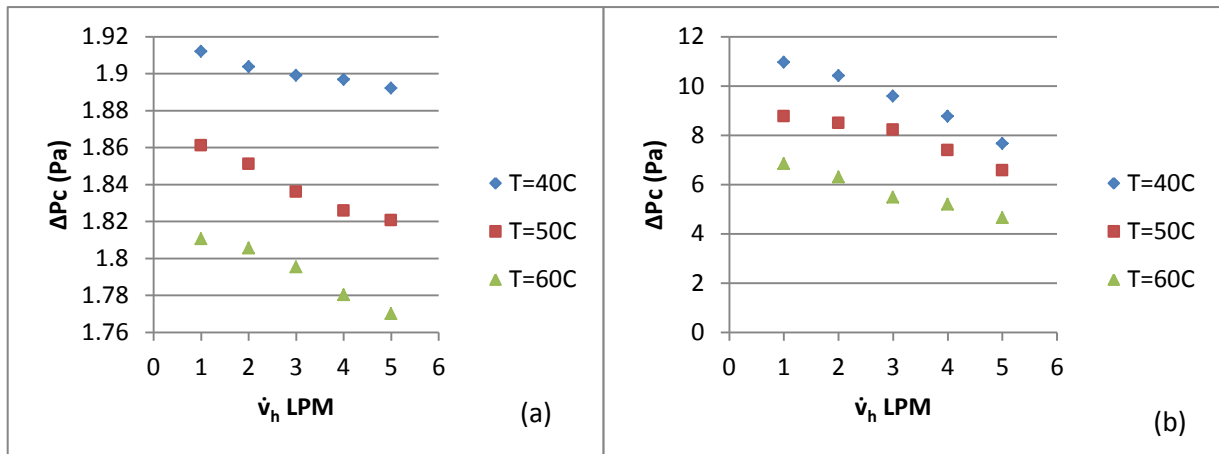
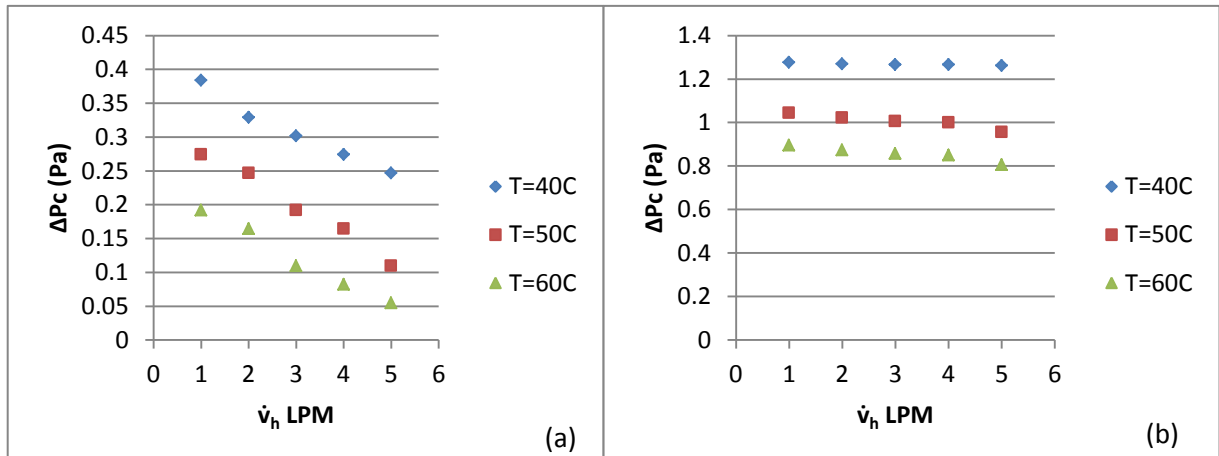
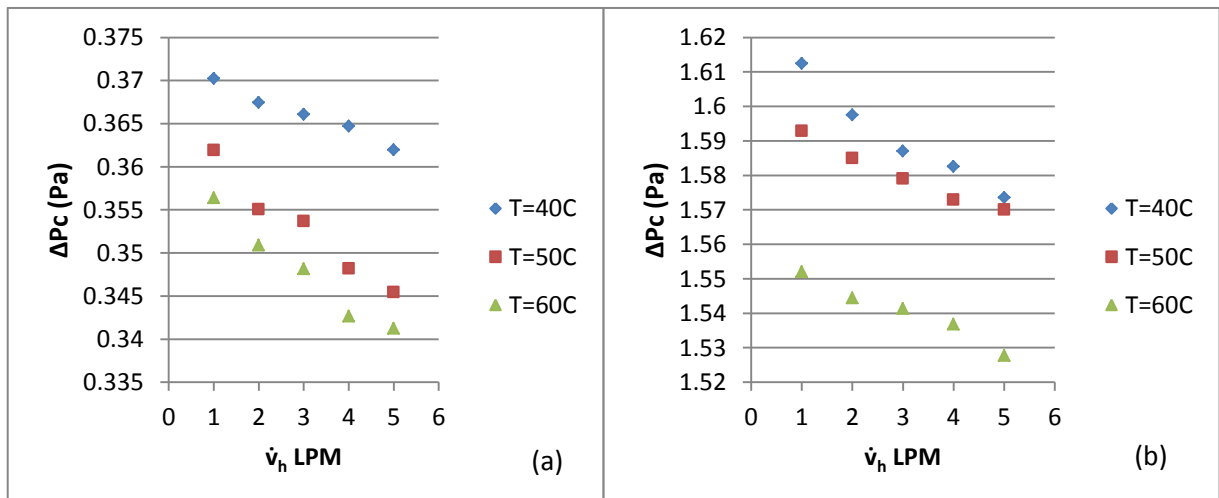


Figure (5-28) Effect of hot mass flow rate on pressure drop in smooth tube at

(a) $\dot{v}_c = 3$ LPM (b) $\dot{v}_c = 7$ LPMFigure (5-29) Effect of hot mass flow rate on pressure drop in corrugated tube ($z/d=1$) at(a) $\dot{v}_c = 3$ LPM (b) $\dot{v}_c = 7$ LPMFigure (5-30) Effect of hot mass flow rate on pressure drop in corrugated tube ($z/d=0.5$) at(a) $\dot{v}_c = 3$ LPM (b) $\dot{v}_c = 7$ LPM

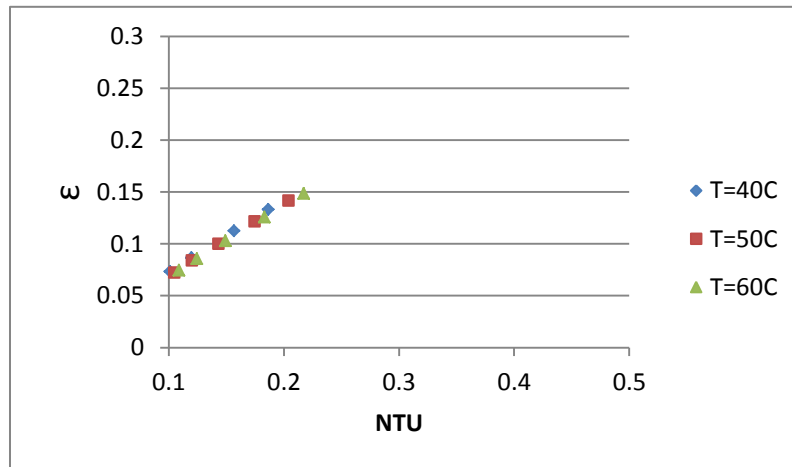


Figure (5-31) Variation of effectiveness with number of transfer units (NTU) in smooth tube at $\dot{v}_c = 3\text{LPM}$ in different temperatures

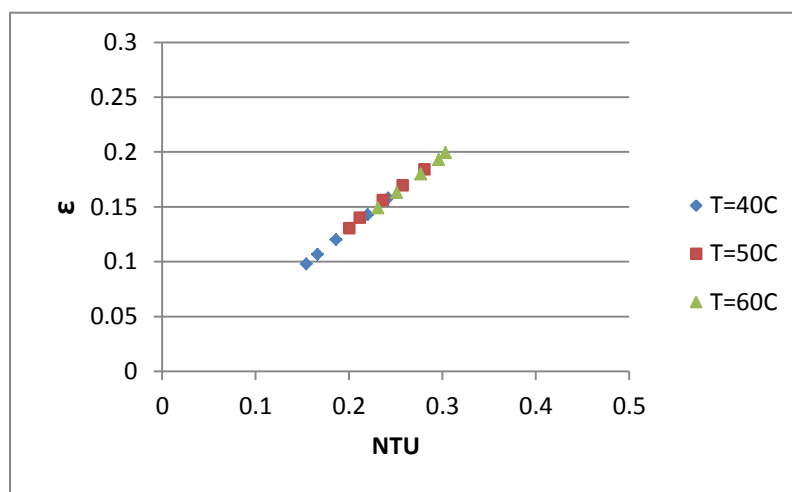


Figure (5-32) Variation of effectiveness with number of transfer units (NTU) in corrugated tube ($z/d = 1$) at $\dot{v}_c = 3\text{LPM}$ in different temperatures

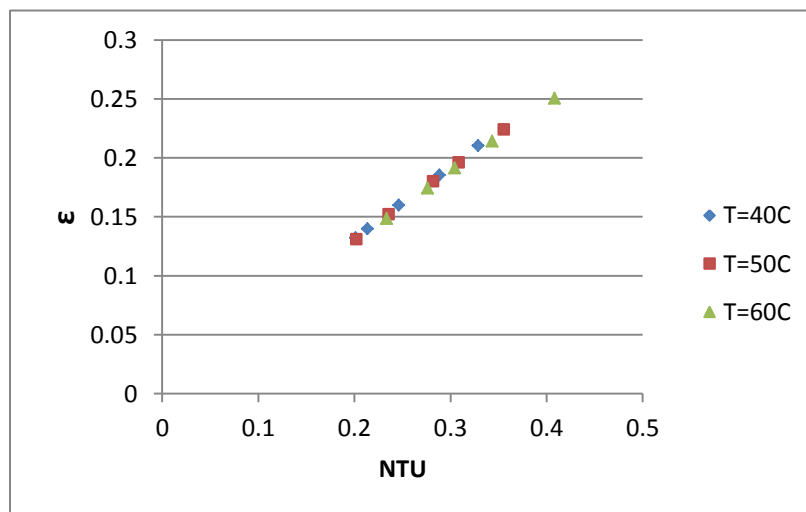


Figure (5-33) Variation of effectiveness with number of transfer units (NTU) in corrugated tube ($z/d = 0.5$) at $\dot{v}_c = 3\text{LPM}$ in different temperatures

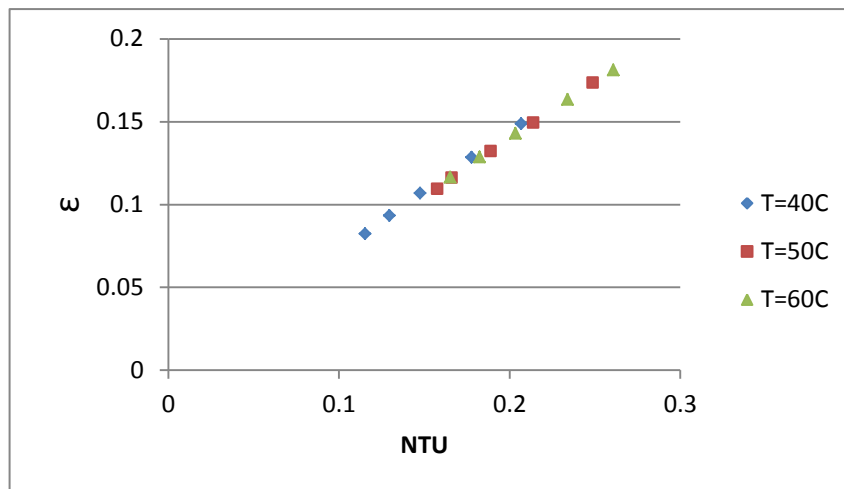


Figure (5-34) Variation of effectiveness with number of transfer units (NTU) in smooth tube at $\dot{v}_c=7\text{LPM}$ in different temperatures

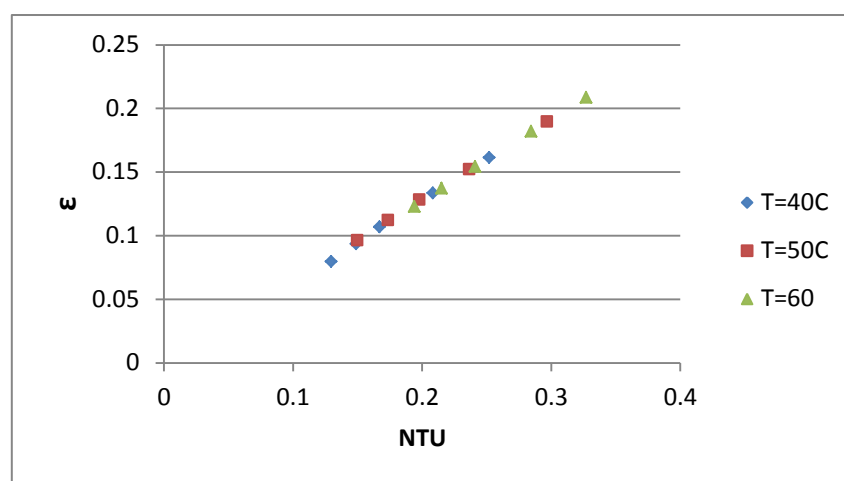


Figure (5-35) Variation of effectiveness with number of transfer units (NTU) in corrugated tube ($z/d=1$) at $\dot{v}_c=7\text{LPM}$ in different temperatures

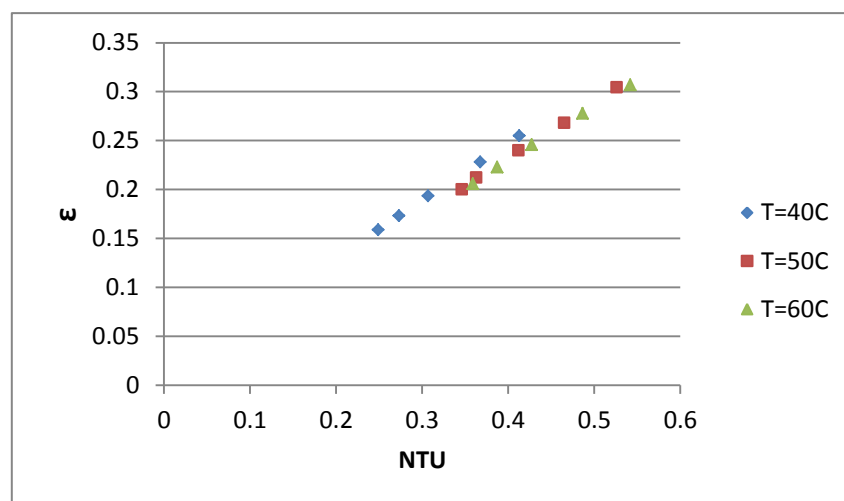


Figure (5-36) Variation of effectiveness with number of transfer units (NTU) in corrugated tube ($z/d=0.5$) at $\dot{v}_c=3\text{LPM}$ in different temperatures

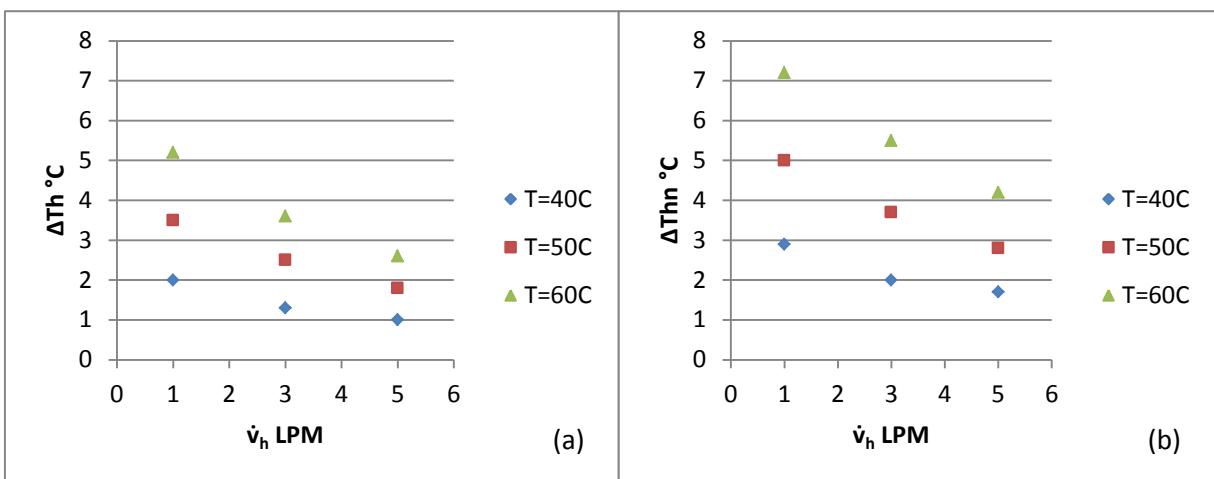


Figure (5-37) Effect of hot mass flow rate on hot temperature difference in smooth tube at $v_c = 3$ LPM in different temperatures for (a) water and (b) Nano fluid

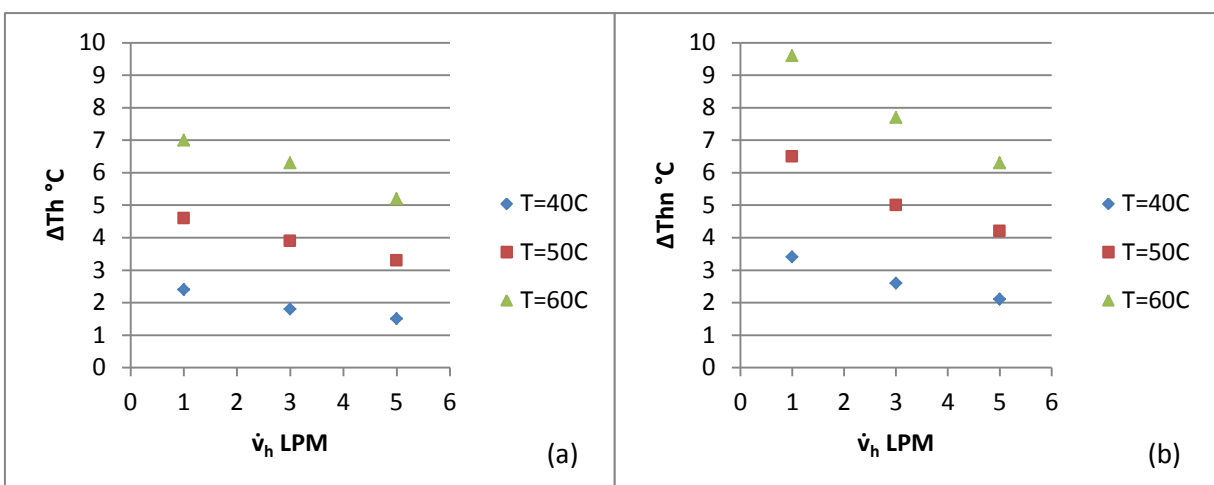


Figure (5-38) Effect of hot mass flow rate on hot temperature difference in corrugated tube ($z/d = 1$) at $v_c = 3$ LPM in different temperatures for (a) water and (b) Nano fluid

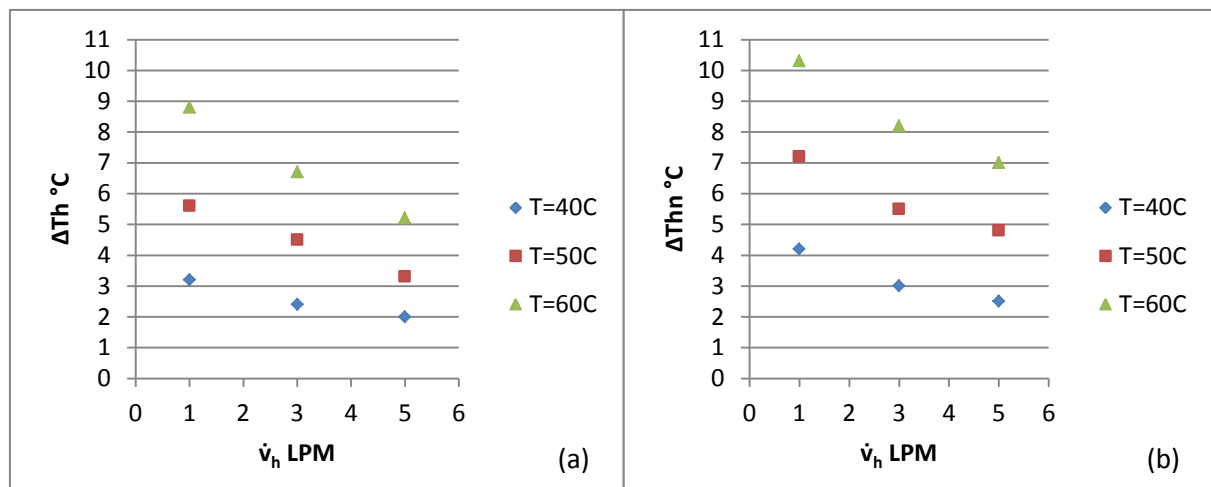


Figure (5-39) Effect of hot mass flow rate on hot temperature difference in corrugated tube ($z/d = 0.5$) at $v_c = 3$ LPM in different temperatures for (a) water and (b) Nano fluid

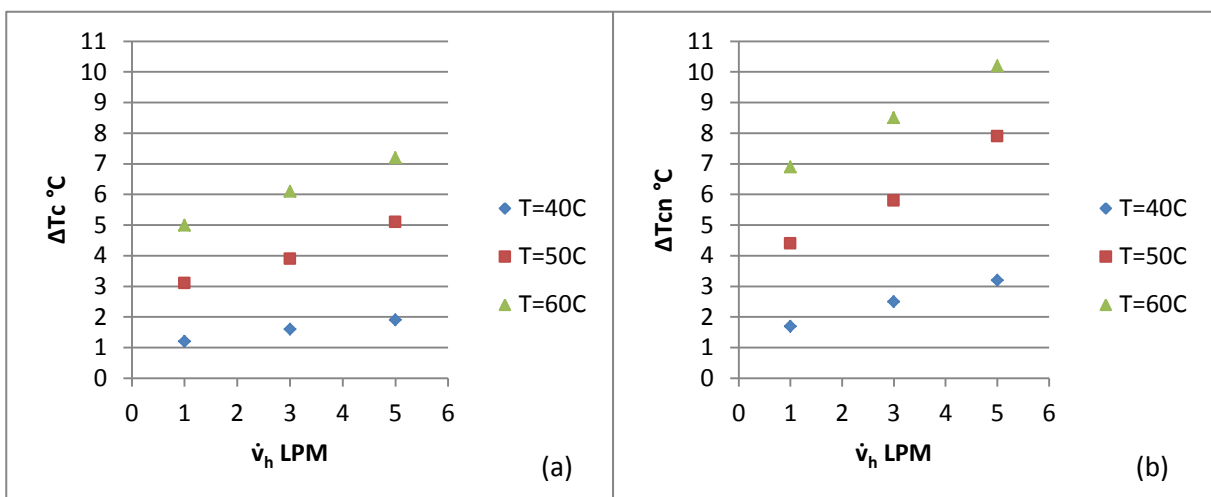


Figure (5-40) Effect of hot mass flow rate on cold temperature difference in smooth tube at $\dot{v}_c = 3$ LPM in different temperatures for (a) water and (b) Nano fluid

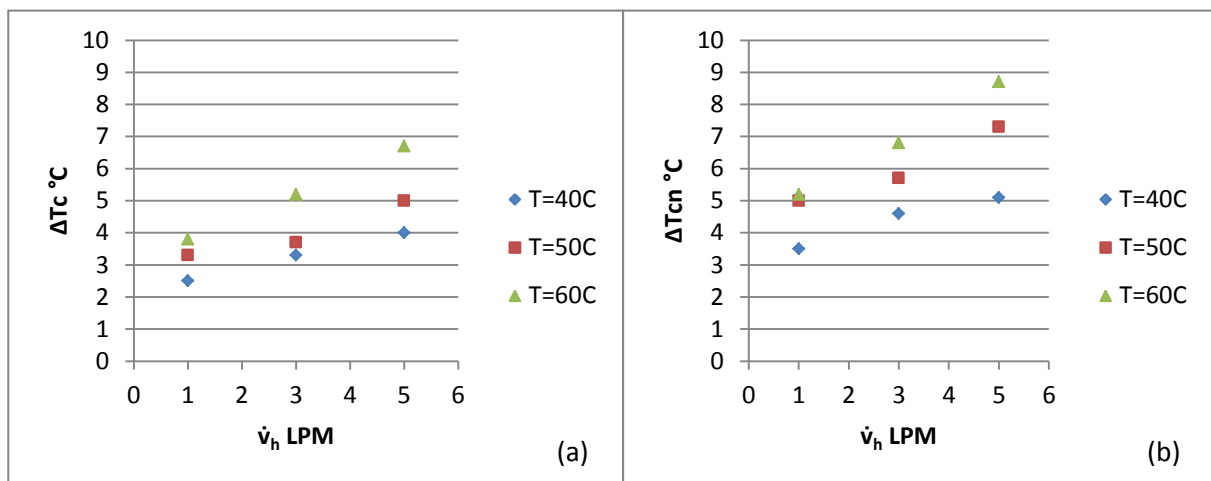


Figure (5-41) Effect of hot mass flow rate on cold temperature difference in corrugated tube ($z/d = 1$) at $\dot{v}_c = 3$ LPM in different temperatures for (a) water and (b) Nano fluid

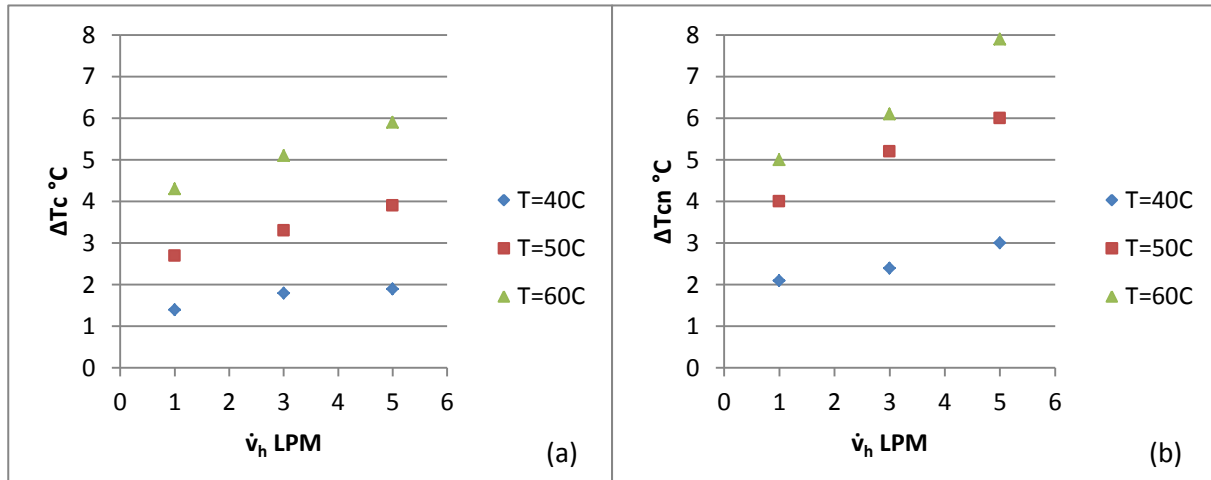


Figure (5-42) Effect of hot mass flow rate on cold temperature difference in corrugated tube ($z/d = 0.5$) at $\dot{v}_c = 3$ LPM in different temperatures for (a) water and (b) Nano fluid

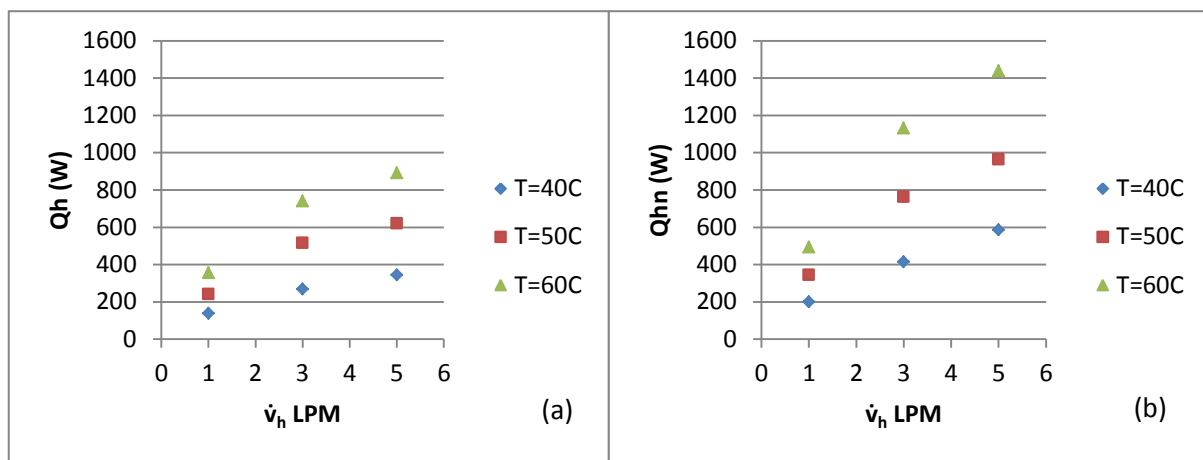


Figure (5-43) Effect of hot mass flow rate on hot heat dissipation in smooth tube at $\dot{v}_c=3$ LPM in different temperatures in (a) water and (b) Nano fluid

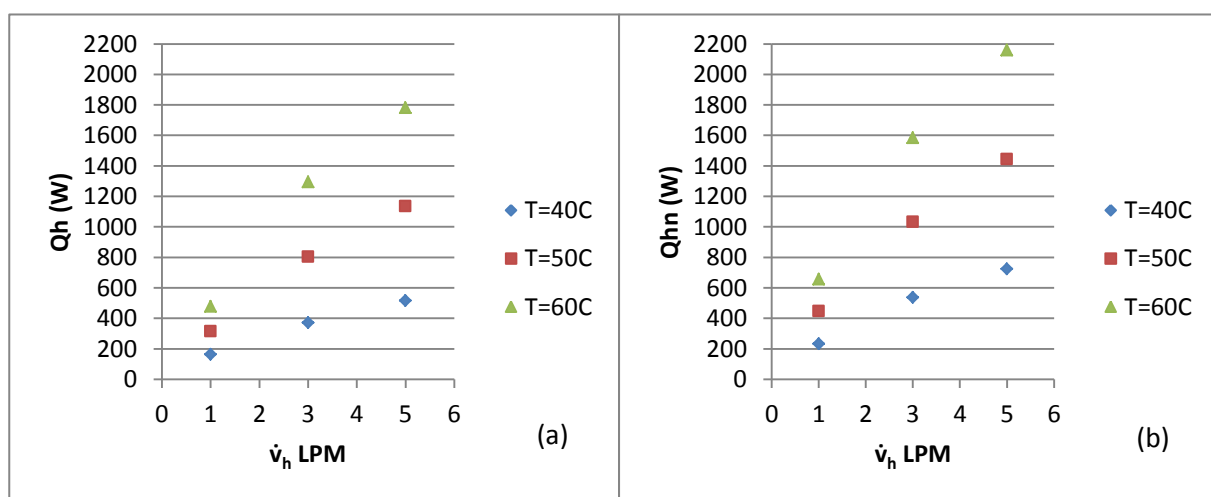


Figure (5-44) Effect of hot mass flow rate on hot heat dissipation in corrugated tube ($z/d=1$) at $\dot{v}_c=3$ LPM in different temperatures in (a) water and (b) Nano fluid

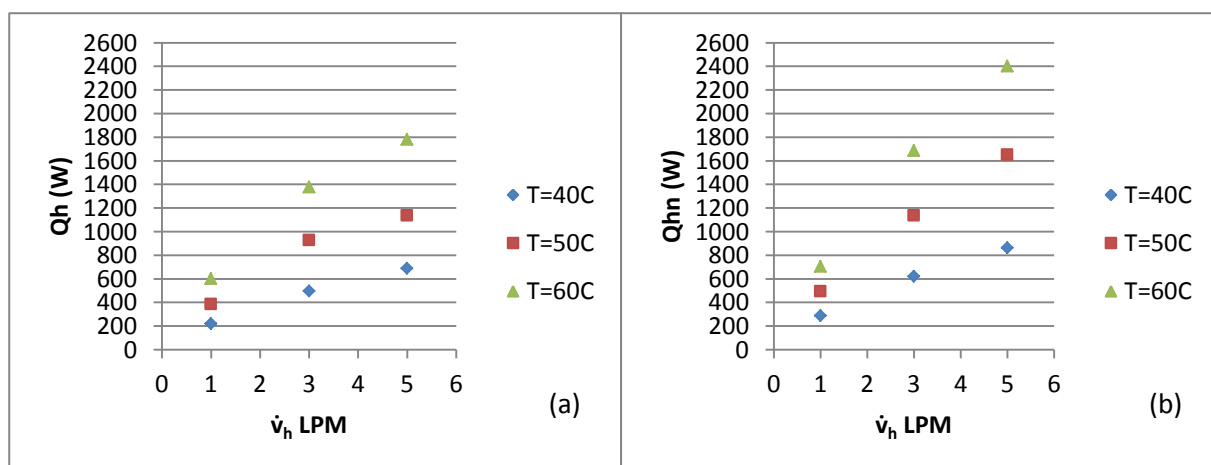


Figure (5-45) Effect of hot mass flow rate on hot heat dissipation in corrugated tube ($z/d=0.5$) at $\dot{v}_c=3$ LPM in different temperatures in (a) water and (b) Nano fluid

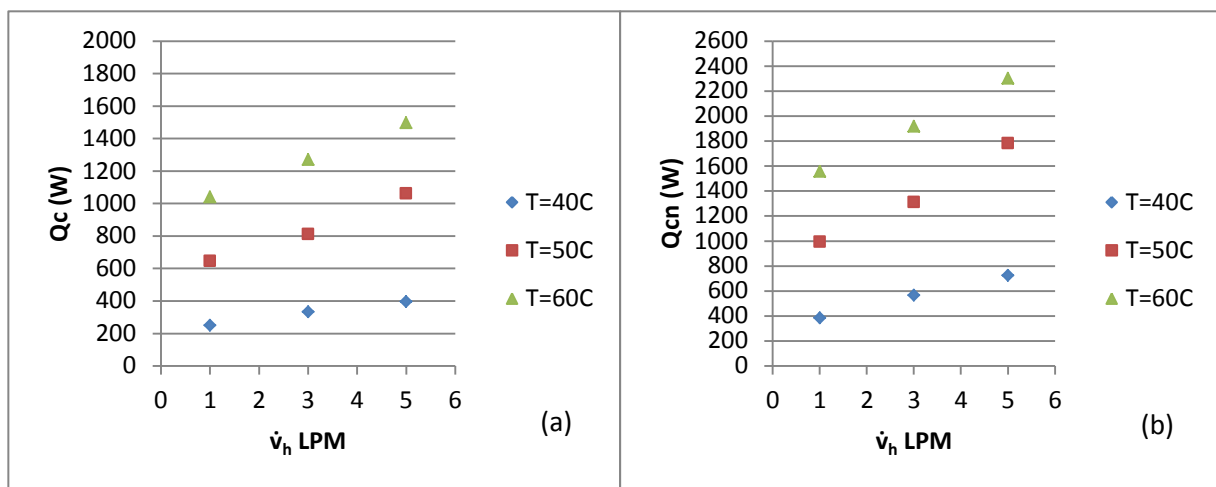


Figure (5-46) Effect of hot mass flow rate on cold heat dissipation in smooth tube at $\dot{v}_c = 3$ LPM in different temperatures in (a) water and (b) Nano fluid

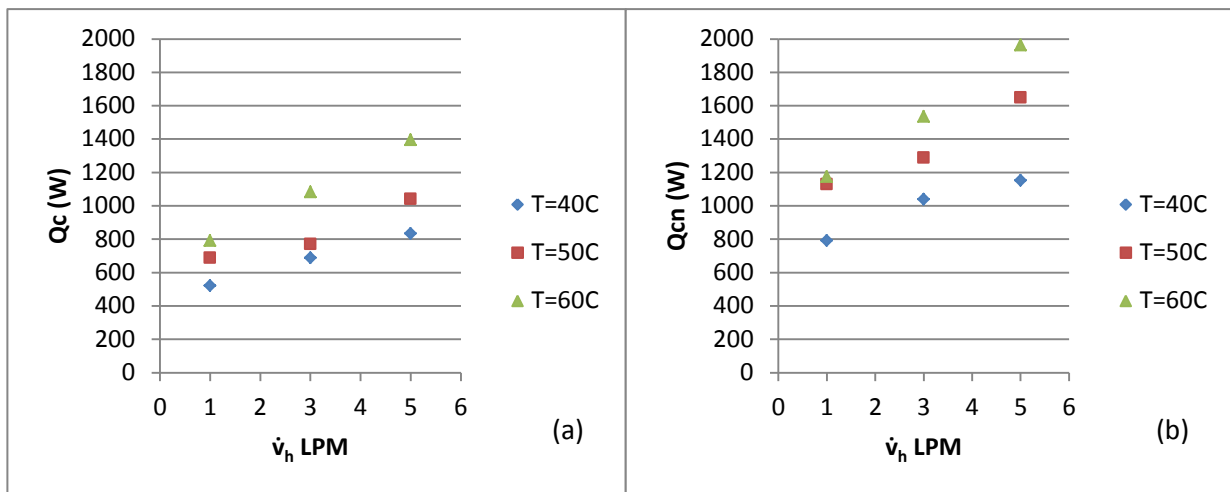


Figure (5-47) Effect of hot mass flow rate on cold heat dissipation in corrugated tube ($z/d = 1$) at $\dot{v}_c = 3$ LPM in different temperatures in (a) water and (b) Nano fluid

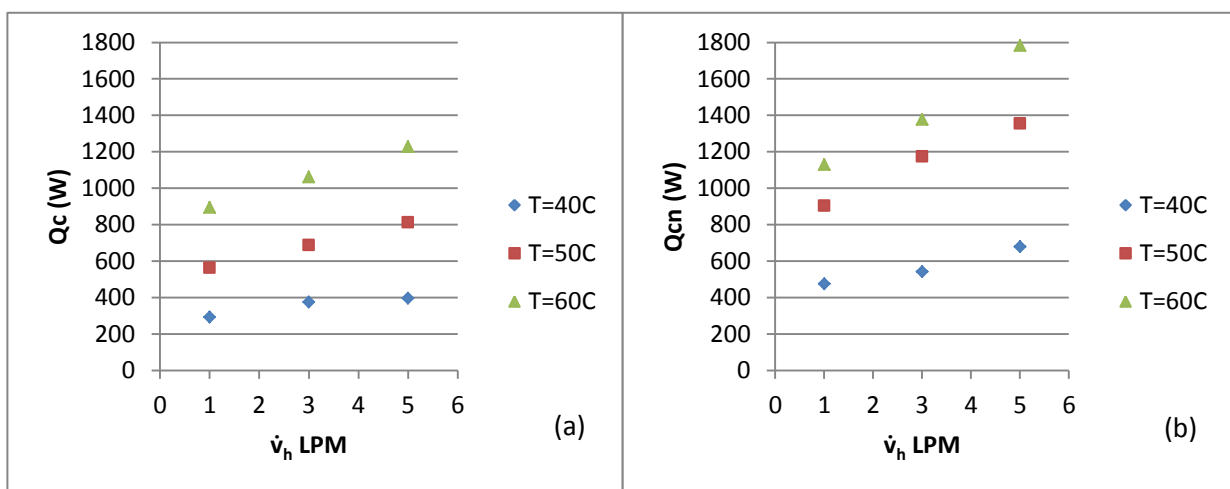


Figure (5-48) Effect of hot mass flow rate on cold heat dissipation in corrugated tube ($z/d = 0.5$) at $\dot{v}_c = 3$ LPM in different temperatures in (a) water and (b) Nano fluid

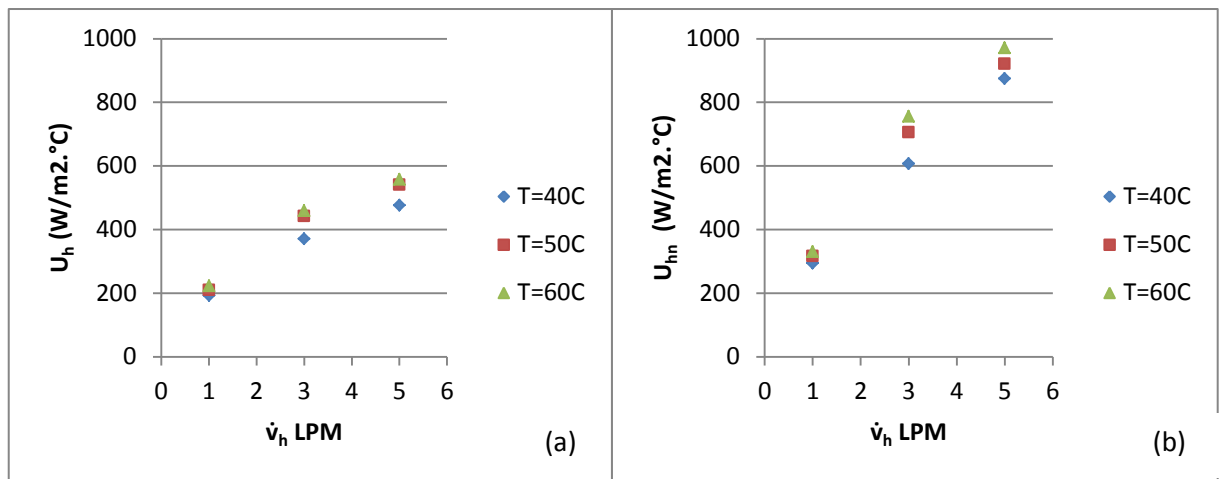


Figure (5-49) Effect of hot mass flow rate on hot overall heat transfer coefficient in smooth tube at $\dot{v}_c = 3$ LPM in different temperatures in (a) water and (b) Nano fluid

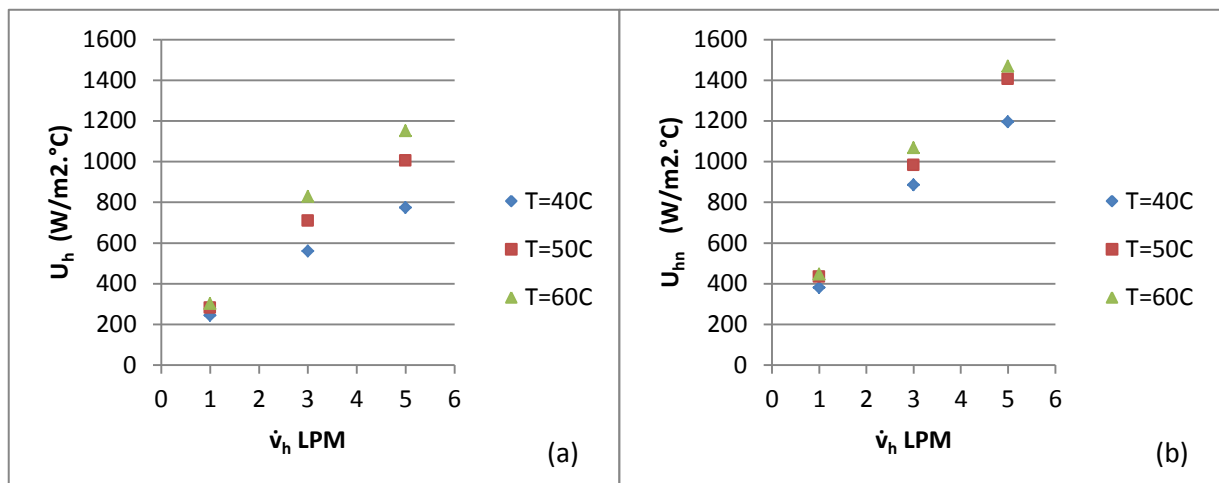


Figure (5-50) Effect of hot mass flow rate on hot overall heat transfer coefficient tube ($z/d = 1$) at $\dot{v}_c = 3$ LPM in different temperatures in (a) water and (b) Nano fluid

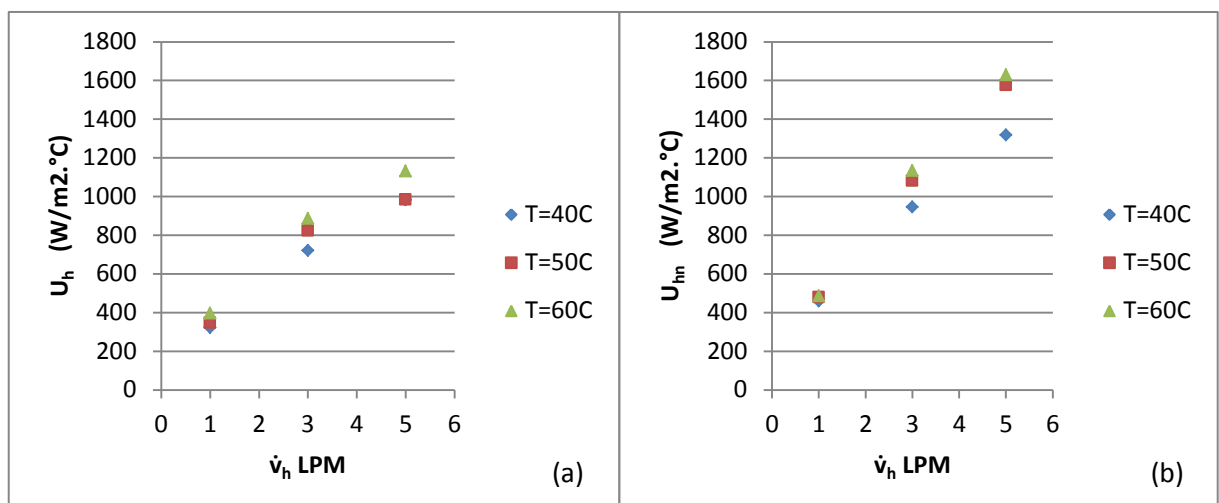


Figure (5-51) Effect of hot mass flow rate on hot overall heat transfer coefficient tube ($z/d = 0.5$) at $\dot{v}_c = 3$ LPM in different temperatures in (a) water and (b) Nano fluid

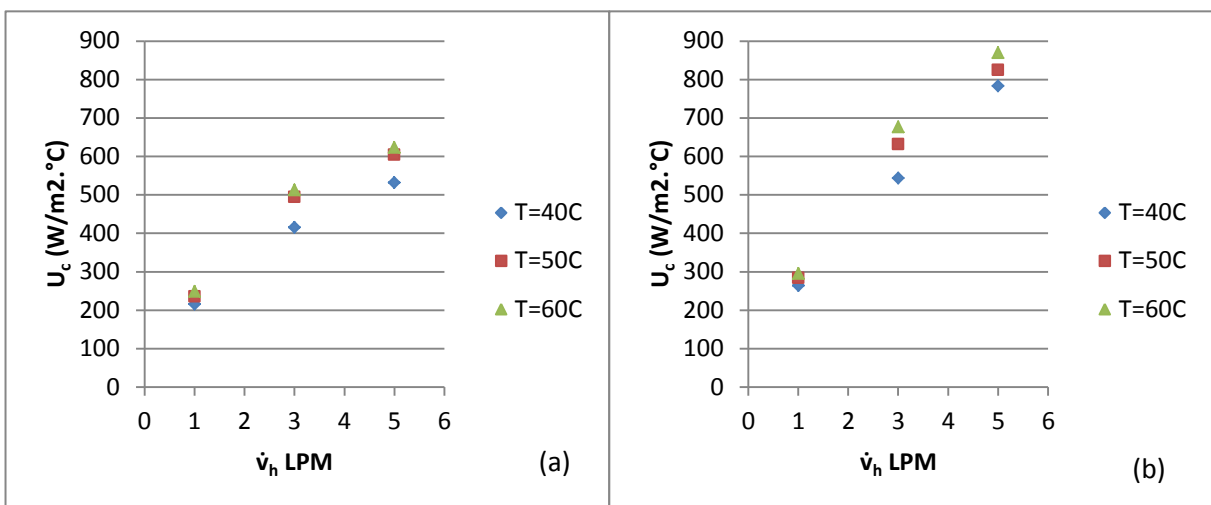


Figure (5-52) Effect of hot mass flow rate on cold overall heat transfer coefficient in smooth tube at $\dot{v}_c = 3$ LPM in different temperatures in (a) water and (b) Nano fluid

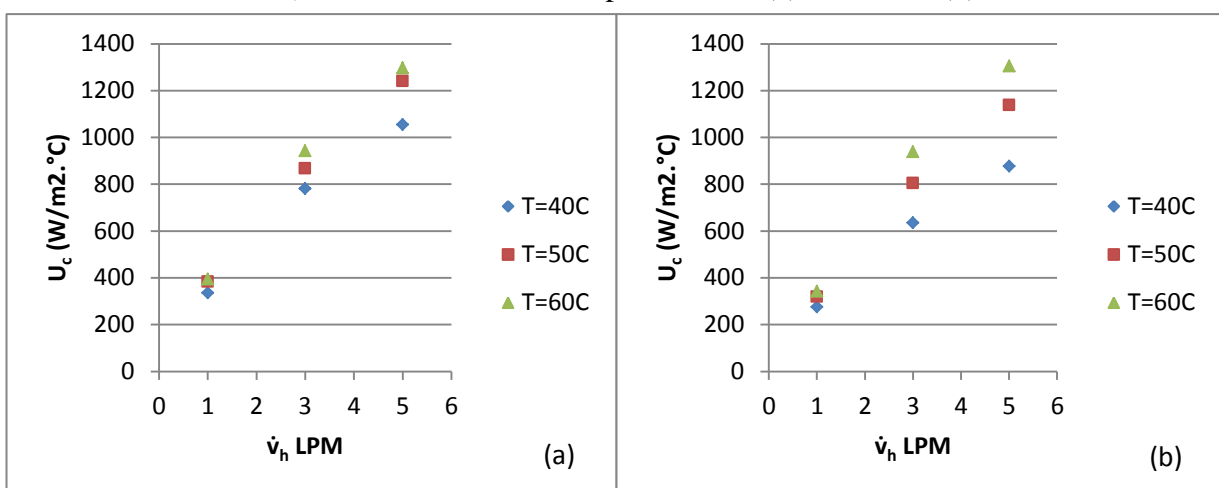


Figure (5-53) Effect of hot mass flow rate on cold overall heat transfer coefficient tube ($z/d = 1$) at $\dot{v}_c = 3$ LPM in different temperatures in (a) water and (b) Nano fluid

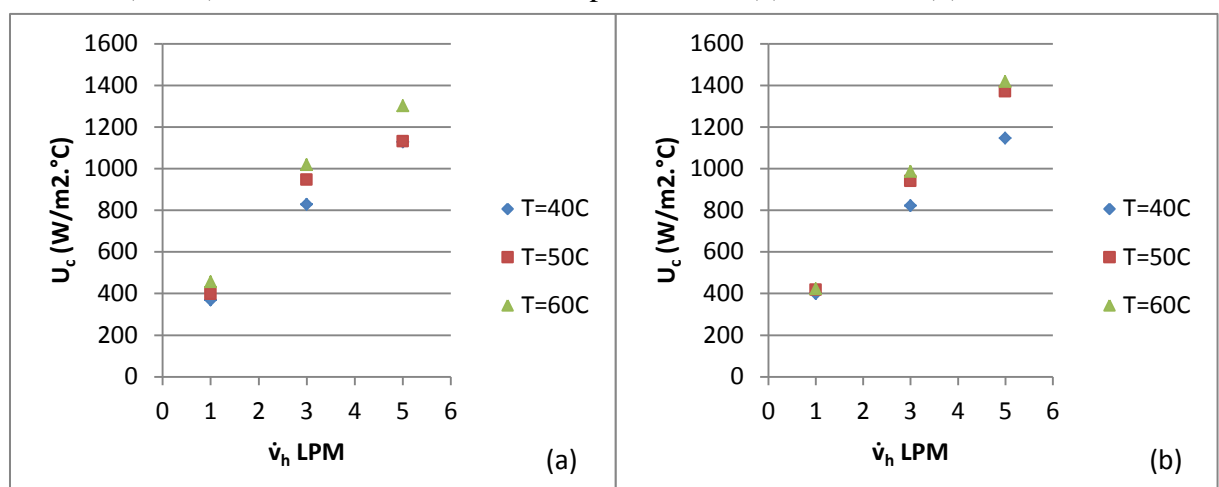


Figure (5-54) Effect of hot mass flow rate on cold overall heat transfer coefficient tube ($z/d = 0.5$) at $\dot{v}_c = 3$ LPM in different temperatures in (a) water and (b) Nano fluid

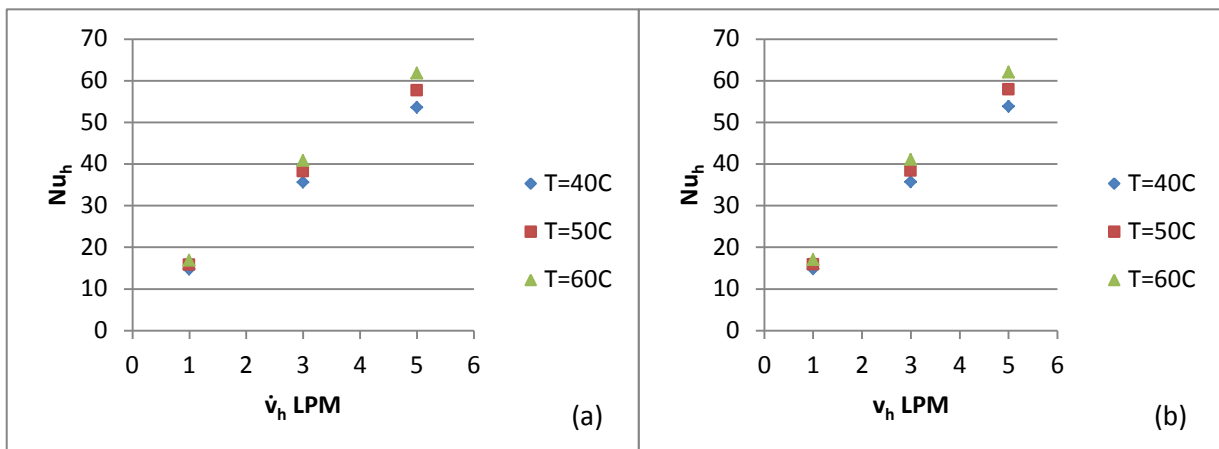


Figure (5-55) Effect of hot mass flow rate on hot Nusselt number in smooth tube at $\dot{v}_c=3$ LPM in different temperatures in (a) water and (b) Nano fluid

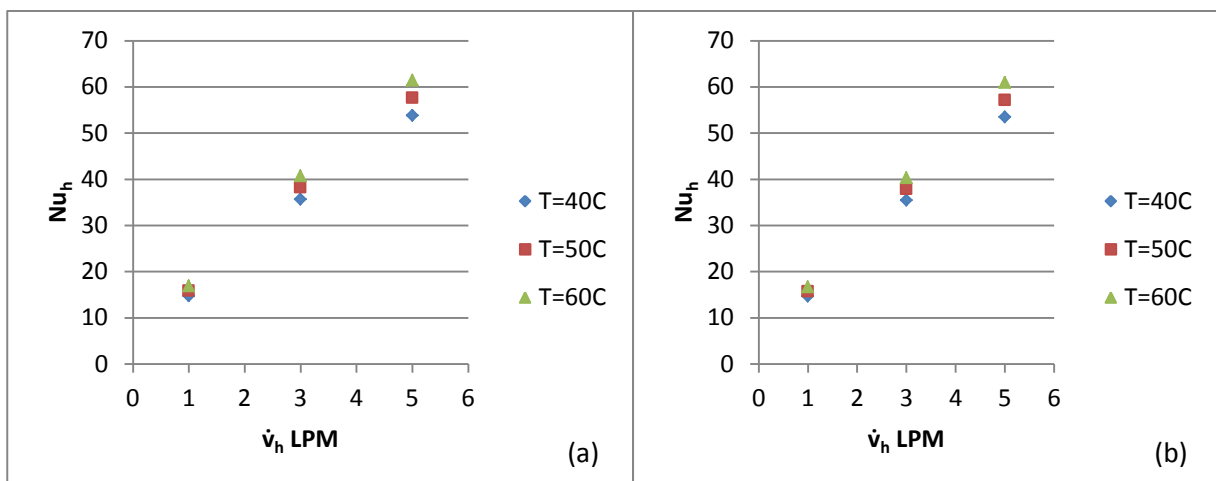


Figure (5-56) Effect of hot mass flow rate on hot Nusselt number in corrugated tube ($z/d=1$) at $\dot{v}_c=3$ LPM in different temperatures in (a) water and (b) Nano fluid

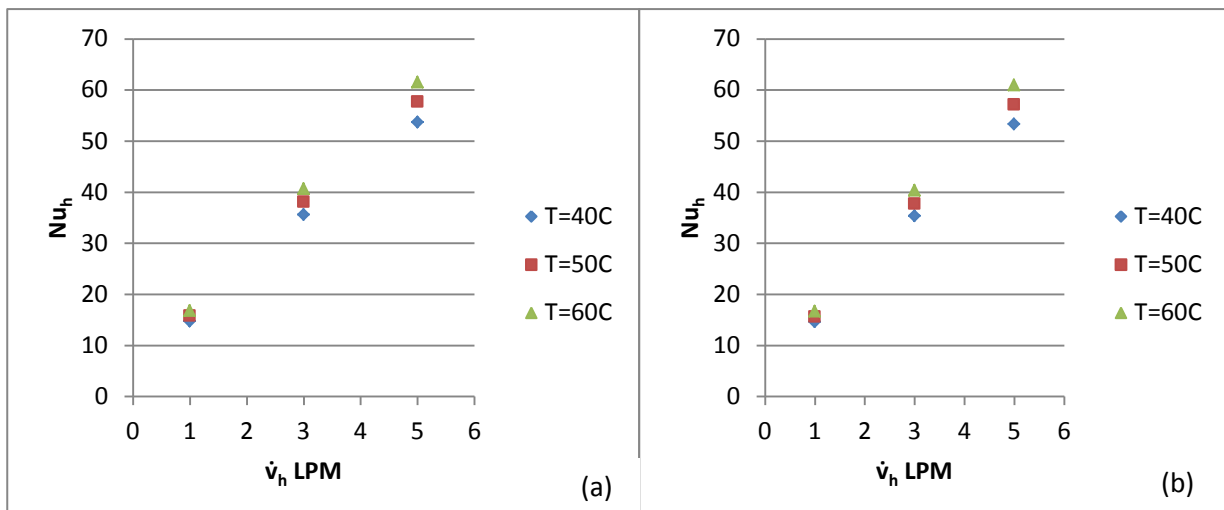


Figure (5-57) Effect of hot mass flow rate on hot Nusselt number in corrugated tube ($z/d=0.5$) at $\dot{v}_c=3$ LPM in different temperatures in (a) water and (b) Nano fluid

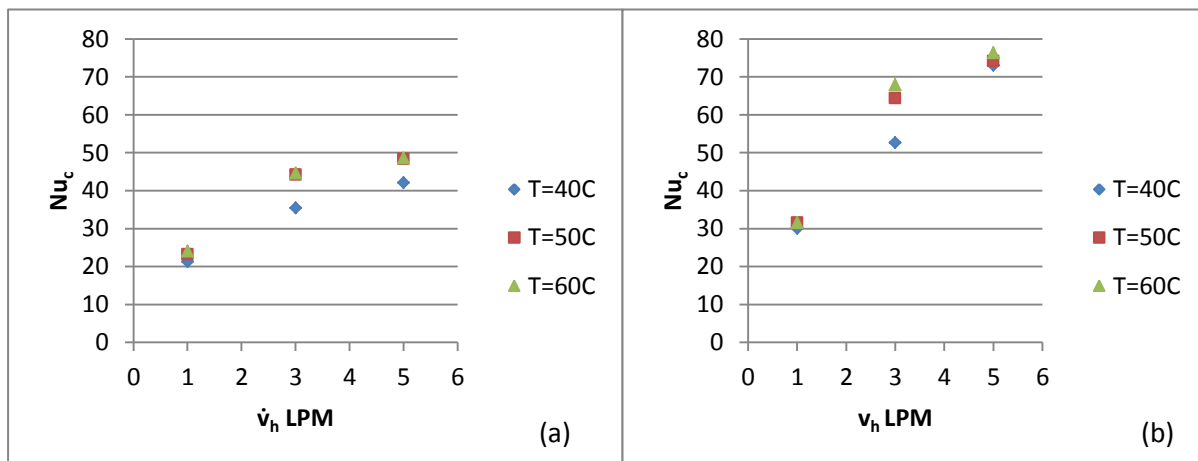


Figure (5-58) Effect of hot mass flow rate on cold Nusselt number in smooth tube at $\dot{v}_c=3$ LPM in different temperatures in (a) water and (b) Nano fluid

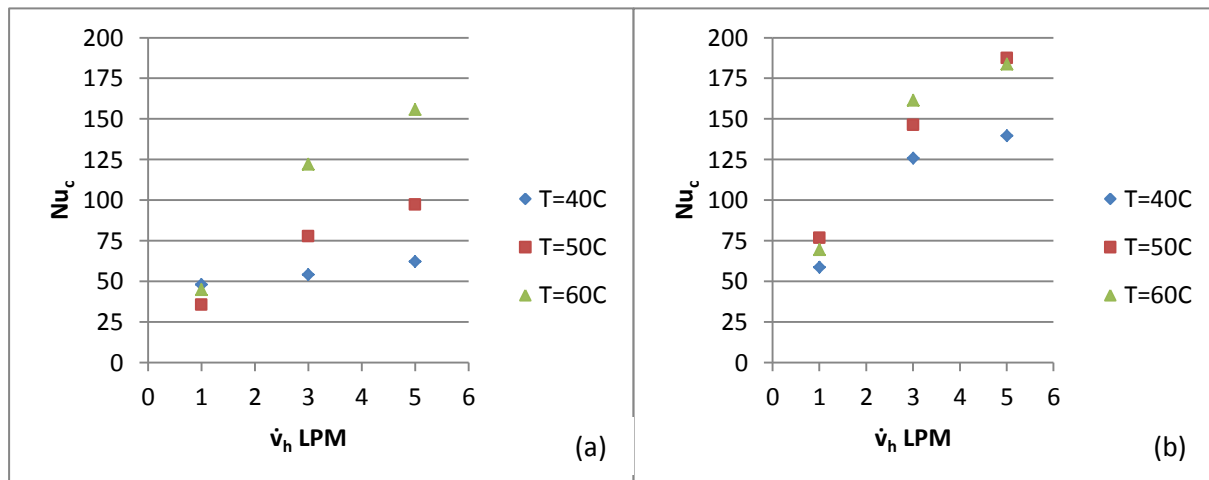


Figure (5-59) Effect of hot mass flow rate on cold Nusselt number in corrugated tube ($z/d=1$) at $\dot{v}_c=3$ LPM in different temperatures in (a) water and (b) Nano fluid

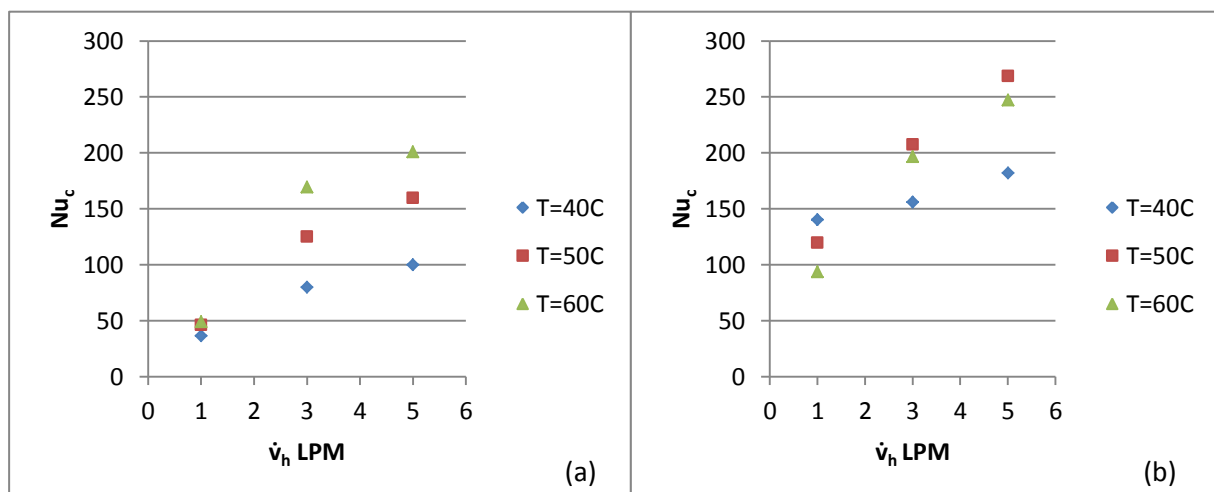


Figure (5-60) Effect of hot mass flow rate on cold Nusselt number corrugated tube ($z/d=0.5$) at $\dot{v}_c=3$ LPM in different temperatures in (a) water and (b) Nano fluid

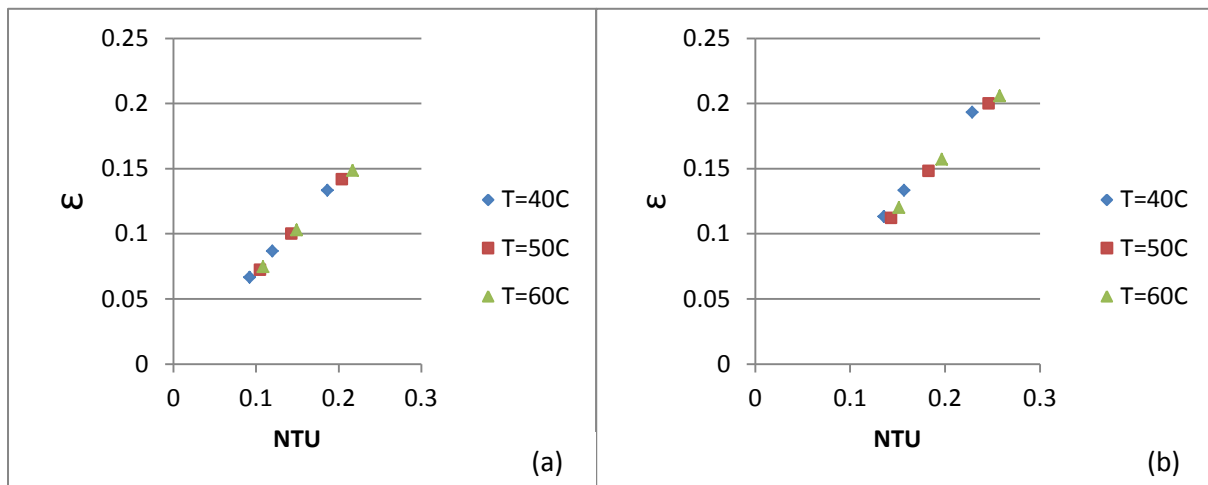


Figure (5-61) Variation of effectiveness with number of transfer units (NTU) in smooth tube at $\dot{v}_c=3\text{LPM}$ in different temperatures in (a) water and (b) Nano fluid

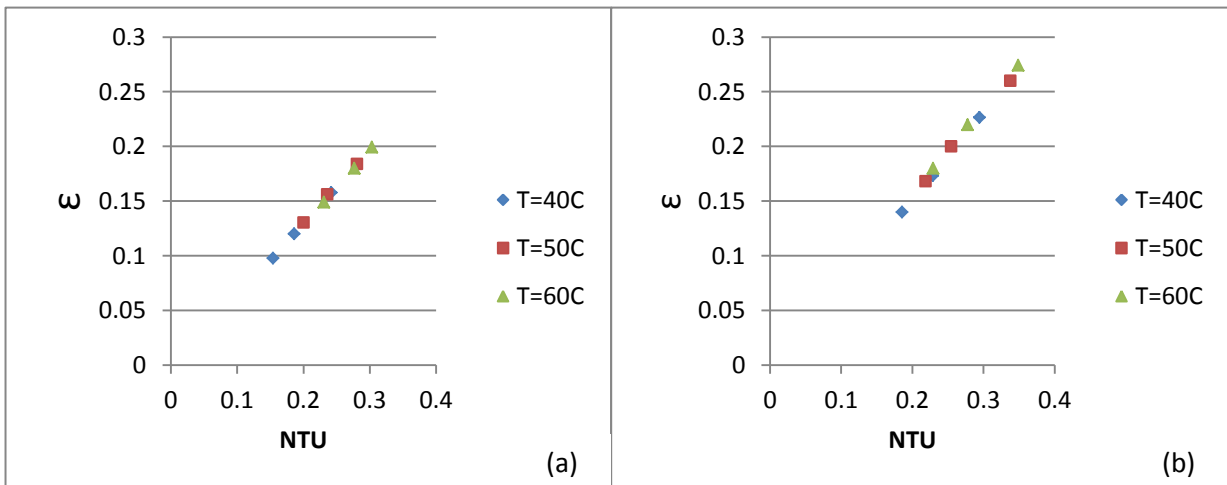


Figure (5-62) Variation of effectiveness with number of transfer units (NTU) in corrugated tube ($z/d=1$) at $\dot{v}_c=3\text{LPM}$ in different temperatures in (a) water and (b) Nano fluid

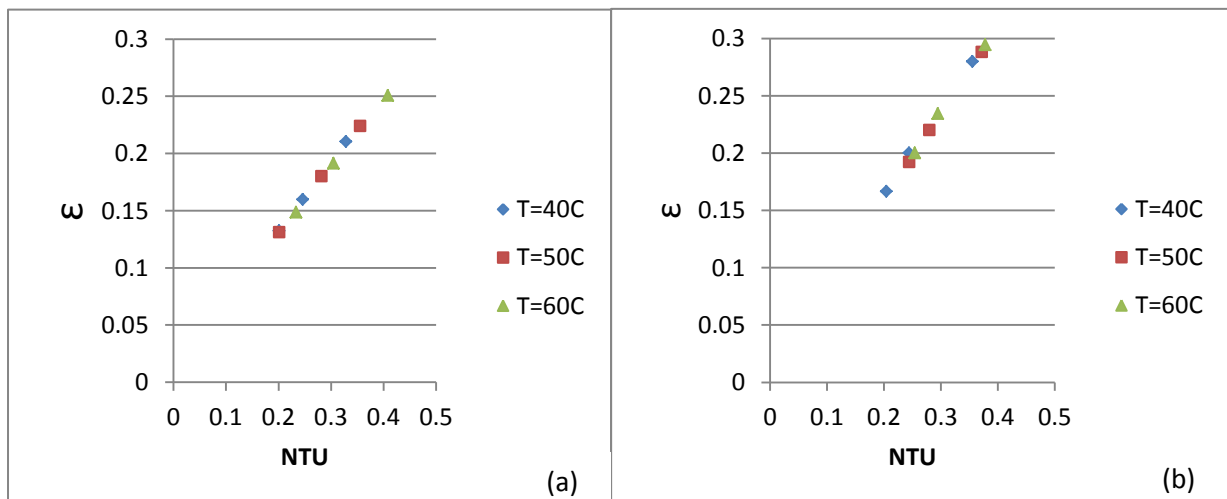


Figure (5-63) Variation of effectiveness with number of transfer units (NTU) in corrugated tube ($z/d=0.5$) at $\dot{v}_c=3\text{LPM}$ in different temperatures in (a) water and (b) Nano fluid

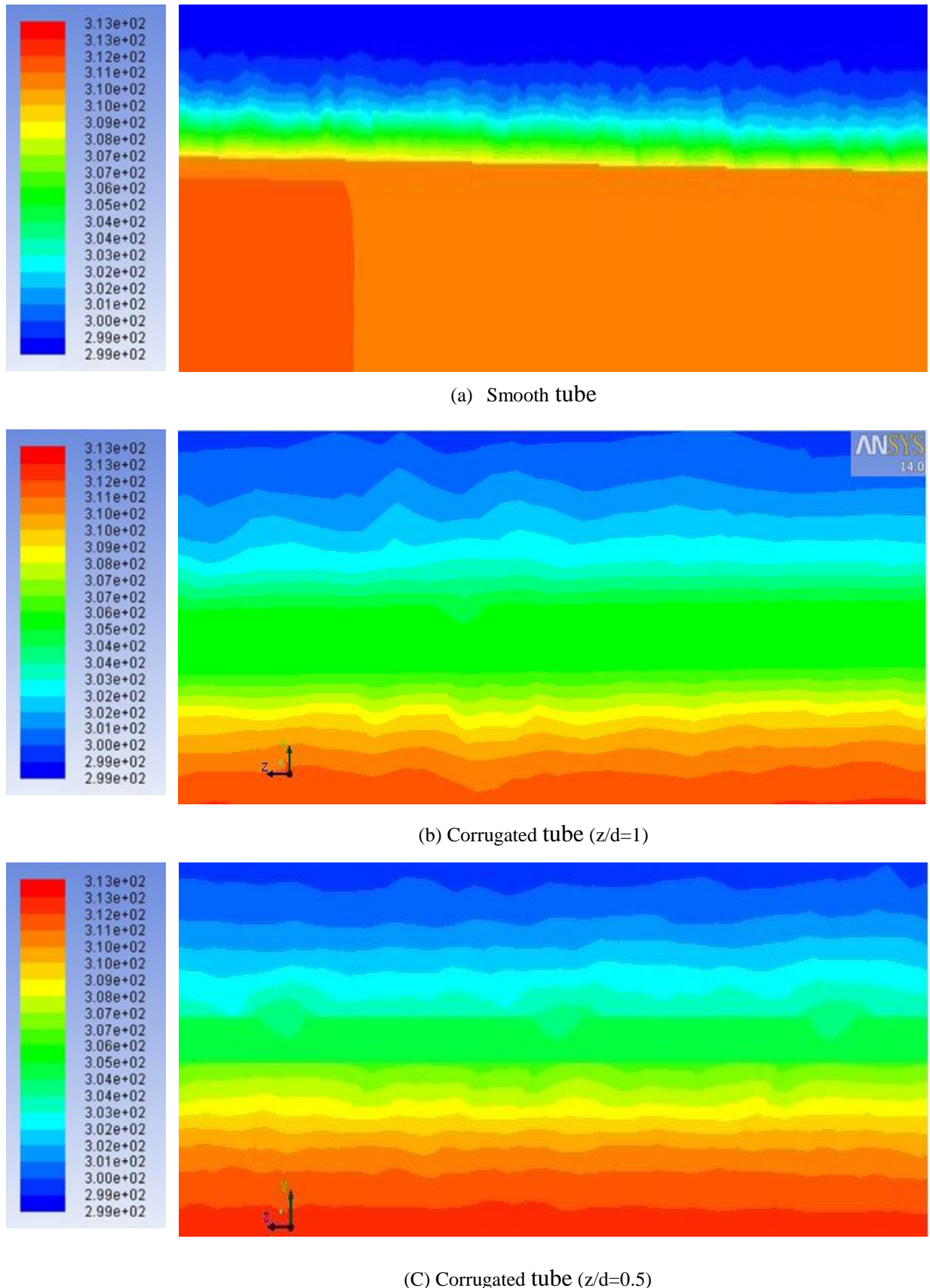
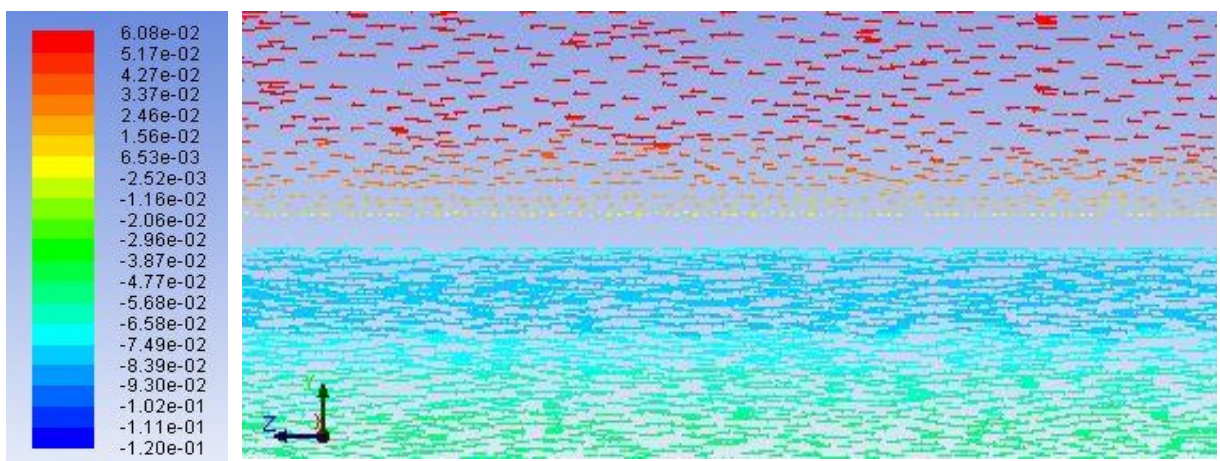


Figure (5-64) longitudinal section in tubes show the effect of corrugated in heat transfer



(a) Smooth tube

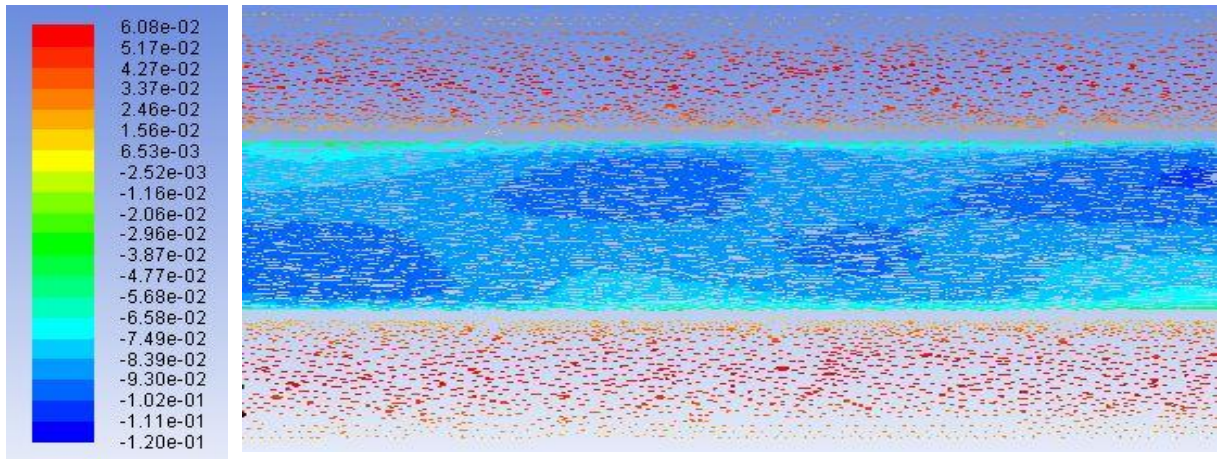
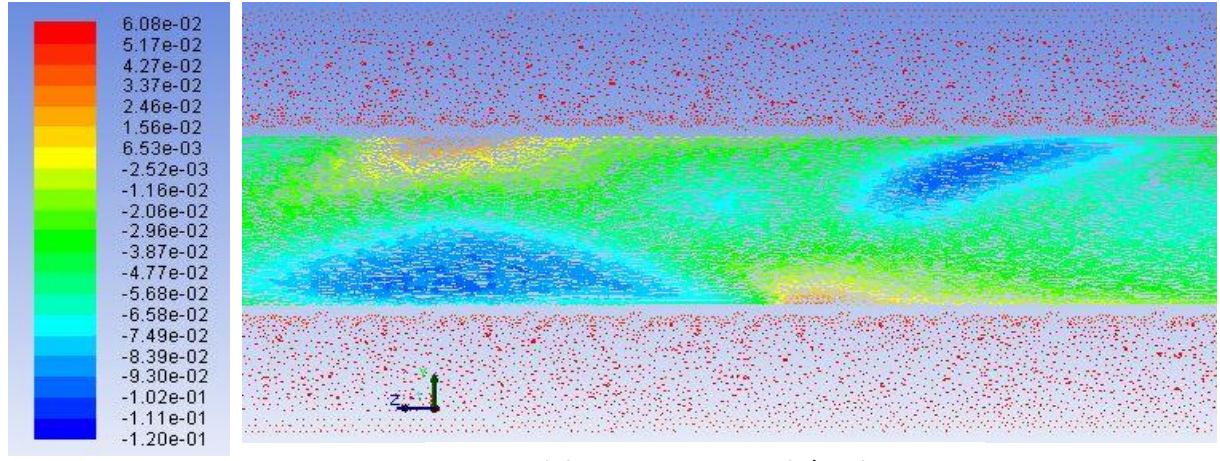
(b) Corrugated tube ($z/d=1$)(b) Corrugated tube ($z/d=1$)

Figure (5-65) longitudinal section in tubes show the effect of corrugated in velocity

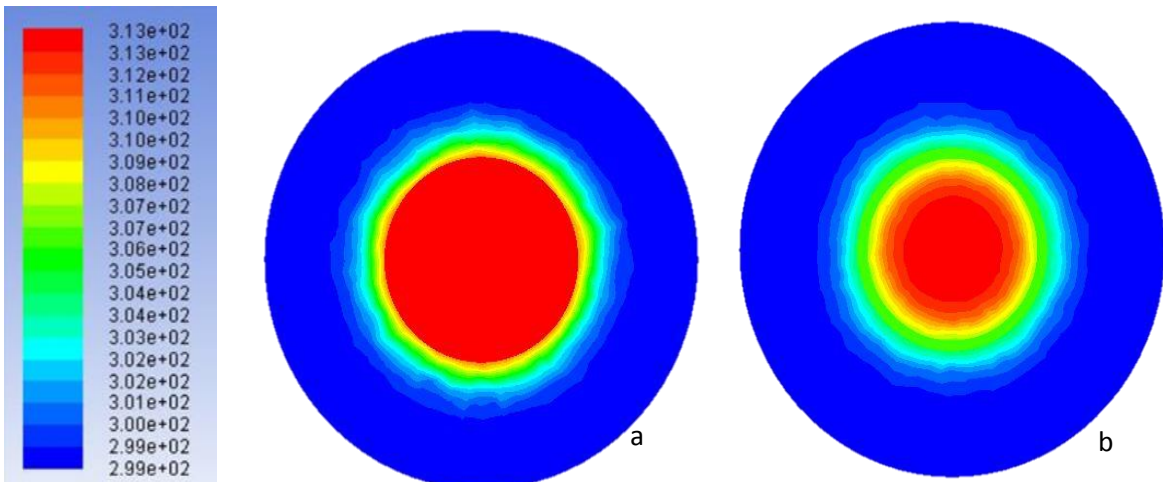


Figure (5-66) section in $z=50\text{cm}$ in test section smooth tube at $T_h=40\text{ }^{\circ}\text{C}$
 (a) at $\dot{v}_c=3\text{LPM}$ (b) at $\dot{v}_c=7\text{LPM}$

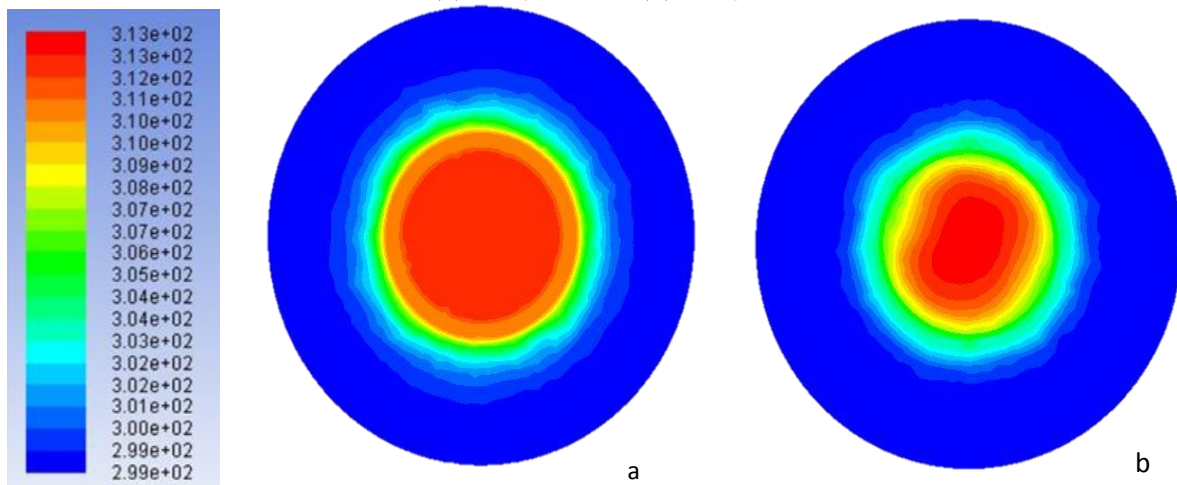


Figure (5-67) section in $z=50\text{cm}$ in test section corrugated tube ($z/d=1$) at $T_h=40\text{ }^{\circ}\text{C}$
 (a) at $\dot{v}_c=3\text{LPM}$ (b) at $\dot{v}_c=7\text{LPM}$

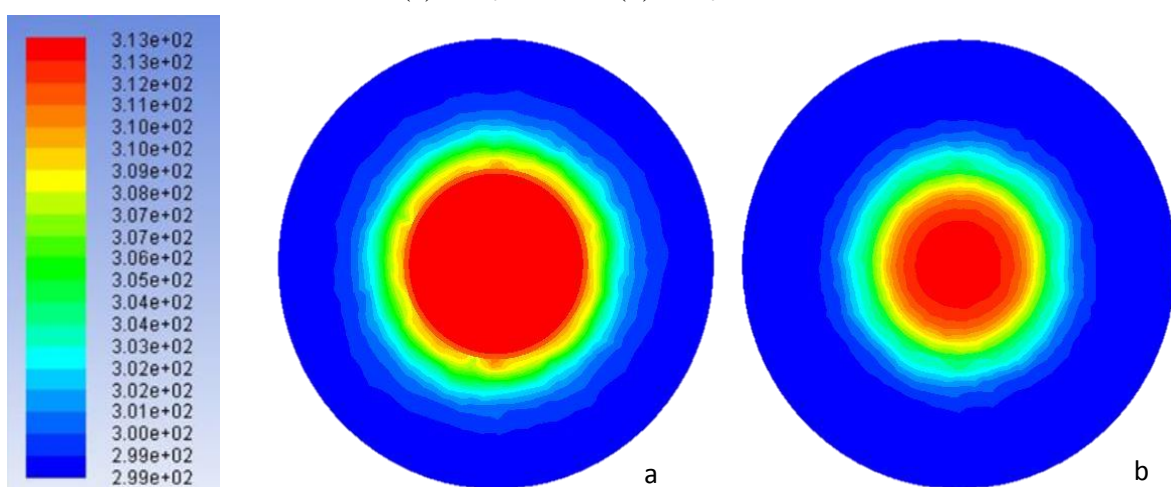
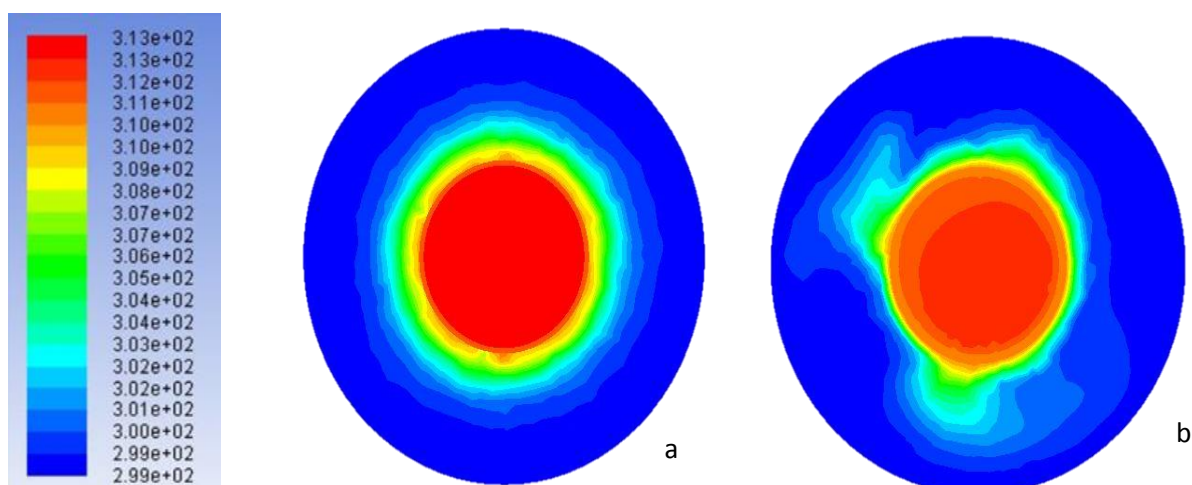
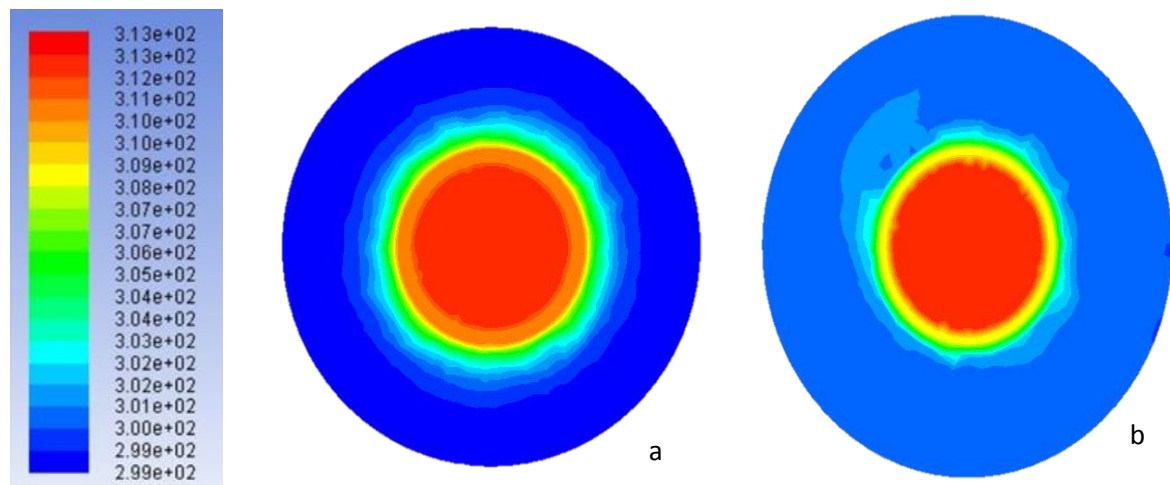
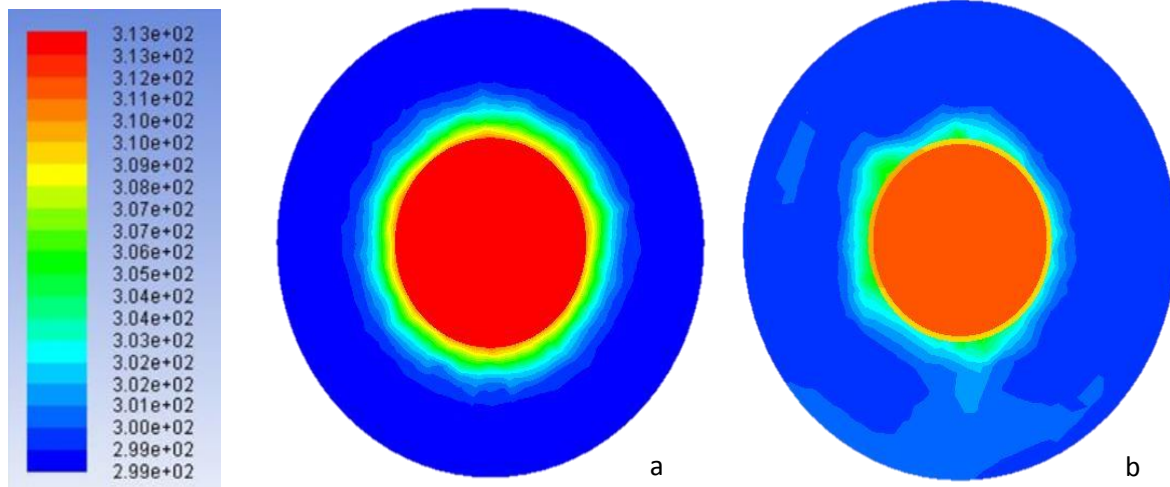


Figure (5-68) section in $z=50\text{cm}$ in test section corrugated tube ($z/d=0.5$) at $T_h=40\text{ }^{\circ}\text{C}$
 (a) at $\dot{v}_c=3\text{LPM}$ (b) at $\dot{v}_c=7\text{LPM}$



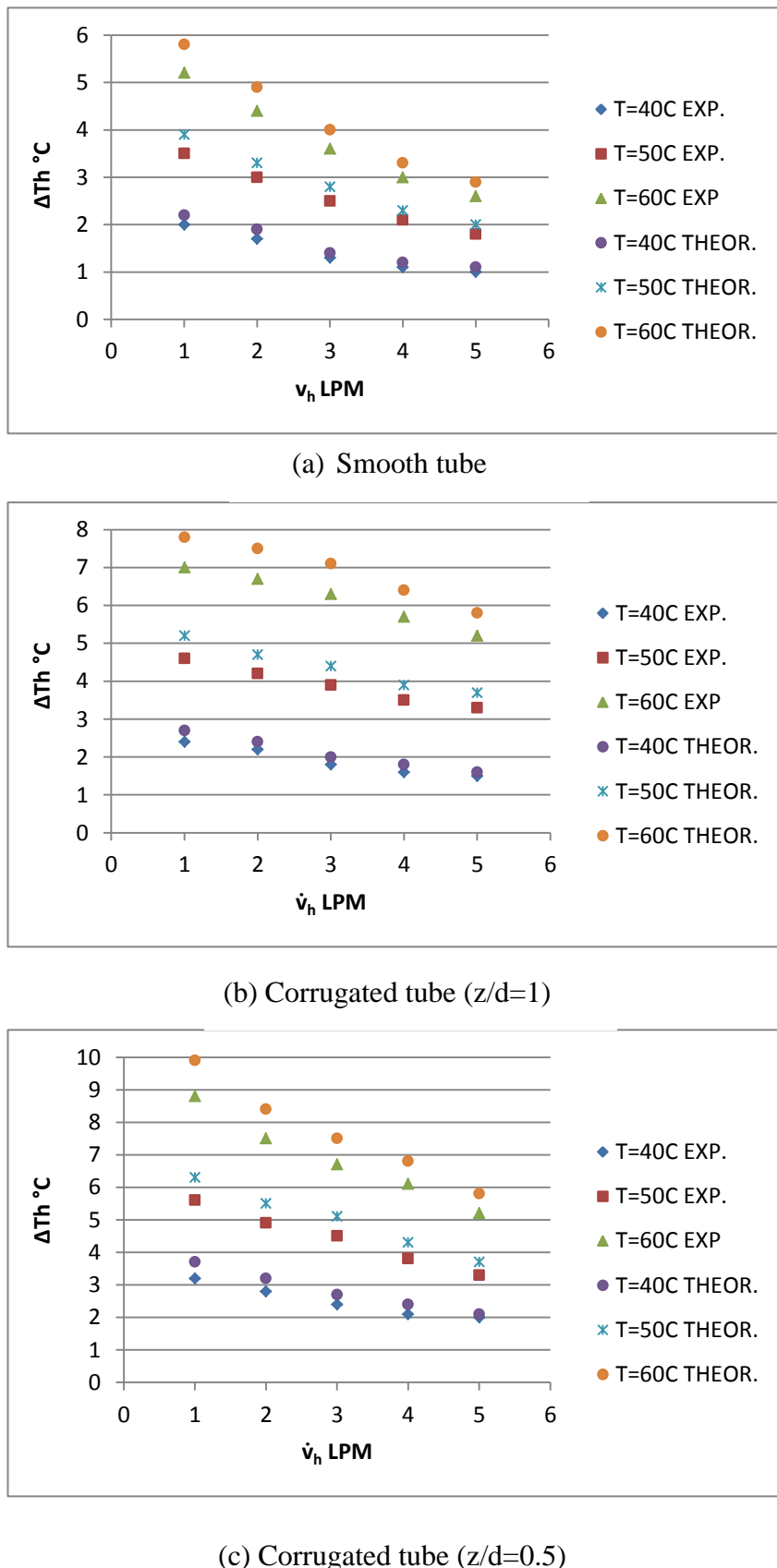


Figure (5-72) Comparison of experimental results and theoretical work

Chapter Six

Conclusions and Recommendations

Introduction

The present work studies experimentally and numerically the effect of change the tube geometry and used Nano particles on heat transfer in heat exchanger at different hot and cold temperatures as well as hot mass flow rates.

In this chapter, the conclusions of this study and the recommendations for the future search have been viewed.

6.1 Conclusions

Important conclusions resulting from this work will be summarized in the following points:

1. The corrugated tube enhancement heat transfer in heat exchanger, this is clear in hot temperature difference and heat dissipation , the behavior of change show clearly as directly proportional for both.
2. The maximum enhancement percentages in hot temperature difference for two corrugated pipes ($z/d= 1, 0.5$) are (36.43, 50.31), (42.44, 51.12) and (44.26, 52.12) at temperatures (40, 50, 60°C) respectively.
3. The maximum enhancement percentages in heat dissipation for two corrugated pipes ($z/d= 1, 0.5$) are (40.4, 52.2), (45.4, 52.69) and (47.66, 52.78) at temperatures (40, 50, 60°C) respectively.
4. The behavior of the hot temperature difference is inversely with increase hot water mass flow rates, but the heat dissipation directly proportionally.
5. The behavior of cold temperature different increase directly proportional with volumetric hot water flow rate and inversely with volumetric cold water flow rate.

6. The important enhancement in effectiveness heat exchanger by using corrugated on outer surface of inner pipe. Directly proportionally behavior with change tube geometry and increase cold mass flow rates and maximum enhancement is 69.17%.
7. Adding AL₂O₃ nanoparticles to base fluid (water) causes prominent augmentation in heat transfer for heat exchanger. The maximum enhancement percentages for used Nano fluid are (46.91, 55.67), (50.32, 55.43) and (51.69, 55.29) for smooth and corrugated pipes ($z/d=1, 0.5$) respectively.
8. Numerical simulation proved that the corrugated tube would enhance heat dissipation during the heat exchanger greater than smooth tube. It is noted that the behavior of heat transfer increases by change tube geometry and increase volumetric cold water flow rate.
9. Numerical simulation shows the enhancement in heat transfer by using Nano fluid.

6.2 Recommendations

The following recommendations are suggested for an amplification of the present work in the future:

1. Studying the effect of new tubes with different geometry like longitudinal grooves with different ratio of height and width.
2. Studying the effect of longitudinal fins that made from the same tube and the effect of change high and numbers of fins.
3. Research the effect of new type's inner surface of the shell (pins, serrated..... etc.).
4. Study the effect of inner corrugated surfaces pipe on heat transfer in the counter flow heat exchanger
5. Studying the effect of adding natural type's nanoparticles.
6. Studying the effect of select other types of base fluids such as refrigerants.

REFERENCES

1. Resat Selbaş, Önder Kızılıkana, Marcus Reppichb, “A new design approach for shell-and-tube heat exchangers using genetic algorithms from economic point of view”, Chemical Engineering and Processing: Process Intensification, Volume 45, Issue 4, April 2006, Pages 268–275.
2. Kevin M. Lunsford, “Increasing Heat Exchanger Performance”, Bryan Research and Engineering, Inc. – Technical Papers, Bryan, Texas, 1998.
3. Yunus A. Cengel, “heat transfer”, 2nd edition by Mc Graw Hill International Edition companies, 2003.
4. B. Chandra Sekhar, D. Krishnaiah, F. Anand Raju, “Thermal Analysis of Multi Tube Pass Shell and Tube Heat Exchanger”, International Journal of Innovative Research in Science, Engineering and Technology, vol. 3, Issue 11, November 2014, Pages 17605-17612.
5. Version 2011 © European Aluminum Association (auto@eaa.be)
6. Jelly Workz, Ukraine, 2013 – 2015, Products & Services / Product Portfolio / Applications.
7. Sondex Spiral Heat Exchangers, Sondex A/S , Jernet 9, DK-6000 Kolding , Denmark • info@sondex.dk, www.sondex.dk
8. Computer cooling, From Wikipedia, the free encyclopedia, 2015.
9. Spirax-Sarco Limited, Charlton House, Cheltenham, Gloucestershire, GL53 8ER, UK, enquiries@uk.spiraxsarco.com, 2014 Spirax-Sarco is a registered trademark of Spirax-Sarco Limited.
10. GE oil and Gas, Ge.com/oil and gas, 2011, General Electric Company.
11. Heat exchangers for hygienic use, by Alfa Laval, www.alfalaval.com, 2015.
12. Dr. Arun Muley, “Advanced Heat Exchangers for Enhanced Air-Side Performance: A Design and Manufacturing Perspective”, Boeing

Reference

- Research and Technology, Huntington Beach, CA, USA, in ARPA-E Advanced Dry Power Plant Cooling Workshop, Chicago, IL, May 12-13.
- 13. Office of Energy Efficiency and Renewable Energy, Washington, DC, USA, 2015.
 - 14. Plate Heat Exchanger for Marine Application, www.tranter.com, marine@se.tranter.com, 2010.
 - 15. Chemical industry GEA Heat Exchangers, 2015.
 - 16. Heat Exchanger Services Vancouver, “Heat Exchangers in an Aircraft”, 2013.
 - 17. Petrochemicals, API Schmidt-Bretten, GmbH Co. KG, Langenmorgen 4, 75015 Bretten, Germany, info@apischmidt-bretten.de, 2015.
 - 18. Calgavin Limited, “Most common Heat Exchanger Problems”, Station Road, Alcester, Warwickshire, B49 5ET, UK, <mailto:website@calgavin.com>, November 23, 2011.
 - 19. Chem-Engineering Services, “Solving Heat Exchanger Problems”, 1500 Glenmar Avenue Monroe, Louisiana 71201 USA, glenng@chemengservices.com, 2015.
 - 20. K. Boomsma, D. Poulikakos, F. Zwick, “ Metal foams as compact high performance heat exchangers”, Mechanics of Materials, Vol. 35, Issue 12, December 2003, Pages 1161–1176.
 - 21. N. Sahiti, F. Durst, A. Dewan, “Heat transfer enhancement by pin elements”, IJHMT, vol. 48, Issues 23–24, November 2005, Pages 4738–4747.
 - 22. Simin Wang, Jian Wen, Yanzhong Li, “An experimental investigation of heat transfer enhancement for a shell and tube heat exchanger”, Applied Thermal Engineering, Vol. 29, Issues 11–12, August 2009, Pages 2433–2438.
 - 23. Chinaruk Thianponga, Petpices Eiamsa-arda, Khwanchit Wongchareeb, Smith Eiamsa-ardc, “ Compound heat transfer enhancement of a dimpled

Reference

- tube with a twisted tape swirl generator”, International Communications in Heat and Mass Transfer, Vol. 36, Issue 7, August 2009, Pages 698–704.
24. Qasim J. M. Slaiman, Abbas N. Znad, “Enhancement of Heat Transfer in The Tube-Sid of A Double Pipe Heat Exchanger by Wire Coils”, Nahraian University, College of Engineering Journal (NUCEJ), Vol.16, No.1, 2013, pp.51-57.
25. K. Vijay, S A K Jilani, A Ramakrishna, “Heat Transfer Analysis through Corrugated Twisted Pipe”, IJMECA, Vol 2, Issue 5, Sept - Oct- 2014, pp. 155 -159.
26. Shweta Y. Kulkarni, Jagadish S.B., Manjunath M.B., “Analyses Comparing Performance of a Conventional Shell and Tube Heat Exchanger using Kern, Bell and Bell Delaware Method”, IJRET, Vol. 3, Issue 3,May 2014,pp.486-496.
27. Sidi El Bécaye Maïga, Cong Tam Nguyen, Nicolas Galanis, Gilles Roy, Thierry Maré, Mickaël Coqueux, “Heat transfer enhancement in turbulent tube flow using Al₂O₃ nanoparticle suspension”, International Journal of Numerical Methods for Heat & Fluid Flow, Vol. 16, 2006,Iss: 3, pp.275 – 292.
28. Paisarn Naphon, , Pichai Assadamongkol, Teerapong Borirak, “ Experimental investigation of titanium Nano fluids on the heat pipe thermal efficiency”, International Communications in Heat and Mass Transfer ,Volume 35, Issue 10, December 2008, Pages 1316–1319.
29. sk. M. Z. M. Saqheeb Ali, k. Mohan Krishna, S. D. V. V. S. Bhimesh Reddy, sk.R.S.M.Ali, “Thermal Analysis of Double Pipe Heat Exchanger by Changing the Materials Using CFD”, IJETT, Vol. 26 Number 2, August 2015, pp. 95-102. 46
30. Eiyad Abu-Nada, “ Effects of variable viscosity and thermal conductivity of Al₂O₃-water Nano fluid on heat transfer enhancement in natural

- convection”, International Journal of Heat and Fluid Flow Volume 30, Issue 4, August 2009, Pages 679–690.
31. K.B. Anoop, T. Sundararajan, Sarit K. Das, “Effect of particle size on the convective heat transfer in Nano fluid in the developing region”, International Journal of Heat and Mass Transfer Vol. 52, Issues 9–10, April 2009, Pages 2189–2195.
32. K.Y. Leonga, R. Saidura, T.M.I. Mahliaa, Y.H. Yaua, “Modeling of shell and tube heat recovery exchanger operated with Nano fluid based coolants”, IJHMT, Vol. 55, Issue 4, 31 January 2012, Pages 808–816.
33. Reza Aghayari, Heydar Maddah, Malihe Zarei, Mehdi Dehghani, Sahar Ghanbari Kaskari Mahalle, “Heat Transfer of Nano fluid in a Double Pipe Heat Exchanger”, International Scholarly Research Notices Volume 2014, Article ID 736424, 7 pages.
34. V. Santhosh Cibi, K. Gokul raj, P. Kathiravan, R. RajeshKanna, B. Ganesh, Dr. S. Sivasankaran, V. VedhagiriEswaran, “Convective heat transfer enhancement of graphite Nano fluids in shell and tube heat exchanger”, IJIRSET, Vol. 3, Special Issue 2, April 2014, pp.270-275.
35. Aphichat Danwittayakul, Cattaleeya Pattamaprom, “Investigation of Heat Transfer Efficiency of Alumina Nano fluids in Shell and Tube Heat Exchanger”, IPCBEE, Vol.82, 2015, pp. 68-72.
36. Arun Kumar Tiwari, “Thermal Performance of Shell and Tube Heat Exchanger Using Nano fluids”, IJAPME, Vol. 1, Issue -1, 2015, 27-31.
37. Somchandra Patel, Vijay Patel, Vishal Thakkar, “Experimental Investigation of Diameter effect of Al_2O_3 Nano fluid on Shell and tube heat exchanger in laminar flow regime”, IJAREST, Vol. 2, Issue No. 5, May-2015,pp.1-5.
38. Asmaa H.Dhiaa, Majid I. Abdulwahab, S.M.Thahab, “Study the Convective Heat Transfer of TiO_2 /Water Nano fluid in Heat Exchanger System”, the authors would like to acknowledge the assistance offered by

- Nanotechnology and Advanced Materials Research Unit (NAMRU),
College of Engineering /University of Kufa /Iraq, 2015, pp. 1-15.
39. Mon M. S. and Gross U., "Numerical study of Fin-Spacing Effects in Annular-Finned Tube Heat Exchangers", International Journal of heat and Mass Transfer, Vol. 47, pp. 1953-1964, 2004.
 40. Lars Davidson, "An Introduction to Turbulence Models", department of thermos and fluid dynamics, Chalmers University of Technology, Sweden, 2009.
 41. Rebay S., "Efficient Unstructured Mesh Generation By Means Of Delainay Triangulation and Bowyer–Watson Algorithm", Journal of Computational Physics, Vol.106, pp.125-138, 1993.
 42. "ANSYS Fluent User's Guide", ANSYS Inc., South pointe 275 Technology Drive Canonsburg, 2011.
 43. Versteeg H. K., Malalasekera W., "An Introduction to Computational Fluid Dynamics, the Finite Volume", Longman Group Limited, 1995.
 44. Nitesh B. Dahare, "Review on Experimental Analysis and Performance Characteristic of Heat Transfer In Shell and Twisted Tube Heat Exchanger", International Journal of Engineering Research and General Science Vol. 3, pp. 981-985, Issue 1, January-February, 2015.
 45. Petukhov, B.S. Heat transfer and friction in turbulent referred to in hand –book of single-phase convective pipe flow with variable physical properties. In heat transferred. T.F. Irvine and J.P. New York, Wiley Interscience, 1987. Hartnett, Vol. 6, Academic Press, New York, 1970.
 46. Maxwell J. C., Garnett, "Colors in Metals Glasses and in Metallic Films", Philosophical transactions of the Royal Society of London. Series A, Containing Papers of a Mathematical or Physical Character, Vol.203, pp.385–420, 1904.

Reference

47. Yu, W. and S. U. S. Choi, "The Role of Interfacial Layers in the Enhanced Thermal Conductivity of Nano fluids: A Renovated Maxwell Model", Journal of Nanoparticles Research, Vol.5, pp.167–171, 2003.
48. Buongiorno, J., "Convective Transport in Nano fluids", Journal of Heat Transfer, pp.128–240, 2006.
49. Sudarmadji Sudarmadji, Sudjito Soeparman, Slamet Wahyudi, Nurkholis Hamidy, "Effects of Cooling Process of Al₂O₃-water Nano fluid on Convective Heat Transfer", IJERGS, VOL. 42, No 2, pp. 155-160, 2014.
50. David R. Lide, "CRC Handbook of Chemistry and Physics", Former Director, Standard Reference Data, National Institute of Standards and Technology, 2005.
51. Fei Duan, "Thermal Property Measurement of Al₂O₃-Water Nano fluids", School of Mechanical and Aerospace Engineering, Nanyang Technological University, Singapore.
52. Visinee Trisaksri, Somchai Wongwises, "Critical Review of Heat Transfer Characteristics of Nano fluids", King Mongkut's University of Technology Thonburi, Bangkok, Thailand , 2006.
53. J. P. Hollman, " Heat Transfer", Department of Mechanical Engineering, Southern Methodist University, 10th edition by Mc Graw. Hill International Edition companies, 2010.
54. Wen D., Ding Y. , "Experimental Investigation into Convective Heat Transfer of Nano fluids at the Entrance Region under Laminar Flow Conditions", International Journal of Heat and Mass Transfer Vol.47, pp.5181-5188, 2004.
55. Ramesh K. Shah, Dušan P. Sekulić, "Fundamentals of Heat Exchanger Design", Jon Wiley & Sons, 2003.
56. Wang, X., Xu X. and Choi S. U. S., "Thermal Conductivity of Nanoparticle–fluid Mixture", Journal of Thermo physics and Heat Transfer, Vol.13, pp.474-480, 1999.

Reference

57. Palm S. J., Roy G., Nguyen C. T., "Heat Transfer Enhancement with the Use of Nano fluids in Radial Flow Cooling Systems Considering Temperature–Dependent Properties", Applied Thermal Engineering, Vol.26, pp. 2209-2218, 2006.
58. Özden Ağra, Hakan Demir, Ş. Özgür Atayılmaz, Fatih Kantaş, Ahmet Selim Dalkılıç, "Numerical investigation of heat transfer and pressure drop in enhanced tubes", International Communications in Heat and Mass Transfer, Vol. 38, pp. 1384-1391, 2011.

APPENDIX [A] EQUATIONS

A.1. Mean Temperature.

All properties of the hot and cold water with and without nanoparticles calculated at the mean temperature as shown in the following equation.

$$T_m = \frac{T_{in} + T_{out}}{2} \quad (A.1)$$

A.2. Mass Flow Rate

The mass flow rate can be calculated by using the following equation with unit (kg/sec).

$$\dot{m} \frac{\text{kg}}{\text{sec}} = \dot{V} \frac{\text{L}}{\text{M}} \times \frac{1\text{M}}{60 \text{ sec}} \times \rho \frac{\text{kg}}{\text{m}^3} \times \frac{1\text{m}^3}{1000\text{L}} \quad (A.2)$$

A.3. Non-dimensional Numbers

The dimensionless numbers are essential parameters in the calculation forced or free convection, and all the physical properties which are required in the calculation of the dimensionless numbers are taken at the mean temperature.

A.3.1 Reynolds Number

Reynolds number is the ratio between the inertia forces to the viscous force of the boundary layer of velocity [53].

$$\text{For hot side: } Re_h = \frac{u_h \rho_h d_i}{\mu_h} \quad (A.3)$$

$$\text{For cold side: } Re_c = \frac{u_c \rho_c D_h}{\mu_c} \quad (A.4)$$

$$u = \frac{\dot{m}}{\rho A_c} \quad (A.5)$$

$$\text{For hot side: } A_{c,ip} = \frac{\pi}{4} d_i^2 \quad (A.6)$$

$$\text{For cold side (smooth), } A_{cs} = \frac{\pi}{4} (D_i^2 - d_o^2) \quad (A.7)$$

Appendix [A]

Hydraulic diameter finds by following equations.

$$D_h = \frac{4A_{cs}}{P} \quad (A.8)$$

$$P = \pi D_i \quad (A.9)$$

For cold side (corrugated), find two outer diameters in the pipe,

$$d_{o1} = 19.05 \text{ mm}, d_{o2} = 18.55 \text{ mm}$$

Then use mean outer diameter, $d_{om} = \frac{d_{o1} + d_{o2}}{2}$

$$A_{cs,c} = \frac{\pi}{4} (D_i^2 - d_{om}^2) \quad (A.10)$$

A.3.2 Nusselt Number

The ratio between the conduction thermal resistance to the convection thermal resistance and it is represented by the following formula [3].

$$Nu = \frac{hd}{k_f} \quad (A.11)$$

For laminar flow and corrugated outer surface [3]

$$Nu_c = \frac{h_c D_{hc}}{k_c} \quad (A.12)$$

For laminar flow and Nano fluid [37]

$$Nu_{nf} = 0.031(Re Pr)^{0.68}(1 + \varphi)^{95.73} \quad (A.13)$$

For turbulent flow [3]

$$Nu = 0.023Re^{0.8}Pr^n \quad (A.14)$$

Where, [n = 0.3 for cooling, n = 0.4 for heating]

With condition, [$Re \geq 10000$, $0.6 \leq Pr \leq 160$, $\frac{L}{D} \geq 10$]

A.3.3 Prandtl Number

Prandtl number can be obtained from [3]:

$$Pr = \frac{\mu C_p}{k} \quad (A.15)$$

For Nano fluid [57]

$$Pr_{nf} = \frac{\mu_{nf} C_{p,nf}}{k_{nf}} \quad (A.16)$$

A.4. Heat Dissipation

The heat dissipation of both sides under these conditions [3]:

$$Q_c = \dot{m}_c C_{pc} (T_{co} - T_{ci}) \quad (\text{A.17})$$

And:

$$Q_h = \dot{m}_h C_{ph} (T_{ho} - T_{hi}) \quad (\text{A.18})$$

The product of mass flow rate and specific heat is called heat capacity rate:

$$C_c = \dot{m}_c C_{pc} \quad \text{And} \quad C_h = \dot{m}_h C_{ph} \quad (\text{A.19})$$

Can be expressed equations (A-17) and (A-18) as:

$$Q_c = C_c (T_{co} - T_{ci}) \quad (\text{A.20})$$

And

$$Q_h = C_h (T_{ho} - T_{hi}) \quad (\text{A.21})$$

The heat dissipation during this study is calculated by using the temperature difference on the water side in equation (A.17) and (A.18). This is because parameters are measured accurately in this zone.

In the heat exchanger, the heat dissipation can also be expressed as:

$$Q = U * A_s * \text{LMTD} * F \quad (\text{A.22})$$

The correction factor can be taken (1). This is because of the counter flow arrangement and has one pipe and one shell within the present heat exchanger.

A.5. Log Mean Temperature Difference (LMTD)

The following equation is used to estimate the log mean temperature difference according to counter flow arrangement [3]:

$$\text{LMTD} = \frac{\Delta T_2 - \Delta T_1}{\ln\left(\frac{\Delta T_2}{\Delta T_1}\right)} = \frac{\Delta T_1 - \Delta T_2}{\ln\left(\frac{\Delta T_1}{\Delta T_2}\right)} \quad (\text{A.23})$$

Where, $\Delta T_1 = T_{hi} - T_{co}$ And $\Delta T_2 = T_{ho} - T_{ci}$

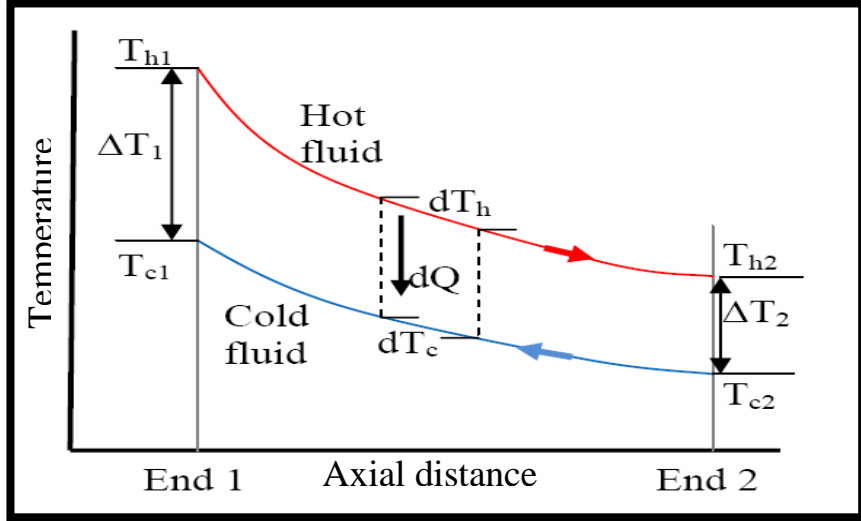


Figure (A.1) temperature distribution in counter flow heat exchanger

A.6. Overall Heat Transfer Coefficient (U)

The heat exchanger system contains two flowing fluids separated by a solid wall. The overall heat transfer coefficient of this mechanism can be expressed [55]:

$$\frac{1}{UA} = \frac{1}{U_i A_i} = \frac{1}{U_o A_o} = \frac{1}{h_i A_i} + \frac{\ln\left(\frac{d_o}{d_i}\right)}{2\pi k_t L} + \frac{1}{h_o A_o} \quad (A.24)$$

Because of the high value of thermal conductivity of the copper tube, the thermal resistance (third term on the left side) can be neglected.

For smooth pipe:

$$A_i = \pi d_i L \quad \text{and} \quad A_o = \pi d_o L \quad (A.25)$$

For corrugated pipe [53]:

$$A_{oc} = A_{os,s} + N A_c \quad (A.26)$$

$$A_{oss} = \pi d_o (L - N * S_{corr.}) \quad (A.27)$$

$$A_c = 121.04 * 10^{-6} m^2 \quad (A.28)$$

In equation (A.9), the overall heat transfer coefficients (U_o and U_i) appear due to the difference between the two heat transfer areas (A_o and A_i):

$$U_o A_o = U_i A_i \quad (A.29)$$

A.7. Inner Side Heat Transfer Coefficient (h_i)

The heat transfer coefficient of water in the inner side (hot water) calculated by the Newton's law of cooling [3]:

$$h_i = \frac{Q_h}{A_i \Delta T_h} \quad (\text{A.30})$$

$$\Delta T_h = T_{hi} - T_{ho} \quad (\text{A.31})$$

and heat transfer rate is calculated from equation:

$$Q_h = \dot{m}_h C_{ph} \Delta T_h \quad (\text{A.32})$$

A.8. Outer Side Heat Transfer Coefficient (h_o)

The cold water side heat transfer coefficient in annuli for both smooth tube and corrugated tube will be discussed as follows [3]:

A.8.1 Smooth Pipe

To calculate the cold side heat transfer coefficient for smooth copper pipe can be calculated by using the following relation.

$$h_o = \frac{1}{\frac{1}{U_o} + \frac{A_o}{h_i A_i}} \quad (\text{A.33})$$

A.8.2 Corrugated Pipe

Cold side heat transfer coefficient with corrugated pipe on the outer surface of inner pipe can be calculated by using the relation:

$$h_o = \frac{1}{\frac{1}{U_o} + \frac{A_o}{h_i A_i}} \quad (\text{A.34})$$

$$D_h = \frac{4A_{c,e}}{P_e} \quad (\text{A.35})$$

$$A_{c,e} = \frac{\pi}{4} D_e^2 \quad (\text{A.36})$$

$$P_e = \pi D_e \quad (\text{A.37})$$

$$D_e = \frac{D_s + D_c}{2} \quad (\text{A.38})$$

A.9 Pressure Drop (ΔP)

The value of pressure drop can be found by using the equation [3]:

$$\Delta P = f \frac{L}{d} \rho \frac{u_m^2}{2g_c} \quad (\text{A.39})$$

Darcy friction factor find by equation

Laminar flow [53]:

$$f = \frac{64}{\text{Re}_d} \quad (\text{A.40})$$

For laminar flow with Nano fluid [37]:

$$f_{nf} = 26.4 \text{Re}^{-0.8737} (1 + \varphi)^{156.23} \quad (\text{A.41})$$

For turbulent flow Blasius's equation

$$f = \frac{0.316}{\text{Re}^{0.25}} \quad 2000 \leq \text{Re} \leq 100000 \quad (\text{A.42})$$

A.10 Thermo-physical Properties of Nanofluid

Specific heat, density, viscosity and thermal conductivity formulas and correlations will be included in the following sections:

A.10.1 Volume Concentration

The volume concentration for nanoparticles in base fluid is finding by the relation:

$$\varphi \% = \frac{\left(\frac{m_p}{\rho_p}\right)}{\left(\frac{m_p}{\rho_p}\right) + \left(\frac{m_{bf}}{\rho_{bf}}\right)} \quad (\text{A.43})$$

A.10.2 Thermal Conductivity

Buongiorno equation [48]:

$$k_{nf} = k_{bf}(1 + 7.47\varphi) \quad (\text{A.44})$$

A.10.3 Dynamic Viscosity

The viscosity of (Al_2O_3) Nanofluid given by **Wang et al.** [56] as follows:

$$\mu_{nf} = \mu_{bf}(123\varphi^2 + 7.3\varphi + 1) \quad (\text{A.45})$$

A.10.4 Density

To calculate density of Nano fluid using mixture rule as follow:

$$\rho_{nf} = (1 - \varphi)\rho_{bf} + \varphi\rho_p \quad (\text{A.46})$$

A.10.5 Specific Heat

The calculation of specific heat by **Palm et al.** [57] equation:

$$Cp_{nf} = (1 - \varphi)Cp_{bf} + \varphi C_p \quad (\text{A.47})$$

A.11 Heat Exchanger Effectiveness

“The effectiveness is the ratio of the actual heat transfer to the maximum possible amount of heat transfer during the operation of heat exchanger”. It can be written as follows [3]:

$$\varepsilon = \frac{\Delta T_{login}}{T_{hi} - T_{ci}} \quad (\text{A.48})$$

APPENDIX [B]
Sample of calculation

In smooth pipe at the condition:

Hot side (pipe side) Cold side (shell side)

$$T_{hin} = 40 \text{ } ^\circ\text{C} \quad T_{cin} = 25 \text{ } ^\circ\text{C}$$

$$T_{hout} = 39 \text{ } ^\circ\text{C} \quad T_{cout} = 26.9 \text{ } ^\circ\text{C}$$

$$\dot{v}_{hin} = 5 \text{ LPM} \quad \dot{v}_{cin} = 3 \text{ LPM}$$

All water properties taken at T_m for hot and cold water

$$T_m = \frac{T_{in} + T_{out}}{2}$$

$$T_{hm} = \frac{40+39}{2} = 39.5 \text{ } ^\circ\text{C}$$

$$T_{cm} = \frac{25+26.9}{2} = 25.95 \text{ } ^\circ\text{C}$$

T_m $^\circ\text{C}$	ρ kg/m ³	μ kg/m.s	k kW/m. $^\circ\text{C}$	C_p J/kg. $^\circ\text{C}$	Pr
39.5	992.26	0.00066	0.632	4174	4.38
25.95	996	0.00088	0.613	4179	5.97

$$\dot{m} \frac{\text{kg}}{\text{sec}} = \dot{m} \frac{\text{L}}{\text{M}} \times \frac{1\text{M}}{60 \text{ sec}} \times \rho \frac{\text{kg}}{\text{m}^3} \times \frac{1\text{m}^3}{1000\text{L}}$$

$$\dot{m}_{hin} \frac{\text{kg}}{\text{sec}} = 5 \frac{\text{L}}{\text{M}} \times \frac{1\text{M}}{60 \text{ sec}} \times 992.26 \frac{\text{kg}}{\text{m}^3} \times \frac{1\text{m}^3}{1000\text{L}} = 0.0827 \frac{\text{kg}}{\text{sec}}$$

$$\dot{m}_{cin} \frac{\text{kg}}{\text{sec}} = 3 \frac{\text{L}}{\text{M}} \times \frac{1\text{M}}{60 \text{ sec}} \times 996 \frac{\text{kg}}{\text{m}^3} \times \frac{1\text{m}^3}{1000\text{L}} = 0.0498 \frac{\text{kg}}{\text{sec}}$$

For hot side

$$A_{c,ip} = \frac{\pi}{4} d_{pin}^2$$

$$d_{ip} = 0.01705 \text{ m}$$

$$A_{c,ip} = \frac{\pi}{4} * 0.01705^2 = 0.000228 \text{ m}^2$$

For cold side

Appendix [B]

$$A_{c,is} = \frac{\pi}{4} (D_{is}^2 - d_{op}^2)$$

$$d_{op} = 0.01905 \text{ m}$$

$$D_{is} = 0.0426 \text{ m}$$

$$A_{cs} = \frac{\pi}{4} (0.0426^2 - 0.01905^2) = 0.00114 \text{ m}^2$$

$$D_{hs} = \frac{4A_{cs}}{P}$$

$$P = \pi D_{is}$$

$$P_{s\ in} = \pi * 0.0426 = 0.134 \text{ m}$$

Hydraulic diameter for cold section:

$$D_{hs} = \frac{4*0.00114}{0.134} = 0.034 \text{ m}$$

Velocity

$$u = \frac{\dot{m}}{\rho A_c}$$

$$u_h = \frac{0.0827}{992.26*0.000228} = 0.366 \frac{\text{m}}{\text{sec}}$$

$$u_c = \frac{0.0498}{996*0.00114} = 0.0439 \frac{\text{m}}{\text{sec}}$$

$$Re = \frac{u \rho d}{\mu} = \frac{ud}{v}$$

$$Re_h = \frac{0.366*992.26*0.01705}{0.00066} = 9381.82$$

$$Re_c = \frac{0.0439*996*0.034}{0.00088} = 1689.35$$

- Hot side is turbulent flow
- Cold side is laminar flow

For hot side (turbulent flow):

$$Nu = 0.023 Re^{0.8} Pr^n$$

n = 0.3 for cooling

$$Nu_h = 0.023 \times 9381.82^{0.8} \times 4.38^{0.3} = 53.95$$

$$h = \frac{Nu k}{d}$$

$$h_i = \frac{53.95*0.632}{0.01705} = 1999.79 \frac{\text{kW}}{\text{m}^2 \cdot ^\circ\text{C}}$$

$$Q_h = \dot{m} C_p \Delta T$$

$$Q_h = UA_s LMTD F$$

Appendix [B]

$$A_{is} = \pi d_{ip} L$$

$$A_{os} = \pi d_{op} L$$

F=1 because have one pipe and one shell

$$Q_h = 0.0827 * 4174 * (40 - 39) = 345.2 \frac{J}{sec} = 345.2 W$$

$$Q_c = 0.0498 * 4179 * (26.9 - 25) = 395.42 \frac{J}{sec} = 395.42 W$$

$$LMTD = \frac{\Delta T_1 - \Delta T_2}{\ln\left(\frac{\Delta T_1}{\Delta T_2}\right)}$$

$$\Delta T_1 = T_{hi} - T_{co}$$

$$\Delta T_2 = T_{ho} - T_{ci}$$

$$\Delta T_1 = 40 - 26.9 = 13.1 ^\circ C$$

$$\Delta T_2 = 39 - 25 = 14 ^\circ C$$

$$LMTD = \frac{13.1 - 14}{\ln\left(\frac{13.1}{14}\right)} = 13.54^\circ C$$

$$U_i = \frac{345.2}{\pi * 0.01705 * 13.54 * 1 * 1} = 475.97 \frac{W}{m^2 \cdot ^\circ C}$$

$$\frac{1}{U_i A_i} = \frac{1}{U_o A_o}$$

$$U_o = U_i \left(\frac{A_i}{A_o} \right)$$

$$A_{is} = \pi * 0.01705 * 1 = 0.0536 m^2$$

$$A_{os} = \pi * 0.01905 * 1 = 0.0598 m^2$$

$$U_o = 475.97 * \left(\frac{0.0536}{0.0598} \right) = 426.62 \frac{W}{m^2 \cdot ^\circ C}$$

For cold side

From equation

$$\frac{1}{U_o A_o} = \frac{1}{h_i A_i} + \frac{1}{h_o A_o}$$

$$h_o = \frac{1}{\frac{1}{U_o} - \frac{A_o}{h_i A_i}}$$

$$h_o = \frac{1}{\frac{1}{426.62} - \frac{0.0536}{1999.79 * 0.0598}} = 426.7 \frac{kW}{m^2 \cdot ^\circ C}$$

$$Nu_c = \frac{426.7 * 0.034}{0.613} = 23.67$$

Appendix [B]

Pressure drop

$$\Delta P = \frac{f L \rho u_m^2}{2d}$$

Where:

For laminar flow Darcy equation

$$f = \frac{64}{Re}$$

For turbulent flow Blasius's equation

$$f = \frac{0.316}{Re^{0.25}} \quad 2000 \leq Re \leq 100000$$

sample	Unit	Hot side	Cold side
L	m	1	1
ρ	kg/m ³	992.26	996
d	m	0.01705	0.034
u	m/sec	0.366	0.0439

Hot side

$$f = \frac{0.316}{9381.82^{0.25}} = 0.0317$$

$$\Delta P = \frac{f L \rho u_m^2}{2d}$$

$$\Delta P = \frac{0.0317 * 1 * 992.26 * 0.366^2}{2 * 0.01705} = 123.6 \text{ Pa} = 1.236 \text{ mbar}$$

Cold side

$$f = \frac{64}{1689.35} = 0.0379$$

$$\Delta P = \frac{0.0379 * 1 * 996 * 0.0439^2}{2 * 0.034} = 1.07 \text{ Pa} = 0.0107 \text{ mbar}$$

Effectiveness

$$\varepsilon = \frac{1.9}{15} = 0.126$$

Appendix [B]

Sample of calculation in corrugated pipe at the condition:

Corrugated ratio ($z/d=1$)

Hot side (pipe side)

$$T_{hin} = 40.2 \text{ } ^\circ\text{C}$$

$$T_{hout} = 38.7 \text{ } ^\circ\text{C}$$

$$\dot{V}_{hin} = 5 \text{ LPM}$$

Cold side (shell side)

$$T_{cin} = 24.9 \text{ } ^\circ\text{C}$$

$$T_{cout} = 27.2 \text{ } ^\circ\text{C}$$

$$\dot{V}_{cin} = 3 \text{ LPM}$$

$$\dot{m} \frac{\text{kg}}{\text{sec}} = \dot{m} \frac{\text{L}}{\text{M}} \times \frac{1\text{M}}{60 \text{ sec}} \times \rho \frac{\text{kg}}{\text{m}^3} \times \frac{1\text{m}^3}{1000\text{L}}$$

All water properties taken at T_m for hot and cold water

$$T_m = \frac{T_{in} + T_{out}}{2}$$

$$T_{hm} = \frac{40.2 + 38.7}{2} = 39.45 \text{ } ^\circ\text{C}$$

$$T_{cm} = \frac{24.9 + 27.2}{2} = 26.05 \text{ } ^\circ\text{C}$$

T_m $^\circ\text{C}$	ρ kg/m^3	μ kg/m. s	k $\text{kW/m.}^\circ\text{C}$	C_p $\text{J/kg.}^\circ\text{C}$	Pr
39.45	992.28	0.00066	0.632	4174	4.38
26.05	995.98	0.00087	0.613	4179	5.95

$$\dot{m}_{hin} \frac{\text{kg}}{\text{sec}} = 5 \frac{\text{L}}{\text{M}} \times \frac{1\text{M}}{60 \text{ sec}} \times 992.28 \frac{\text{kg}}{\text{m}^3} \times \frac{1\text{m}^3}{1000\text{L}} = 0.0827 \frac{\text{kg}}{\text{sec}}$$

$$\dot{m}_{cin} \frac{\text{kg}}{\text{sec}} = 3 \frac{\text{L}}{\text{M}} \times \frac{1\text{M}}{60 \text{ sec}} \times 995.98 \frac{\text{kg}}{\text{m}^3} \times \frac{1\text{m}^3}{1000\text{L}} = 0.0498 \frac{\text{kg}}{\text{sec}}$$

For hot side

$$A_{c,ip} = \frac{\pi}{4} d_{pin}^2$$

$$d_{ip} = 0.01705 \text{ m}$$

$$A_{c,ip} = \frac{\pi}{4} * 0.01705^2 = 0.000228 \text{ m}^2$$

For cold side

$$d_{om} = \frac{d_{o1} + d_{o2}}{2}$$

Appendix [B]

$$d_{om} = \frac{19.05+18.55}{2} = 18.8\text{mm}$$

$$A_{cs,c} = \frac{\pi}{4} (D_i^2 - d_{om}^2)$$

$$A_{cs,c} = \frac{\pi}{4} (0.0426^2 - 0.0188^2) = 0.001148 \text{ m}^2$$

$$D_h = \frac{4*0.001148}{0.134} = 0.034\text{m}$$

$$u = \frac{\dot{m}}{\rho A_c}$$

$$u_h = \frac{0.0827}{992.28*0.000228} = 0.366 \frac{\text{m}}{\text{sec}}$$

$$u_c = \frac{0.0498}{995.98*0.001148} = 0.0436 \frac{\text{m}}{\text{sec}}$$

$$Re = \frac{u \rho d}{\mu} = \frac{ud}{v}$$

$$Re_h = \frac{0.366*992.28*0.01705}{0.00066} = 9382$$

$$Re_c = \frac{0.0436*995.98*0.034}{0.00087} = 1697.06$$

- Hot side is turbulent flow
- Cold side is laminar flow

For hot side (turbulent flow):

$$Nu = 0.023 Re^{0.8} Pr^n \quad n = 0.3 \text{ for cooling}$$

$$Nu_h = 0.023 \times 9382^{0.8} \times 4.38^{0.3} = 53.95$$

$$h = \frac{Nu k}{d}$$

$$h_i = \frac{53.9*0.632}{0.01705} = 1997.94 \frac{\text{kW}}{\text{m}^2 \cdot ^\circ\text{C}}$$

$$Q_h = \dot{m} C_p \Delta T$$

$$Q_h = U A_s LMTD F$$

$$F=1$$

$$A_{is} = \pi d_{ip} L$$

$$A_{os} = A_{cs} + A_{sm}$$

$$A_{oc} = N A_c$$

$$A_{sm} = \pi d_{op} (L - NS)$$

Appendix [B]

$$Q_h = 0.0827 * 4174 * (40.2 - 38.7) = 517.78 \frac{J}{sec} = 517.78 W$$

$$Q_c = 0.0498 * 4179 * (27.2 - 24.9) = 478.66 \frac{J}{sec} = 478.66 W$$

$$LMTD = \frac{\Delta T_1 - \Delta T_2}{\ln\left(\frac{\Delta T_1}{\Delta T_2}\right)}$$

$$\Delta T_1 = T_{hi} - T_{co}$$

$$\Delta T_2 = T_{ho} - T_{ci}$$

$$\Delta T_1 = 40.2 - 27.2 = 13^{\circ}C$$

$$\Delta T_2 = 38.7 - 24.9 = 13.8 ^{\circ}C$$

$$LMTD = \frac{13 - 13.8}{\ln\left(\frac{13}{13.8}\right)} = 13.4^{\circ}C$$

$$U_i = \frac{478.66}{\pi * 0.01705 * 13.4 * 1 * 1} = 666.88 \frac{W}{m^2 \cdot ^\circ C}$$

$$\frac{1}{U_i A_i} = \frac{1}{U_o A_o}$$

$$U_o = U_i \left(\frac{A_i}{A_o} \right)$$

$$A_{is} = \pi * 0.01705 * 1 = 0.0536 m^2$$

$$A_{os} = A_{s,os} + A_{c,os}$$

$$A_{corrug.} = 121.04 mm^2 = 1.2104 * 10^{-4} m^2$$

$$A_{cs} = 49 * 1.2104 * 10^{-4} = 0.00593 m^2$$

$$A_{s,s} = \pi * 0.01905 * (1 - 49 * 0.00173) = 0.0548 m^2$$

$$A_{s,corrug.} = 0.00593 + 0.0548 = 0.06073 m^2$$

$$U_o = 666.88 * \left(\frac{0.0536}{0.06073} \right) = 588.585 \frac{W}{m^2 \cdot ^\circ C}$$

$$h_o = \frac{1}{\frac{1}{588.585} - \frac{0.06073}{1997.94 * 0.0536}} = 883.47 \frac{kW}{m^2 \cdot ^\circ C}$$

$$Nu_c = \frac{883.47 * 0.034}{0.613} = 49 \frac{kW}{m^2 \cdot ^\circ C}$$

Pressure drop

$$\Delta P = \frac{f L \rho u_m^2}{2d}$$

Where:

For laminar flow

Appendix [B]

$$f = \frac{64}{Re}$$

For turbulent flow

$$f = \frac{0.316}{Re^{0.25}}$$

sample	Unit	Hot side	Cold side
L	m	1	1.02
ρ	kg/m^3	992.28	995.98
d	m	0.01705	0.034
u	m/sec	0.366	0.0436

Hot side

$$f = \frac{0.316}{9382^{0.25}} = 0.032$$

$$\Delta P = \frac{f L \rho u_m^2}{2d}$$

$$\Delta P = \frac{0.032 * 1 * 992.28 * 0.366^2}{2 * 0.01705} = 124.74 \text{ Pa} = 1.2474 \text{ mbar}$$

Cold side

$$f = \frac{64}{1697.06} = 0.038$$

$$\Delta P = \frac{0.038 * 1.02 * 995.98 * 0.0436^2}{2 * 0.034} = 1.079 \text{ Pa} = 0.01079 \text{ mbar}$$

Effectiveness

$$\varepsilon = \frac{2.3}{14.3} = 0.16$$

Sample of calculation in Nano fluid smooth pipe at the condition:

Hot side (pipe side)

$$T_{hin} = 40 \text{ } ^\circ\text{C}$$

$$T_{hout} = 38.6 \text{ } ^\circ\text{C}$$

$$\dot{V}_{hin} = 5 \text{ LPM}$$

Cold side (shell side, Nano side)

$$T_{cin} = 25 \text{ } ^\circ\text{C}$$

$$T_{cout} = 26.3 \text{ } ^\circ\text{C}$$

$$\dot{m} \frac{\text{kg}}{\text{sec}} = \dot{m} \frac{\text{L}}{\text{M}} \times \frac{1\text{M}}{60 \text{ sec}} \times \rho \frac{\text{kg}}{\text{m}^3} \times \frac{1\text{m}^3}{1000\text{L}}$$

Appendix [B]

All water properties taken at Tm for hot and cold water

$$T_m = \frac{T_{in} + T_{out}}{2}$$

$$T_{hm} = \frac{40 + 38.6}{2} = 39.3 \text{ } ^\circ\text{C}$$

$$T_{cm} = \frac{25 + 26.3}{2} = 25.65 \text{ } ^\circ\text{C}$$

T _m °C	ρ kg/m ³	μ kg/m. s	k kW/m. °C	C _p J/kg. °C	Pr
39.5	992.34	0.00066	0.632	4174	4.396
25.95	996.01	0.00088	0.612	4179	6.02

For hot side:

$$\dot{m}_{hin} \frac{\text{kg}}{\text{sec}} = 5 \frac{\text{L}}{\text{M}} \times \frac{1\text{M}}{60 \text{ sec}} \times 992.34 \frac{\text{kg}}{\text{m}^3} \times \frac{1\text{m}^3}{1000\text{L}} = 0.0827 \frac{\text{kg}}{\text{sec}}$$

$$A_{c,ip} = \frac{\pi}{4} d_{pin}^2$$

$$d_{ip} = 0.01705 \text{ m}$$

$$A_{c,ip} = \frac{\pi}{4} * 0.01705^2 = 0.000228 \text{ m}^2$$

$$u = \frac{\dot{m}}{\rho A_c}$$

$$u_h = \frac{0.0827}{992.26 * 0.000228} = 0.366 \frac{\text{m}}{\text{sec}}$$

$$Re = \frac{u \rho d}{\mu} = \frac{ud}{v}$$

$$Re_h = \frac{0.366 * 992.26 * 0.01705}{0.00066} = 9381.82$$

Properties for Nano fluid

$$\rho_{nf} = (1 - \varphi) \rho_{bf} + \varphi \rho_p$$

$$\rho_{nf} = \left(1 - \frac{0.8}{100}\right) * 996.01 + \frac{0.8}{100} * 3970 = 1019.8 \frac{\text{kg}}{\text{m}^3}$$

$$\mu_{nf} = \mu_{bf}(123\varphi^2 + 7.3\varphi + 1)$$

$$\mu_{nf} = 0.00088 * \left(123 * \left(\frac{0.8}{100}\right)^2 + 7.3 * \frac{0.8}{100} + 1\right) = 0.00094 \frac{\text{kg}}{\text{m.s}}$$

$$k_{nf} = k_{bf}(1 + 7.47\varphi)$$

$$k_{nf} = 0.612 * \left(1 + 7.47 * \frac{0.8}{100}\right) = 0.649 \frac{\text{kW}}{\text{m. } ^\circ\text{C}}$$

Appendix [B]

$$Cp_{nf} = (1 - \varphi)Cp_{bf} + \varphi Cp_{pf}$$

$$Cp_{nf} = \left(1 - \frac{0.8}{100}\right) * 4179 + \frac{0.8}{100} * 765 = 4151.69 \frac{\text{J}}{\text{kg.}^{\circ}\text{C}}$$

$$Pr_{nf} = \frac{Cp_{nf}\mu_{nf}}{k_{nf}}$$

$$Pr_{nf} = \frac{4151.69 * 0.00094}{0.649} = 6.01$$

T _m °C	ρ kg/m ³	μ kg/m. s	k kW/m.°C	Cp J/kg.°C	Pr
25.65	1019.8	0.00094	0.632	4151.69	4.396

For cold side (Nano fluid) work at same (Re = 1689.35)

$$Re = \frac{u\rho d}{\mu} = \frac{ud}{v}$$

$$A_{c,is} = \frac{\pi}{4} (D_i^2 - d_{op}^2)$$

$$d_{op} = 0.01905 \text{ m}$$

$$D_{is} = 0.0426 \text{ m}$$

$$A_{cs} = \frac{\pi}{4} (0.0426^2 - 0.01905^2) = 0.00114 \text{ m}^2$$

$$D_{hs} = \frac{4A_{cs}}{P}$$

$$P = \pi D_{is}$$

$$P_s = \pi * 0.0426 = 0.134 \text{ m}$$

Hydraulic diameter for cold section:

$$D_{hs} = \frac{4 * 0.00114}{0.134} = 0.034 \text{ m}$$

Then:

$$1689.35 = \frac{u * 1019.8 * 0.034}{0.00094}$$

$$u = 0.0458 \frac{\text{m}}{\text{sec}}$$

$$u = \frac{\dot{m}}{\rho A_c}$$

$$0.0458 = \frac{\dot{m}_{nf}}{1019.8 * 0.00114}$$

Appendix [B]

$$\dot{m}_{nf} = 0.0532 \frac{\text{kg}}{\text{sec}}$$

$$0.0532 \frac{\text{kg}}{\text{sec}} = \dot{v}_{nf} \frac{\text{L}}{\text{M}} \times \frac{1\text{M}}{60 \text{ sec}} \times 1019.8 \frac{\text{kg}}{\text{m}^3} \times \frac{1\text{m}^3}{1000\text{L}}$$

$$\dot{v}_{nf} = 3.13 \frac{\text{L}}{\text{M}}$$

- Hot side is turbulent flow
- Cold side is laminar flow

For hot side (turbulent flow):

$$\text{Nu} = 0.023 \text{Re}^{0.8} \text{Pr}^n \quad n = 0.3 \text{ for cooling}$$

$$\text{Nu}_h = 0.023 \times 9326.05^{0.8} \times 4.396^{0.3} = 53.75$$

For cold side (Nano fluid laminar flow):

$$\text{Nu}_{nf} = 0.031(\text{Re Pr})^{0.68}(1 + \varphi)^{95.73}$$

$$\text{Nu}_{nf} = 0.031(1689.35 * 6.01)^{0.68} * \left(1 + \frac{0.8}{100}\right)^{95.73} = 35.25$$

$$Q_h = \dot{m}C_p\Delta T$$

$$Q_h = U A_s \text{LMTD} F$$

$$A_{is} = \pi d_{ip} L$$

$$A_{os} = \pi d_{op} L$$

F=1 because have one pipe and one shell

$$Q_h = 0.0827 * 4174 * (40 - 38.6) = 483.27 \frac{\text{J}}{\text{sec}} = 483.27 \text{ W}$$

$$Q_{nf} = 0.0545 * 4151.69 * (26.3 - 25) = 294.15 \frac{\text{J}}{\text{sec}} = 294.15 \text{ W}$$

$$\text{LMTD} = \frac{\Delta T_1 - \Delta T_2}{\ln\left(\frac{\Delta T_1}{\Delta T_2}\right)}$$

$$\Delta T_1 = T_{hi} - T_{nfo}$$

$$\Delta T_2 = T_{ho} - T_{nfi}$$

$$\Delta T_1 = 40 - 26.3 = 13.7^\circ\text{C}$$

$$\Delta T_2 = 38.6 - 25 = 13.6^\circ\text{C}$$

$$\text{LMTD} = \frac{13.7 - 13.6}{\ln\left(\frac{13.7}{13.6}\right)} = 13.65^\circ\text{C}$$

Appendix [B]

$$U_i = \frac{483.27}{\pi * 0.01705 * 13.65 * 1 * 1} = 660.97 \frac{W}{m^2 \cdot ^\circ C}$$

$$\frac{1}{U_i A_i} = \frac{1}{U_o A_o}$$

$$U_o = U_i \left(\frac{A_i}{A_o} \right)$$

$$A_{is} = \pi * 0.01705 * 1 = 0.0536 m^2$$

$$A_{os} = \pi * 0.01905 * 1 = 0.0598 m^2$$

$$U_o = 660.97 * \left(\frac{0.0536}{0.0598} \right) = 591.58 \frac{W}{m^2 \cdot ^\circ C}$$

$$h = \frac{Nu k}{d}$$

$$h_i = \frac{53.75 * 0.632}{0.01705} = 1992.38 \frac{kW}{m^2 \cdot ^\circ C}$$

$$h_{nf} = \frac{35.04 * 0.649}{0.034} = 668.85 \frac{kW}{m^2 \cdot ^\circ C}$$

Pressure drop

$$\Delta P = \frac{f L \rho u_m^2}{2d}$$

Where:

For laminar flow (Nano fluid)

$$f_{nf} = 26.4 Re^{-0.8737} (1 + \varphi)^{156.23}$$

For turbulent flow Blasius's equation

$$f = \frac{0.316}{Re^{0.25}}$$

sample	Unit	Hot side	Cold side
L	m	1	1
ρ	kg/m^3	992.34	1019.8
d	m	0.01705	0.034
u	m/sec	0.366	0.0454

Hot side

$$f = \frac{0.316}{9326.05^{0.25}} = 0.032$$

$$\Delta P = \frac{f L \rho u_m^2}{2d}$$

Appendix [B]

$$\Delta P = \frac{0.032 * 1 * 992.34 * 0.366^2}{2 * 0.01705} = 124.7 \text{ Pa} = 1.247 \text{ mbar}$$

Cold side

$$f_{nf} = 26.4 * 1689.35^{-0.8737} \left(1 + \frac{0.8}{100}\right)^{156.23} = 0.14$$

$$\Delta P = \frac{0.14 * 1 * 1019.8 * 0.0458^2}{2 * 0.034} = 4.4 \text{ Pa} = 0.044 \text{ mbar}$$

Effectiveness

$$\varepsilon = \frac{1.4}{15} = 0.1$$

APPENDIX [C]

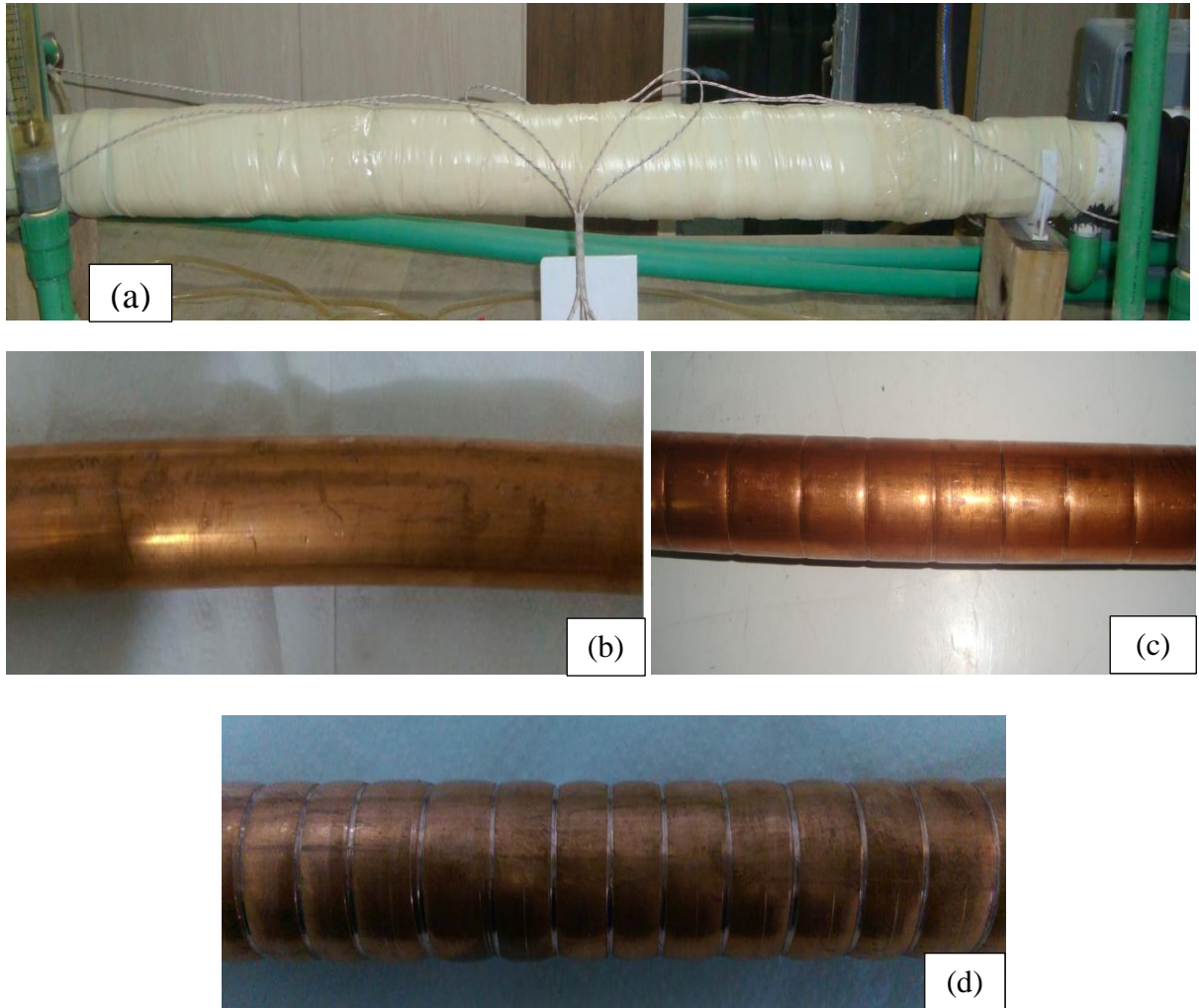


Figure (C-1 a, b, c, d) photograph show test section



Figure (C-2) photograph show test pipe and insulation connect with data logger



Figure (C-3) photograph show hot water vessel

Appendix [C]



Figure (C-4) photograph show
Cold water vessel



Figure (C-5) photograph show
water pump



Figure (C-6) photograph show water valves

Appendix [C]



Figure (C-7) photograph show flow meter



Figure (C-8) photograph show cooling unit



Figure (C-9) photograph show Installation of thermocouple



Figure (C-10) photograph show manometer



Figure (C-11) photograph show Nanoparticle

C.1 Calibration of Flow Meter

In order to calibrate the flow meter, graduated vessel and stop watch were used and the sample of calibration test results is described below:

Samples of Flow Meter Calibrations

By using flow meter

Volumetric flow rate reading = 1 l/min.

Test No.1:

Time for observation = 1min.

Volumetric flow rate in graduate container = 0.98 l/min.

Test No.2:

Time for observation = 1minute

Volumetric flow rate in graduated container = 0.99 l/min.

Test No.3:

Time for observation = 1min.

Volumetric flow rate in graduated container = 0.97 l/min.

Test No.4:

Time for observation = 1min.

Volumetric flow rate in graduated container = 0.97 l/min.

The net volumetric flow rate by graduated vessel and stop watch was:

$$\dot{V} = \frac{\dot{V}_1 + \dot{V}_2 + \dot{V}_3 + \dot{V}_4}{4} = \frac{0.98 + 0.99 + 0.97 + 0.97}{4} = 0.9775 \text{ l/min.}$$

From the above tests it is obvious that:

Measuring difference = $1 - 0.9775 = 0.0225$

Measuring error = $\frac{1 - 0.9775}{1} = 2.25\%$

Appendix [C]

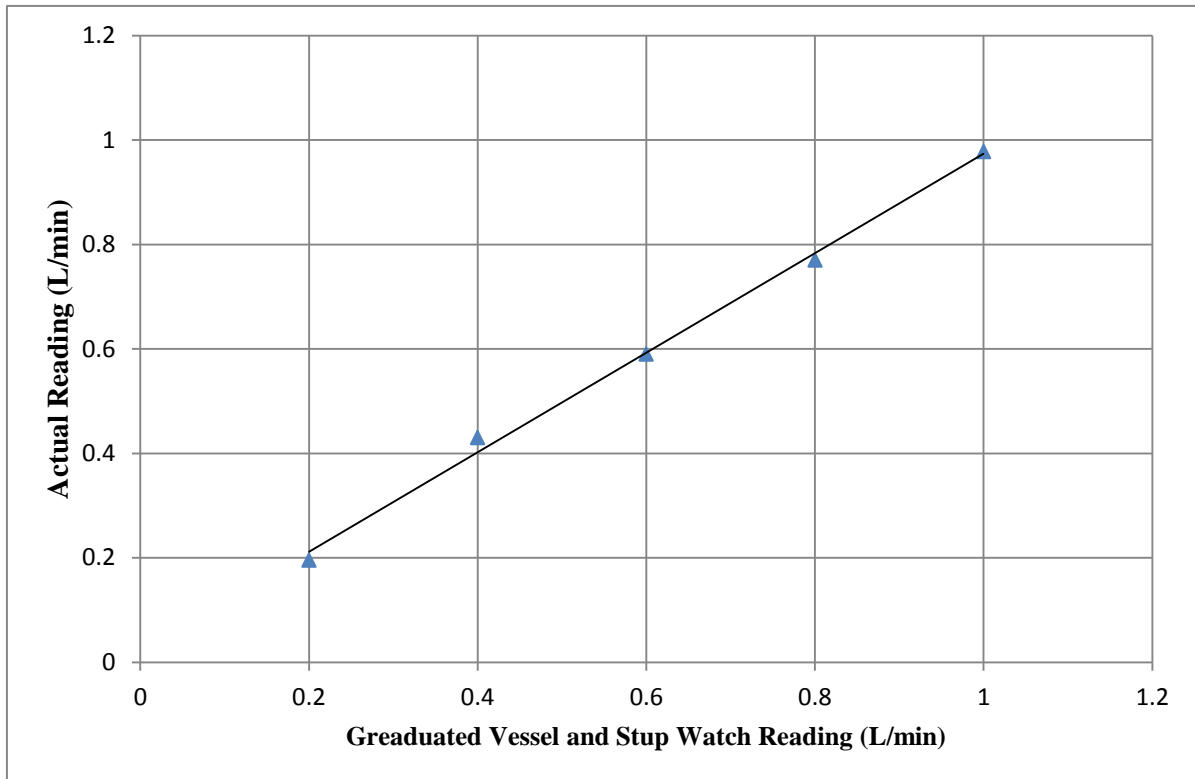


Figure (C-12) show the results of experimental calibration for water flow rates calibration in this study

Appendix [C]



Calibration Certificate

Central Organization for Standardization and Quality

Control (COSQC)

Metrology Department

P.O. Box 13032 Algeria street, Baghdad ,Tel:7765180

E-Mail : cosqc@yahoo.com

Certificate No.: PH

607 / 2016

Date of issue :

28/08/2016

Customer			
Name:	طالب الماجستير صفاء عبد محمد		
Address:	العراق - الكويت		
Item under calibration			
Description:	Thermocouple Type K		
Manufacturer:	_____		
Model:	_____		
Serial number:	1		
Other identification:	(0.0 ----- 200) °C		
Date of reception:	18/08/2016		
Condition of reception:	GOOD		
Standard(s) used in the calibration			
Description:	Multimeter	PT100	Temperature Calibrator
Manufacturer:	Agilent	Fluke / USA	BETA
Model:	34420A	5626	PTC-8010
Serial number:	MY42999734	3408	01-023-00
Other identification:	_____	_____	_____
Calibration information			
Date of calibration:	25/08/2016		
Place of calibration:	Temperature measurement lab		
Method(s) of calibration:	Calibration method using Working Thermometer - Calibration Procedure 2008		
Calibrated quantity:	Temprature / Celcius / °C		
Results of calibration:	Attached a complete result in Annex 1 of this certificate		
Measurement uncertainty:	The reported expanded uncertainty is based on GUM Standard and the standard Uncertainty multiplied by coverage factor k=2 to give confidence level of 95%		
Metrological traceability:	The traceability of measurement results to the SI units is assured by the National standard maintained at Central Organization for standardization and Quality Control through calibration at :- - Temp. measurement lab. (Cert. PH -01-124-00) - NVLAB (REPORT NO. B3114057)		
Environmental conditions of calibration:	Temp. (27 °C):	±1°C	R. H.(50%) ±5%
Observations, opinions or recommendations:			

Performed by :

Ahmed

Approved by:

Lamyia I.M.Saad Ayoub

1 of 1

This certificate is issued in accordance with the laboratory accreditation requirements. It provides tracibility of measurement to recognized national standards, and to the units of measurement realized at the COSQC or other recognized national standards laboratories. This certificate may not be reproduced other than in full by photographic process. This certificate refers only to the particular item submitted for calibration

(a)

Appendix [C]

Calibration Certificate

Central Organization for Standardization and Quality
Control (COSQC)
Metrology Department

P.O. Box 13032 Algeria street, Baghdad, Tel: 7765180 E-Mail : cosqc@yahoo.com
Certificate No.: P 607 / 2016
Date of issue : 28/08/2016

Results

Set Value C°	Reference Value C°	Indicate Value C°	Correction C°	Uncertainty C°
25	25.1408	25	0.1408	0.6100
40	40.47	39.9	0.57	0.6100
50	50.59	49.9	0.697	0.6100
60	60.75	59.3	1.453	0.6100

Performed by:
Ahmed

Reviewed by:
S

Approved by:
Lamyia I.M.Saad Ayoub

2 of 1
This certificate is issued in accordance with the laboratory accreditation requirements. It provides traceability of measurement to recognized national standards, and to the units of measurement realized at the COSQC or other recognized national standards laboratories. This certificate may not be reproduced other than in full by photographic process. This certificate refers only to the particular item submitted for calibration

(b)

Figure (C-13a, b) Thermocouples Calibration Certificate



Figure (C-14) photograph show Ultrasonic Vibration Device

Digital Ultrasonic Cleaner 10L

Tank Size: 300×240×150 mm

Machine Size: 330×270×280mm

Ultrasonic Power: 240W

Frequency: from 20khz to 135kHz

Timer: 1-30min

Heater: 20-80°C

Volume: 10L.

APPENDIX [D]

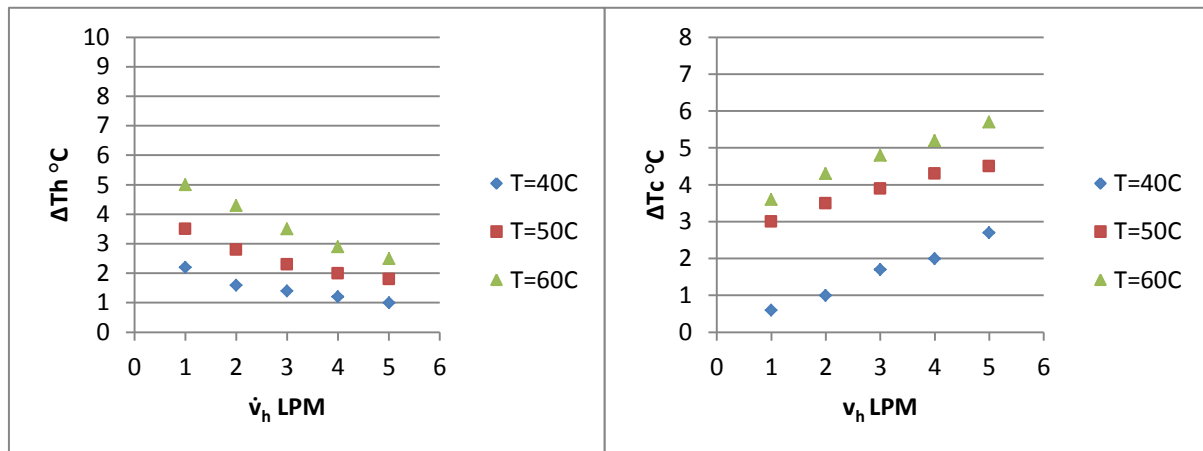


Figure (D-1) Effect of hot mass flow rate on temperature difference in smooth tube at $\dot{V}_c = 4 \text{ LPM}$ in different temperatures

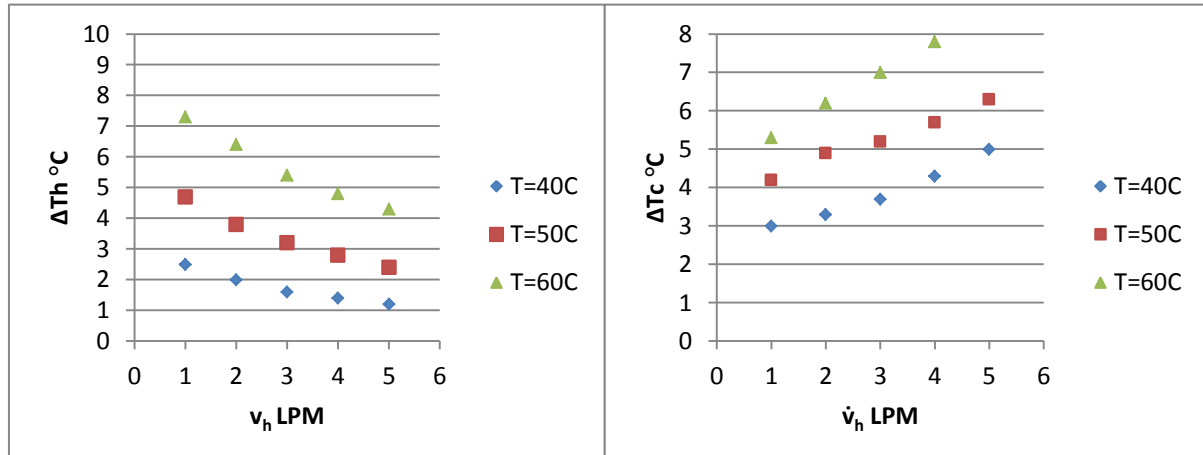


Figure (D-2) Effect of hot mass flow rate on temperature difference in corrugated tube ($z/d = 1$) at $\dot{V}_c = 4 \text{ LPM}$ in different temperatures

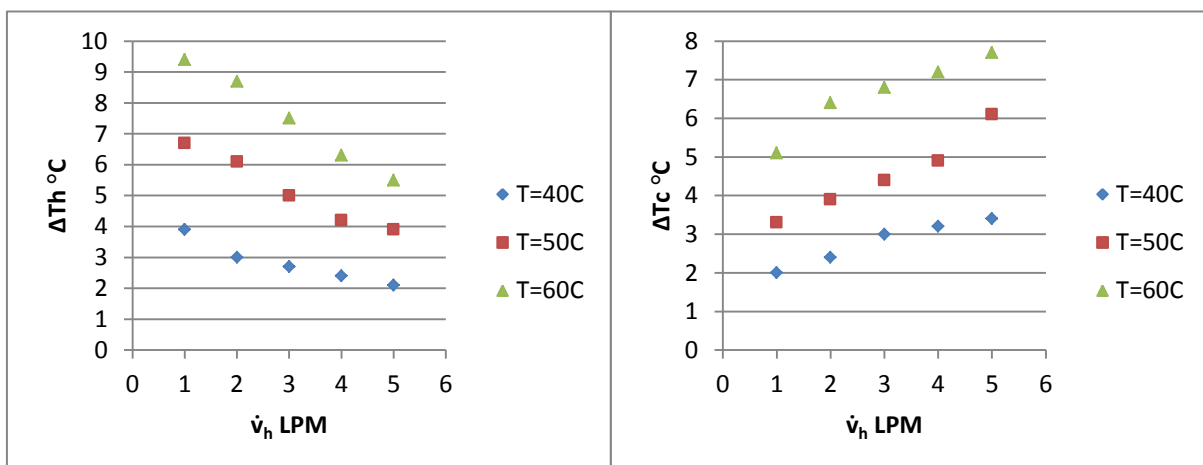


Figure (D-3) Effect of hot mass flow rate on temperature difference in corrugated tube ($z/d = 0.5$) at $\dot{V}_c = 4 \text{ LPM}$ in different temperatures

Appendix [D]

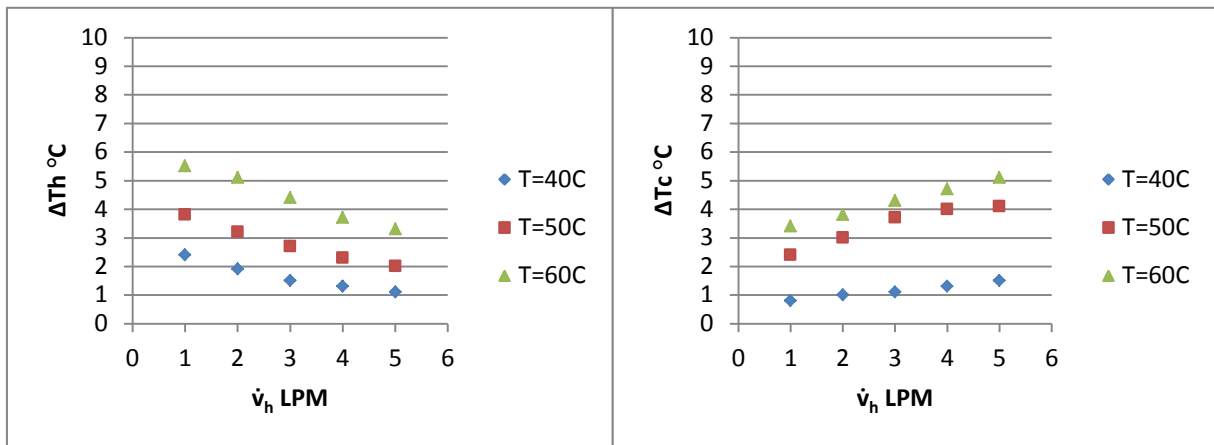


Figure (D-4) Effect of hot mass flow rate on temperature difference in smooth tube at $\dot{v}_c = 5$ LPM in different temperatures

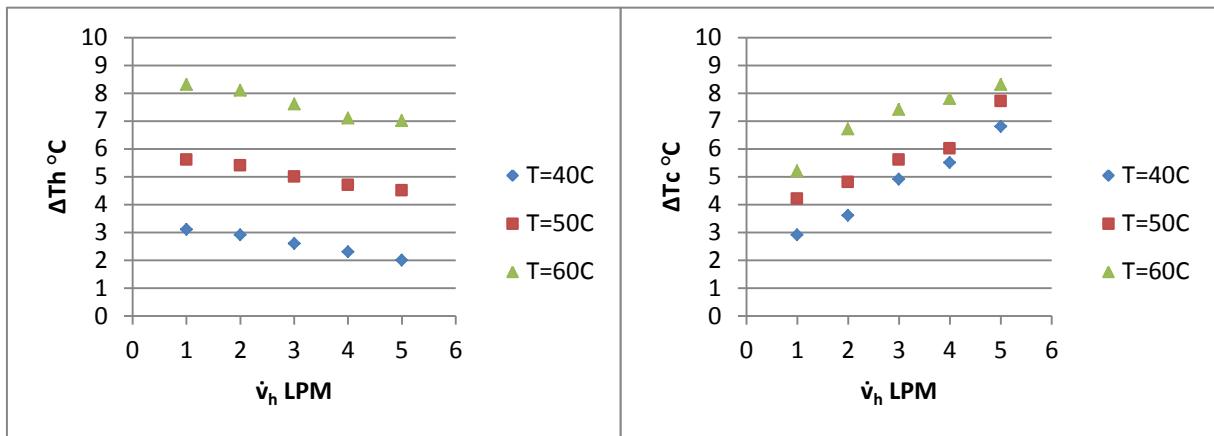


Figure (D-5) Effect of hot mass flow rate on temperature difference in corrugated tube ($z/d = 1$) at $\dot{v}_c = 5$ LPM in different temperatures

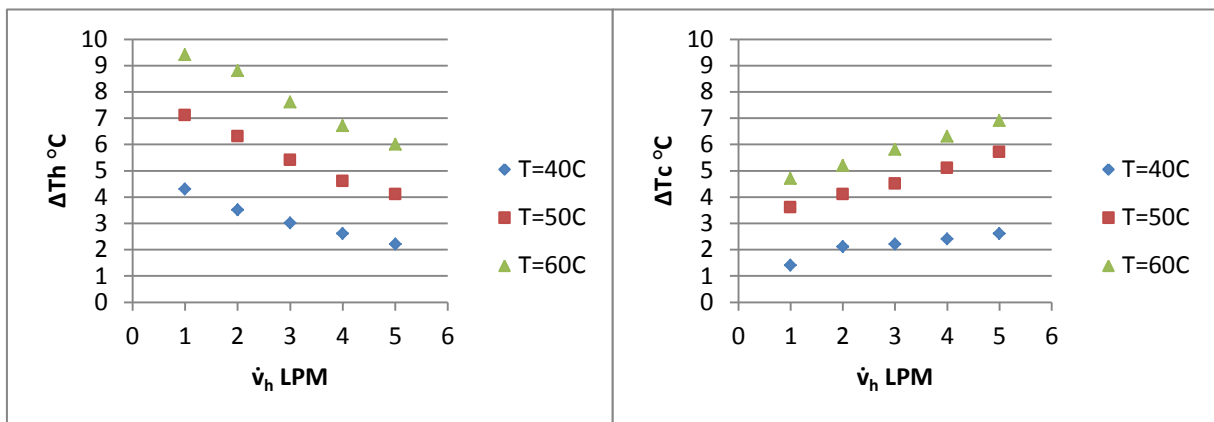


Figure (D-6) Effect of hot mass flow rate on temperature difference in corrugated tube ($z/d = 0.5$) at $\dot{v}_c = 5$ LPM in different temperatures

Appendix [D]

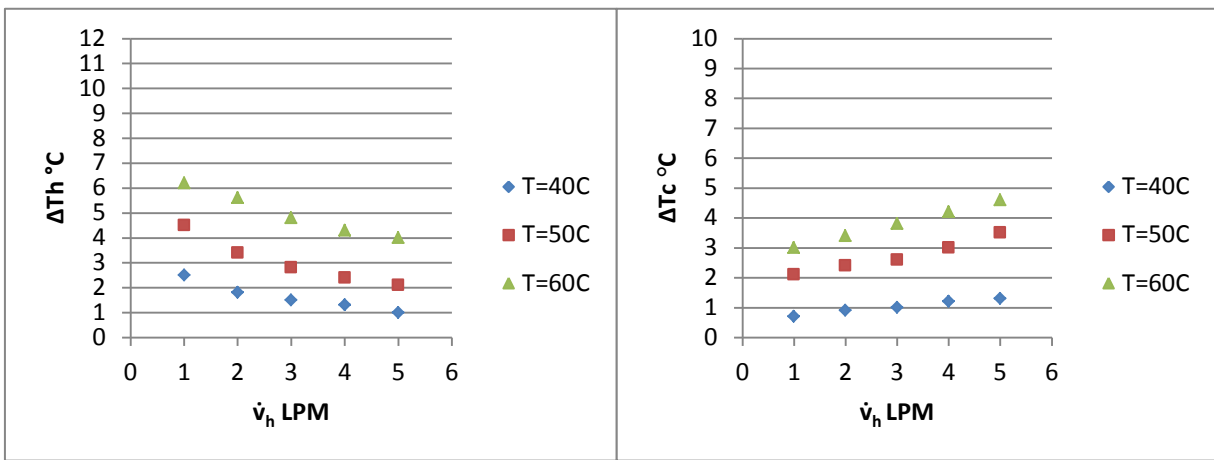


Figure (D-7) Effect of hot mass flow rate on temperature difference in smooth tube at $\dot{v}_c = 6$ LPM in different temperatures

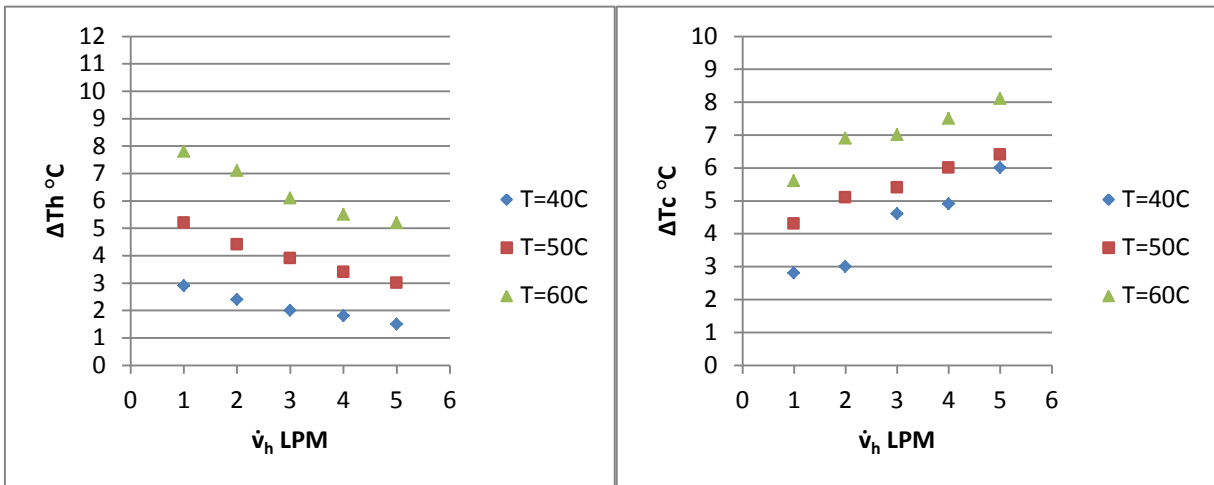


Figure (D-8) Effect of hot mass flow rate on temperature difference in corrugated tube ($z/d = 1$) at $\dot{v}_c = 6$ LPM in different temperatures

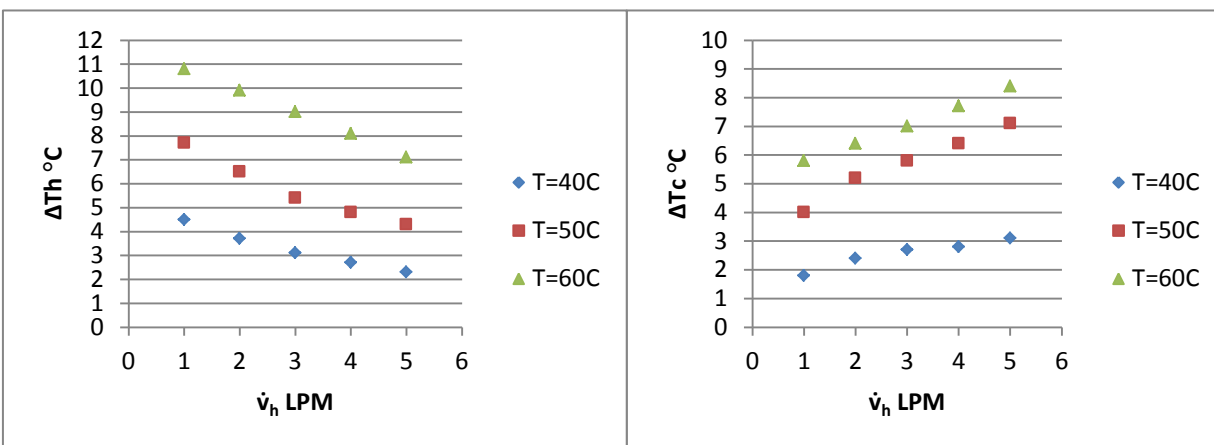


Figure (D-9) Effect of hot mass flow rate on temperature difference in corrugated tube ($z/d = 0.5$) at $\dot{v}_c = 6$ LPM in different temperatures

Appendix [D]

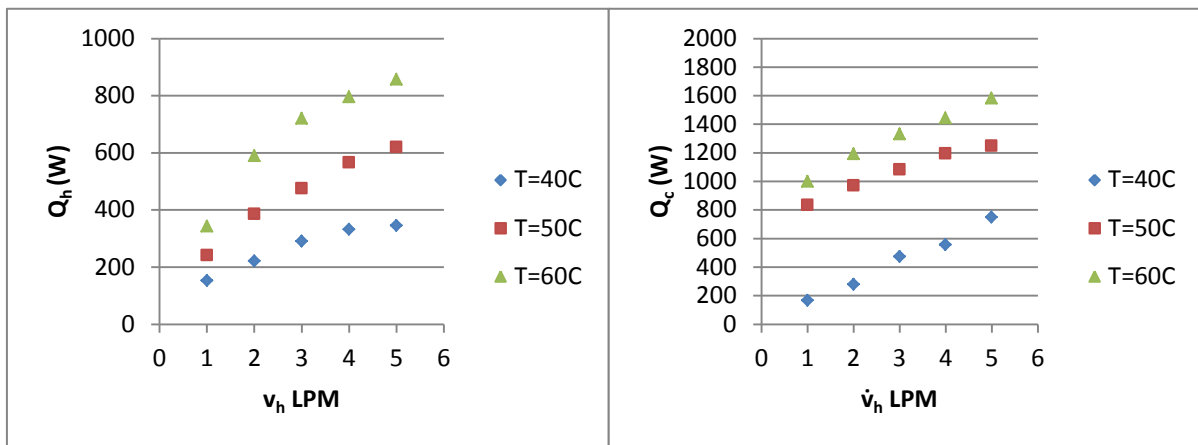


Figure (D-10) Effect of hot mass flow rate on heat dissipation in smooth tube at $\dot{v}_c = 4$ LPM in different temperatures

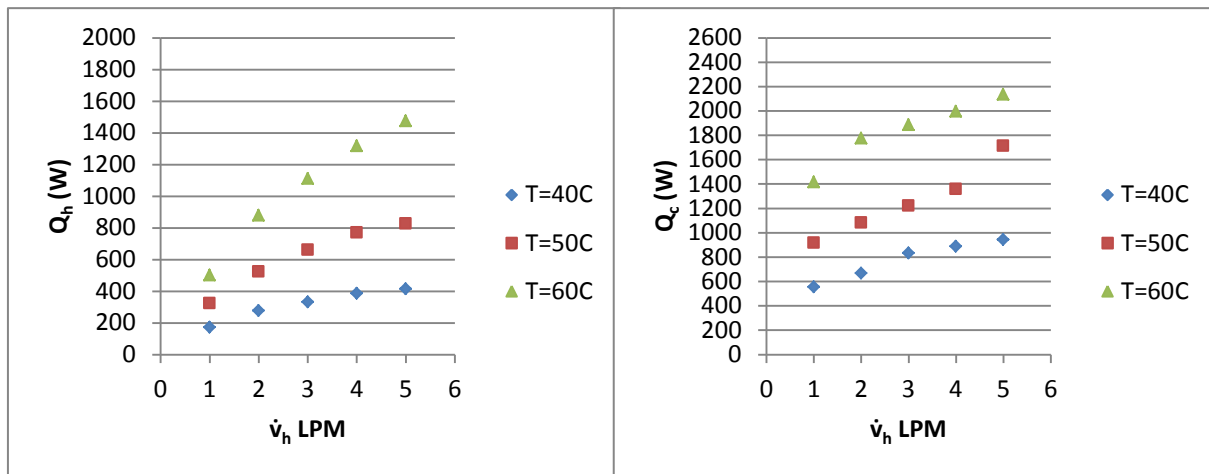


Figure (D-11) Effect of hot mass flow rate on heat dissipation in corrugated tube ($z/d = 1$) at $\dot{v}_c = 4$ LPM in different temperatures

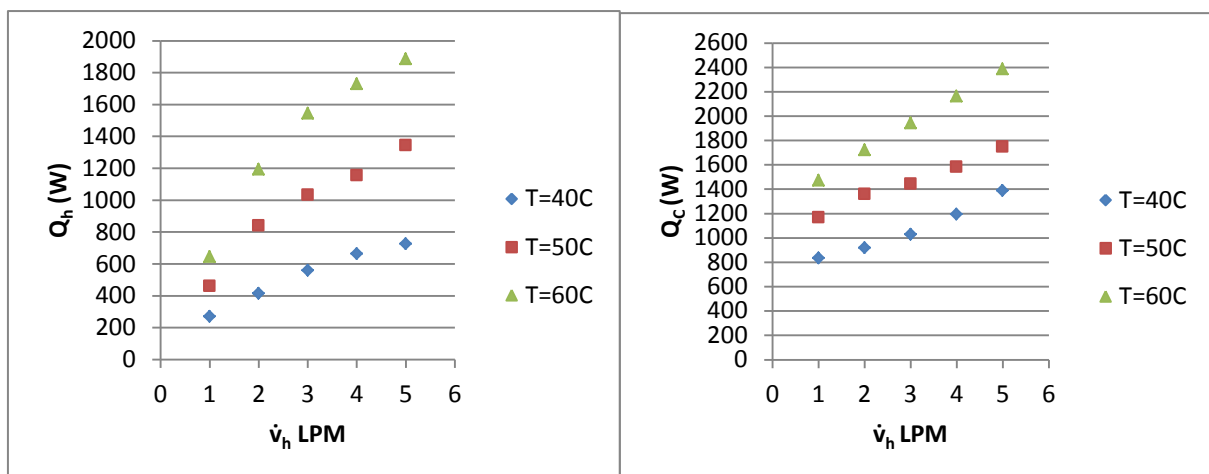


Figure (D-12) Effect of hot mass flow rate on heat dissipation in corrugated tube ($z/d = 0.5$) at $\dot{v}_c = 4$ LPM in different temperatures

Appendix [D]

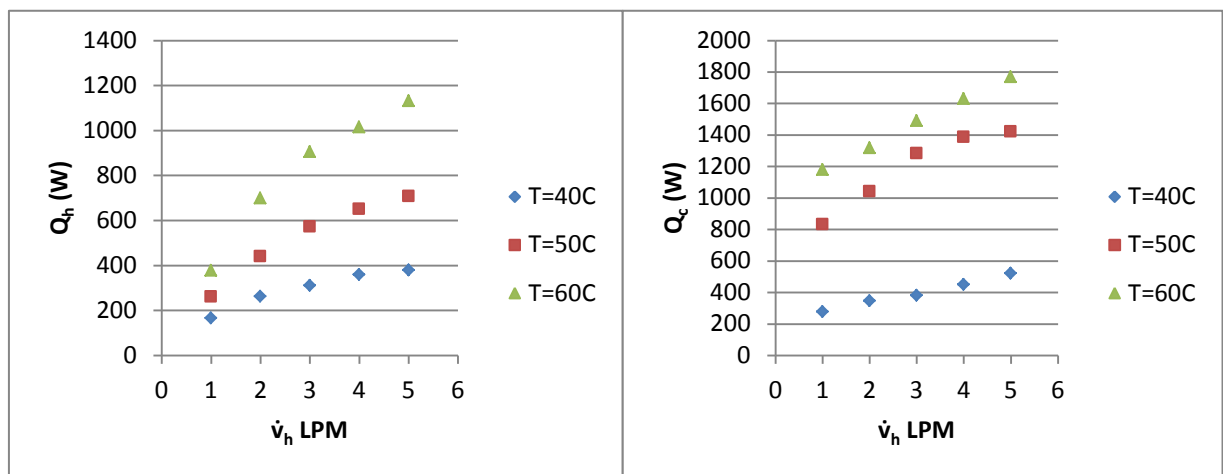


Figure (D-13) Effect of hot mass flow rate on heat dissipation in smooth tube at $\dot{v}_c = 5$ LPM in different temperatures

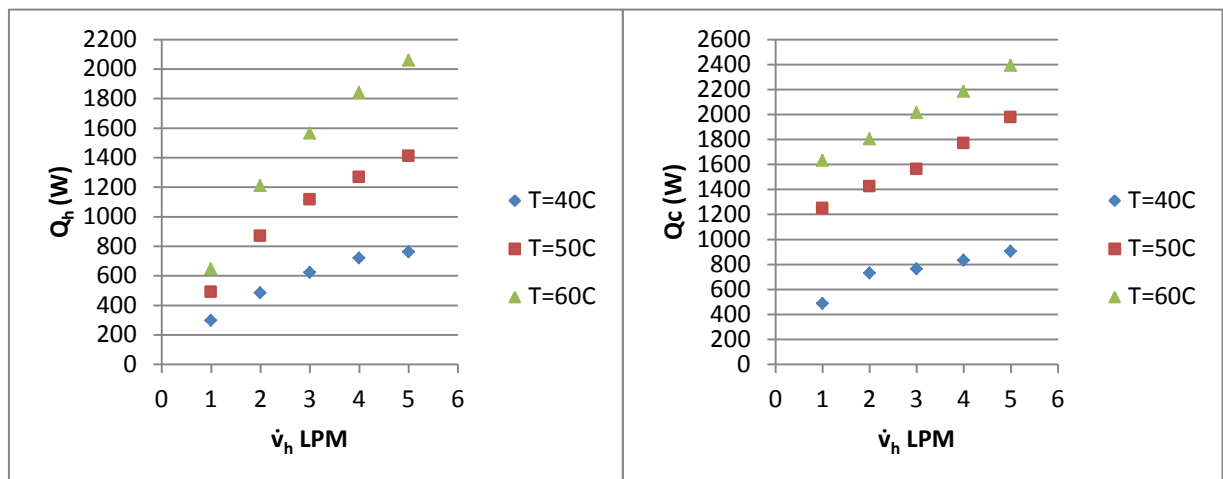


Figure (D-14) Effect of hot mass flow rate on heat dissipation in corrugated tube ($z/d = 1$) at $\dot{v}_c = 5$ LPM in different temperatures

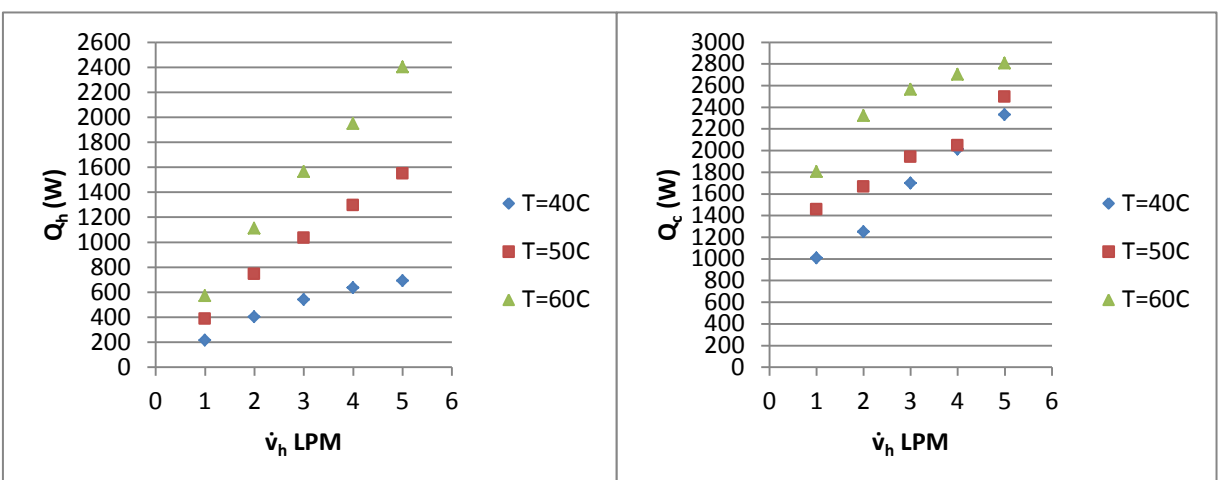


Figure (D-15) Effect of hot mass flow rate on heat dissipation in corrugated tube ($z/d = 0.5$) at $\dot{v}_c = 5$ LPM in different temperatures

Appendix [D]

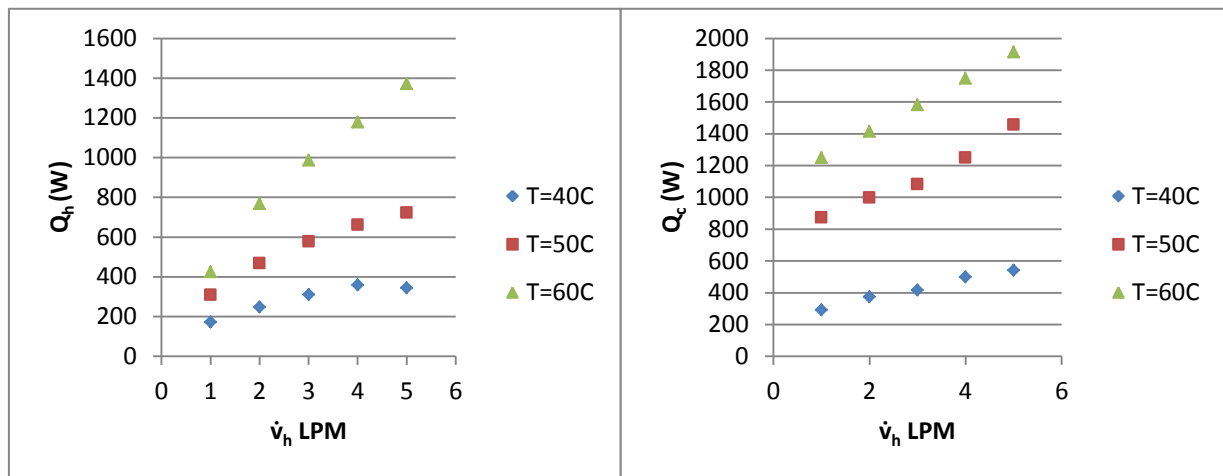


Figure (D-16) Effect of hot mass flow rate on heat dissipation in smooth tube at $\dot{v}_c = 6$ LPM in different temperatures

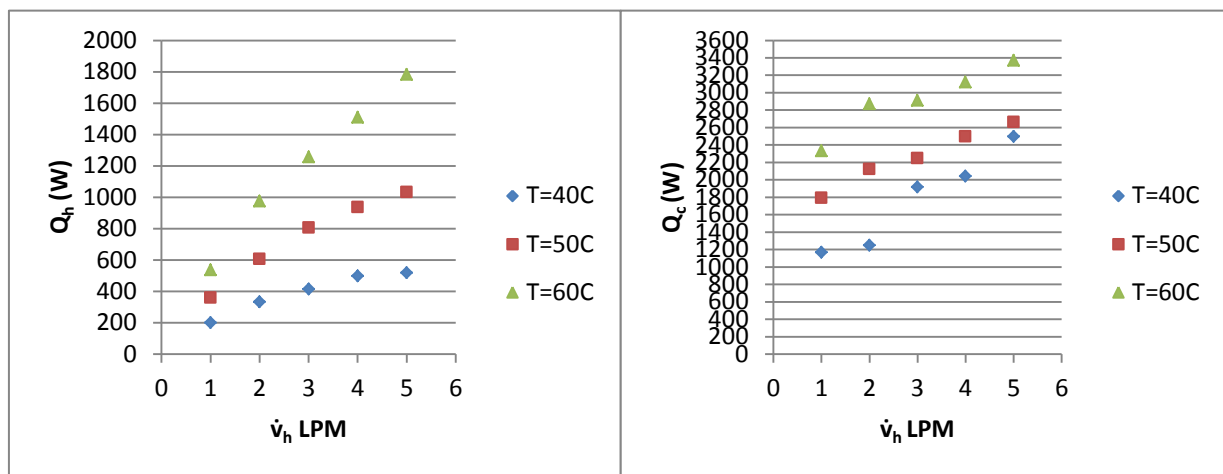


Figure (D-17) Effect of hot mass flow rate on heat dissipation in corrugated tube ($z/d = 1$) at $\dot{v}_c = 6$ LPM in different temperatures

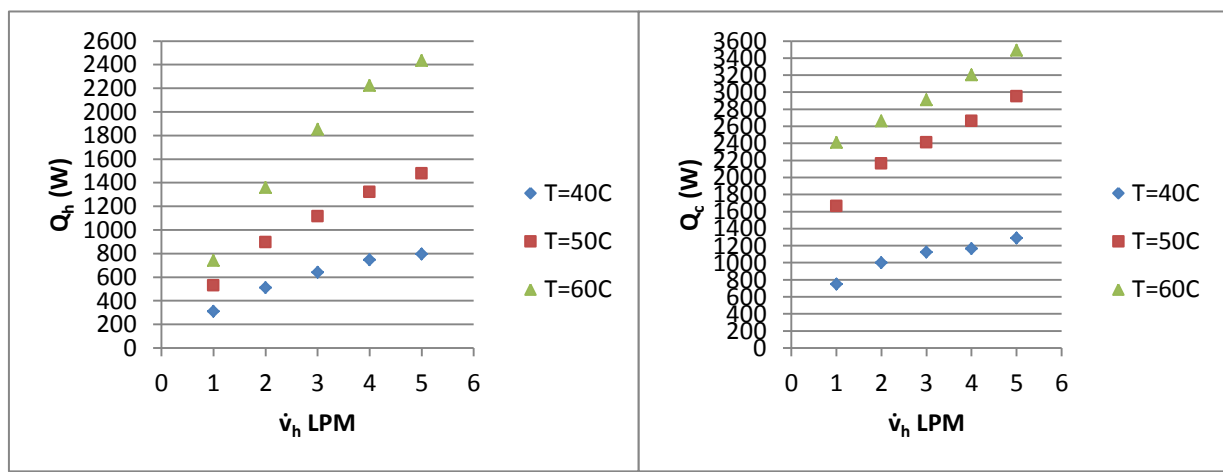


Figure (D-18) Effect of hot mass flow rate on heat dissipation in corrugated tube ($z/d = 0.5$) at $\dot{v}_c = 6$ LPM in different temperatures

Appendix [D]

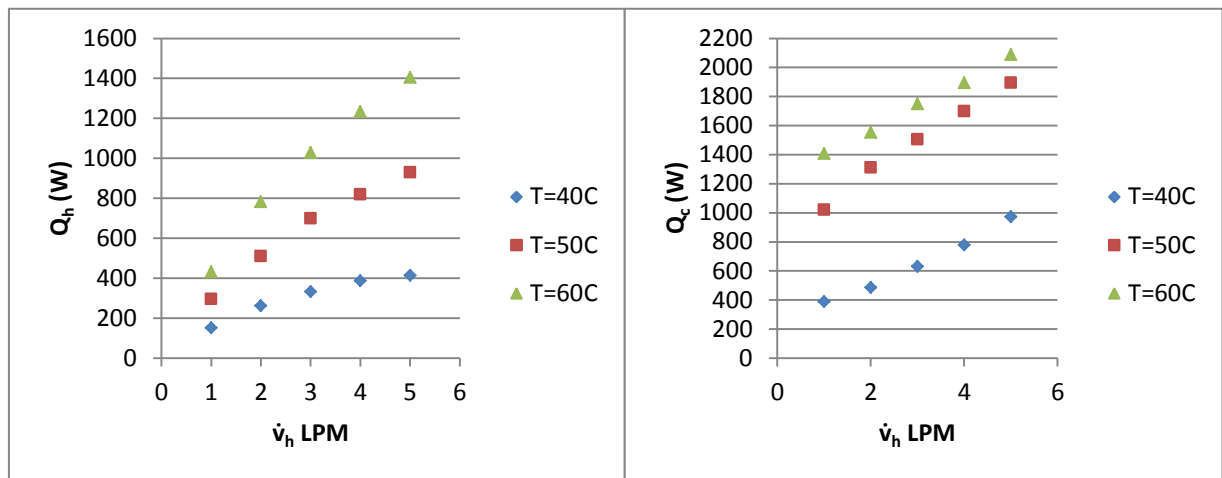


Figure (D-19) Effect of hot mass flow rate on heat dissipation in smooth tube at $\dot{v}_c = 7$ LPM in different temperatures

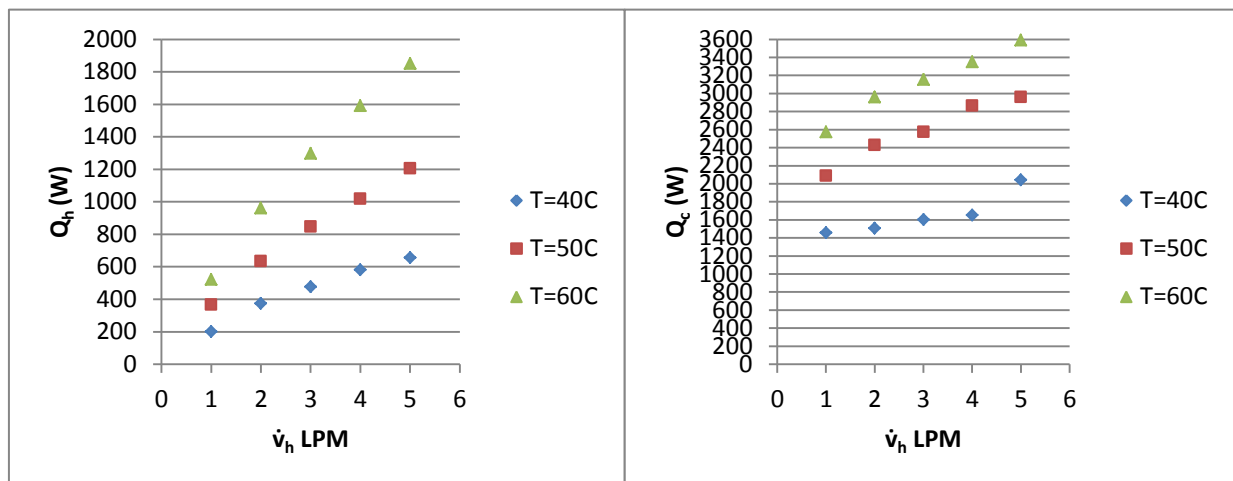


Figure (D-20) Effect of hot mass flow rate on heat dissipation in corrugated tube ($z/d = 1$) at $\dot{v}_c = 7$ LPM in different temperatures

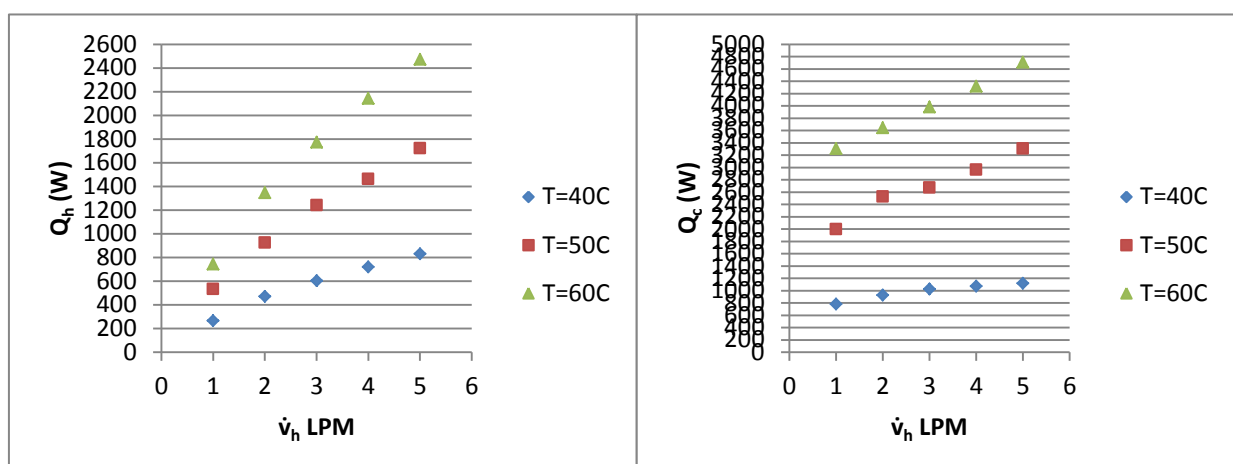


Figure (D-21) Effect of hot mass flow rate on heat dissipation in corrugated tube ($z/d = 0.5$) at $\dot{v}_c = 7$ LPM in different temperatures

Appendix [D]

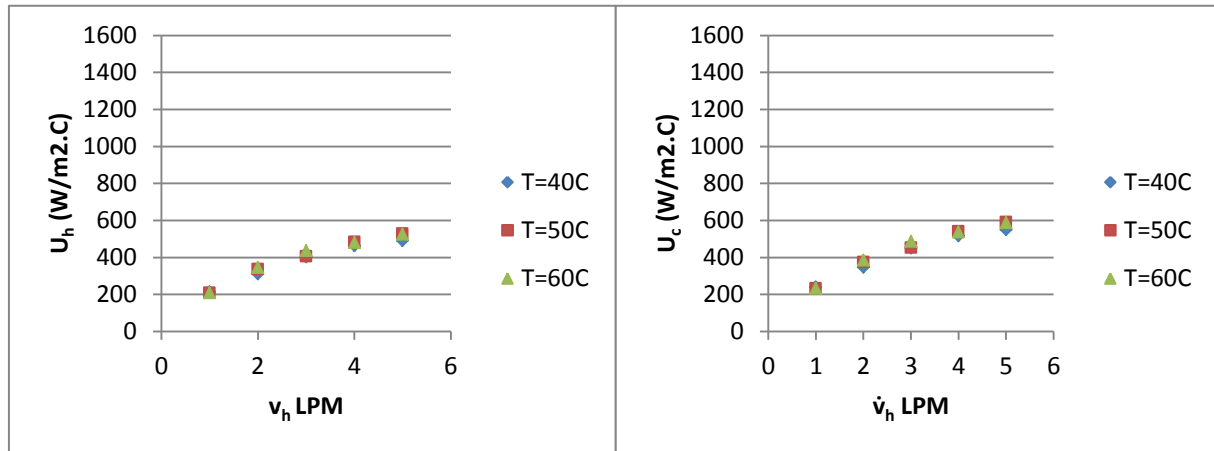


Figure (D-22) Effect of hot mass flow rate on overall heat transfer coefficient in smooth tube at $\dot{v}_c=4$ LPM in different temperatures

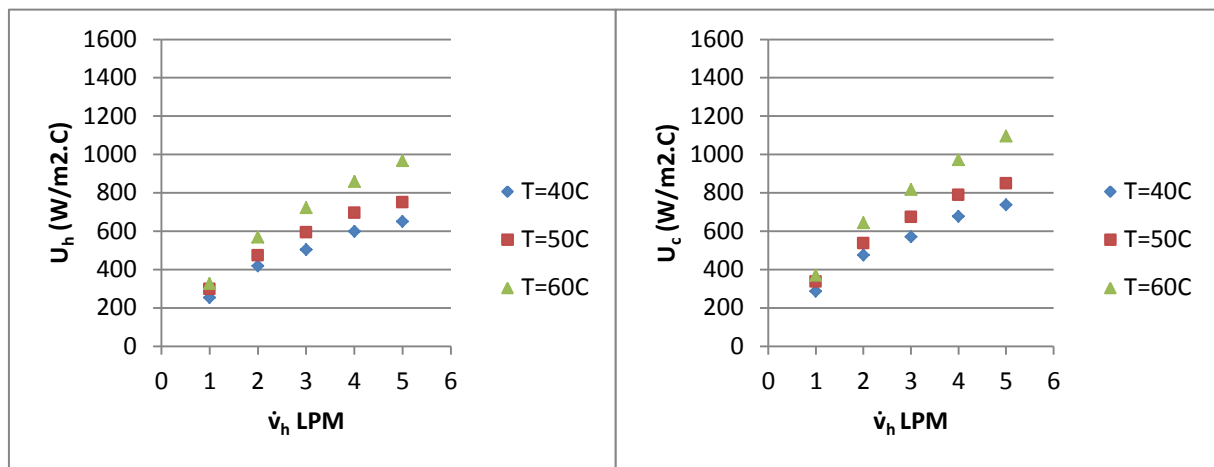


Figure (D-23) Effect of hot mass flow rate on overall heat transfer coefficient in corrugated tube ($z/d=1$) at $\dot{v}_c=4$ LPM in different temperatures

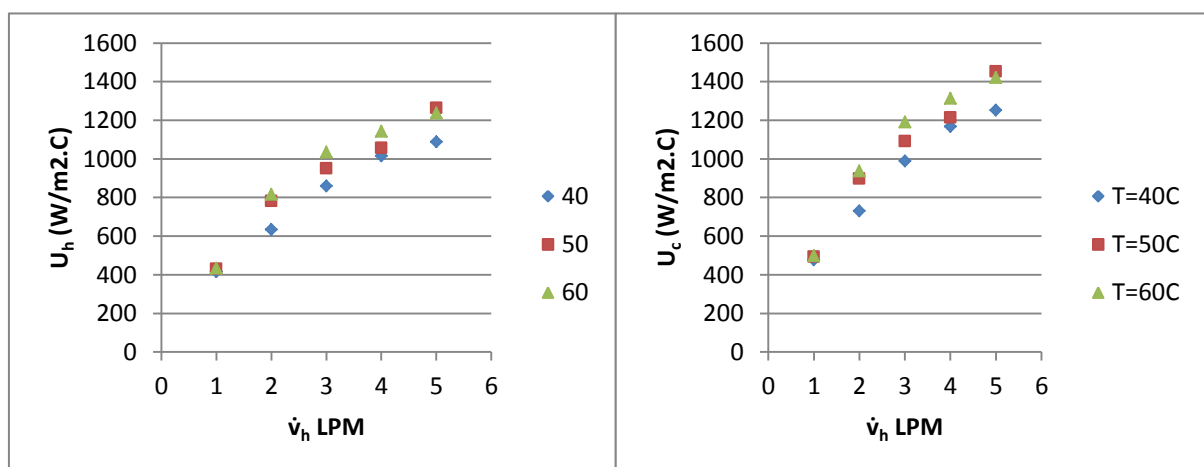


Figure (D-24) Effect of hot mass flow rate on overall heat transfer coefficient in corrugated tube ($z/d=0.5$) at $\dot{v}_c=4$ LPM in different temperatures

Appendix [D]

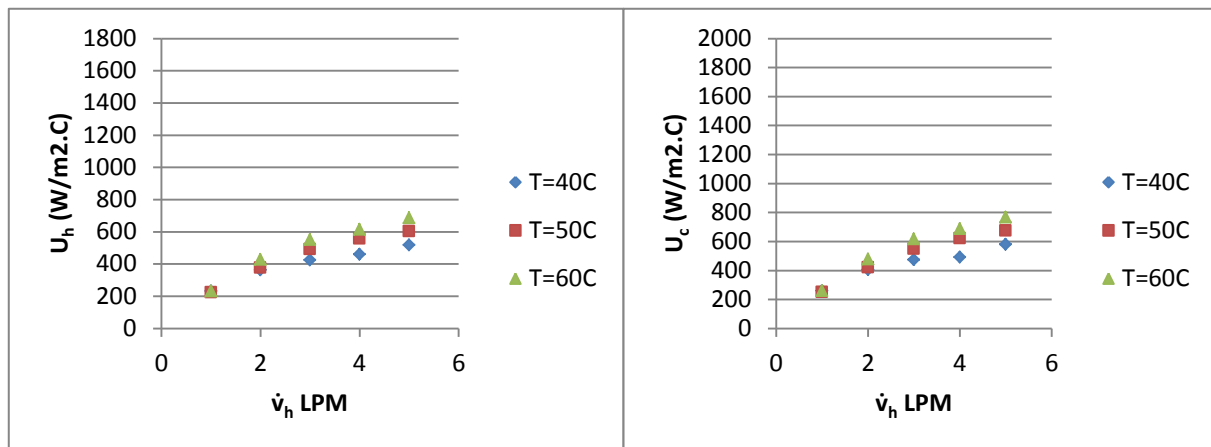


Figure (D-25) Effect of hot mass flow rate on overall heat transfer coefficient in smooth tube at $\dot{v}_c=5$ LPM in different temperatures

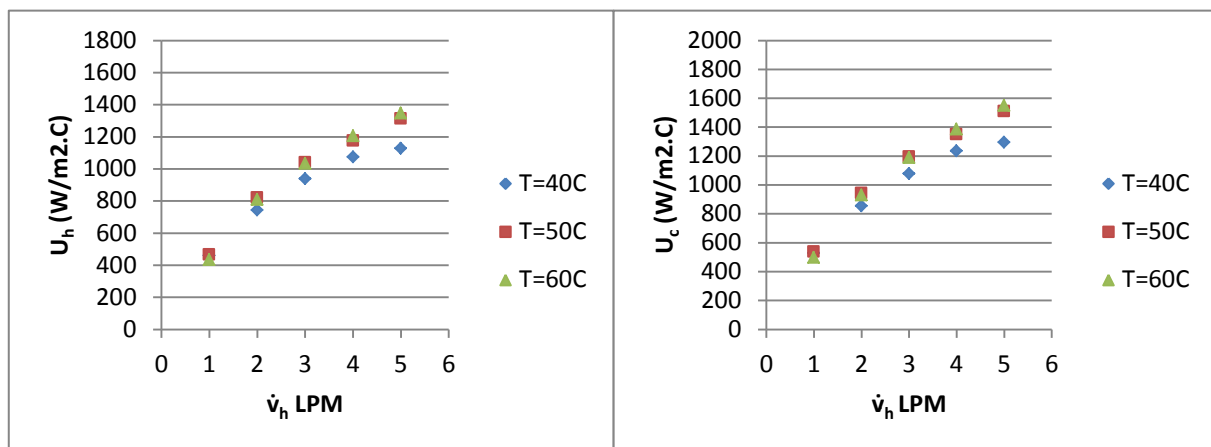


Figure (D-26) Effect of hot mass flow rate on overall heat transfer coefficient in corrugated tube ($z/d=1$) at $\dot{v}_c=5$ LPM in different temperatures

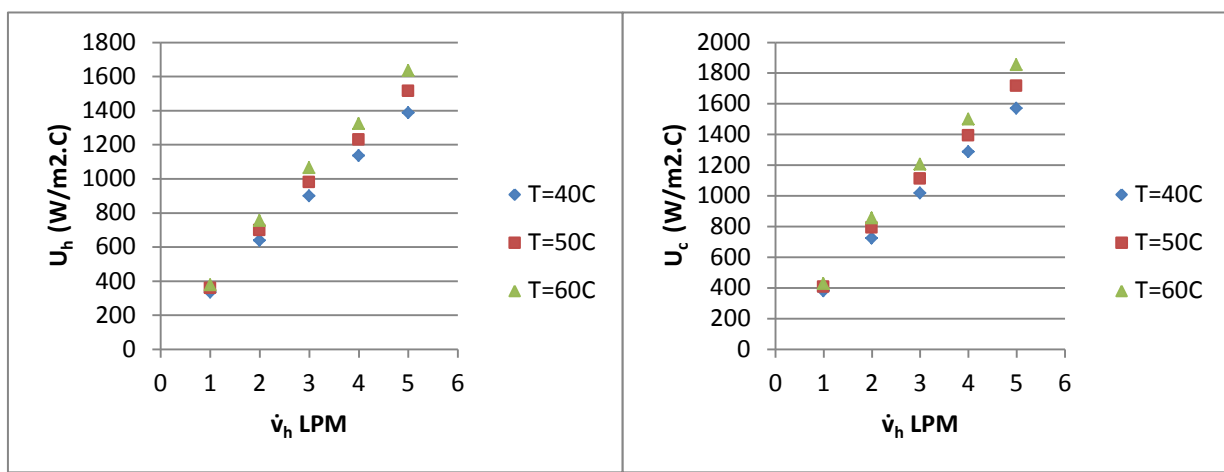


Figure (D-27) Effect of hot mass flow rate on overall heat transfer coefficient in corrugated tube ($z/d=0.5$) at $\dot{v}_c=5$ LPM in different temperatures

Appendix [D]

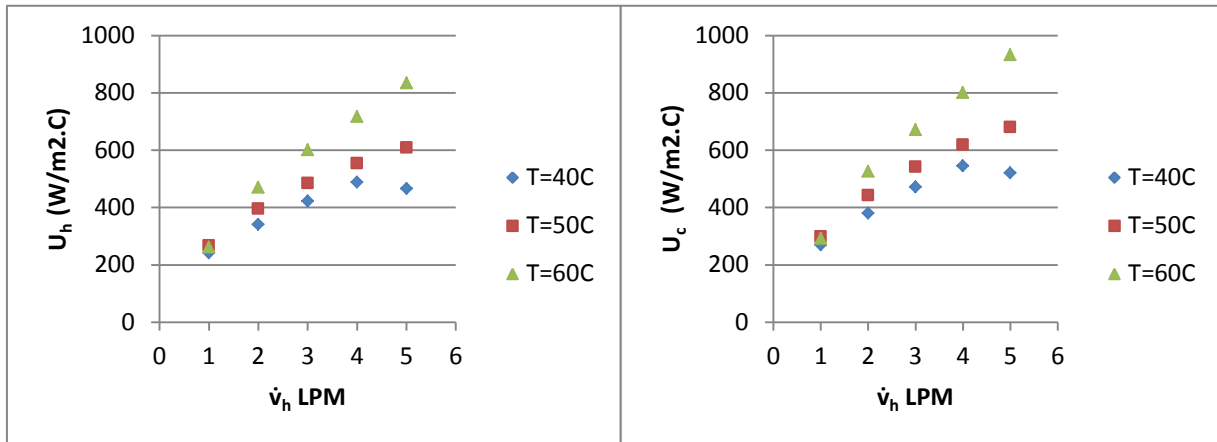


Figure (D-28) Effect of hot mass flow rate on overall heat transfer coefficient in smooth tube at $\dot{v}_c=6$ LPM in different temperatures

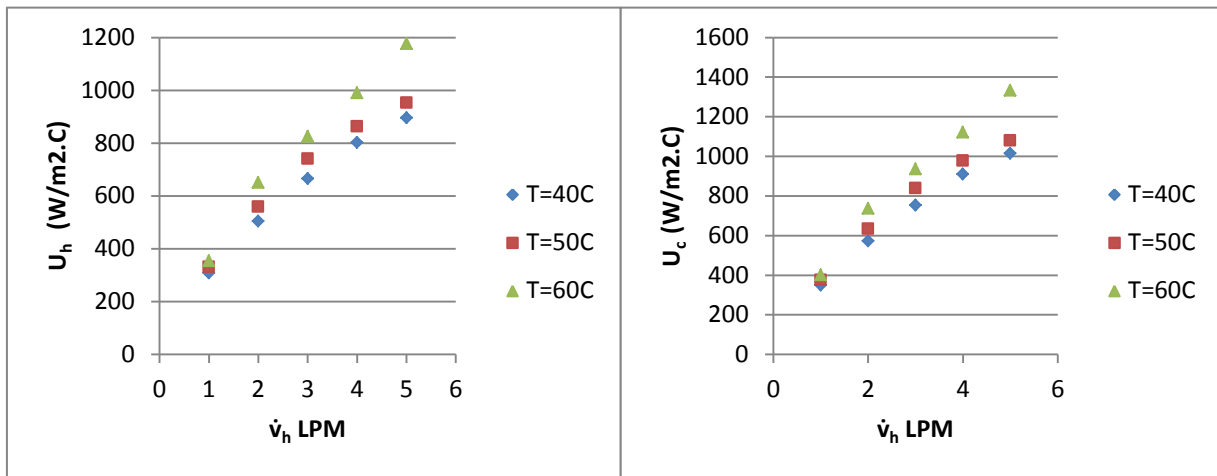


Figure (D-29) Effect of hot mass flow rate on overall heat transfer coefficient in corrugated tube ($z/d=1$) at $\dot{v}_c=6$ LPM in different temperatures

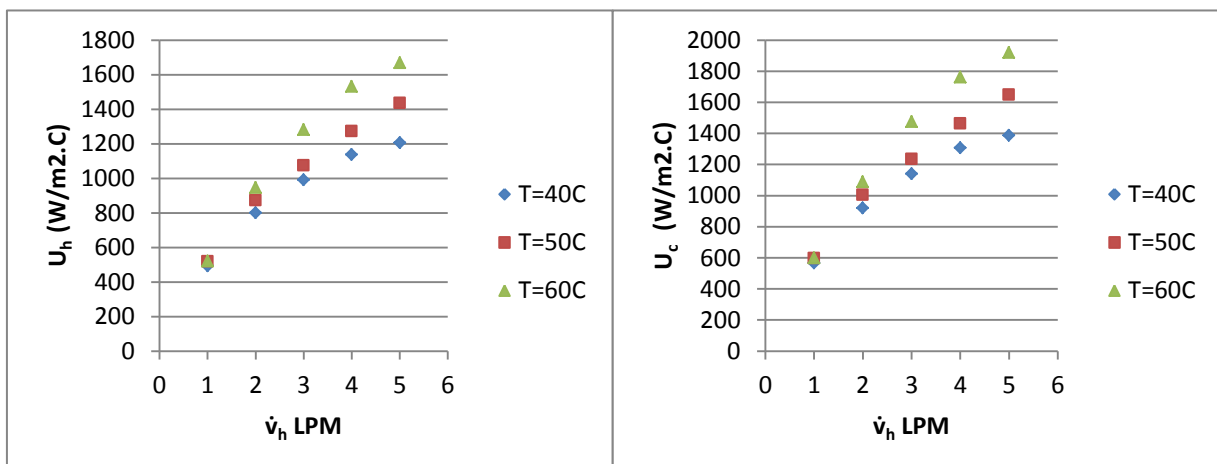


Figure (D-30) Effect of hot mass flow rate on overall heat transfer coefficient in corrugated tube ($z/d=0.5$) at $\dot{v}_c=6$ LPM in different temperatures

Appendix [D]

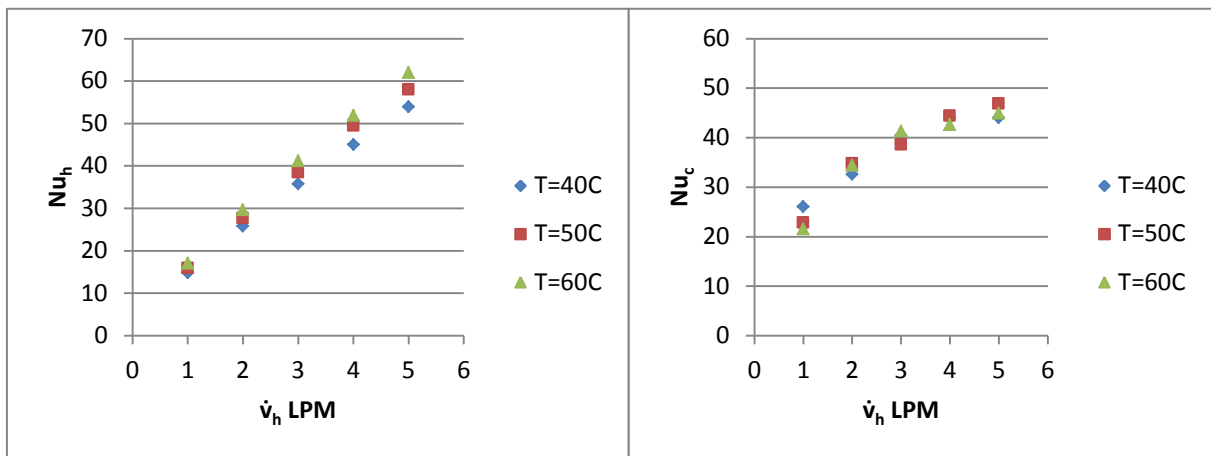


Figure (D-31) Effect of hot mass flow rate on Nusselt Number in smooth tube at $\dot{v}_c=4$ LPM in different temperatures

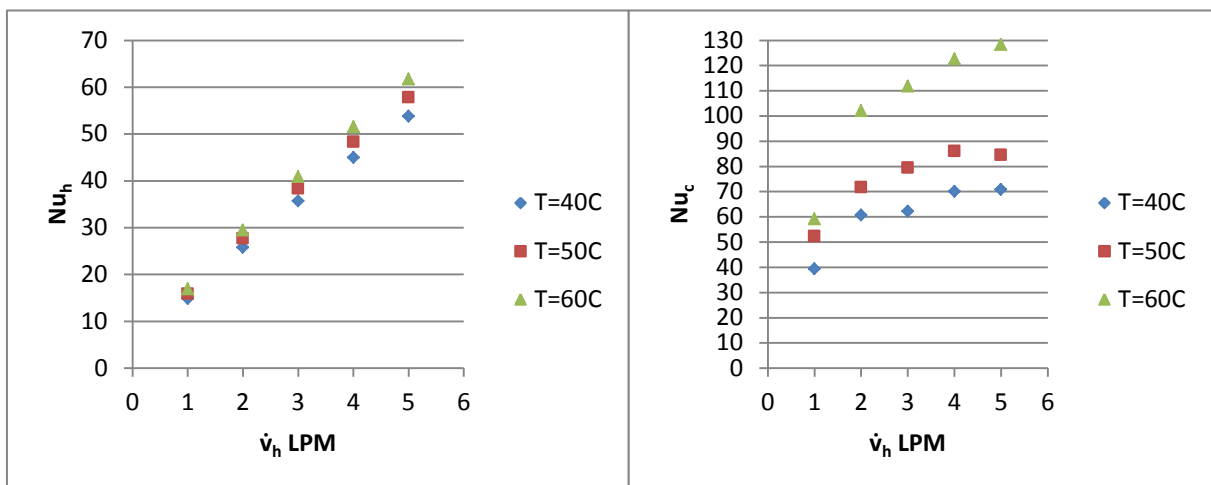


Figure (D-32) Effect of hot mass flow rate on Nusselt Number in corrugated tube ($z/d=1$) at $\dot{v}_c=4$ LPM in different temperatures

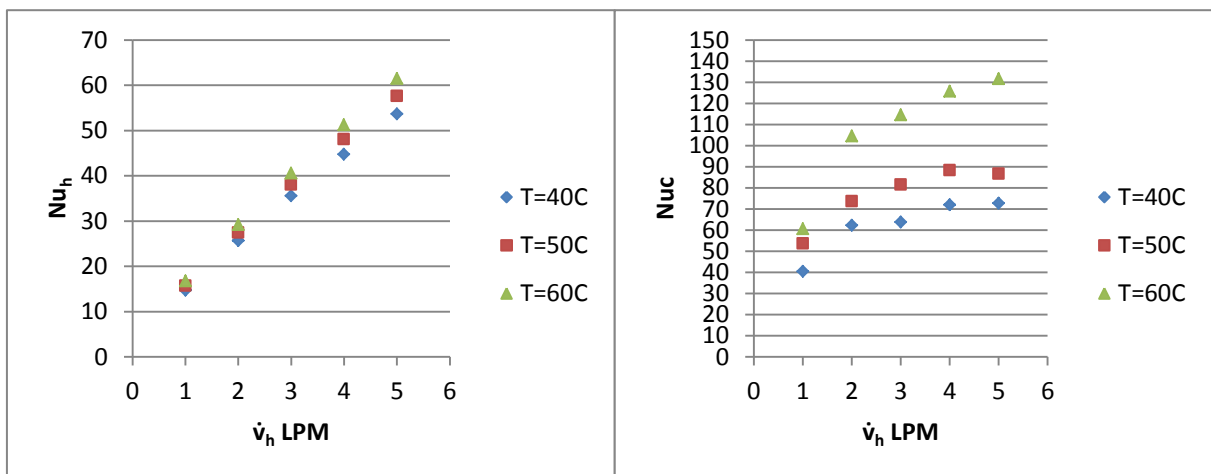


Figure (D-33) Effect of hot mass flow rate on Nusselt Number in corrugated tube ($z/d=0.5$) at $\dot{v}_c=4$ LPM in different temperatures

Appendix [D]

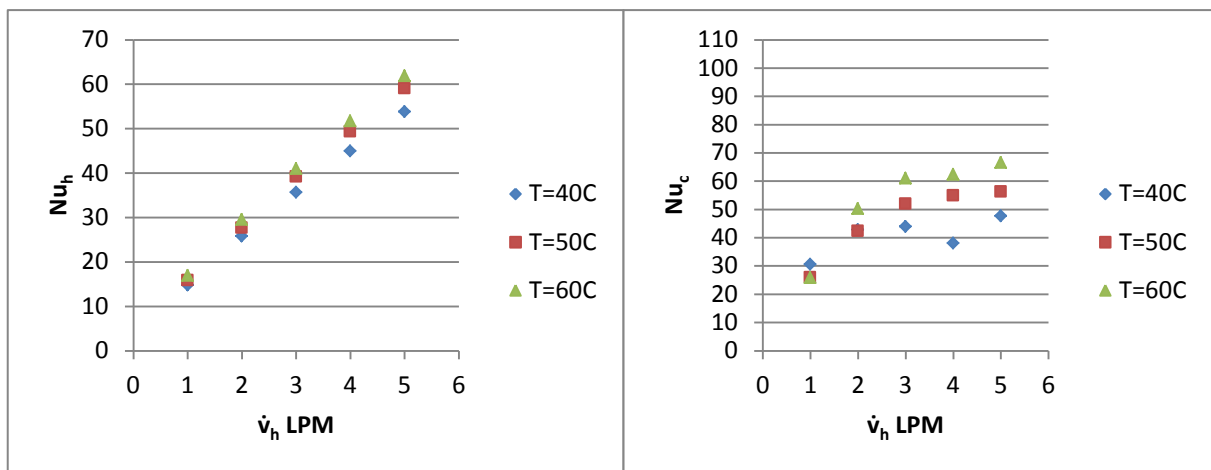


Figure (D-34) Effect of hot mass flow rate on Nusselt Number in smooth tube at $\dot{v}_c=5$ LPM in different temperatures

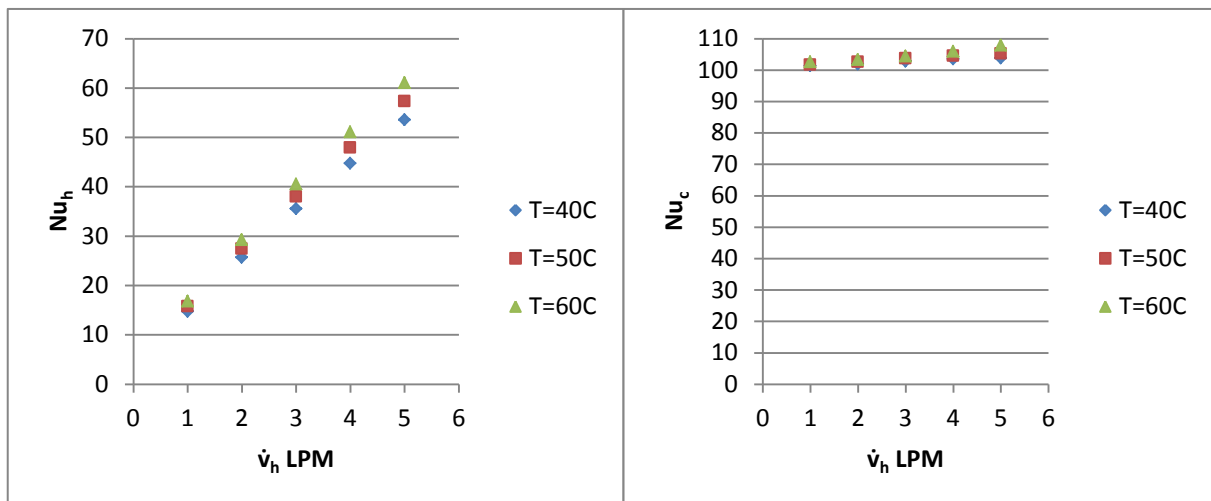


Figure (D-35) Effect of hot mass flow rate on Nusselt Number in corrugated tube ($z/d=1$) at $\dot{v}_c=5$ LPM in different temperatures

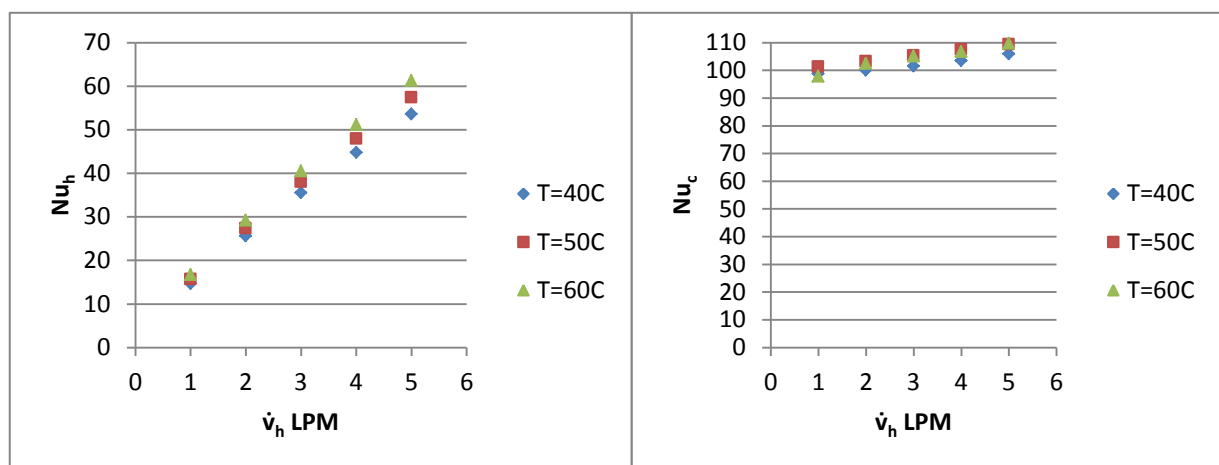


Figure (D-36) Effect of hot mass flow rate on Nusselt Number in corrugated tube ($z/d=0.5$) at $\dot{v}_c=5$ LPM in different temperatures

Appendix [D]

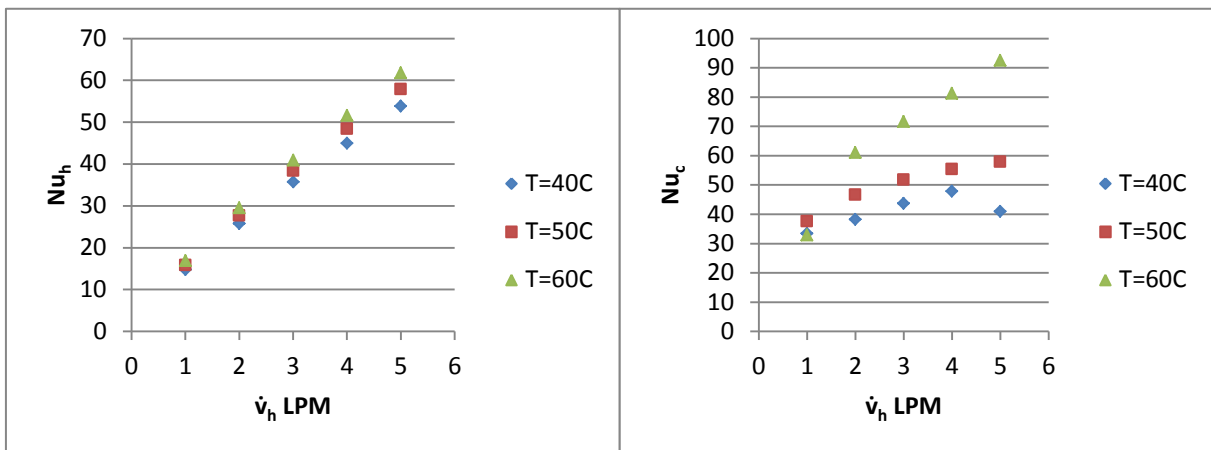


Figure (D-37) Effect of hot mass flow rate on Nusselt Number in smooth tube at $\dot{v}_c = 6$ LPM in different temperatures

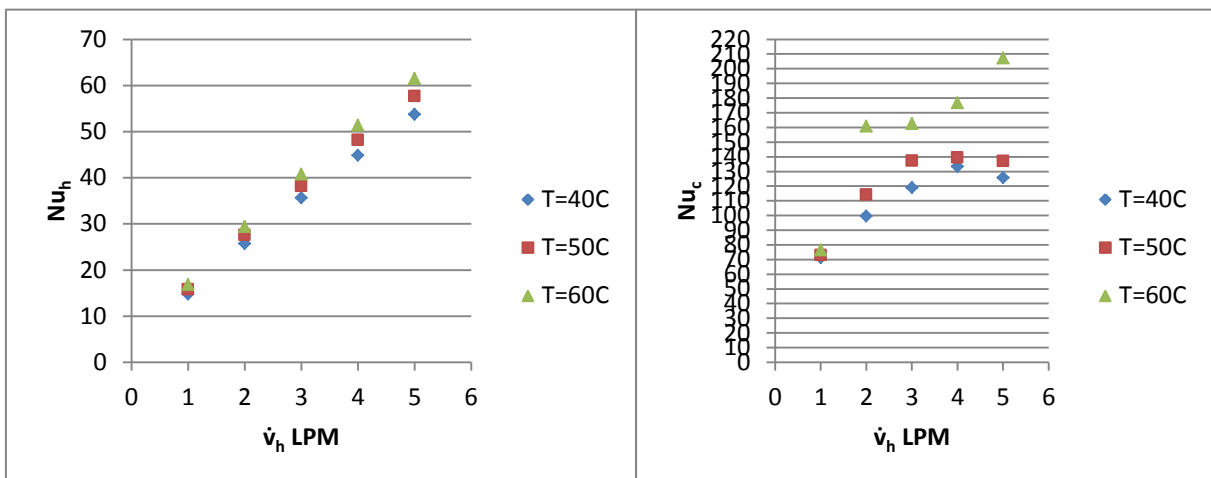


Figure (D-38) Effect of hot mass flow rate on Nusselt Number in corrugated tube ($z/d = 1$) at $\dot{v}_c = 6$ LPM in different temperatures

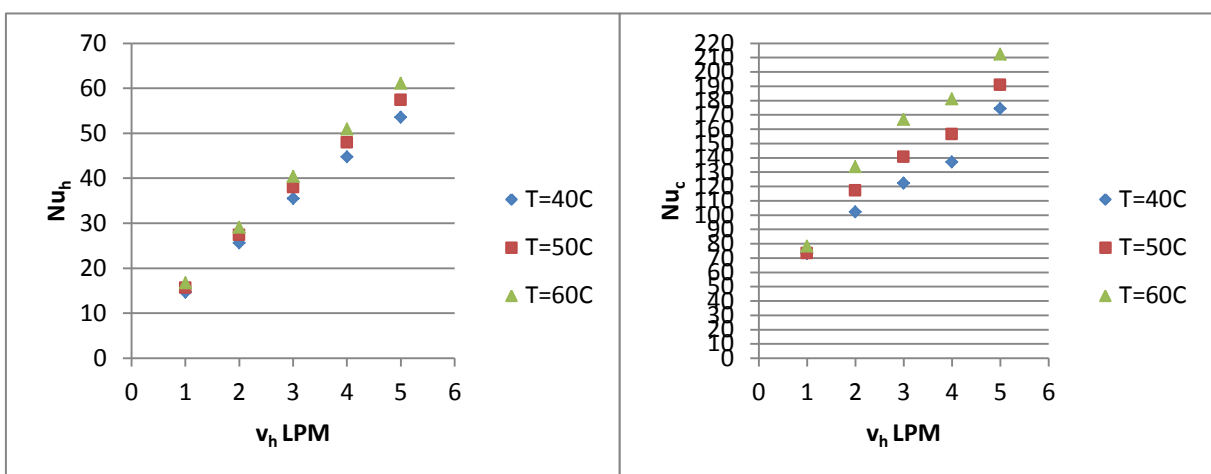


Figure (D-39) Effect of hot mass flow rate on Nusselt Number in corrugated tube ($z/d = 0.5$) at $\dot{v}_c = 6$ LPM in different temperatures

Appendix [D]

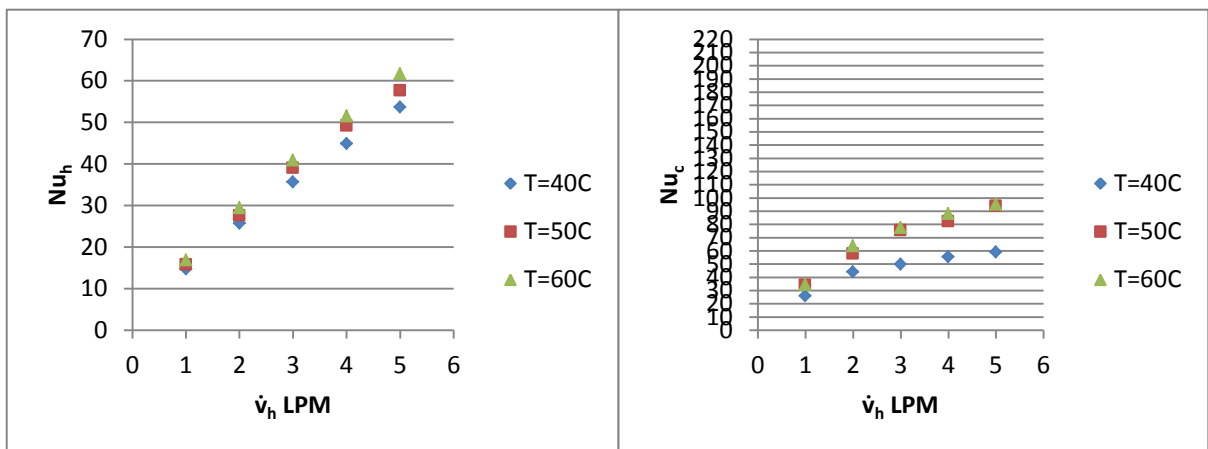


Figure (D-40) Effect of hot mass flow rate on Nusselt Number in smooth tube at $\dot{v}_c = 7$ LPM in different temperatures

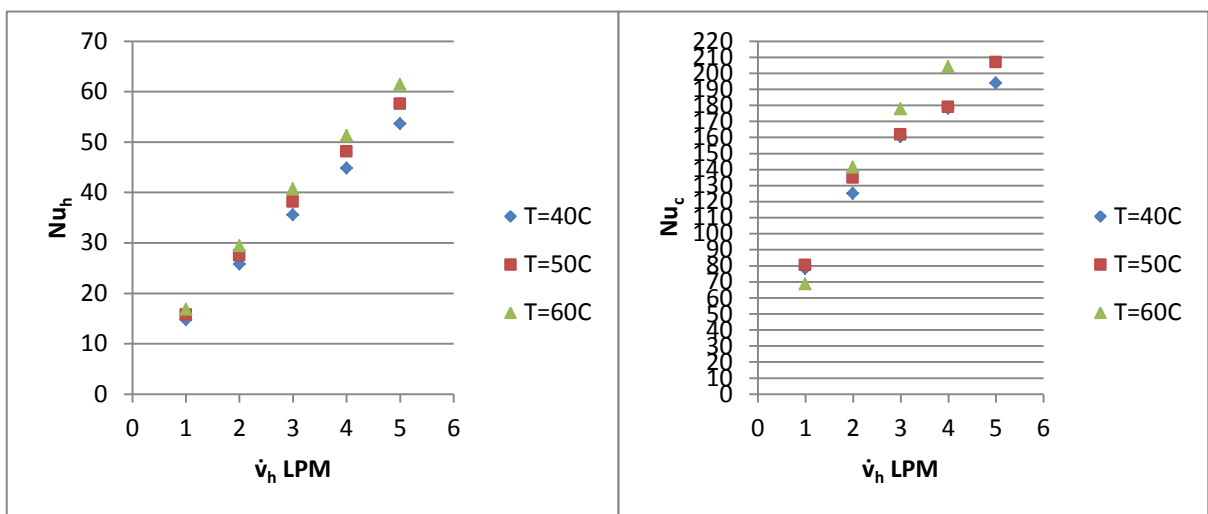


Figure (D-41) Effect of hot mass flow rate on Nusselt Number in corrugated tube ($z/d = 1$) at $\dot{v}_c = 7$ LPM in different temperatures

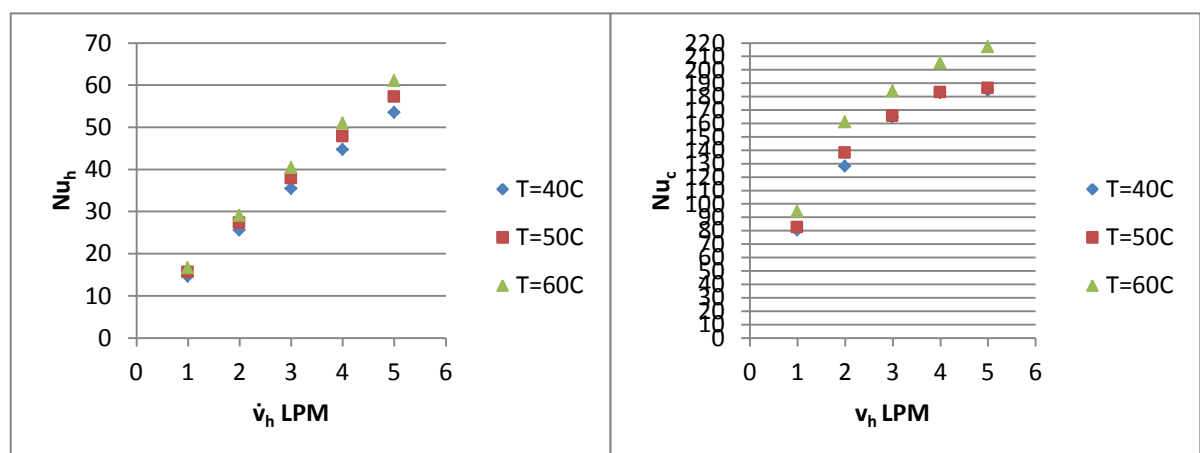


Figure (D-42) Effect of hot mass flow rate on Nusselt Number in corrugated tube ($z/d = 0.5$) at $\dot{v}_c = 7$ LPM in different temperatures

Appendix [D]

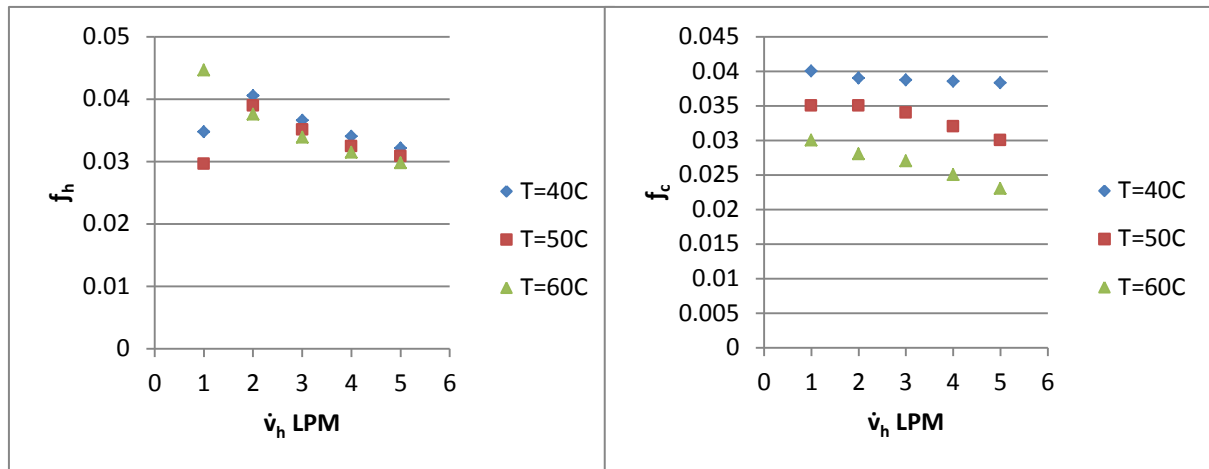


Figure (D-43) Effect of hot mass flow rate on fraction factor in smooth tube at $\dot{v}_c = 4$ LPM in different temperatures

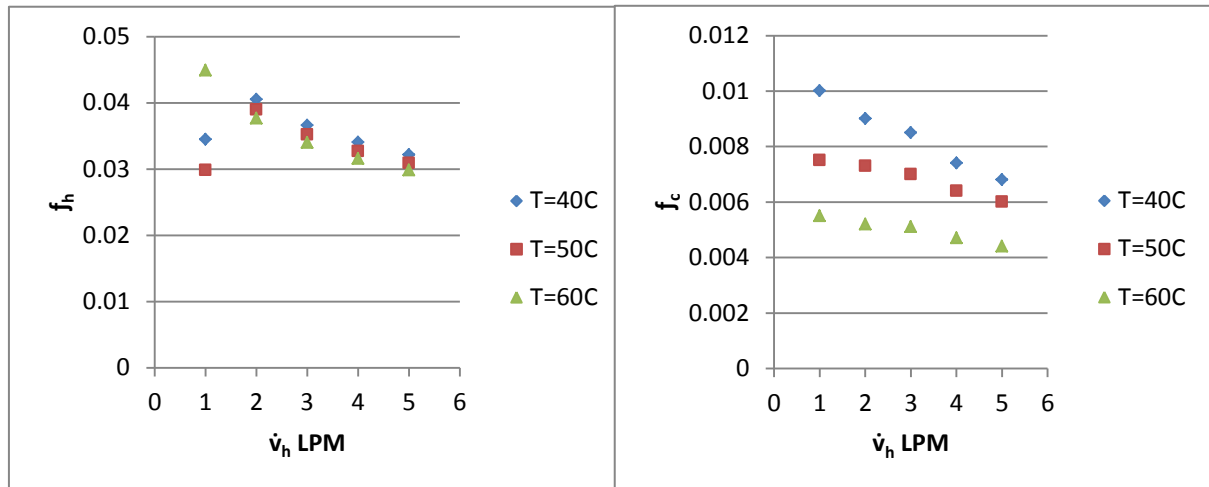


Figure (D-44) Effect of hot mass flow rate on fraction factor in corrugated tube ($z/d = 1$) at $\dot{v}_c = 4$ LPM in different temperatures

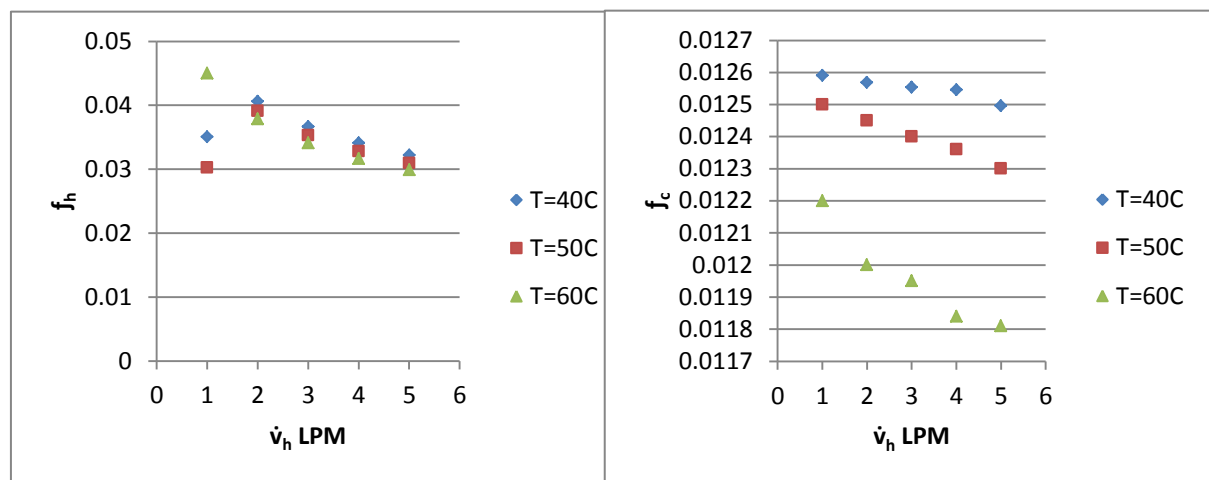


Figure (D-45) Effect of hot mass flow rate on fraction factor in corrugated tube ($z/d = 0.5$) at $\dot{v}_c = 4$ LPM in different temperatures

Appendix [D]

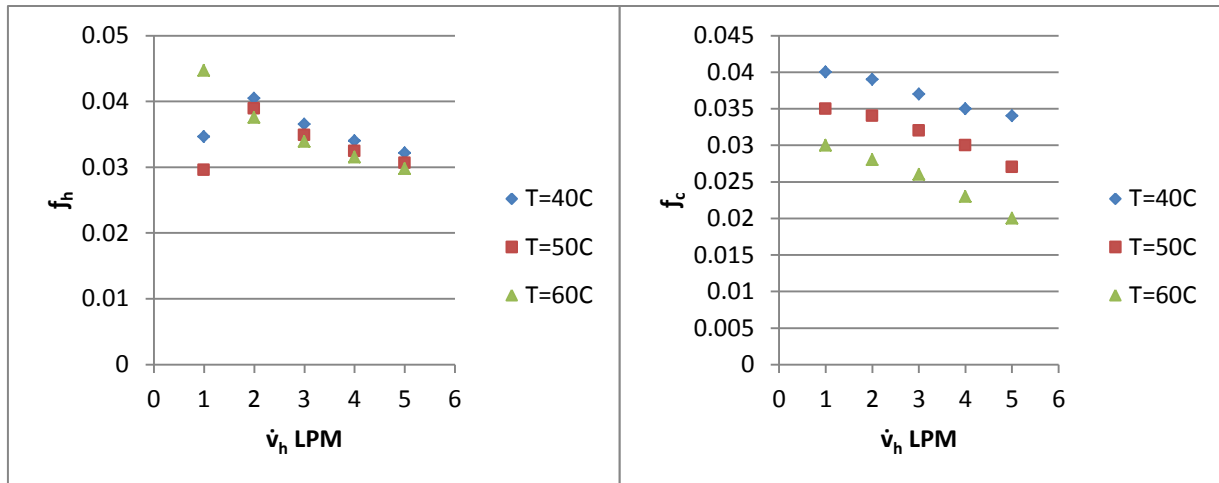


Figure (D-46) Effect of hot mass flow rate on fraction factor in smooth tube at $\dot{v}_c = 5$ LPM in different temperatures

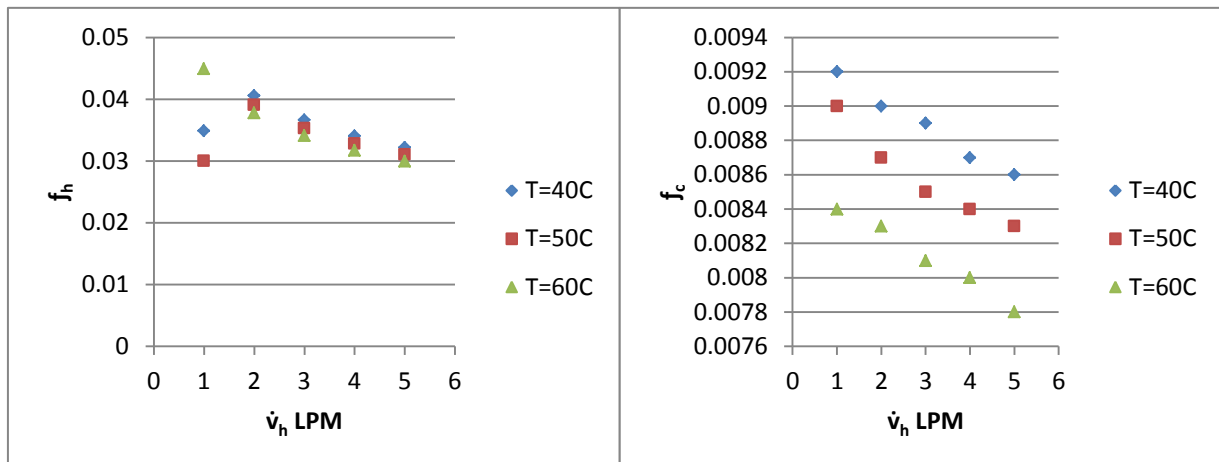


Figure (D-47) Effect of hot mass flow rate on fraction factor in corrugated tube ($z/d = 1$) at $\dot{v}_c = 5$ LPM in different temperatures

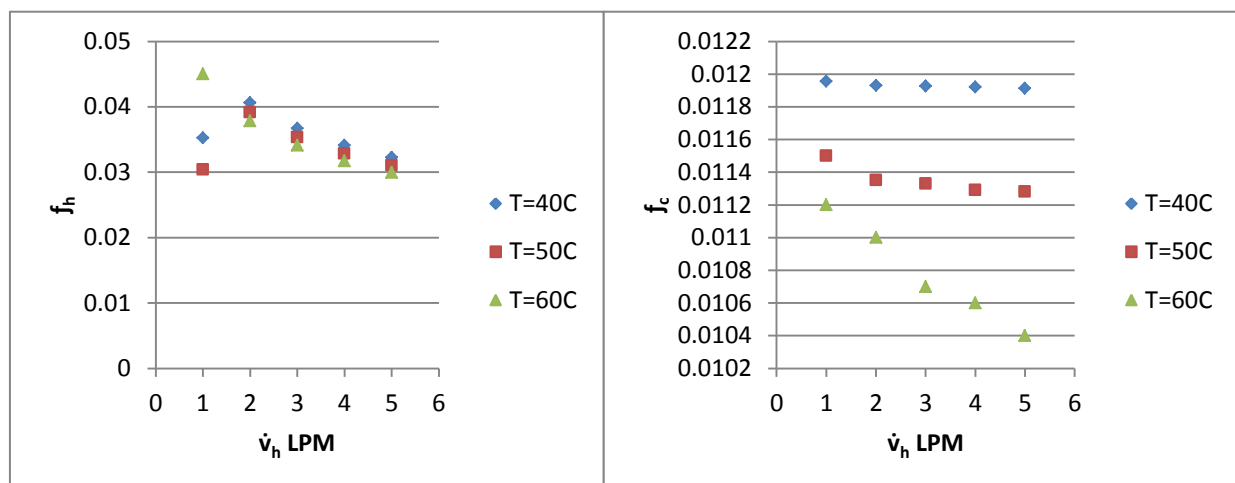


Figure (D-48) Effect of hot mass flow rate on fraction factor in corrugated tube ($z/d = 0.5$) at $\dot{v}_c = 5$ LPM in different temperatures

Appendix [D]

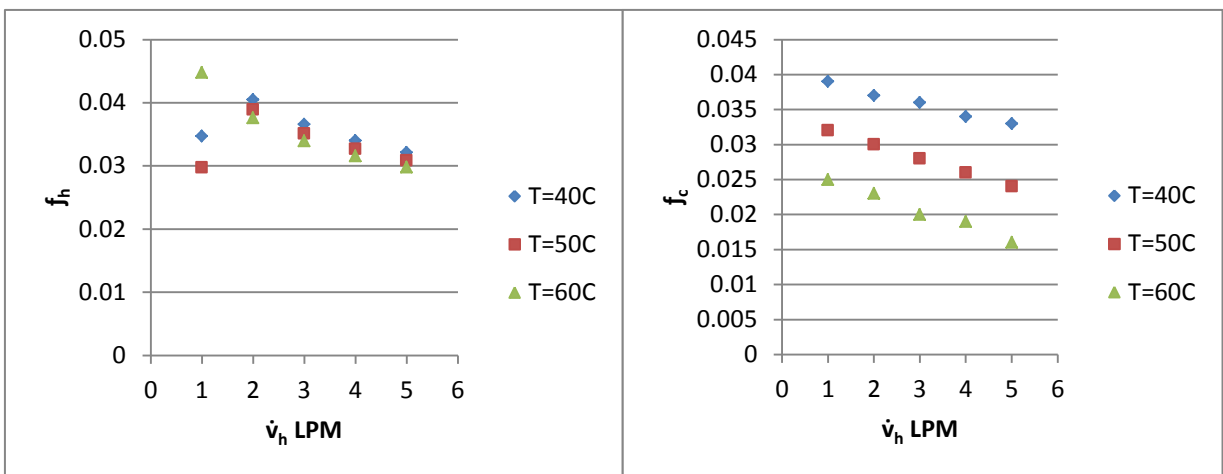


Figure (D-49) Effect of hot mass flow rate on fraction factor in smooth tube at $\dot{v}_c=6$ LPM in different temperatures

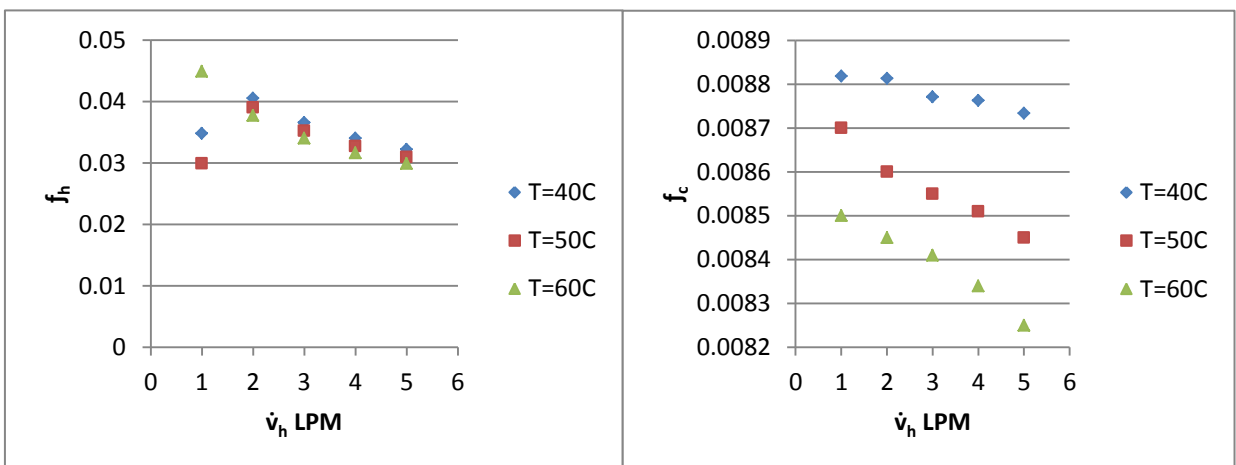


Figure (D-50) Effect of hot mass flow rate on fraction factor in corrugated tube ($z/d=1$) at $\dot{v}_c=6$ LPM in different temperatures

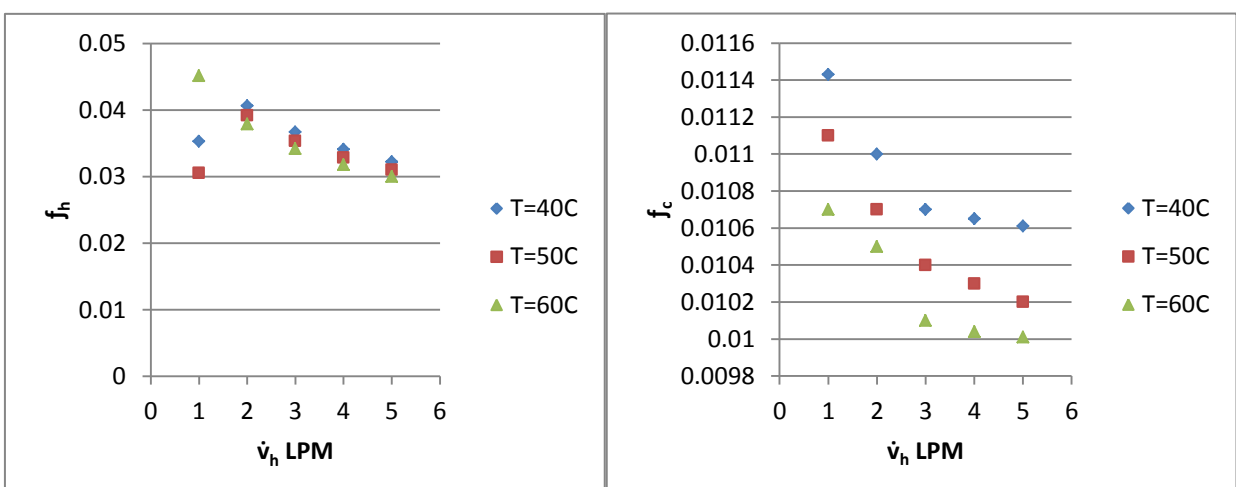


Figure (D-51) Effect of hot mass flow rate on fraction factor in corrugated tube ($z/d=0.5$) at $\dot{v}_c=6$ LPM in different temperatures

Appendix [D]

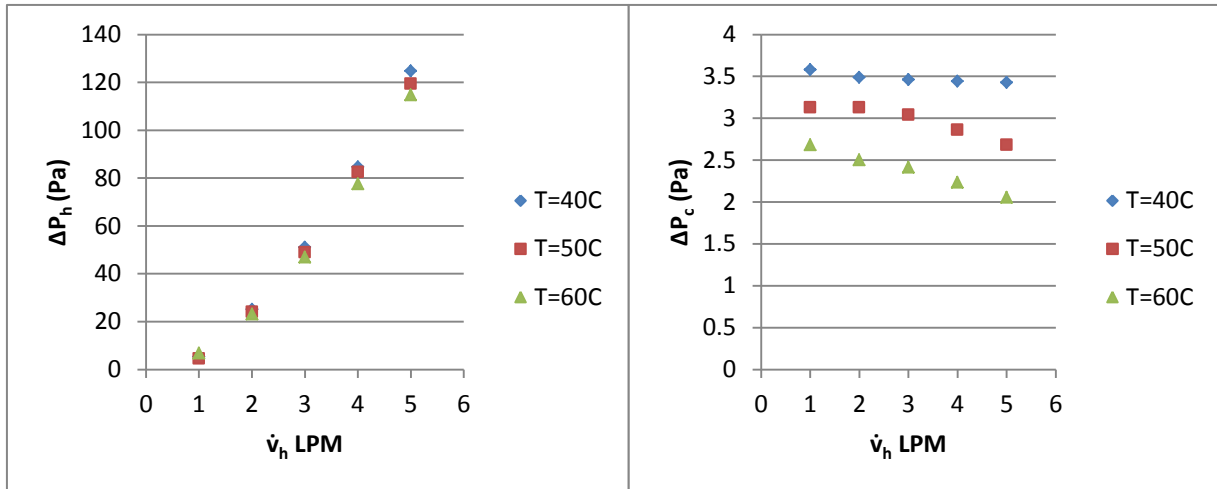


Figure (D-52) Effect of hot mass flow rate on pressure drop in smooth tube at $\dot{v}_c=4$ LPM in different temperatures

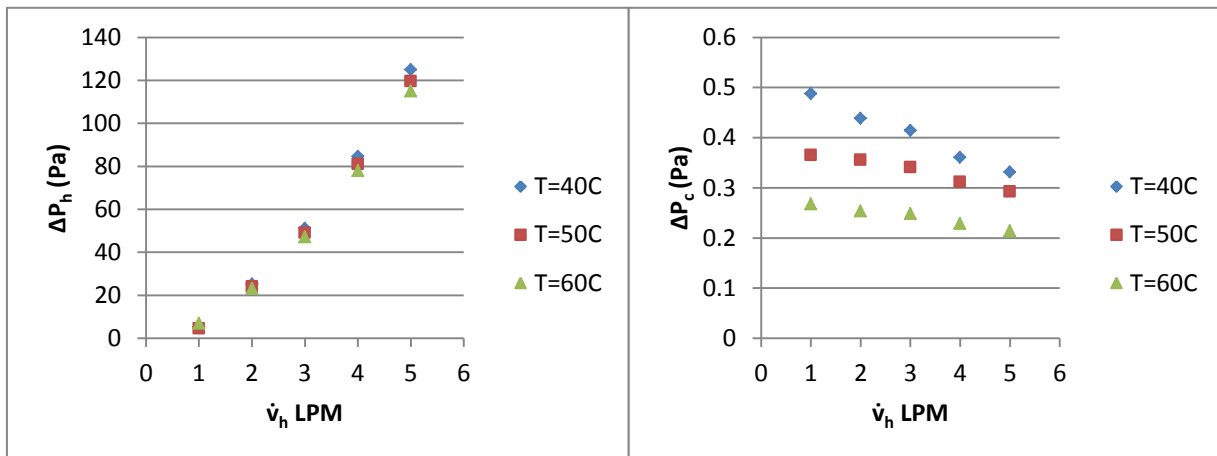


Figure (D-53) Effect of hot mass flow rate on pressure drop in corrugated tube ($z/d=1$) at $\dot{v}_c=4$ LPM in different temperatures

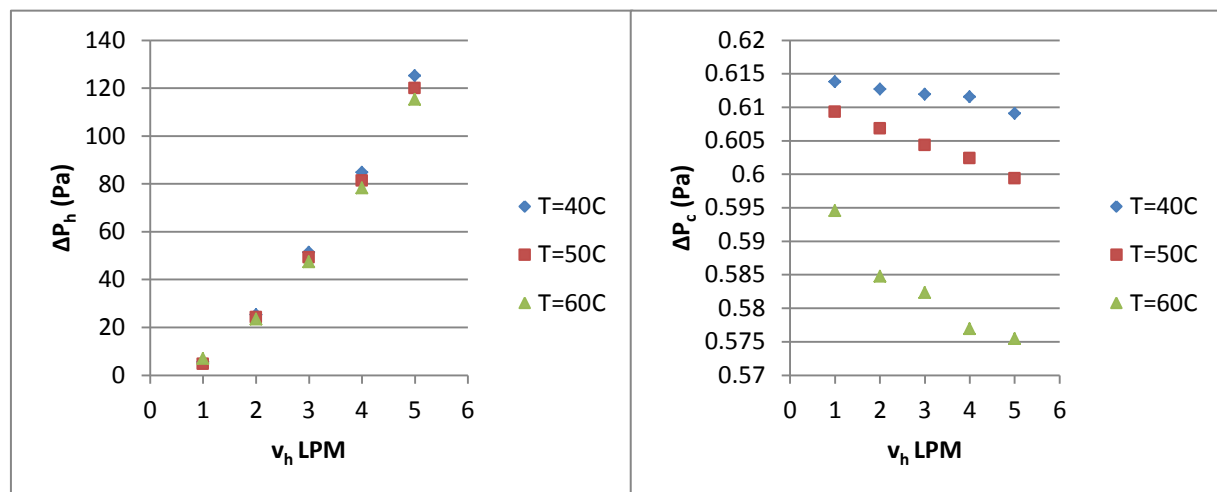


Figure (D-54) Effect of hot mass flow rate on pressure drop in corrugated tube ($z/d=0.5$) at $\dot{v}_c=4$ LPM in different temperatures

Appendix [D]

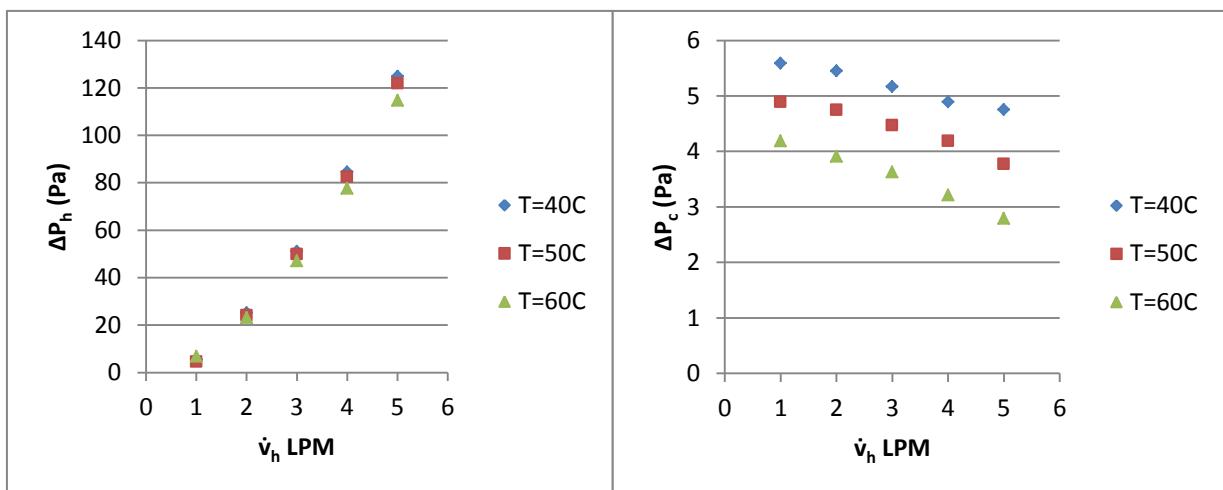


Figure (D-55) Effect of hot mass flow rate on pressure drop in smooth tube at $\dot{v}_c=5$ LPM in different temperatures

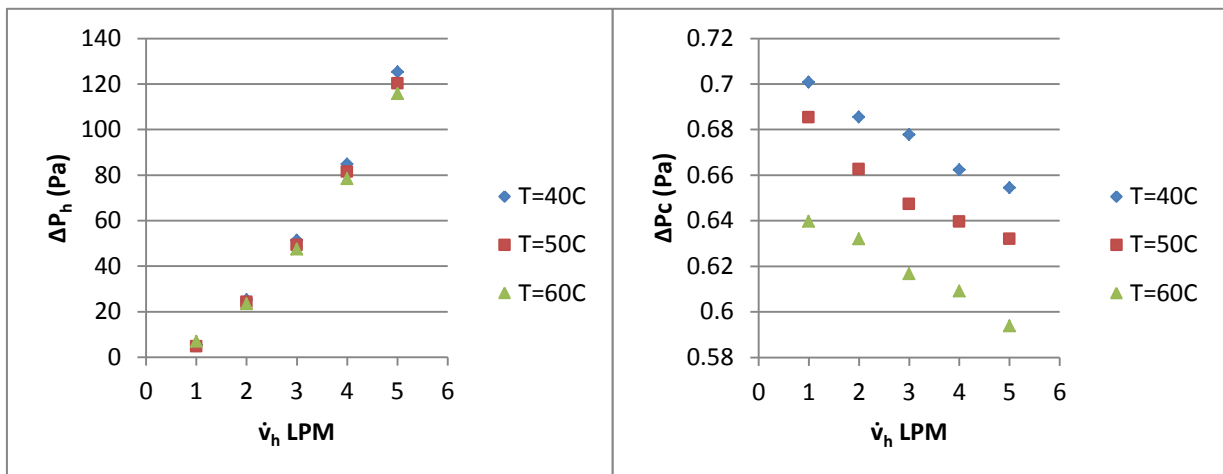


Figure (D-56) Effect of hot mass flow rate on pressure drop in corrugated tube ($z/d=1$) at $\dot{v}_c=5$ LPM in different temperatures

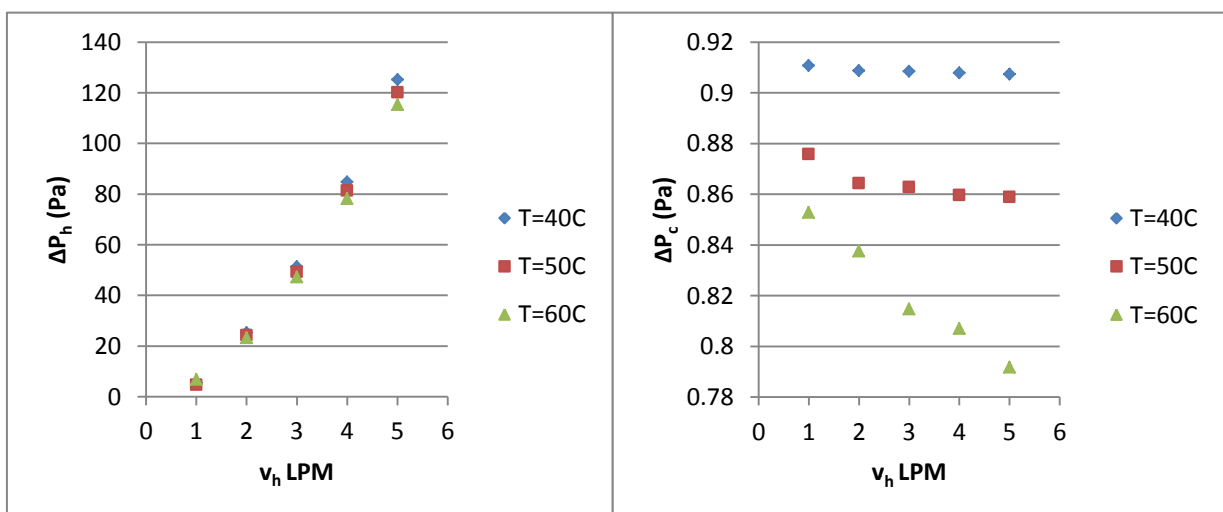


Figure (D-57) Effect of hot mass flow rate on pressure drop in corrugated tube ($z/d=0.5$) at $\dot{v}_c=5$ LPM in different temperatures

Appendix [D]

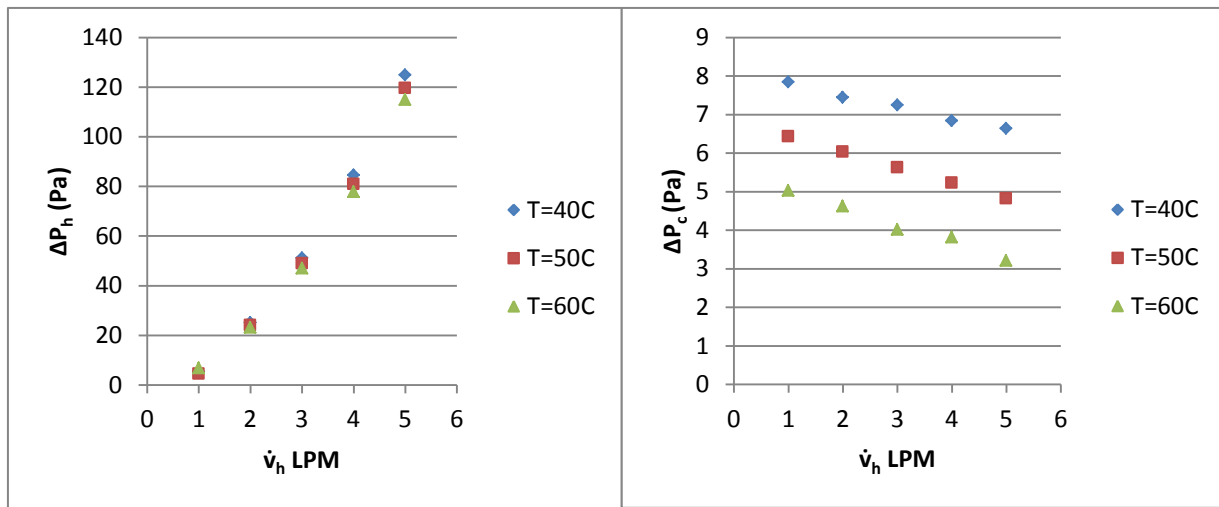


Figure (D-58) Effect of hot mass flow rate on pressure drop in smooth tube at $\dot{v}_c = 6$ LPM in different temperatures

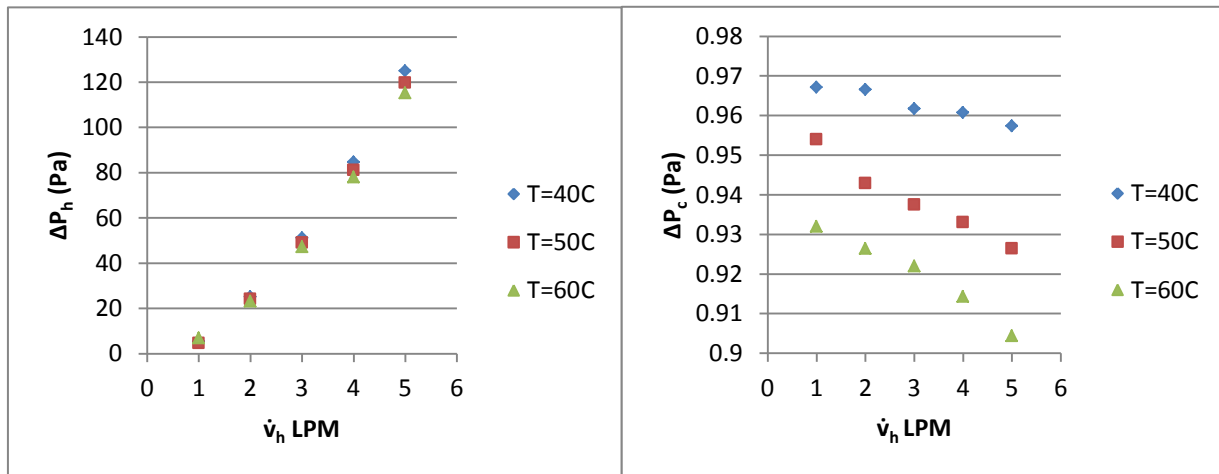


Figure (D-59) Effect of hot mass flow rate on pressure drop in corrugated tube ($z/d = 1$) at $\dot{v}_c = 6$ LPM in different temperatures

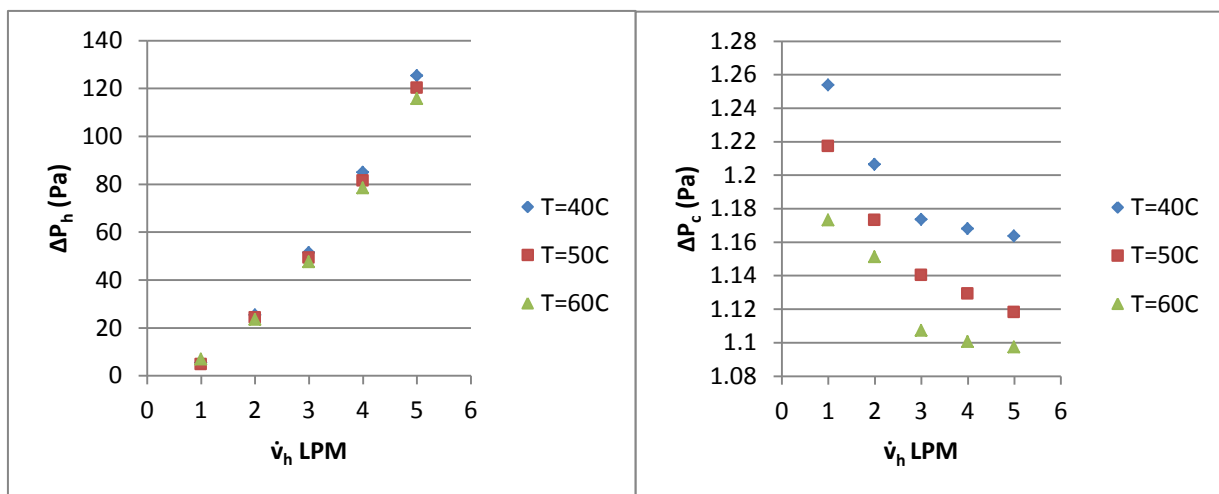


Figure (D-60) Effect of hot mass flow rate on pressure drop in corrugated tube ($z/d = 0.5$) at $\dot{v}_c = 6$ LPM in different temperatures

Appendix [D]

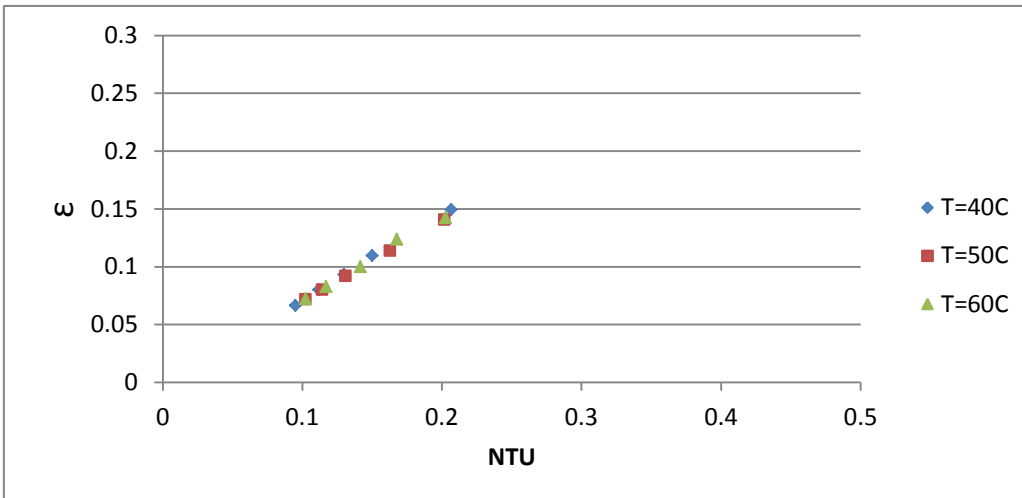


Figure (D-61) Variation of effectiveness with number of transfer units (NTU) in smooth tube at $\dot{v}_c = 4\text{LPM}$ in different temperatures

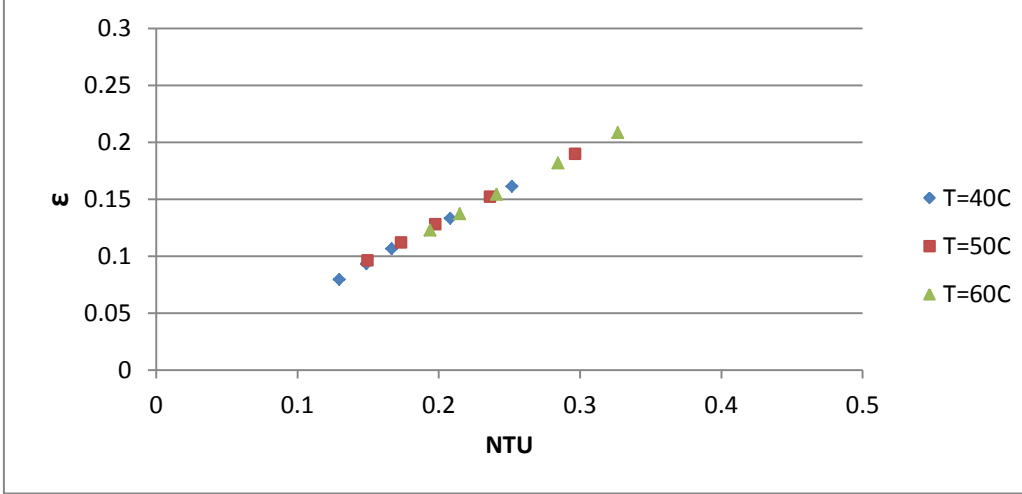


Figure (D-62) Variation of effectiveness with number of transfer units (NTU) in corrugated tube ($z/d=1$) at $\dot{v}_c = 4\text{LPM}$ in different temperatures

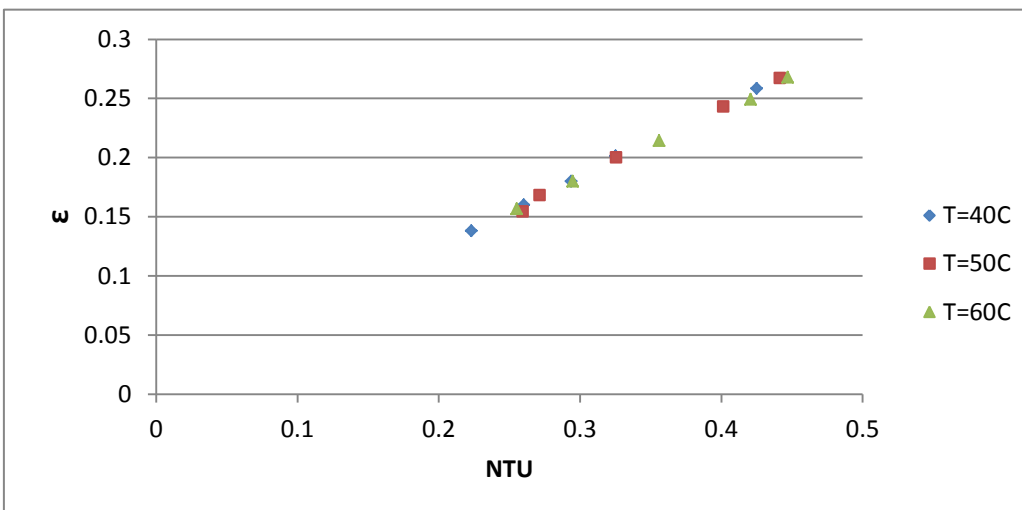


Figure (D-63) Variation of effectiveness with number of transfer units (NTU) in corrugated tube ($z/d=0.5$) at $\dot{v}_c = 4\text{LPM}$ in different temperatures

Appendix [D]

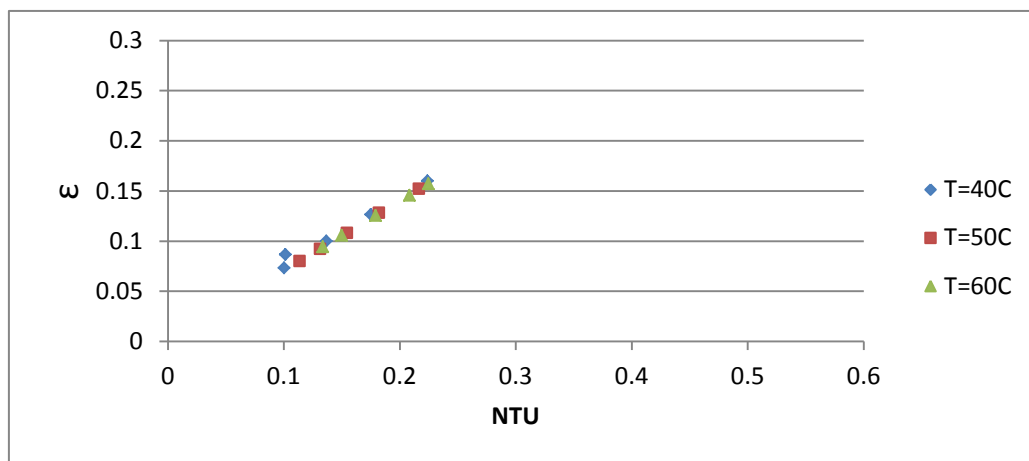


Figure (D-64) Variation of effectiveness with number of transfer units (NTU) in smooth tube at $\dot{v}_c=5\text{LPM}$ in different temperatures

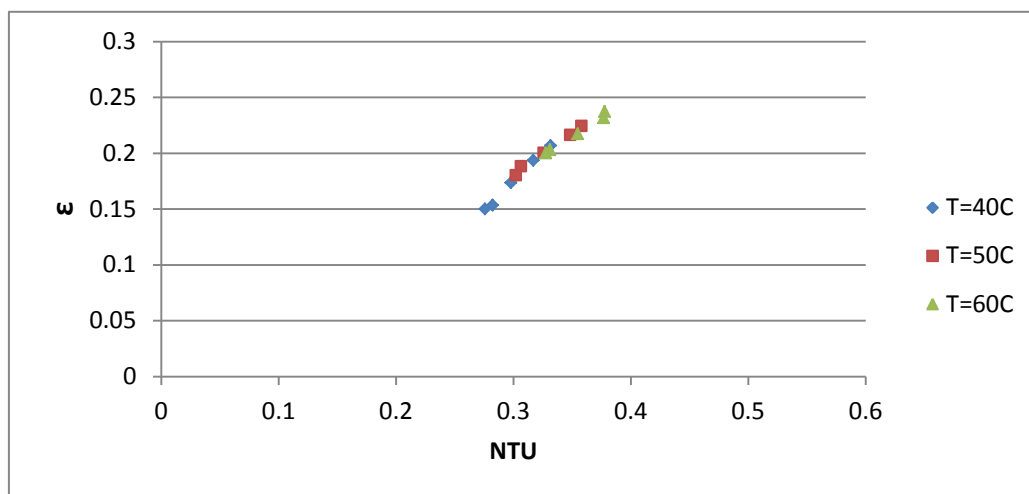


Figure (D-65) Variation of effectiveness with number of transfer units (NTU) in corrugated tube ($z/d=1$) at $\dot{v}_c=5\text{LPM}$ in different temperatures

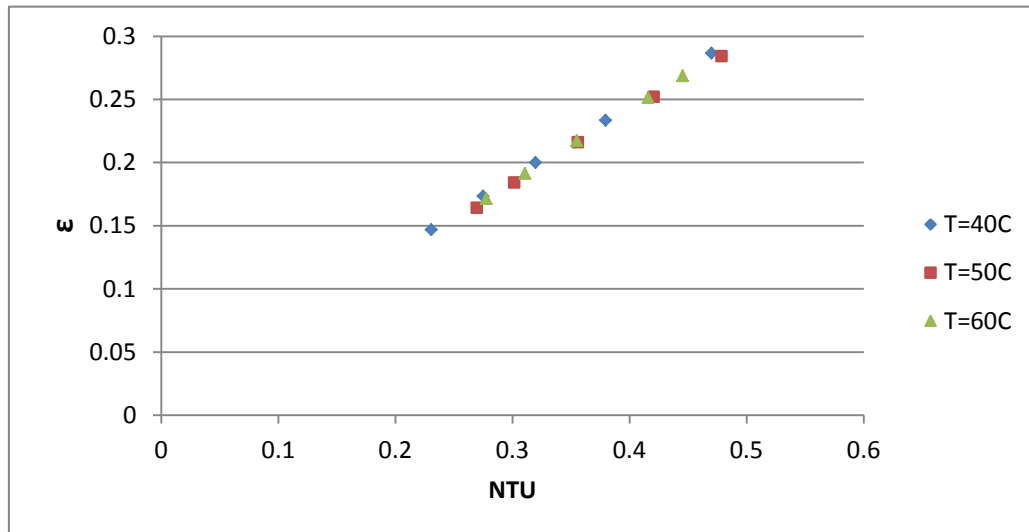


Figure (D-66) Variation of effectiveness with number of transfer units (NTU) in corrugated tube ($z/d=0.5$) at $\dot{v}_c=5\text{LPM}$ in different temperatures

Appendix [D]

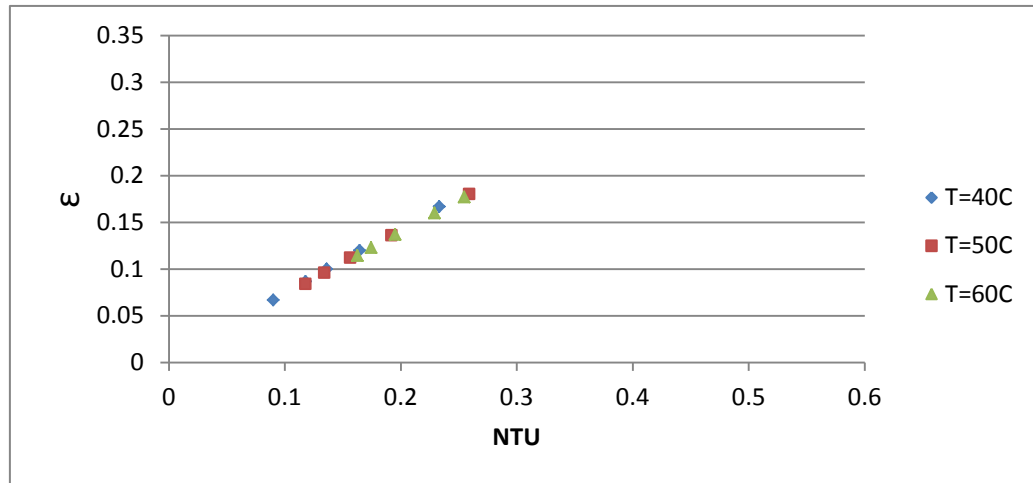


Figure (D-67) Variation of effectiveness with number of transfer units (NTU) in smooth tube at $\dot{v}_c=6\text{LPM}$ in different temperatures

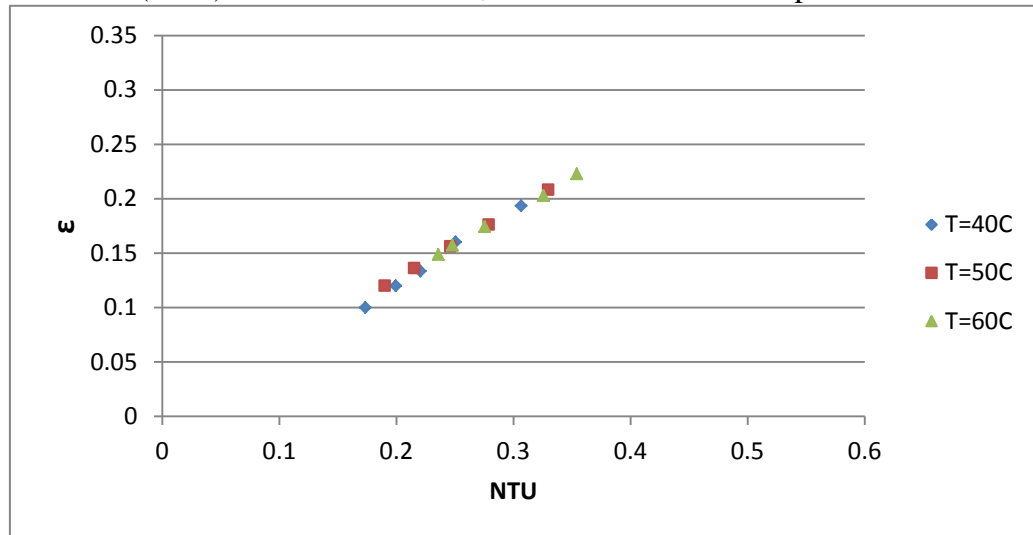


Figure (D-68) Variation of effectiveness with number of transfer units (NTU) in corrugated tube ($z/d=1$) at $\dot{v}_c=6\text{LPM}$ in different temperatures

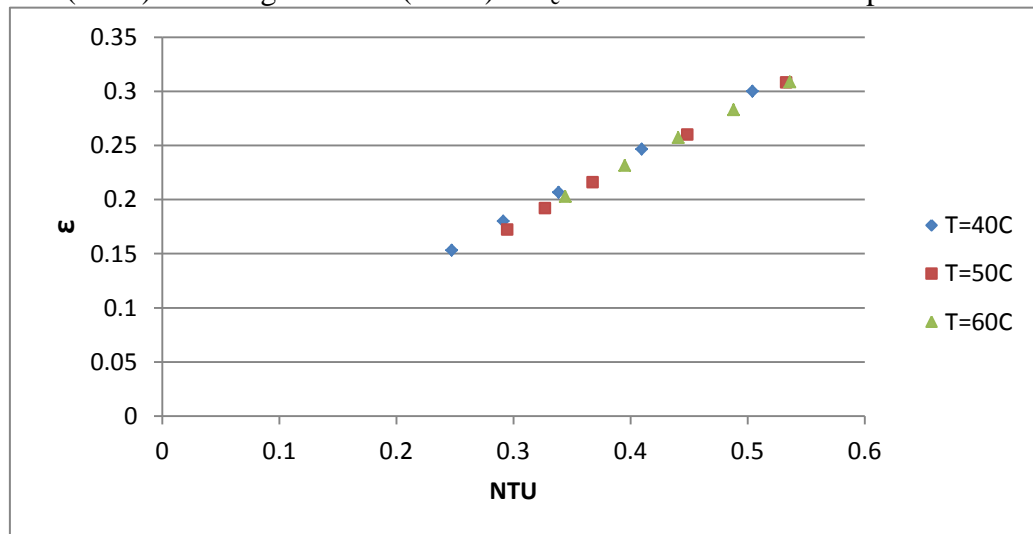


Figure (D-69) Variation of effectiveness with number of transfer units (NTU) in corrugated tube ($z/d=0.5$) at $\dot{v}_c=6\text{LPM}$ in different temperatures

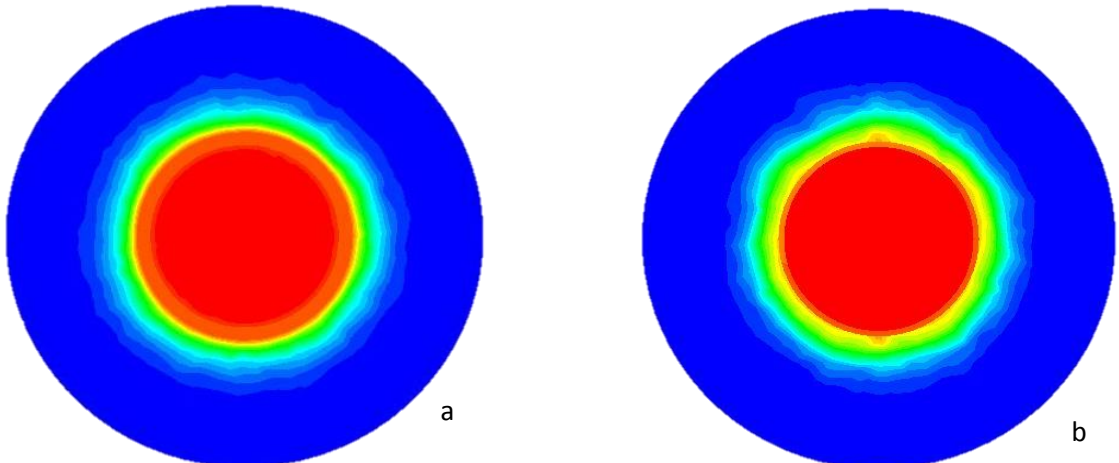


Figure (D-70) section in $z=50\text{cm}$ in test section smooth tube at $\dot{v}_h=2\text{LPM}$
(a) water (b) Nano fluid

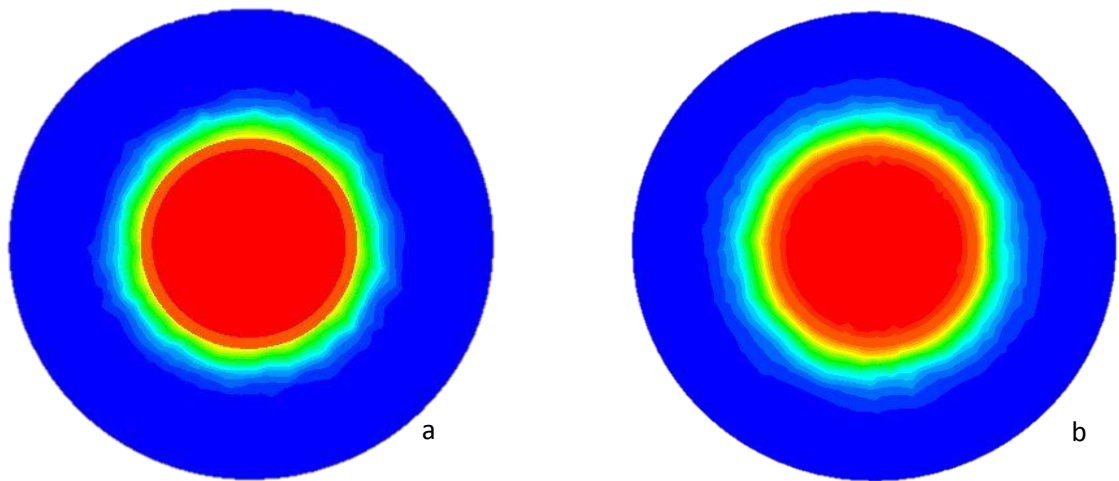


Figure (D-71) section in $z=50\text{cm}$ in test section smooth tube at $\dot{v}_h=3\text{LPM}$
(a) water (b) Nano fluid

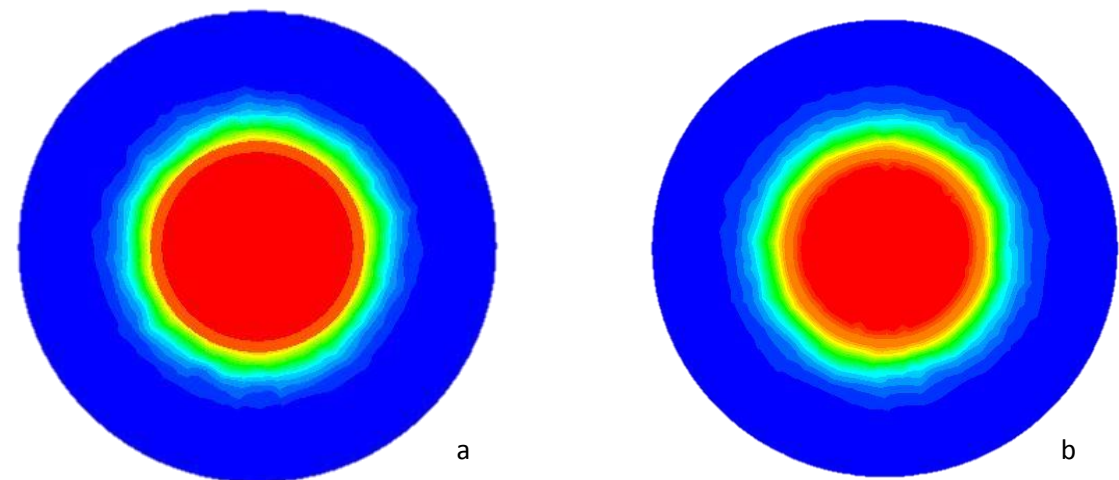
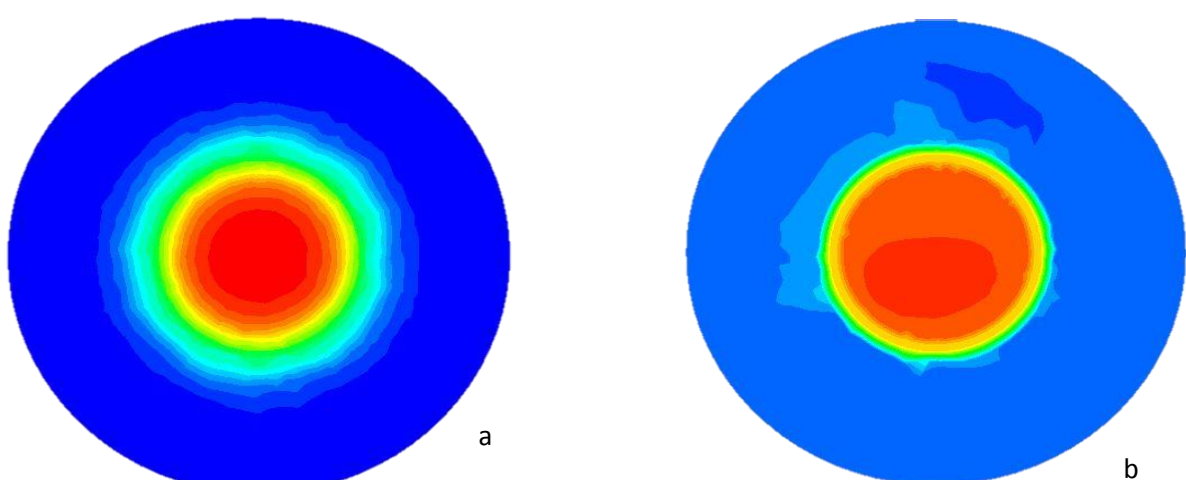
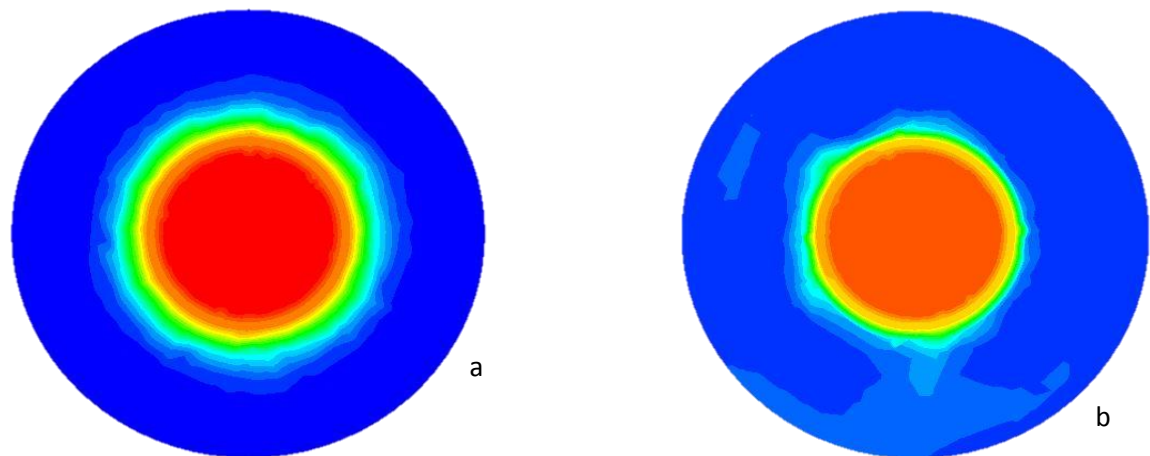
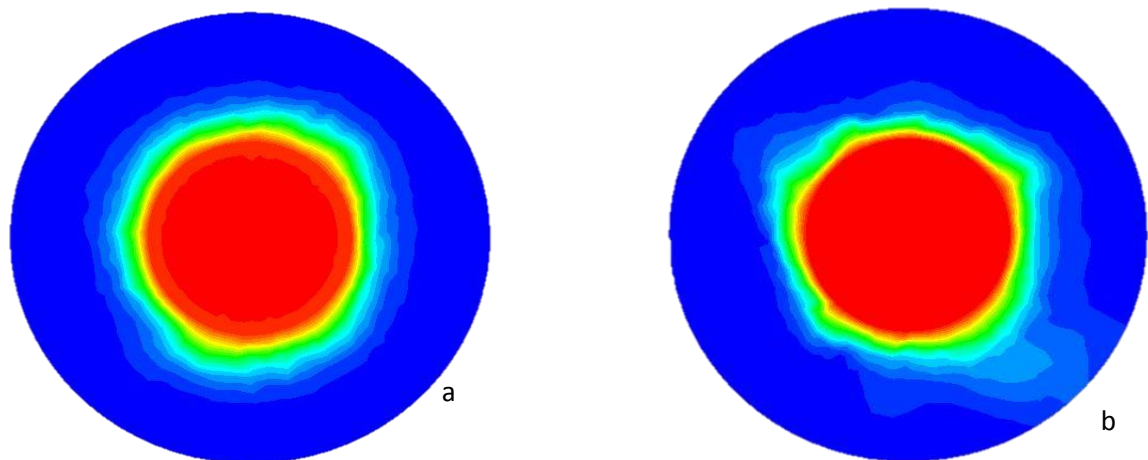


Figure (D-72) section in $z=50\text{cm}$ in test section smooth tube at $\dot{v}_h=4\text{LPM}$
(a) water (b) Nano fluid

Appendix [D]



Appendix [D]

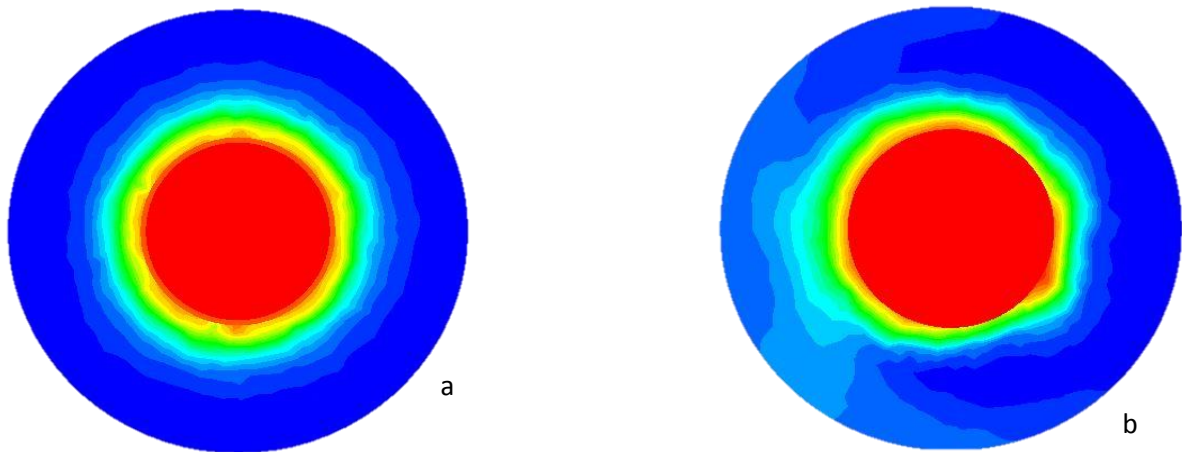


Figure (D-76) section in $z=50\text{cm}$ in test section corrugated tube ($z/d=0.5$)
at $\dot{v}_h = 2\text{LPM}$ (a) water (b) Nano fluid

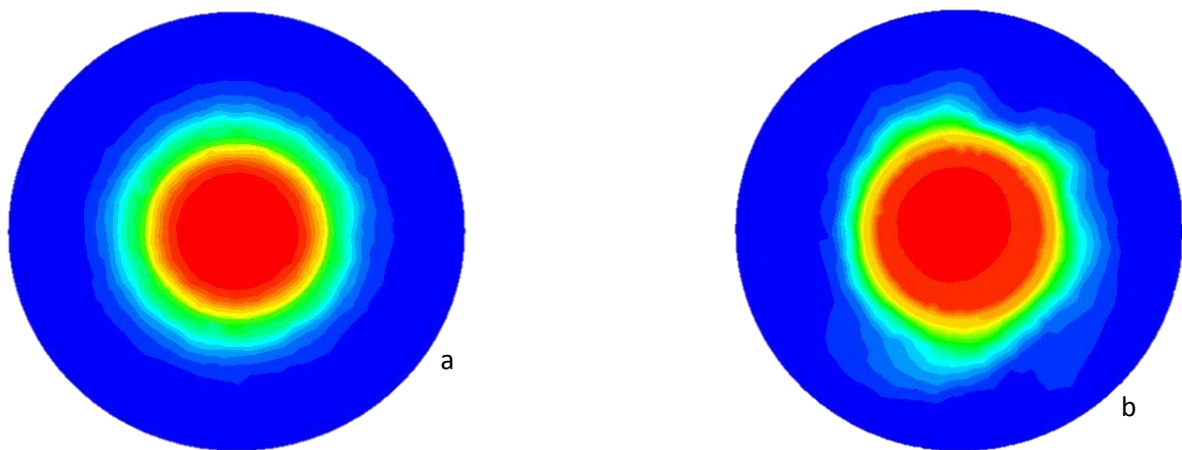


Figure (D-77) section in $z=50\text{cm}$ in test section corrugated tube ($z/d=0.5$)
at $\dot{v}_h = 3\text{LPM}$ (a) water (b) Nano fluid

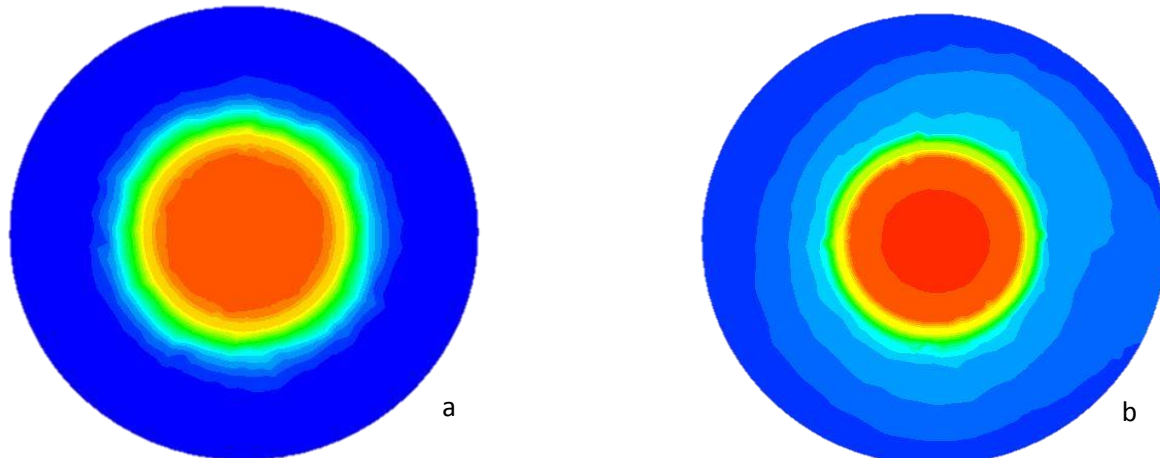


Figure (D-78) section in $z=50\text{cm}$ in test section corrugated tube ($z/d=0.5$)
at $\dot{v}_h = 4\text{LPM}$ (a) water (b) Nano fluid

APPENDIX [E]

Table (E.1) Enhancement percentages by change pipe geometry

T hot	\dot{m}_c L/M	ΔT_h		ΔT_c		Q_h	
		corrugated $z/d=1$	corrugated $z/d=0.5$	corrugated $z/d=1$	corrugated $z/d=0.5$	corrugated $z/d=1$	corrugated $z/d=0.5$
40°C	3	14.94	43.2	52.14	29.34	15.29	45.65
	4	23.58	45.03	58.55	33.66	26.77	46.3
	5	25.26	47.44	60.59	42.86	28.36	48.7
	6	30.25	47.52	75.95	46.73	32.33	49.09
	7	36.43	50.31	76.06	60.16	40.4	52.2
50°C	3	20.28	41.63	8.051	9.88	20.01	43.23
	4	23.62	44.95	26.99	15.04	26.32	44.6
	5	26.63	47.04	39.22	25.22	26.65	48.69
	6	33.85	49.09	42.48	44.77	37.68	48.88
	7	42.44	51.12	50	52.28	45.4	52.69
60°C	3	20.25	42.08	16.79	20	21.52	42.34
	4	21.45	42.86	32.38	26.3	21.88	43.57
	5	35.46	44.54	39.83	28.93	37.43	45.07
	6	39.16	45.19	44.41	46.18	43.51	47.22
	7	44.26	52.34	45.87	56.45	47.66	52.78

Table (E.2) Enhancement percentages by change pipe geometry

T hot	\dot{m}_c L/M	Q_c		U_i		U_o	
		corrugated $z/d=1$	corrugated $z/d=1$	corrugated $z/d=1$	corrugated $z/d=0.5$	corrugated $z/d=1$	corrugated $z/d=0.5$
40°C	3	52.14	52.14	22.36	47.89	23.46	49.36
	4	58.54	58.54	33.68	49.54	34.62	50.97
	5	60.58	60.58	38.04	53.17	38.92	54.49
	6	76.04	76.04	38.32	54	39.2	55.78
	7	76.16	76.16	54.54	55.72	55.66	58.91
50°C	3	20.04	20.04	25.32	44.16	26.38	45.73
	4	26.98	26.98	30.17	50.85	31.16	52.24
	5	37.88	37.88	32.9	53.27	33.86	54.59
	6	42.46	42.46	38.96	55.35	39.83	56.61
	7	49.98	49.98	52.93	56.24	53.6	57.48
60°C	3	16.77	16.77	26.82	47.93	27.85	49.4
	4	32.35	32.35	27.77	48.77	28.8	50.21
	5	39.46	39.46	42.03	50.12	42.85	51.53
	6	44.38	44.38	45.13	51.55	45.91	52.92
	7	45.84	45.84	51.21	57.27	51.9	58.48

Appendix [E]

Table (E.3) Enhancement percentages by change pipe geometry

T hot	\dot{m}_c L/M	Nu_c		ϵ		NTU	
		corrugated $z/d=1$	corrugated $z/d=1$	corrugated $z/d=1$	corrugated $z/d=0.5$	corrugated $z/d=1$	corrugated $z/d=0.5$
40°C	3	37.81	37.81	13.03	42.95	23.35	48.64
	4	38.31	38.31	23.58	44.56	32.23	51.72
	5	60.16	60.16	24.44	46.76	35.51	54.57
	6	62.8	62.8	28.92	47.43	37.91	55.99
	7	66.1	66.1	37.64	50.3	51.01	58.56
50°C	3	45.16	45.16	19.9	41.16	27.72	46
	4	49.9	49.9	23.61	44.46	31.77	53.84
	5	54.87	54.87	26.48	47.03	32.38	56.28
	6	56.04	56.04	33.38	49.09	37.03	56.37
	7	58.51	58.51	44.44	51.73	51.32	58.06
60°C	3	49.01	49.01	20.08	41.82	27.52	50.02
	4	55.84	55.84	21.45	42.85	29.36	50.36
	5	56.72	56.72	35.19	44.54	41.99	52.51
	6	62.81	62.81	39.21	45.1	42.36	53.89
	7	64.76	64.76	42.25	51.17	49.32	58.76

Table (E.4) Enhancement percentages by change pipe geometry

T hot	\dot{m}_c L/M	f_c		ΔP_c	
		corrugated	$z/d=1$	corrugated	$z/d=1$
		$z/d=0.5$		$z/d=0.5$	
40°C	3	78.56	69.61	88.34	83.44
	4	76	69.21	86.92	83.22
	5	75.47	67.75	86.64	82.43
	6	75.44	67.74	86.62	82.41
	7	70.34	64.65	83.84	80.74
50°C	3	80.31	64.79	89.26	80.81
	4	79.39	64.08	88.77	80.42
	5	76.6	63.24	87.25	79.96
	6	72.85	62.64	85.2	79.64
	7	69.42	62.36	83.33	79.48
60°C	3	87.65	64.39	93.27	80.59
	4	81.27	57.56	89.7	76.87
	5	72.41	55.04	84.96	75.49
	6	68.03	50.37	82.57	72.95
	7	59.27	50.15	77.8	72.83

Appendix [E]

Table (E.5) Enhancement percentages by change pipe geometry and used Nano

T hot	\dot{m}_c L/M	ΔT_h			
		Without Nano		With Nano	
		corrugated $z/d=1$	corrugated $z/d=0.5$	corrugated $z/d=1$	corrugated $z/d=0.5$
40°C	3	14.94	43.2	43.82	48.98
	5	25.26	47.44	43.82	50.98
	7	36.43	50.31	46.91	55.67
50°C	3	20.28	41.63	36.81	42.78
	5	26.63	47.04	43.71	50.29
	7	44.44	52.12	50.32	55.43
60°C	3	20.25	42.08	36.360	38.65
	5	35.46	44.54	42.36	46.99
	7	42.26	51.34	51.69	55.29

Table (E.6) Enhancement percentages by change pipe geometry and used Nano

T hot	\dot{m}_c L/M	Q_h			
		Without Nano		With Nano	
		corrugated $z/d=1$	corrugated $z/d=0.5$	corrugated $z/d=1$	corrugated $z/d=0.5$
40°C	3	15.29	45.65	45.17	53.41
	5	28.36	48.7	48.14	53.93
	7	40.4	52.2	49.79	57.61
50°C	3	20.01	43.23	35.75	42.74
	5	26.65	48.69	45.01	51.03
	7	47.4	52.69	52.94	58.08
60°C	3	21.52	42.34	36.72	38.680
	5	37.43	45.07	44.63	48.39
	7	45.66	52.78	54.88	58.56

Appendix [F]

To calculate the uncertainty of the experimental results the following parameter is concerned:

$$1) \text{ The mean value of the variable } x \text{ calculated as: } \bar{x}_{\text{mean}} = x_{\text{average}} = \frac{\sum_1^n x_i}{n}$$

$$2) \text{ The standard deviation of } x, \text{ given by: } \sigma = \sqrt{\frac{\sum_1^n (x_i - \bar{x})^2}{n-1}}$$

$$3) \text{ The standard error is given by: } \sigma_m = \frac{\sigma}{\sqrt{n}}$$

$$4) \text{ The uncertainty of variable } x \text{ given by: } x = \bar{x} \pm \sigma_m = \bar{x} \pm \frac{\sigma}{\sqrt{n}}$$

While the variables which are measured their uncertainty percentage for hot and cold side are the heat dissipation (Q), heat transfer coefficient (h), the overall heat transfer coefficient (U), the Nusselt number (Nu) ; the calculation shown in the table (G-1) without use Nano-fluid and table (G-2) with Nano-fluid.

Table (G-1) The Uncertainty Calculations Without Nano-Fluid

No	Pipe type	T_h °C	Q_h	U_i	Nu_h	h_i	Q_c	U_o	Nu_c	h_o
1	Smooth	40	0.14	0.135	0.2	0.205	0.14	0.135	0.09	0.09
		50	0.155	0.155	0.21	0.21	0.09	0.155	0.115	0.115
		60	0.165	0.165	0.205	0.205	0.075	0.165	0.135	0.135
2	Corrugated $z/d=0.5$	40	0.165	0.155	0.205	0.205	0.075	0.155	0.068	0.067
		50	0.165	0.165	0.205	0.21	0.085	0.165	0.067	0.068
		60	0.18	0.17	0.21	0.21	0.065	0.17	0.068	0.069
3	Corrugated $z/d=1$	40	0.165	0.18	0.2	0.2	0.105	0.18	0.066	0.16
		50	0.18	0.185	0.205	0.205	0.075	0.185	0.068	0.165
		60	0.195	0.195	0.205	0.205	0.075	0.195	0.068	0.19

Table (G-2) The Uncertainty Calculations With Nano-Fluid

No	Pipe type	T_h °C	Q_n	U_n	Nu_n	h_n
1	Smooth	40	0.225	0.29	0.205	0.245
		50	0.17	0.3	0.245	0.245
		60	0.125	0.31	0.27	0.27
2	Corrugated z/d=0.5	40	0.065	0.31	0.205	0.185
		50	0.295	0.46	0.38	0.4
		60	0.1	0.33	0.22	0.285
3	Corrugated z/d=1	40	0.1	0.33	0.17	0.19
		50	0.105	0.325	0.175	0.165
		60	0.11	0.33	0.19	0.25

الخلاصة

هذا العمل هو التعامل مع التنفيذ التجاري والعددي لاستعادة الفائدة عن طريق تغيير شكل الأنابيب في المبادل الحراري وتحسين نقل الحرارة باستخدام الماء كسائل لنقل الحرارة في الحالة الأولى، ثم النانو فلود كسائل لنقل الحرارة.

وأجريت الاختبارات التجريبية عن طريق تصميم و تصنيع نظام اختبار كامل لمبادل الحرارة متعاكس الجريان. تم اجراء الاختبارات على نظام يتكون من أنبوب النحاس بطول ١٢.٥ متر قطر داخلي ١٧.٥ ملم وقطر خارجي ١٩.٥ ملم تتمركز داخل أنبوب خارجي مصنوعة من كلوريد بولي فينيل (P.V.C) قطره الداخلي ٤٣ ملم والقطر الخارجي ٥٠ ملم عزل من الخارج باستخدام رغوة بيضاء للحد من فقدان الحرارة. تم تصنيع الأنابيب المعدل الذي يحتوي على أحاديد عرضية بعمق ٥.٥ ملم وهذا يساوي نصف سماك أنبوب النحاس مع نسبة (z/d=1, 0.5) (z : المسافة من مركز إلى مركز الأخدود، d: قطر الأنابيب الخارجي)

استخدمت التجربة المختبرية معدل التدفق الحجمي للمياه الساخنة التي تتراوح بين ١ إلى ٥ لتر في الدقيقة ورقم رينولد من ٤٠٠٠ إلى ٣٠٠٠٠ ويمر داخل الأنابيب النحاسي الداخلي. تم استخدام مياه التبريد في الحالة الأولى مع معدل التدفق الحجمي الذي يتراوح بين ٣ إلى ٧ لتر في الدقيقة ورقم رينولد من ٥٠٠ إلى ٢٢٠٠. وفي الحالة الثانية تم اضافة جزيئات الومينا النانوية AL₂O₃ ذات قطر 20nm إلى الماء بتركيز ٨٪. وكانت درجات حرارة السائل الساخن ٤٠، ٥٠ و ٦٠ درجة مئوية ودرجة حرارة سائل التبريد ٢٥ درجة مئوية.

أظهرت النتائج التجريبية أن التحسن في معامل انتقال الحرارة الكلي يتراوح من ٥٤.٥٤٪ إلى ٥٥.٧٢٪ عند درجة حرارة ٤٠ درجة مئوية و ٥٢.٩٣٪ إلى ٥٦.٢٤٪ عند درجة حرارة ٥٠ درجة مئوية و ٥١.٢١٪ إلى ٥٧.٢٧٪ عند درجة حرارة ٦٠ درجة مئوية، لكل من الأنابيب المموجة بالمقارنة مع الأنابيب غير المعدل دون استخدام الجسيمات النانوية. عند إضافة الجسيمات النانوية من AL₂O₃ بتركيز ٨٪ زيادة عملياً في نقل الحرارة بنسبة ١١.٧٠٪.

تم عمل المحاكاة العددية لتحليل عمل المبادل الحراري ونقل الحرارة باستخدام برنامج الأنسيز فلوينت ٤. وقد تم استخدام البرنامج لحل معادلات الطاقة والزخم والاستمرارية لتحليل تدفق السوائل من خلال المبادل حراري. تم إجراء التحليل لكل الأنابيب باستخدام سوائل التبريد بدون استخدام الجسيمات النانوية وباستخدامها وتم فرض السلوك النيوتيني وثلاثي الأبعاد. في المحاكاة العددية تم استخدام معدل التدفق الحجمي للمياه الساخنة التي تتراوح بين ١ إلى ٥ لتر في الدقيقة ورقم رينولد من ٤٠٠٠ إلى ٣٠٠٠٠ ويمر داخل الأنابيب النحاسي الداخلي. تم استخدام مياه التبريد في الحالة الأولى مع معدل التدفق الحجمي الذي يتراوح بين ٣ إلى ٧ لتر في الدقيقة ورقم رينولد من ٥٠٠ إلى ٢٢٠٠. وتم استخدام النانو فلود AL₂O₃ بحجم جزيئي ٨٪.

وأظهرت النتائج تباين طفيف بين النتائج العملية والنظرية بنسبة ٨.٩٧٪ إلى ١١.٣٥٪ ولكن أن لديهم نفس السلوك والظاهرة.

تم استنتاج المعادلات التجريبية للعلاقة بين قيم رقم الرينولد ورقم النسلت كما هو مبين في الفصل ٥، لجميع المتغيرات ولكل نوع من الأنابيب ولنوعي سائل التبريد باستخدام برنامج لاب فيت المصمم من قبل الجامعة الفيدرالية دي كامبيينا غراندي في البرازيل.

$$Nu_c = 449.8 + 1443R_e^{0.1749} \quad (1)$$

$$Nu_{cn} = 621.3 + 1157R_{en}^{0.1096} \quad (2)$$



جمهورية العراق

وزارة التعليم العالي والبحث العلمي

جامعة واسط / كلية الهندسة

قسم الهندسة الميكانيكية

تحسين انتقال الحرارة في مبادل حراري قشرة وانبوب متعاكس الجريان

مقدمة الى مجلس كلية الهندسة في جامعة واسط

وهي جزء من متطلبات نيل شهادة الماجستير في كلية الهندسة/ قسم الهندسة الميكانيكية

فرع توليد الطاقة

من قبل الطالب

صفاء عبد محمد

بأشراف الأستاذ الدكتور

زينه خليفة كاظم

تشرين الاول ٢٠١٦ م

محرم ١٤٣٨ هـ